Pressure ripple propagation in hydraulic systems.

Butler, Malcolm David

Award date:
1984

Awarding institution:
University of Bath

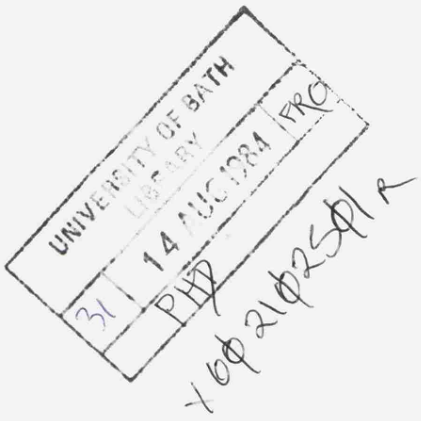
UNIVERSITY OF BATH
LIBRARY
14 AUG 1984
PHD
Y04210254

PRESSURE RIPPLE PROPAGATION IN HYDRAULIC SYSTEMS

A thesis submitted by

MALCOLM DAVID BUTLER

for the degree of

Ph.D.

of

University of Bath

1983

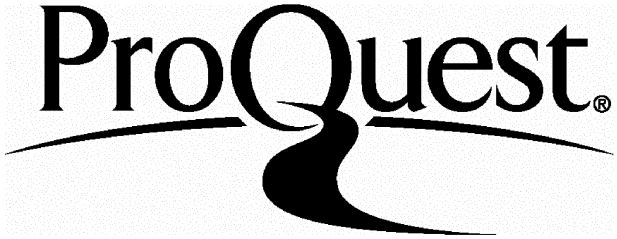

ACKNOWLEDGEMENTS:-

The author would like to thank:

His supervisor Professor Ted Bowns for his help and guidance.

All the staff of the school of engineering. With particular thanks to Dr. Derek Tilley for his counsel and encouragement and Dr. Kevin Edge for proof reading the manuscript.

Mrs. Yvonne Stratton for the typing of the manuscript.

SUMMARY

The problem of pressure ripple propagation in fluid filled pipelines has been understood for a long time. To-date, however, mathematical representations of pressure ripple standing waves generated in hydraulic systems have been limited to very simple systems operating at low mean pressure levels and over limited frequency ranges.

This report details the evaluation and development of the mathematical impedance representation of hydraulic systems and system components. With the result that these can be used to predict, with confidence, pressure ripple levels in hydraulic circuits under normal conditions of operation and over a wide frequency range. The confidence comes from the detailed practical examination of the pressure ripple levels created in hydraulic systems, made up from standard hydraulic components, operated under normal conditions of pressure and flow. Although the test circuits used are only representative of practical systems, they do not perform any specific function, they incorporate all the major features of circuit design, including branch lines and impedances (components) in series.

Lastly, the ability to model with accuracy the pressure ripple levels within a hydraulic circuit provides the means by which they can become part of the overall design specification for a hydraulic system. This thesis illustrates the difficulties which restrict the practical implementation of this ideal.

CONTENTS:

LIST OF FIGURES:

Notation:

Symbol		Definition	Units
a	-	Velocity of sound in the hydraulic fluid	$m.s^{-1}$
a_o	-	Velocity of sound in air	$m.s^{-1}$
a_s	-	Velocity of sound in steel	$m.s^{-1}$
d	-	Distance along pipeline	$m.$
k	-	Pipe wall thickness	$m.$
l	-	Length of pipeline	$m.$
l'	-	Length of pump discharge line	$m.$
n	-	Polytropic index of the orifice equation	-
p	-	Incremental pressure	$N.m^{-2}$
t	-	Time	$s.$
v	-	Velocity of vibration	$m.s^{-1}$
x	-	Distance along pipeline	$m.$
A	-	Cross sectional area	m^2
B	-	Bulk modulus	$N.m^{-2}$
B_T	-	Isentropic tangent bulk modulus	$N.m^{-2}$
B_T'	-	B_T including pipe wall flexibility	$N.m^{-2}$
B_s	-	Isentropic secant bulk modulus	$N.m^{-2}$
B_{so}	-	B_s at zero pressure	$N.m^{-2}$
B_{sp}	-	B_s at pressure P	$N.m^{-2}$
D	-	Pipe diameter	$m.$
E	-	Youngs modulus for steel	$N.m^{-2}$
F	-	Wave propagation equation constant	-
F_p	-	Pressure force	$N.$
G	-	Wave propagation equation constant	-
H_A	-	Dimensionless parameter	-
K	-	Orifice equation constant	-
P	-	Pressure	$N.m^{-2}$
P_M	-	Mean pressure	$N.m^{-2}$
Q	-	Flow	$m^3.s^{-1}$

Q_L	-	Leakage flow	$m^3.s^{-1}$
Q_Z	-	Flow through valve	$m^3.s^{-1}$
R	-	Pipeline friction coefficient	-
T	-	Temperature	^oC
V	-	Volume	m^3
V_p	-	Pipeline vibration velocity	$m.s^{-1}$
W_A	-	Actual acoustic power	W
W_I	-	Ideal acoustic power	W
Z	-	Impedance	$N.s.m^{-5}$
Z_I	-	Inertance of a pipeline	$N.s.m^{-5}$
Z_o	-	Characteristic impedance of a pipeline	$N.s.m^{-5}$
Z_{se}	-	System Impedance	$N.s.m^{-5}$
Z_v	-	Impedance of a closed volume	$N.s.m^{-5}$

Greek symbols

α	-	Attenuation value $(R_e(\gamma))$	-
β	-	Change of phase value $(I(\gamma))$	-
γ	-	Propagation constant	-
λ	-	Wavelength	m.
ρ	-	Density	$Kg.m^{-3}$
ρ'	-	ρ including frequency effects	$Kg.m^{-3}$
ρ_s	-	Reflection coefficient at the pump	-
ρ_T	-	Reflection coefficient at the termination	-
μ	-	Viscosity	$N.s.m^{-2}$
μ'	-	μ including frequency effects	$N.s.m^{-2}$
σ	-	Radiation efficiency	-
ω	-	Frequency	Hz
ω_c	-	Coincidence frequency	Hz
ω_o	-	Resonant frequency	Hz

General suffices:-

1,2,3,4	-	Denote different positions or conditions
bp	-	boost pump

c	-	chamber
e, E	-	entrance to pipelines
f	-	flowmeter
in	-	inlet conditions
J	-	junction
m	-	motor
max	-	maximum value
min	-	minimum value
$mean$	-	mean value
o	-	outlet conditions
p	-	pump
RMS	-	root mean squared value
s	-	pump
ss	-	steady state value
T	-	termination
v	-	due to pipe vibration
x	-	position along a pipeline

CHAPTER 1

INTRODUCTION

INTRODUCTION

101 In recent years more attention has been paid to the general standards of the working environment present in all sections of industry. Concern over potential health hazards has lead to the introduction of changes in working practices whilst in more severe cases legislation has been used to provide more stringent safeguards. More recently attention has been focused on the problem of noise as a major health hazard, which has until now been regarded simply as a discomfort. Research has shown that a person's hearing can be seriously impaired by prolonged exposure to high noise levels. This has led to the introduction, in this and many other industrial nations, of legislation which limits the amount of time that any person may be subjected to a given noise level in the course of a normal working day. As a result, purchasers of industrial equipment are including noise level limits in their specifications for new equipment.

102 In themselves hydraulic components are only as noisy as equivalent electrical or mechanical components but they often excite high levels of vibration and noise in other system components. They can, therefore, contribute significantly to the general noise level in many industrial applications. Clearly a reduction in the noise levels of hydraulic components or systems would make them more attractive to potential users. The potential value to the hydraulics industry of such a reduction in the noise levels generated by hydraulic systems was demonstrated by the scale of a research programme initiated by the Department of Industry (D.O.I.) in 1976. The aim of this research was to investigate the noise problems associated with hydraulic components and to devise and develop ways in which these noise levels could be reduced.

103 The overall pattern of the noise generated by a hydraulic system is best illustrated by considering a typical circuit. In any system there are several potential sources of vibration, the cause of all the unwanted noise, and several paths along which the vibration can be transmitted, as illustrated on Fig. 1.1. The figure shows the sources of vibration to include the prime mover and load in addition to the hydraulic components. Hydraulic pumps and motors are particularly strong generators of noise because of the rapid changes in pressure that occur within them. Valves can also generate high levels of vibration especially when high pressures and flows are involved.

104 Noise is radiated from any vibrating external surface which may not be the surface of a component which could be considered a primary source of vibration. The vibrations are transmitted from their component source to all other components to which they are mechanically coupled. Thus a surface some distance from the initial source of the vibration may be a significant distributer of noise if it is mechanically more responsive to that particular frequency. This transmission of vibration is known as structure borne noise. With hydraulic systems we have an additional transmission path, the hydraulic fluid. Vibrating components can interact directly with the fluid to create pressure ripples which are transmitted through the fluid in the form of pressure waves. The dominant source of pressure ripple is, however, the positive displacement pump. Large variations in the flow delivered by the pump, an unavoidable consequence of the pumping mechanism, generate significant levels of pressure ripple. These are transmitted through the fluid and hence throughout the system where they can induce vibration

in other components. This generation and transmission of pressure ripple is referred to as Fluid Borne Noise (F.B.N.) and it is this aspect of hydraulic system noise in which we are interested.

The Source of Fluid Borne Noise

105 As mentioned above the pump is the primary source of F.B.N. in a hydraulic system. The discharge from a positive displacement pump is not steady but, due to the discrete flows from each piston, gear tooth or vane, consists of a mean flow with a superimposed periodic fluctuation. If we consider an axial piston pump in which the motion of the pistons is simple harmonic then the ideal flow, obtained by neglecting the effects of compressibility and port plate timing, is given by the sum of the flows from each of the cylinders which are open to the discharge line at any instant. The idealised flow for a 7 piston pump is illustrated on Fig. 1.2, which shows the summation of the individual piston flows to give the total flow as a function of the angle of rotation of the pump. This illustration shows that the ripple frequency for the idealised flow from a pump with an odd number of pistons is twice piston frequency. It can be shown that the ripple frequency is the same as the piston frequency for a pump with an even number of pistons. The discharge flowrate from many real pumps approaches this idealised flowrate when the discharge line pressure is very low.

106 Under normal operating conditions, with a high discharge line pressure, fluctuations can occur in the flow from each piston as it opens to the delivery line due to the compressibility of the fluid. The effect of the discharge line pressure on the instantaneous pump flowrate is shown on Fig. 1.3. This shows that

as the discharge port opens to the delivery line a reverse flow takes place until the cylinder pressure rises to the pressure of the delivery line. Helgestad et al (1) have shown that the magnitude of these flow irregularities is a function of the delivery pressure, pump speed and port plate geometry.

107 Other types of pump produce similar instantaneous flow ripple, although the reverse flow due to compressibility may not be so significant in some of these. For example, in external gear pumps the pressure rise occurs gradually around the casing, the rate of the rise governed by the leakage across the sides and tips of the gear teeth. The backflow into each pocket of fluid is therefore not as significant as with an axial piston pump. In this case the flow ripple is predominantly due to the discontinuous nature of the flow delivery created as the two gears mesh.

Transmission of Fluid Borne Noise

108 The instantaneous flow from a positive displacement pump is complex. However, as the flow fluctuation is periodic it can be separated into a series of sine wave components by Fourier analysis. These will consist of a fundamental component at piston, gear tooth or vane frequency plus the higher harmonics at integer multiples of this frequency.

109 The flow ripple interacts with the system producing a complex pressure ripple which is superimposed upon the mean system pressure level. This pressure wave is then propagated along the pipeline at the local speed of sound. When the wave encounters a discontinuity, such as a valve, it is partially reflected back towards the pump. Partial reflection will again occur when the wave reaches the pump. With the further reflections of this and the subsequent

pressure waves from the pump we end up with two sets of travelling pressure waves. One set travelling away from the pump and the other travelling in the reverse direction. All these waves interfere with each other to produce a standing wave of the pressure ripple, the amplitude and phase of which varies along the pipeline.

Previous Work

110 The theory of pressure ripple propagation and generation of standing waves has been understood for a long time and a number of investigators have produced successful theoretical models of simple hydraulic or pneumatic systems. Many have used the concept of impedance to represent the circuit component parameters which they then combined using wave propagation theory to produce a mathematical representation of the pressure standing wave. This process is directly analogous to the transmission line theory used for electrical circuits.

111 Much of the early work was in connection with the transmission of sound in ducts and one such investigator, Stewart (2), considered pneumatic systems at atmospheric pressure with relatively low ripple frequencies. The frequency range and mean pressure levels were limited by the performance of the pressure transducers available at the time. Although these pneumatic systems provided a convenient means of examining pressure standing waves the effects of pressure transients in liquids was also considered around this time through the investigation of water hammer by such as Joukowsky (3).

112 More recently there have been a number of investigations into cyclic pressure variations which generate the pressure standing waves within hydraulic systems, by for example Waller (4). Some such as

Constantinesco (5) and Foster (6) were concerned with maximising the pressure amplitudes in order to use the wave motion to transmit power through the fluid. However, later investigators such as Willekens (7) have concentrated on the modelling of systems with the aim of reducing pressure ripple levels. However, these investigations were limited to low pressure systems and limited frequency range.

113 This work is part of a more detailed and extensive program of work mounted at the University of Bath and supported by the Department of Industry. Its aim is to extend and improve the mathematical models used to-date to include systems operating at higher more realistic pressure levels and over a wider frequency range. In addition, the range of systems is to be extended to include circuits containing branch lines and impedances in series.

CHAPTER 2

INSTRUMENTATION

INTRODUCTION

201 The experimental work presented in this thesis covers a variety of test rigs and procedures. Specific details of each rig and experimental procedure are provided in the relevant chapters. However, the instrumentation and data acquisition techniques are universally applied.

202 Consider, for example, the extending pipeline test rig employed in chapter 3, as outlined on Fig. 3.6 and illustrated on Figs. 3.5 and 3.7. The basic variable parameters needed to define the operating conditions and fluid properties in this simple circuit are the mean pressure, mean flowrate, temperature of the oil and rotational speed of the pump drive shaft. These parameters are easily measured using standard pieces of test equipment such as pressure gauges.

203 To examine the pressure ripple within the circuit a more specialised form of instrumentation is required. In this case a pressure transducer with good frequency response characteristics, such as those provided by the piezo electric type of transducer. Figs. 3.6 and 3.7 show two such transducers mounted at the ends of the test pipeline, where the test conditions are more defined.

204 The output from such a transducer, or more specifically the output of the amplifier used to boost the small transducer signal to a useful level, is in the form of a voltage level which varies with time. A typical trace is shown on Fig. 2.2. Such signals in the time domain are of limited use in the analysis of the pressure ripple. However, the signals are periodic so they can be transferred to the frequency domain, which defines the signal in terms of harmonic

amplitudes and phases. The transfer from the time to the frequency domain could be achieved mathematically using Fourier Analysis. However, there is now a range of instrumentation available that will perform this test automatically. One such device was the Solartron Frequency Response Analyser used here.

205 In addition to the specialised forms of test equipment several more standard instruments were used to monitor and/or record data. These included a digital voltmeter, frequency counter and oscilloscope. These and other instruments together with the interfaces between transducers, analysers and data acquisition computer are shown on Fig. 2.1.

206 The instrumentation mentioned above, together with some additional pieces of test equipment used at some point during the experimental work, are discussed in detail below. The method of data acquisition using a mini computer is also detailed.

TRANSDUCERS

Mean Pressure

207 The mean pressures in the test pipelines were measured using Bourdon type gauges. These were connected close to the entrance to the pipeline. To ensure that the line connecting the pressure gauge to the pipeline did not introduce any standing wave effects which would interfere with the transient pressure levels within the test line the pressure tapping was made through a very small bleed hole, 1mm. diameter, as illustrated on Fig. 2.3. In addition, a small needle valve was mounted adjacent to the mounting block which could be used to isolate the gauge line during those periods when the transient pressures were recorded. However,

subsequent tests showed that it was not necessary to isolate the gauge line.

Transient Pressure

208 The measurement of pressure fluctuations associated with pressure wave propagation within a hydraulic system requires a pressure transducer and amplifier system with a good frequency response. Hence, piezo electric transducers were used together with charge amplifiers. The use of charge amplifiers as opposed to voltage amplifiers eliminates the need for relatively short, fixed length, calibrated cables connecting the transducers and amplifiers. With charge amplifiers virtually any length of cable can be used which is more suited to the extending pipeline length test procedures used here.

209 The piezo electric transducers (Vibrometer Type 6QP500) are very small, with a diaphragm of approximately 4mm. in diameter. Variations in pressure over the measuring diaphragm due to standing waves could therefore be ignored even at the highest frequencies considered. To prevent any degradation in the detection of the pressures in the pipeline, care was taken to ensure that the diaphragms were flush with the internal surface of the pipe wall, as shown in Fig. 2.3. Thus, the presence of the transducers would not cause any disturbance in the flow. The transducers were generally located at either end of each test pipeline, the actual locations are given on the relevant circuit diagrams, Figs. 3.8, 4.2, 5.3, 6.6 and 7.4.

Mean Flow

210 To obtain a measure of the mean flowrate in the

test pipeline a turbine flowmeter was installed in the low pressure return line. The flowmeter was positioned downstream of the filter to prevent ingress of dirt, as illustrated for example on Fig. 3.6. The output from the flowmeter, in the form of voltage pulses, can be measured directly as pulses per second using a frequency counter or as a voltage level using a frequency to voltage convertor and a voltmeter. The later system can be set to give a voltage readout which corresponds directly to a flowrate measurement. For example, 1.7 volts for 1.7 litres/sec. Both of these methods were used during the investigations.

Transient Flow

211 The measurement of transient flows in hydraulic systems has always been difficult due to the limited frequency response of standard flowmeters. However, the Hot Film Sensor Anemometer recently developed at Bath University, by Tilley (8), can detect dynamic flows at frequencies of several kilohertz.

212 The transient flowmeter was used to establish the flow ripple in a hydraulic circuit, Chapter 5, in order to validate the relationship between the pressure, impedance and flow. This relationship, which is analogous to that of voltage, impedance and current in electrical theory, means that fluid borne noise can be considered solely in terms of pressure and impedance.

213 This result has practical advantages since the small piezo electric pressure transducers can be used extensively to monitor pressure ripple. Their small size allows them to be located in almost any position along a pipeline without hindrance to the measured flow within the pipeline. On the other hand, a

different transient flowmeter would be required for each pipe size. In addition to this, their size and geometry restrict the areas in a system where such devices can be located.

Shaft Speed

214 The shaft speed or more appropriately the piston frequency was detected using a magnetic pick up unit positioned to detect equi-spaced teeth on the circumference of a steel disc mounted on the pump drive shaft. The number of teeth on the disc correspond to the number of pistons within the pump. Thus the number of pulses per revolution is equivalent to the piston frequency.

215 The pulse levels produced vary with the speed of rotation and the distance between the teeth and the magnetic pick up unit. Slight differences in the spacing of the teeth, due to machining tolerances, and in the width of the gap, often caused by vibration, create irregular pulse periods and peak voltage levels. Such irregularities can lead to a variation in the piston frequency when detected by more sensitive types of instrumentation, such as Frequency Response Analysers. The introduction of a phased locked loop, shown in block diagram form on Fig. 2.4, provided an average frequency signal with a regular pulsed waveform.

Oil Temperature

216 A knowledge of the operating temperature of the oil in the test pipeline was essential in order to evaluate the properties of the oil. The oil temperature was measured using a thermocouple mounted in the reservoir. This can be taken to be the termperature of the oil in the test pipeline once steady conditions had been established at each test condition.

217 In the series impedance tests, chapter 7, the oil temperatures in the two test pipelines are different. The temperature in the second pipeline was measured using a thermocouple clamped, using a pad of insulating material, against the pipe wall.

218 A constant oil temperature level, 40°C, was maintained by adjusting the flow of water through the oil cooler. For the majority of the tests, this was done manually with temperatures maintained within 2°C. By the later tests an automatic controller had been installed which gave a higher degree of control. Temperatures could now be maintained within 1°C.

Vibration

219 In addition to the measurement of transient pressures and flows a need arose to measure vibration. Firstly to measure the vibration of a pipeline in the branch line tests, Chapter 6. Secondly, to observe the vibration of a valve body in order to detect the presence of cavitation, during the series impedance tests, Chapter 7.

220 The vibration was measured using piezo electric accelerometers combined with voltage amplifiers. Each transducer had its own calibrated cable for connection to the voltage amplifier. The sensitivity of each transducer and cable was known which allowed for correlations to be made between the amplifier outputs and the mechanical quantity measured.

221 In all cases the accelerometers were mounted onto the test rig in the required orientation using small magnetic bases.

Calibration

222 All the measuring devices were regularly recalibrated during the investigations to ensure that there was no variation in the sensitivity of the test equipment which would introduce errors into the analysis of the results.

SIGNAL ANALYSERS

Frequency Response Analyser

223 To analyse the complex time domain signal registered by the piezo electric pressure transducers the signal was transferred to the frequency domain and the harmonic components were obtained. This was achieved using a Solartron 1170 Frequency Response Analyser (F.R.A.)

224 The normal application of this type of instrument is to use the frequency generator stage of the F.R.A. to input a sinusoidal signal of known frequency and amplitude into a system. The response of the system is then monitored at the same frequency. The F.R.A. compares the two signals to give information concerning the phase shift and attenuation produced by the system at that frequency.

225 To analyse the pressure signals no output was required from the F.R.A. as the excitation was provided by the pump itself. The internal generator of the F.R.A. could be synchronised to an external frequency source, or to integer multiples, up to ten, of that frequency. Any input to the instrument, in this case the pressure signal, was monitored and the amplitude of the frequency content corresponding to the internal generator frequency was displayed. Also displayed was

the phase shift between the input and the internally generated signal.

226 In this case the synchronising frequency was provided by the pulses from the shaft speed measurement described above, Section 215. Thus the first harmonic or fundamental frequency was the piston frequency of the pump. The response of the system, in terms of amplitude and phase, was obtained at this frequency and at each harmonic, up to the tenth. The trigger pulses also served as the reference for the phase measurement. Although the phase of each harmonic was completely arbitrary when viewed in isolation all the phase were measured relative to the same reference and so the relative phases were correct. Hence the results could be recombined to provide the original time domain signal.

Spectrum Analyser

227 In addition to the F.R.A. discussed above, a Hewlett-Packard Spectrum Analyser, Model 3582A, was used on occasions to examine the frequency content of the pressure transducer signals. Unlike the F.R.A., the spectrum analyser examines the signal over a frequency band rather than at discrete frequencies. The analyser uses a fast fourier transform algorithm to derive the amplitude/frequency or phase/frequency relationship for a periodic signal over a selected frequency band. In this case from 0 to 2.5 KHz.

228 The analyser is a two channel device and the phase valves for these channels are related. However, in order to synchronise the phases with the piston frequency, one channel had to be used to measure the output of the shaft speed detector. This would reduce the analyser to a single channel unit. For this reason

the analyser was only used to examine the frequency content of a signal or comparing spectrums of pressures at two positions, were absolute references were not required.

229 The results are displayed in the form of amplitude/frequency or phase/frequency plots on an inbuilt visual display unit. A permanent record of a result can be obtained by connecting the analyser to a X-Y plotter. This analyser has the facility to transfer results from the display or from one of its memory areas directly to a suitable plotter. Typical results recorded in this way can be seen on Fig. 7.10.

DATA ACQUISITION

230 Experience has shown that, in general, ten harmonics are sufficient to describe most pressure signals. Nevertheless the amount of data to be gathered was still considerable, consisting of the amplitude and phase of ten harmonics of between two and six transducers. Because of the large amount of data an on line digital computer (PDP8) was used to control the F.R.A. during the test and to record and store the information. The computer program was designed to cycle through ten harmonics of each pressure reading, averaging a set number of readings at each harmonic, normally five, and then switch to the next transducer to repeat the process. The information, extracted via a digital interface on the rear of the F.R.A., was stored by the computer on magnetic disc or tape for later analysis or printing.

231 The computer recorded information at a very much faster rate than could be achieved manually, even taking five readings for each harmonic. This means that there was less likelihood of any changes occuring

in the test conditions whilst the results were taken. The readings were generally found to be very stable although the stability decreased for the higher harmonics. Typical variations for the first harmonic could be .1 dB and .5 degree whilst for the tenth variations of 5 or 6 dB and 10 to 20 degrees would not be uncommon. Such variations of the pressure signal with time may be attributed to two factors. Firstly, small variations in the pump speed give rise to small changes in the piston frequency about a nominal value. This frequency variation will, of course, be multiplied for the higher harmonics. That is a variation of 1 Hz at the fundamental leads to a variation of 10 Hz at the tenth harmonic, which may well alter the levels recorded. Secondly, the pressure pulse delivered by each pumping element in turn will not be identical. Discrepancies in this area would again be characterised by variations in the higher harmonics.

CHAPTER 3

Characteristics of an Axial Piston Pump, Pipeline, and Restrictor Valve System

INTRODUCTION

301 The work detailed in this chapter follows on directly from the work carried out recently at the University of Bath in modelling simple oil hydraulic systems using an impedance model derived from plane wave propagation theory for transmission lines as often applied in electrical systems.

302 The usefulness of this technique for modelling fluid transients has been known for a long time. For example Stewart (2) used a similar technique in the early 1920's to explain the effect of simple filter sections in fluid systems. These early applications were limited to air at low or atmospheric pressure levels and low frequencies. Gradually the technique was applied to water and oil hydraulic systems to model pressure transient effects such as water hammer.

303 More recently the improvements in instrumentation and data handling systems have made possible the application of this technique to more practical hydraulic systems with increased mean pressure levels and higher frequencies. This work has been carried out by among others Willekens (7). However, up till now the systems covered used relatively low mean pressure levels, when compared to practical applications. Furthermore, the simplified impedance models employed for various circuit components restricted the accuracy of the model to the first few harmonics of the disturbing frequency.

304 Most recently Tilley (8) obtained good results over an increased frequency range with a system using

a 70 bar mean pressure level. This was achieved by paying closer attention to the individual component impedances. The major aspect of this work was a demonstration of the performance of a transient flowmeter from which he was able to obtain experimentally the flow ripple values to complement their corresponding pressure ripple levels. However, in order to model the pressure and flow ripple standing waves, several assumptions were made which require further investigation. These arose mainly from the design of the test rig which included many superfluous components which could, and in some instances obviously did, affect the pressure and flow ripple levels. In addition the use of an artificially high value for the pipe friction factor in the mathematical analysis also invites further attention.

305 It is the aim, therefore, of the work reported in this chapter to remove these uncertainties from both the test arrangements and the mathematical models. In addition the experimental work will be undertaken using a hydraulic system operating with higher, more realistic, pressure levels.

306 To achieve these aims an experimental rig was designed and constructed to give the simplest hydraulic circuit possible using practical, off the shelf, hydraulic components, whilst eliminating bends, relief valves and changes in section. To complement this basic approach the test procedure was confined to fixed speed running of the pump with the pressure ripple measured at fixed points along the pipeline, for many different pipe lengths. In this way the circuit not only represents the many fixed speed systems in use but also ensures that the component impedances remain the same for each pipe length used. This allows a simple averaging or statistical approach to be used to improve the accuracy of the analysis.

MATHEMATICAL MODEL OF A SIMPLE SYSTEM

307 The equations describing the pressure and flow ripple standing wave patterns are adopted from the electrical theory for transmission lines, which can be found in several electrical text books such as Chipman (9). The mathematical derivation, based upon the two major variables of flow and pressure change, is outlined in Tilley (8). A detailed summary is included here to show the derivation of the salient parameters, for which we can then demonstrate how they influence the generation of the pressure and flow standing waves.

308 Consider a fluid element in a pipeline subject to a plane travelling wave, as shown in Fig. 3.1.

By continuity, $$-\frac{\partial Q}{\partial x} = \frac{A}{B} \cdot \frac{\partial P}{\partial t} \qquad (3\cdot1)$$

By force equilibrium, $$-\frac{\partial P}{\partial x} = QR + \frac{P}{A} \cdot \frac{\partial Q}{\partial t} \qquad (3\cdot2)$$

Combining these expressions we get the wave equations,

$$\frac{\partial^2 Q}{\partial x^2} = \gamma^2 Q \qquad (3\cdot3)$$

$$\frac{\partial^2 P}{\partial x^2} = \gamma^2 P \qquad (3\cdot4)$$

Where the propogation constant

$$\gamma = \left(\frac{RA}{B} \cdot S + \frac{\rho}{B} \cdot S^2\right)^{1/2} \qquad (3\cdot5)$$

309 The general solutions to the wave equations (3.3) and (3.4) are given by:-

$$P = Fe^{-\gamma x} + Ge^{\gamma x} \qquad (3.6)$$

$$Q = \frac{1}{Z_o}\left(Fe^{-\gamma x} - Ge^{\gamma x}\right) \qquad (3.7)$$

Where the Characteristic Impedance of the pipeline

$$Z_o = \left[\frac{R + S/A \cdot S}{A/B \cdot S}\right]^{1/2} \qquad (3.8)$$

and the constants F and G can be evaluated for a particular system.

310 It is clear from the equations (3.6) and (3.7) that the pressure and flow fluctuations in a pipeline generate two wave systems. One propagating in the forward direction given by the term $Fe^{-\gamma x}$ and one in the reverse direction given by $Ge^{\gamma x}$. The magnitude of these waves depend upon the values of the constants F and G, which are obtained by considering the end conditions for the system.

311 Consider the simple pump, pipeline and termination system as shown on Fig. 3.2.

At the termination, where $x = \ell$, the impedance

$$Z_T = \frac{P_T}{Q_T} = Z_o \cdot \left[\frac{Fe^{-\gamma\ell} - Ge^{\gamma\ell}}{Fe^{-\gamma\ell} - Ge^{\gamma\ell}}\right] \qquad (3.9)$$

Rearranging this expression gives,

$$F = \frac{Ge^{2\gamma\ell}}{\rho_T} \qquad (3.10)$$

Where the Reflection Coefficient at the termination

$$\rho_T = \frac{Z_T - Z_o}{Z_T + Z_o} \qquad (3.11)$$

gives the magnitude and phase of the reflected wave compared to the incident wave.

312 At the pump, where $x = 0$, the pump flow

$$Q_s = Q_E + Q_L \qquad (3.12)$$

Where Q_E is the flow entering the pipeline and Q_L is the leakage flow through the pump which is given by

$$Q_L = \frac{P_E}{Z_s}$$

Substituting for equations (3.6) and (3.7) into (3.12) we get

$$Q_s = \frac{1}{Z_s}(F + G) + \frac{1}{Z_o}(F - G)$$

which when rearranged gives,

$$Q_s = \frac{Z_s + Z_o}{Z_s Z_o}(F - \rho_s G) \qquad (3.13)$$

Where the Reflection Coefficient at the pump

$$\rho_s = \frac{Z_s - Z_o}{Z_s + Z_o} \qquad (3.14)$$

313 Substituting for F from equation (3.10)

$$Q_s = G \cdot \frac{Z_s + Z_o}{Z_s Z_o} \cdot \left(\frac{e^{2\gamma l}}{\rho_T} - \rho_s \right)$$

which rearranged gives,

$$G = \frac{Q_s Z_s Z_o}{Z_s + Z_o} \cdot \frac{1}{\left(\frac{e^{2\gamma l}}{\rho_T} - \rho_s \right)} \qquad (3.15)$$

similarly $$F = \frac{Q_s Z_s Z_o}{Z_s + Z_o} \cdot \frac{e^{2\gamma l}}{\left(\frac{e^{2\gamma l}}{\rho_T} - \rho_s \right)} \qquad (3.16)$$

Substituting for these values of F and G into equations (3.6) and (3.7)

$$P = \frac{Q_s Z_s Z_o}{Z_s + Z_o} \cdot \frac{\left(\frac{e^{2\gamma l}}{\rho_T} e^{-\gamma x} + e^{\gamma x} \right)}{\left(\frac{e^{2\gamma l}}{\rho_T} - \rho_s \right)}$$

$$Q = \frac{Q_s Z_s}{Z_s + Z_o} \cdot \frac{\left(\frac{e^{2\gamma l}}{\rho_T} e^{-\gamma x} - e^{\gamma x} \right)}{\left(\frac{e^{2\gamma l}}{\rho_T} - \rho_s \right)}$$

Rearranging gives

$$P = \frac{Q_s Z_s Z_o}{Z_s + Z_o} \cdot \frac{\left(e^{-\gamma x} + \rho_T e^{-\gamma(2l-x)} \right)}{\left(1 - \rho_s \rho_T e^{-2\gamma l} \right)} \qquad (3.17)$$

$$Q = \frac{Q_s Z_s}{Z_s + Z_o} \cdot \frac{\left(e^{-\gamma x} - \rho_T e^{-\gamma(2l-x)} \right)}{\left(1 - \rho_s \rho_T e^{-2\gamma l} \right)} \qquad (3.18)$$

Equations (3.17) and (3.18) can be used to model the transmission of pressure and flow waves in a fluid pipeline, irrespective of the nature of the disturbance.

314 These relatively involved expressions for the pressure and flow at any point in the pipeline can be better understood by considering the physical significance of the terms in the equation. If we consider a harmonic disturbance as generated by a pump, then the incident pressure wave at the pipe entry is given by:-

$$P_E = Q_S \cdot \frac{Z_S Z_o}{Z_S + Z_o} \qquad (3\cdot19)$$

As the wave passes down the pipeline the value of this incident wave at any point is given by:-

$$P_x = Q_S \cdot \frac{Z_S Z_o}{Z_S + Z_o} \cdot e^{-\gamma x} \qquad (3\cdot20)$$

The propagation constant γ can be replaced by the index $\alpha + j\beta$ where α denotes the attenuation of the wave due to friction and β, which is given by ω/a, gives the phase change as the wave propagates along the line. Thus the incident wave decreases in amptitude as it passes down the line and at the same time its phase lag increases.

315 At the termination the incident wave is partially reflected and partially transmitted. The magnitude and change in phase for the reflected wave is given by the reflection coefficient, ρ_T. The reflected wave is then attenuated and its phase lag increased as it passes back along the pipeline. The value for this reflected wave is given by:-

$$P_x = Q_S \cdot \frac{Z_S Z_o}{Z_S + Z_o} \cdot \rho_T e^{-\gamma(2l-x)} \qquad (3\cdot21)$$

Thus the pressure at any point along the pipeline will be the sum of the two travelling waves.

316 When the reflected wave reaches the pump it is reflected again. The magnitude and change in phase for this reflected wave is given by the reflection coefficient, ρ_s. Thus the overall pattern for the pressure fluctuations in the pipeline are due to the multiple reflections from both the pump and termination. The sum of the pressure values for each wave at any point along the pipeline gives the value of the pressure standing wave at that point. This summation is given by the term,

$$\left(1 - \rho_s \rho_T e^{-2\gamma\ell}\right)^{-1} \qquad (3.22)$$

If this expression were to be expanded Binomially it would show mathematically the attenuation and phase change associated with each wave reflection.

MODELLING OF THE FLUID PROPERTIES

317 Effect of Oscillatory Flow

The wave propagation equations derived above assume that the wavefront was plane, which does not occur in practice. However, it has been shown by Uchida (10) that the velocity distribution for oscillatory flow tends towards a plane profile as the frequency of the oscillation increases. It was found that the actual velocity profile depends upon the value of a non dimensional quantity H_A, given by the expression:-

$$H_A = \frac{D}{2}\left(\frac{\omega \rho}{\mu}\right)^{1/2} \qquad (3.23)$$

318 Foster and Parker (6) found that it was possible to allow for the non plane waveform by applying correction factors to the fluid density and friction coefficient based on this parameter H_A. The change in density is given by:-

$$\rho' = \rho\left(1 + \frac{\sqrt{2}}{H_A}\right) \qquad (3.24)$$

The change in the friction coefficient is brought about by applying a correction to the dynamic viscosity of the fluid, which is given by the expression:-

$$\mu' = \mu\left(.425 + .175\, H_A\right) \qquad (3.25)$$

Equations (3.24) and (3.25) are valid provided that $H_A > 10$.

319 Now the pressure drop per unit length for steady laminar flow in a pipeline is given by Poiseuille's equation:-

$$\frac{dp}{dx} = \frac{128\,\mu Q}{\pi D^4} \qquad (3.26)$$

Alternatively $\frac{dp}{dx} = RQ$ where R is the friction factor $\left(\frac{128\mu}{\pi D^4}\right)$

Substituting for μ from equation (3.25) we get

$$R = \frac{128}{\pi D^4}\mu(\cdot 425 + \cdot 175\, H_n) \qquad (3.27)$$

Hence the friction coefficient increases with frequency.

320 <u>Value of the Bulk Modulus</u>

The bulk modulus β of a hydraulic fluid is dependent upon the pressure and temperature of the fluid. This variation with temperature and pressure is non linear, as illustrated on Fig. 3.3, and this leads to two definitions for the bulk modulus.

i) If the strain is measured as a finite increase in pressure then a secant value of β is used.

ii) If the strain is an infinitesimal increment in pressure then a Tangent value of β is used.

321 In addition when the fluid is compressed some of the work done is turned into heat, and if this compression is rapid the temperature of the fluid will rise. This gives rise to two compression curves for the fluid. One corresponding to an isentropic compression and the other to an isothermal compression. There are, therefore, four different values which can

be used for the Bulk Modulus. The use of any particular one is dependent upon the system conditions.

322 In this particular application the pressure changes created by the propagation of the pump flow ripple are both small and rapid. We will use, therefore, the isentropic tangent bulk modulus B_T. This can be calculated using the method proposed by Hayward (11) as follows:-

The isentropic tangent bulk modulus B_T is given by:-

$$B_T = \frac{B_{sp}\,(B_{sp} + P)}{B_{so}} \qquad (3.28)$$

Where B_s, the isentropic secant bulk modulus is given by:-

$$B_s = \left(1.78 + 7(\rho - .86)\right)\left(10^{(.0024(20-T))}\right)\cdot 10^4 + 5.6\,P \qquad (3.29)$$

$B_{sp} = B_s$ with a system pressure P

$B_{so} = B_s$ with zero system pressure $(P = 0)$

323 A further allowance must also be made for the elasticity of the pipe wall. This results in a reduction in the effective value of the bulk modulus as given by the expression.

$$B_T' = \frac{B_T}{\left(1 + \frac{B_T D}{k E}\right)} \qquad (3.30)$$

MODELLING THE SYSTEM COMPONENTS

324 The Pipeline

The pipeline is represented in the mathematical model for the system by two paramenters, the characteristic impedance Z_o and the propagation constant γ, as defined by equations (3.5) and (3.8). These values, however, do not represent the pipeline as a distinct system element but describe the interaction between the pipeline and the fluid flowing through it.

325 The Termination - Variable Restrictor Valve

If we assume that the restrictor valve provides a purely restrictive termination then its impedance can be determined by the use of the small perturbation technique.

e.g. for an orifice $$Q = f(P) \qquad (3.31)$$

where P is the pressure difference across the orifice.

For small changes in P $$\Delta Q = \frac{\partial Q}{\partial P} \cdot \Delta P$$

Denoting ΔQ and ΔP by q and p respectively then:-

$$q = \frac{\partial Q}{\partial P} \cdot p \qquad (3.32)$$

Now if we have fully developed turbulent flow across the orifice then:-

$$Q = k\sqrt{P} \qquad (3.33)$$

Substituting for equation (3.33) in (3.32) we get:-

$$q = \frac{K P^{-\frac{1}{2}}}{2} \cdot p \qquad (3.34)$$

Substituting for K gives $q = \frac{Q}{2P} \cdot p$

That is the termination impedance Z_T which is given by p/q is equal to:-

$$Z_T = \frac{2P}{Q} \qquad (3.35)$$

326 It is known, however, that the characteristics of a restrictor valve are more closely approximated using a polytropic index, and this is shown experimentally in later sections.

That is $Q = K P^n \qquad (3.36)$

thus $q = \frac{Q}{nP} \cdot p \qquad (3.37)$

Which gives a termination impedance value:-

$$Z_T = \frac{nP}{Q} \qquad (3.38)$$

The polytropic index n can be derived from the pressure and flow characteristics for the valve used.

327 <u>The Pump</u>

A positive displacement pump can be modelled as a flow Q_S and an impedance Z_S, as given by Bowns et al (12)

This can be represented by an equivalent circuit with a flow source and shunt impedance as illustrated on Fig. 3.4. This is equivalent to the Thevenin circuit used in electrical circuit theory. In order to model the pump we must assume that the conditions at the inlet to the pump do not affect the delivery flow.

328 The Pump Impedance

Previous investigators such as Davidson et al (13) assumed that the impedance of a positive displacement pump could be approximated to that of a simple closed volume at low frequencies. That is the pump impedance is given by:-

$$Z_s = Z_v = \frac{\beta}{j\omega V} \qquad (3.39)$$

This implies that the resistive impedance of the pump, which represents the pump leakage, can be ignored.

329 To improve the model, so extending its frequency range, Davidson also suggested the introduction of an inertance term based upon the length of the discharge port l'. This is given by:-

$$Z_I = \frac{j\omega \rho l'}{A} \qquad (3.40)$$

This implies that the pump has a resonant frequency which is given by:-

$$\omega_o = a\sqrt{\frac{A}{l'V}} \qquad (3.41)$$

330 It has, however, been found experimentally; Chapter 5; that this model breaks down at the higher frequencies as the internal geometry of the pump delivery port begins to influence the flow. As the frequency of the ripple increases the dimensions of the discharge port will become significant when compared to the wavelength of the flow ripple. When such conditions arise there is a possibility that standing waves may be generated within the discharge port. Indeed this does occur as will be discussed later in Chapter 5. Furthermore, many pumps have additional internal porting to provide an oil supply to integral control systems or relief valves. In these cases the component impedance can interfere with the pump impedance or again standing waves may be generated in the porting. It is clear, therefore, that the impedance of the pump will have to be determined experimentally.

331 The Pump Flow

The ideal total flow from a multi cylinder pump is created by the addition of the instantaneous flows from the individual pistons. It was shown by Waller (4) that this simple approach produces a flow ripple of minimal amplitude and that its frequency depends as to whether the pump has an odd or even number of pistons. Unfortunately, this analysis neglects the effects of port plate timing which introduces a back flow into the cylinder. This adds a flow component at piston frequency, as shown on Fig. 1.3.

332 The effects of port plate timing have been considered extensively by, among others, Helgestead et al (1) but the basic effects are as follows:-

As a cylinder passes from the suction to the delivery port the pressure in the cylinder is that of the low pressure suction line. If then the delivery port opens at top dead centre (t.d.c.) a transient reverse flow will occur until the pressure in the cylinder rises to that of the delivery line. Should the port opening be delayed then the fluid trapped in the cylinder is compressed by the travel of the piston and its pressure will rise. Thus the ideal time for the port to open is when the pressure in the cylinder equals the delivery line pressure, when no reverse flow would occur. If, however, the opening is delayed further the pressure in the cylinder will rise above that of the delivery line. On opening the cylinder pressure falls to that of the delivery line and this will be accompanied by an initial excess flow from the cylinder. It is evident, therefore, that the ideal timing depends upon the pressure required in the delivery line and upon the angle of the swashplate.

333 If the pressure in the delivery line is increased then a longer delay is required to allow the pressure in the cylinder time to reach the higher level. Similarly, if the pressure in the delivery line was reduced, a shorter delay is needed.

334 A reduction in the angle of the swashplate decreases both the maximum volume of the cylinder, which occurs at t.d.c., and the change in the cylinder volume per unit revolution of the pump. However, the ratio of change in volume to the initial volume at t.d.c. falls as the swashplate angle decreases which implies that a longer delay is required to achieve ideal timing for smaller swashplate angles. This smaller rise in the cylinder pressure due to the reduced change in volume is offset to some degree by

the reduced cylinder volume at the time of the opening of the cylinder to the delivery port. The outcome of this is that the change in the swashplate angle does not have as large an influence upon the back flow valves as a change in the delivery pressure level.

PRACTICAL EVALUATION OF THE CIRCUIT MODEL

335 To evaluate the mathematical model, derived above, for a simple hydraulic system it is necessary to design and construct an experimental test rig. The test rig will also be used to determine values for the various component parameters required by the mathematical model.

336 The major consideration in the design of the test rig was simplicity. By keeping the construction of the hydraulic circuit under test as simple as possible then many of the problems encountered by previous investigators may be avoided.

Experimental Rig

337 A photograph of the test rig, Fig. 3.5 shows the main circuit components; the electric motor, pump, pipeline and variable restrictor valve. A line diagram of the complete circuit is given on Fig. 3.6. The axial piston pump shown, was selected because of its very simple design and because this particular make was known to be particularly noisy. The pump should therefore provide a strong source of flow ripple. The pipeline is connected directly to the pump flange and does not contain any bends, changes in section, or a flowmeter. The latter can be omitted as all the information regarding the standing wave patterns can be derived from the results of pressure alone. A variable restrictor valve was used to terminate the pipeline and so provide a controlled load. Finally, in order to maintain a high level of repeatability for the transient pressure recordings an oil cooling system was incorporated in the return line to allow for control of the oil temperature. Better control of the temperature of the oil will maintain consistant values for the properties of the oil.

Details of the important circuit components are given below:-

Pump

338 The pump used was a Reyrolle A200 variable delivery unit of the axial piston variable swashplate angle design; shown on Figs. 3.5 and 3.7. This has 7 pistons and a maximum displacement of $33cm^3$/rev. The test circuit was arranged as an open loop system with the return line going to the reservoir. Although the pump has a good suction capability, a small positive suction head was provided at the pump inlet by locating the reservoir some 2m above the level of the pump. This provided a static head of .17 bar.

Prime Mover

339 The pump is driven by a 3 phase, 18.5KW electric motor running at a nominal speed of 1470 rev./min. through a flexible coupling. This power level is sufficient to run the pump at full swash with system pressures up to 210 bar. Unfortunately, the electrical supply to the laboratory was limited to 30 amps. A further limitation was imposed as a safety measure, and the current limiter in the control box for the motor was set to operate at 28 amps. Since there is no relief valve in the test circuit, this current limit to the electric motor will avoid the build up of any dangerously high pressure levels due to incorrect operation of the test rig. In addition, this should also prevent the main 30 Amp fuse from blowing should such a mishap occur.

340 Limiting the current to the motor limits the power available to 15.8KW. Thus in order to use system pressures up to 200 bar the pump swashplate

angle was reduced to 93% of its maximum value. This corresponds to a displacement of 31 cm^3/rev, which when operated with a system pressure of 200 bar corresponds to a flowrate of 0.7 l/s, measured in the return line. This gives a maximum power value of 14KW, and an overall value for the efficiency of the pump of 89%.

Pipeline

341 A photograph of the test pipeline is shown on Fig. 3.7. The line consisted of various lengths of rigid steel tubing with a nominal internal diameter of 14.9mm ($\frac{3}{4}$" O/D). All the fittings used to connect the lengths of pipeline together and to the pump and restrictor valve had the same internal diameter as the pipeline. This provided a smooth passage for the flow of oil with no changes in the cross section of the line. The pump was mounted so that the axis of the delivery port was in the horizontal plane. The pipeline connected directly to the pump flange lay along this same axis until its termination at the restrictor valve, with no bends in the circuit as shown by Fig. 3.7 Close attention was paid to the fittings for the pressure transducers and pressure guage to ensure that they did not interfere with the pressure ripple propagation in the test pipeline. Details of these connections have already been discussed in Chapter 2. The relative positions for the two transducers are given in Fig. 3.8.

Load

342 A 19mm ($\frac{3}{4}$") variable restrictor valve was used to provide the load, as this is the simplest form of controllable loading device available. There is no relief valve in this test circuit and so great care is required when operating the system.

Return Line

343 Flexible hose was used for the return line to allow for the movement of the restrictor valve necessary to accommodate the different lengths of test pipeline. The return flow was first passed through a 10μm nominal mesh size filter to prevent the build up of excess contamination in the system. The constant removal and replacement of test pipelines will inevitably lead to a large amount of dirt entering the system. Following the filter, and so protected to a degree from the effects of dirt, a turbine flowmeter is positioned to measure the mean flowrate. Finally, the oil was passed through a cooler before returning to the reservoir. The cooler was of a sufficient size so as to be able to maintain an oil temperature of 40^{o}C with the system operating at its maximum permitted power output.

Evaluation of the Pipeline and Restrictor Valve Impedances

344 Before commencing with the experimental analysis of the pressure standing wave the impedance characteristics of the pipeline and termination were established. The characteristic impedance Z_o and the propagation constant γ were determined using equations 3.8 and 3.5 and details of the steel pipeline as given on Table 3.1.

345 To obtain the impedance of the restrictor valve its pressure and flow characteristics were determined for three settings which are going to be used during the main stages of testing as detailed below. The polytropic index n for the valve at these settings were determined from the results. These were then used to give the impedance values for the valve using equation 3.38, and these are listed on Table 3.2.

Experimental Test Procedure

346 As with the design of the test rig the emphasis of the test procedure was placed on simplicity. The tests must provide results which can be used to determine the values for any unknown parameters required by the impedance model and in addition they must provide the widest possible coverage of the possible pressure ripple standing wave conditions. There are two basic approaches to this problem. One is to use a variable speed drive and the other is to use several different lengths of pipeline.

347 The variable speed test method is not a very practical approach to this problem. Although we can obtain values for the pressure ripple at many different frequencies in a relatively short time the results obtained will only apply to one set of test conditions. This arises because the pump parameter Q_s and Z_s both vary with pump speed and furthermore for each new flowrate the valve impedance Z_T will have to be altered to maintain the required mean pressure level. It would not be possible, therefore, to predict with confidence the values for any component impedance using such a small number of test results.

348 Using different lengths for the test pipeline does not present these difficulties. We can see from equation 3.17 that the line length does not change any of the component impedance values. If, therefore, we use many different lengths of line with a fixed speed pump then we will obtain a large number of results for the pressure ripple standing wave under all possible conditions, from resonance to anti-resonance. Furthermore, with a large number of results we can obtain reliable values for any of the component parameters, as these remain constant for all the test

conditions. This procedure, although time consuming, provides the best method of analysing the pressure standing wave in a hydraulic system.

349 The pump was run at a constant speed of 1470 rev./min. with a fixed swashplate setting as detailed above in Section 340. To begin with, the circuit was arranged as shown on Fig. 3.5 using a short length of pipeline, approximately .1m, to connect the pump and restrictor valve. The valve was adjusted to give a mean system pressure level of 100 bar. The system was then left to allow time for the oil temperature to settle at the desired 40°C. Once steady conditions had been achieved the pressure levels at P_P and P_T were recorded for the first ten harmonics of piston frequency using the F.R.A. described in Chapter 2. Following this the valve was readjusted to give a system pressure of 150 bar and the pressures were recorded once steady conditions had been obtained. Finally, this process was repeated with a system pressure of 200 bar. The oil temperature was maintained at 40°C for all three pressure levels.

350 The pipeline was replaced by one slightly longer, an increase of about 5cm, and the above tests were repeated. This procedure was repeated many more times, ending when the pipeline length reached 4m. This involved the use of 69 different lengths of pipeline.

ANALYSIS OF RESULTS

351 To evaluate the pressure standing wave with regard to the impedance model derived earlier, we need to compare the pressures recorded at P_P and P_T with values predicted for these locations using equation 3.17. Unfortunately, this expression requires values for the pump flow Q_S and the pump impedance Z_S which have yet to be established. Nevertheless, we can proceed by eliminating these parameters from the equation by forming a ratio between pressures for any two points on a pipeline of length .

Elimination of Unknown Parameters Q_S & Z_S

352 If we use the pressures for the transducer locations P_P and P_T using equation 3.17 we can obtain:-

$$\frac{P_T}{P_P} = \frac{e^{-\gamma x_T} + \varsigma_T e^{-\gamma(2\ell - x_T)}}{e^{-\gamma x_P} + \varsigma_T e^{-\gamma(2\ell - x_P)}} \qquad (3.42)$$

This expression requires only the properties of the pipeline γ and Z_o, and the termination impedance Z_T to be able to evaluate the pressure ratio P_T/P_P. Hence, we can use this to examine the accuracy of the predicted pipeline parameters γ and Z_o in conjunction with the experimentally determined values for Z_T.

Comparing the Theoretical and Experimental Values

353 Computer programs, in FORTRAN, were used to determine the values provided by the various mathematical expressions which represent component parameter values and system conditions. In addition, FORTRAN programs were also used to manipulate the experimental results and to present both the experimental and theoretical values in graphical form.

354 In this way, the theoretical values for the pressure ratio P_T/P_p were computed using equation 3.42 with values for the line length ℓ increased by small increments from 0 to 4m and values for the parameters γ, Z_o and Z_T that correspond to the experimental test conditions with a mean system pressure of 200 bar. The results were plotted against line length as shown as a full line on Fig. 3.9. These curves illustrate the change in the conditions of the standing wave, passing from resonance to anti-resonance and back again as the line length is increased. In this case, resonance is defined as the condition when the pressure at all points on the line tend to a maximum. Thus, resonance conditions arise when the pressure ratio is 1. This becomes the case when the line length ℓ is an integer number of half wavelengths, λ.

That is $$\ell = \frac{n\lambda}{2}$$

The peaks shown on Fig. 3.9 correspond to the anti-resonance conditions which occur when the line length is an odd integer number of quarter wavelengths.

That is $$\ell = (2n - 1)\frac{\lambda}{4}$$

355 The experimental results obtained from the readings of P_T and P_p are also plotted as the ratio $|P_T/P_p|$ on Fig. 3.9. It can be seen that these are displaced to the left of the theoretical plot. This out of phase effect is considered to be the result of a discrepancy in the predicted value of the acoustic velocity, a. Although the acoustic velocity, a, does not appear directly in equation 3.42, it influences the position of the standing wave through the propagation constant, γ. We know that γ can be replaced by $\alpha + j\beta$; refer Section 314; where β represents the

phase change as the wave progresses along the line. Now for a lossless line $\beta = s\sqrt{\frac{\rho}{B}}$, furthermore, the acoustic velocity a is given by $\sqrt{\frac{B}{\rho}}$. Thus, in terms of frequency the phase change is given by ω/a.

356 Tilley (8) attributed the error to the value used for the bulk modulus B and used a value reduced by 5% from that determined using Hayward's method to counter the misalignment. He considered that a deviation of this magnitude was quite possible for the following reasons:-

357 Hayward (11) had found that equation, which is sensitive to pressure and temperature as shown in Section 320, gave results accurate to within 2% for pressures common to hydraulic systems. However, later investigators (14) obtained a maximum error of 4.7% using this method. In additon, air entrainment in the oil has the effect of reducing the bulk modulus, due to the increased compressibility of the air. The effect of an increasing level of entrained air on the bulk modulus value is shown on Fig. 3.10, which is taken from (8) and shows how a very small amount of entrained air produces a considerable reduction in the value of the bulk modulus.

358 It was found by trial and error that a 3% reduction in the predicted value for B was sufficient to bring the two curves, shown on Fig. 3.9, into phase. The improved relationship obtained between the pressure ratio values is shown on Fig. 3.11. The corresponding results for the phase relationship are shown on Fig. 3.12 which also shows good agreement between the two curves. Close agreement was also obtained using the results for the remaining test conditions at 150 and 100 bar mean system pressure.

359 The improved curve fit in the present experimental results has been achieved without applying any form of correction factor to the friction coefficient R, as was required by Tilley. This may be due to the elimination of bends and flowmeter from the circuit, although the idea that these elements could affect the friction factor was discounted by Tilley. The improved curve fit for the present experimental results may have been achieved because higher flow velocities were used. This aspect will be referred to again in a later section.

360 Although accurate predictions have been obtained for the pressure ratio P_T/P_P with the mathematical model using a steady state impedance value for the valve Z_T, there is some doubt as to the accuracy of this parameter model. The impedance values as defined by equation 3.38 are purely resistive and it is doubtful whether this can be true for such a device. Thurston (15) showed that a simple square edged orifice in a thin rigid steel plate gave a non-linear and frequency dependent characteristic when acted upon by a sinusoidal flow with or without a superimposed mean flow level. He characterised the pressure and flow relationship for the orifice using resistance and inertance terms to give an impedance value. Furthermore, he found that the values for the individual terms depended upon the geometry of the orifice and the nature of the fluid flow. It is most likely, therefore, that the impedance of a needle valve, which is a much more complex device as illustrated on Fig. 3.13, would consist of resistance, capacitance and inertance terms. In other words, Z_T would be frequency dependent for the valve used.

361 If the impedance of the valve Z_T is complex then it cannot be determined theoretically. It is shown, however, in the next section that it is possible to evaluate a value for Z_T for each of the harmonic frequencies considered during testing.

Prediction of the Termination Impedance

362 We can predict values for the termination impedance Z_T using the experimental results for the pressure ratio P_T/P_P and a rearranged equation 3.42.
Rearranging equation 3.42 we get:-

$$\rho_T = \frac{e^{-\gamma x_T} - P_T/P_P\, e^{-\gamma x_P}}{P_T/P_P\, e^{-\gamma(2l-x_P)} - e^{-\gamma(2l-x_T)}} \qquad (3.45)$$

In addition, if we rearrange equation 3.11 :-

$$Z_T = Z_o \frac{(1+\rho_T)}{(1-\rho_T)} \qquad (3.46)$$

Thus, we can determine values for Z_T by substituting for values of ρ_T, obtained using experimental results of P_P and P_T in equation 3.45, into equation 3.46.

363 In this way, the termination impedance values were computed using the results recorded at P_P and P_T for all 69 lengths of pipeline, for all ten harmonics of piston frequency and for all three system pressure levels. The results contained a large amount of scatter. However, when plotted against the pipeline length, the results for both the amplitude and phase show a variation with line length. This is illustrated on Fig. 3.14 where the amplitude and phase of Z_T are plotted for the first two harmonics of the 100 bar system pressure test. This shows that the greatest variations in these results occur when the pipeline lengths correspond to integer values of half wavelengths for their particular wave frequency. That is, they occur when we use pressure levels recorded when the system was at or close to resonance for the particular harmonic frequency considered.

364 It is extremely difficult, when dealing with any type of system, to measure or predict with accuracy the response of a system that is at or close to a state of resonance. For this reason it was decided that the values derived from results obtained around a resonance condition could be disregarded. Thus all results for which the line length was an integer half wavelength of the harmonic frequency considered, or was within ten per cent of these values were omitted. An arithmetic mean value was then determined using the remaining predictions. The results for the impedance of the valve obtained in this way are shown on Fig. 3.15, which illustrates that both the phase and amplitude of the valve impedance are frequency dependent.

365 Since the pump flow was constant then the different spectra given on Fig. 3.15 show that the valve impedance varies with valve setting as well as with the frequency of the pressure ripple. This is better illustrated using a non-dimensional impedance value, formed by dividing the impedance amplitudes $|Z_T|$ for a given condition by the corresponding steady state impedance Z_{Tss}. Fig. 3.16 shows the variation of these non-dimensional impedances $|Z_T|/Z_{Tss}$ with the harmonic frequency of the pressure ripple plotted logarithmically.

366 Having established the valve impedance spectra we can recompute the plots for the pressure ratio P_T/P_p using the spectra values as given on Fig. 3.15. The curves for the amplitude ratio and phase difference obtained using these values of Z_T are shown on Figs. 3.17 and 3.18, again alongside their respective experimental results. It is noticable that there has been a reduction in the peak amplitude levels. It is possible, therefore, that the erroneous factoring of the friction coefficient R applied in previous

experiments arose as a result of using incorrect, steady state, values for the valve impedance.

367 Having established an accurate model for the pipeline and termination, we can now examine the parameters Z_S and Q_S which define the action of the pump.

Prediction of the Source Impedance

368 We can obtain predictions for the impedance of the pump Z_S by using a similar method to that used to determine the termination impedance Z_T above. We begin by eliminating the unknown source flow term Q_S from the transmission line equation 3.17. This is done by taking the ratio of pressures at the same location along the pipeline x for two different lengths of line l_1 and l_2. This eliminates the source flow Q_S but leaves the reflection coefficient at the pump ς_S which contains the pump impedance Z_S.

369 Taking the ratio of pressures recorded at the pump flange P_{P_1} and P_{P_2} for pipeline lengths l_1, and l_2 using equation 3.17 gives:-

$$\frac{P_{P_1}}{P_{P_2}} = \frac{\left(e^{-\gamma x_P} + \varsigma_T e^{-\gamma(2l_1 - x_P)}\right)\left(1 - \varsigma_T \varsigma_S e^{-2\gamma l_2}\right)}{\left(e^{-\gamma x_P} + \varsigma_T e^{-\gamma(2l_2 - x_P)}\right)\left(1 - \varsigma_T \varsigma_S e^{-2\gamma l_1}\right)} \qquad (3.47)$$

Rearranging this expression gives

$$\varsigma_S = \frac{\frac{P_{P_1}}{P_{P_2}} - \left(\frac{e^{-\gamma x_P} + \varsigma_T e^{-\gamma(2l_1 - x_P)}}{e^{-\gamma x_P} + \varsigma_T e^{-\gamma(2l_2 - x_P)}}\right)}{\varsigma_T \left(e^{-2\gamma l_1}\frac{P_{P_1}}{P_{P_2}} - e^{-2\gamma l_2}\left(\frac{e^{-\gamma x_P} + \varsigma_T e^{-\gamma(2l_1 - x_P)}}{e^{-\gamma x_P} + \varsigma_T e^{-\gamma(2l_2 - x_P)}}\right)\right)} \qquad (3.48)$$

If we now rearrange equation 3.14 we get

$$Z_s = Z_o \frac{(1 + \rho_s)}{(1 - \rho_s)} \qquad (3.49)$$

Thus we can evaluate the pump impedance Z_s using equations 3.48 and 3.49 with pressure levels obtained at P_p for two different lengths of pipeline.

370 The accuracy of any predictions obtained using the above method will depend upon the accuracy of the experimentally determined pressure levels and the relative pipeline lengths for which they were obtained. As with the predictions for the termination impedance Z_T above, pressure values for pipeline lengths corresponding to resonance conditions will be susceptible to errors. In addition, with the method proposed here results obtained for adjacent pipeline lengths, especially those giving low values for the pressure level, will also be sensitive to experimental errors.

371 It would be possible to overcome these problems by careful selection of the pipeline lengths used, and so improve the accuracy of the prediction for Z_s. However, to simplify the process values for Z_s were determined using results for the pressure level recorded at each pipeline length ratioed with the results obtained for several others in turn. This produced over 300 predictions for Z_s at each harmonic of the piston frequency. Although these predictions contained a large amount of scatter, the mean values provided a reasonably accurate value for the pump impedance spectra as shown on Fig. 3.19.

372 The plots for the pump impedance spectra given on Fig. 3.19 show that the pump impedance was purely capacitive. This is indicated by the 90^o phase lag

and amplitude levels which show little variation with mean pressure level. It appears, therefore, that we can apply a simple volumetric model to represent the pump impedance. The impedance of a simple volume is given by equation 3.39. i.e.

$$Z_v = \frac{B}{j\omega V}$$

If we assume that the volume V is that of the pump as 'seen' from the delivery port flange then we can see from Fig. 3.20, which shows a cross section of the delivery port, that this volume comprises of two sections:-

i) the section between the outlet flange and the timing plate.

ii) the volumes in those cylinders open to the outlet port at any given instant in time.

Thus the total volume varies as the pump rotates, and in addition this variation can be separated into two phases which depend on whether there are 3 or 4 cylinders open to the delivery port. This is illustrated on Fig. 3.21 which demonstrates the variation in the pump volume, as described here, with the position of the cylinder barrel. The numerical values quoted on Fig. 321 were derived from the detailed dimensions of the pump supplied by the manufacturer.

373 Two theoretical impedance spectra were calculated using mean values for the pump volume V taken from each of the two phases of the pump flow, as shown on Fig. 3.21, with a bulk modulus value corresponding to a system pressure of 200 bar. The spectra derived in this way are compared with the amplitude spectra predicted for Z_s from the experimental results for the 200 bar system pressure tests, on Fig. 3.22. The figure shows very good agreement for all except the first harmonic.

374 By achieving such a good result we have shown that the simple volumetric impedance model can be applied successfully to axial piston pumps of simple design over a wide frequency range. This is in contrast to the argument outlined earlier in Section 330, in which we dismissed this model on the grounds of its limited frequency range. However, we are dealing here with a pump that has a delivery port of the very simplest design. As mentioned earlier many, if not the majority, of axial piston pumps have ports which are much more complex in design many include integral valving or servo systems to control the swashplate angle or to adjust the port plate timing. Some of the larger units may also possess integral boost pumps. Each of these additional design elements can greatly influence the impedance of a pump as seen at the pump flange. The basic design of the pump considered here ensures that none of these additional effects need be considered. Furthermore, the delivery line is sufficiently short so as to ensure that the first resonant frequency, as proposed by Davidson (13), lies well outside the frequency range considered here.

That is $$\omega_o = a\sqrt{\frac{A}{\ell' V}} = 16{\cdot}8 \ KH\eta.$$

375 This result is very encouraging as it implies that we can model any axial piston pump as a self contained hydraulic system, consisting of a pumping element and associated pipe and valve network. Thus, it should be possible to determine values for the impedance and flow of the pump as lumped parameters at the pump outlet flange, using a volumetric model for the pumping element and transmission line equations to define the pipe network. However, this

does assume that it is possible to apply transmission line theory to pipe networks, which is the subject of later chapters.

376 Before going on to consider the pump flow Q_S we can evaluate the predictions for the pump impedance spectra Z_S using the results of the pressure standing wave.

Evaluation of the Pump Impedance Z_S Using Pressure Standing Wave Values

377 A measure of the accuracy of the predicted pump impedance spectra Z_S can be obtained by comparing theoretical and experimental values for a pressure ratio P_{x_2}/P_{x_1} formed using pressures at the same point x along the pipeline obtained for different pipeline lengths. To assess the results for the complete range of pipeline lengths it is preferable to obtain ratios for pressures obtained at each pipeline length P to a fixed pressure value obtained at a selected line length x, i.e. P/P_x. The most convenient value to use as this reference level is the pressure which provides the minimum pressure amplitude $|P_{min}|$. which occurs at a line length l_{min} . This value may be determined easily from the experimental results, which are well defined around their minima, and likewise simple computation will produce a corresponding reference for the theoretical values.

378 If we use the pressures at P_p and substitute these into equation 3.47 we obtain:-

$$\frac{P_p}{P_{pmin}} = \frac{\left(e^{-\gamma x_p} + \varsigma_T e^{-\gamma(2l-x_p)}\right)\left(1 - \varsigma_s \varsigma_T e^{-2\gamma l_{min}}\right)}{\left(e^{-\gamma x_p} + \varsigma_T e^{-\gamma(2l_{min}-x_p)}\right)\left(1 - \varsigma_s \varsigma_T e^{-2\gamma l}\right)} \qquad (3.50)$$

The pump impedance Z_s does not appear directly in this expression but its influence is included via the reflection coefficient ζ_s.

379 Values for P_p/P_{pmin} were computed using equation 3.50 and values for the line length ℓ increased by small increments from 0 to 4m. The results for the pressure amplitude ratio, which correspond to the test condition with 200 bar mean system pressure, were plotted against line length as shown on Fig. 3.23. The peaks and troughs of this plot illustrate the variation in the pressure level at the pump flange that arises as a result of changes in the line length, ℓ. The actual values of the maximum and minimum pressures cannot be derived until we have obtained values for the pump flow Q_s. Experimental values for the pressure amplitude ratio $|P_p/P_{pmin}|$ derived from the pressures recorded at P_p are also plotted on Fig. 3.23. The good agreement between the theoretical and experimental values shown on this figure suggest that we have obtained an accurate value for the pump impedance Z_s. This implication is supported by the corresponding results for the phase relationship as illustrated on Fig. 3.24.

380 Values predicted for P_p/P_{pmin} for the remaining test conditions with 150 and 100 bar mean system pressure also gave good agreement when plotted alongside the experimental results. Having established the impedance spectra for the pump at each test condition we can now turn our attention to the last unknown parameter, the pump flow Q_s.

Prediction of the Pump Flow

381 The pump flow Q_s is the one unknown parameter required by the impedance model for the pressure ripple

standing wave given by equation 3.17. Thus, we can predict values for Q_s using the results for the pressure standing wave levels and equation 3.17. Using the pressures recorded at P_p then values for Q_s are given by the rearranged equation 3.17.
That is

$$Q_s = P_p \frac{(Z_s + Z_o)}{(Z_s Z_o)} \frac{(1 - \varsigma_s \varsigma_T e^{-2\gamma l})}{(e^{-\gamma x_p} + \varsigma_T e^{-\gamma(2l - x_p)})} \qquad (3.51)$$

382 Values for the pump flow Q_s were computed using the pressures recorded at P_p for all pipeline lengths. Unlike the results for the pump and termination impedances these values contain little scatter. Thus, the flow spectra were derived by evaluating the arithmetic mean values for each harmonic for each of the three test conditions. The flow spectra obtained are illustrated on Fig. 3.25. The phases shown are referred to the synchronising fundamental frequency of the F.R.A., refer to sections 225, 226. The figure shows the change in the pump flow with mean system pressure. However, a better appreciation of the flow mechanism can be obtained by considering the flow on a time rather than frequency basis.

383 The synthesised pump flows as a function of time obtained by combining the harmonics of the pump flow spectra and the mean flow levels are illustrated on Fig. 3.26. The back flows into the cylinders, which are a result of the non ideal port plate timing, refer sections 331 to 334, are well defined by these flow profiles. Likewise, the increase in the magnitude of the back flow as a result of increased system pressure levels can also be seen. This indicates the need for longer delay times for the opening of the delivery port at the higher system pressure levels.

384 The beneficial effects that can be gained by improving the port plate timing are self evident

from the figures obtained above. The high levels of back flow give rise to the high amplitude levels and increased harmonic content of the pump flow spectra. These produce the high levels of pressure ripple since the magnitude of the pressure ripple standing wave is related directly to the value of the pump flow Q_s, as given by equation 3.17. Thus, a reduction in the amplitudes for Q_s, which can be achieved by improving the port plate timing, would lower the pressure standing wave levels and so create a quieter pump and system.

Prediction of Pressure Levels at any Point in the System

385 Now that we have established values for all the system parameters we can predict the pressure levels at any point along the pipeline using equation 3.17. Thus values for P_p and P_T were computed for pipeline lengths ℓ increased in small increments from 0 to 4m for each of the three system conditions. The resulting amplitude and phase values are plotted against line length along with their corresponding experimental results for a test at a mean system pressure level of 200 bar on Figs. 3.27 and 3.30. The peaks and troughs are shown clearly and the mathematical model gives good agreement with the experimental results. Similar results were obtained for the tests at 150 and 100 bar.

DISCUSSION OF RESULTS

386 The results have shown that the theory of transmission lines provides a precise mathematical model for the pressure ripple standing waves generated in a simple hydraulic circuit operating under typical pressure and flow conditions. This was achieved without the need of any extraneous factors. It is evident, however, that the accuracy of the model follows closely the accuracy of the individual component impedance values. Unfortunately, as the results of the investigation have shown, these component impedances cannot be derived either from their design or their steady state characteristics. This is clearly demonstrated by the model for one of the simplest components, the restrictor valve. The impedance of a restrictor valve varies with frequency and setting as illustrated on Fig. 3.16. Clearly a family of impedance spectra would be needed to cover the complete operating range for any valve.

387 Surprisingly, the results for the pump show that a simple volumetric model can be used to represent its impedance spectrum. It may also prove possible to derive the pump flow profiles at any pressure and any swashplate angle by close examination of the pumping mechanism. This approach is being investigated by Kelsey (16). The simple design of this particular axial piston lends itself to easy modelling. However, it is clear that we will not be able to model more complex pumps using such simple formats. Nevertheless, the success of the volumetric model for the impedance of this simple pump implies that the more complex pumps may be modelled as simple hydraulic circuits. For the moment, however, experimentation remains the only reliable method of obtaining impedance and flow spectra.

CHAPTER 4

Effect of Swashplate Angle on the Pump Parameters

INTRODUCTION

401 Upuntil now we have only considered the pump as a fixed displacement unit. However, pumps of the axial piston design may have the facility to alter their flow levels by adjusting the angle of their swashplate. Thus,in order to complete the impedance and flow models for the pump tested in the previous chapter,we need to ascertain the effects that the swashplate angle may have on these parameters.

402 To obtain values for Q_s and Z_s we could repeat the extending pipeline test detailed above with several settings of the pump swashplate angle. Now although such tests would provide accurate results they are also very time consuming. It was decided therefore to try a combination of two shorter test methods outlined in (17) and referred to as the High Impedance Pipe (H.I.P.) and Additional Capacitance (A.C.) tests.

THEORETICAL BASIS FOR THE TWO TEST METHODS

High Impedance Pipeline

403 The basis of this test method is to provide conditions at the pump outlet so that a single measurement of the pressure level at this point can be related directly to the pump parameters, so eliminating the effects due to the rest of the system. To achieve this the pump flow is discharged directly into a pipeline with a small internal diameter. The pipe size is chosen to give an entry impedance very much greater than the impedance of the pump.

404 If we consider a simple circuit as illustrated on Fig. 4.1 then the pressure and flow at any point along the line are given by equations 3.17 and 3.18. Now if we let the pressure and flow at the pump flange, where $x = 0$, be P_o and Q_o then the impedance at the entrance to the pipeline is given by:-

$$Z_E = \frac{P_o}{Q_o} \qquad (4.1)$$

Substituting for P_o and Q_o using equations 3.17 and 3.18 with $x = 0$ we obtain:-

$$Z_E = Z_o \frac{(1 + \varsigma_T e^{-2\gamma\ell})}{(1 - \varsigma_T e^{-2\gamma\ell})} \qquad (4.2)$$

405 The pressure at the pump P_o is given by equation 3.17 which we can expand by substituting for ς_S using equation 3.14. Thus:-

$$P_o = \frac{Q_s Z_s Z_o}{Z_s + Z_o} \cdot \frac{\left(1 + \rho_T e^{-2\gamma l}\right)}{\left(1 - \frac{(Z_s - Z_o)}{(Z_s + Z_o)} \rho_T e^{-2\gamma l}\right)} \qquad (4.3)$$

which when rearranged becomes

$$P_o = Q_s Z_s \cdot \frac{1}{\left(1 + \frac{Z_s}{Z_o} \frac{\left(1 + \rho_T e^{-2\gamma l}\right)}{\left(1 - \rho_T e^{-2\gamma l}\right)}\right)} \qquad (4.4)$$

Now substituting for equation 4.2 the expression simplifies to

$$P_o = \frac{Q_s Z_s}{1 + Z_s / Z_E} \qquad (4.5)$$

If, therefore, the entry impedance Z_E is much greater than the pump impedance Z_s then the pressure at the pump flange becomes simply

$$P_o = Q_s Z_s \qquad (4.6)$$

the product of the two parameters.

406 We can see from equation 4.2 that a high entry impedance can be obtained by increasing the characteristic impedance for the pipeline Z_o. If we assume that the line is lossless then equation 3.8 becomes:-

$$Z_o = \sqrt{\frac{\rho B}{A^2}} = \frac{4\sqrt{\rho B}}{\pi \cdot d^2} \qquad (4.7)$$

Hence the entry impedance can be increased by reducing the diameter of the pipeline, d. However, if this method is to be successful we require very high values for the entry impedance, i.e. $Z_E \gg Z_s$. Unfortunately,

many pumps, such as the axial piston pump considered here, have high impedance levels and in such cases it becomes impractical to arrange for Z_E to be very much greater than Z_S.

Additional Capacitance

407 This method is an extension of the high impedance pipeline test so that it can be used for pumps which have a high impedance value. To allow for this the impedance of the pump is lowered artificially by the addition of a known volumetric impedance. This extra capacitance can be added to the pump in the form of a short expansion chamber of large diameter as illustrated on Fig. 4.2.

408 If the diameter of the expansion chamber is sufficiently large then we know that the characteristic impedance for the chamber Z_{oc} will be very much less than the entry impedance to the high impedance pipe, Z_E.

That is $Z_{oc} \ll Z_E$

Thus the reflection coefficient at the entry to the H.I.P., given by equation 3.11, will tend to 1.0. Now if we measure the pressure P_c at the entry to the pipeline where $x = l_c$ then from equation 3.17

$$P_c = \frac{Q_s Z_s Z_{oc}}{Z_s + Z_{oc}} \cdot \frac{2 e^{-\gamma_c l_c}}{\left(1 - \rho_s e^{-2\gamma_c l_c}\right)} \qquad (4.8)$$

If we substitute for ρ_s using equation 3.14 and rationalise we can obtain the expression:-

$$P_c = \frac{Q_s Z_s Z_{oc}}{Z_s\left(\frac{e^{\gamma_c l_c} - e^{-\gamma_c l_c}}{2}\right) + Z_{oc}\left(\frac{e^{\gamma_c l_c} + e^{-\gamma_c l_c}}{2}\right)} \qquad (4.9)$$

alternatively

$$P_c = \frac{Q_s Z_s Z_{oc}}{Z_s \sinh \gamma_c l_c + Z_{oc} \cosh \gamma_c l_c} \qquad (4.10)$$

409 With its short length and large diameter we can reasonably assume that the chamber acts as a lossless line, i.e. $\gamma_c = j\omega/a$

substituting for γ_c in equation (4.10)

$$P_c = \frac{Q_s Z_s Z_{oc}}{Z_s \, Sinh\, j\frac{\omega l_c}{a} + Z_{oc} \, Cosh\, j\frac{\omega l_c}{a}}$$

Now if $\frac{\omega l_c}{a}$ is small then $Sinh\, j\frac{\omega l_c}{a}$ tends towards $j\frac{\omega l_c}{a}$

and $Cosh\, j\frac{\omega l_c}{a}$ tends towards 1.

Thus
$$P_c = \frac{Q_s Z_s Z_{oc}}{Z_s j\frac{\omega l_c}{a} + Z_{oc}} \qquad (4.11)$$

Rearranging gives:-

$$P_c = \frac{Q_s Z_s \cdot \frac{Z_{oc}}{j\frac{\omega l_c}{a}}}{Z_s + \frac{Z_{oc}}{j\frac{\omega l_c}{a}}} \qquad (4.12)$$

If the chamber is lossless then from equation 4.7,

$$Z_{oc} = \frac{\sqrt{\rho B}}{A_c}$$

Thus
$$X = \frac{Z_{oc}}{j\frac{\omega l_c}{a}} = \frac{\sqrt{\rho B}}{A_c} \cdot \frac{a}{j\omega l_c}$$

Now $A_c l_c = V_c$ the volume of the chamber and the acoustic velocity $a = \sqrt{\frac{B}{\rho}}$ so

$$X = \frac{B}{j\omega V_c} = Z_V$$ the impedance of a volume

So equation (4.12) can be written as

$$P_c = \frac{Q_s Z_s Z_v}{Z_s + Z_v} \qquad (4.13)$$

We may note that the expression $\frac{Z_s Z_v}{Z_s + Z_v}$ represents the combined impedances of the pump and chamber added in parallel.

That is $\frac{1}{Z'} = \frac{1}{Z_s} + \frac{1}{Z_v} = \frac{Z_v + Z_s}{Z_s Z_v}$

410 Unfortunately, we are again left with an expression which alone cannot give the values for the pump flow or impedance. If, however, we apply both of the above test methods or use two additional capacitances of different sizes then we will have two equations which we can solve to obtain the two unknown parameters.

Separation of Pump Parameters

411 If we combine equations 4.5 and 4.13 in terms of $Q_S Z_S$ we get:-

$$\frac{P_o (Z_E + Z_S)}{Z_E} = \frac{P_c (Z_V + Z_S)}{Z_S Z_V} \qquad (4.14)$$

Rearranging $$Z_S = \frac{Z_E Z_V (P_c - P_o)}{P_o Z_V - P_c Z_E} \qquad (4.15)$$

Having established Z_S it is a simple matter of substituting this value into either of equations 4.5 and 4.13 to obtain values for Q_S. In this way we have a much simpler experimental procedure which will provide values for Q_S and Z_S using results of pressure measurements from two simple tests.

412 Both test methods require some knowledge of the circuit impedances. The entry impedance Z_E can be obtained using equation 4.2 provided that the valve impedance Z_T is known, and the impedance of the chamber Z_V can be derived from the dimensions of the chamber using equation 3.39. The need to know the impedance of the restrictor value Z_T is a limitation on the application of the H.I.P. test. The additional capacitance test on the other hand eliminates the details of the pipeline and valve from the evaluation. It would be preferable, therefore, if the additional capacitance test alone could be used.

413 If we let the pressures recorded for two volumes V_1 and V_2 be P_{c1} and P_{c2} then combining the resulting expressions in terms of the product $Q_S Z_S$ we get

$$\frac{P_{c1} (Z_{V1} + Z_S)}{Z_S Z_{V1}} = \frac{P_{c2} (Z_{V2} + Z_S)}{Z_S Z_{V2}} \qquad (4.16)$$

Rearranging:-

$$Z_s = \frac{Z_{v1} Z_{v2} \left(P_{c2} - P_{c1}\right)}{P_{c1} Z_{v2} - P_{c2} Z_{v1}} \qquad (4.17)$$

If we substitute for the volumetric impedances Z_{v1} and Z_{v2} using expressions given by equation 3.39 we get

$$Z_s = \frac{B}{j\omega} = \frac{V_1 V_2 \left(P_{c2} - P_{c1}\right)}{P_{c1} V_2 - P_{c2} V_1} \qquad (4.18)$$

PRACTICAL EVALUATION OF TEST METHODS

Experimental Test Rig

414 To provide an experimental appraisal of the effect of varying the angle of the pump swashplate the additional capacitance test described above was carried out. To achieve this the test pipeline used for the extending line tests described in the previous chapter was replaced by the additional capacitance and high impedance pipeline as illustrated on Fig. 4.2. The remainder of the test circuit remain as for the extending pipeline test circuit as shown on Fig. 3.6.

Experimental Procedure

415 Using the test circuit described above with an additional capacitance of 319 cc. the pump swashplate was set to give the same flowrate as for the extending pipeline tests. That is .7 l/s, measured in the return line, for a system pressure of 200 bar. The restrictor value was adjusted to give a mean pressure of 200 bar in the chamber and the pressure in the chamber P_{c1} was recorded for each of the ten harmonics of piston frequency. Following this the pump swashplate was readjusted to give a flowrate of .525 l/s (75 °/o of the initial flow value) again for a system pressure of 200 bar. The chamber pressure P_{c1} was recorded once the conditions were established. This process was repeated with swashplate settings corresponding to flowrates of .35 and .175 l/s with a system pressure of 200 bar. (50 °/o and 25 °/o respectively of the initial flow value).

416 The additional capacitance was replaced by one of 520 cc. and the test procedure detailed above was repeated. From this we obtain the second set of chamber pressures, P_{c2}. Thus we now have two sets of pressures, P_{c1} and P_{c2}, from which we can derive the pump parameters Q_s and Z_s using the procedure outlined above in Section 413.

Evaluation of the Test Method

417 We can use the results obtained for the initial swashplate setting to evaluate the test method. To do this the pump parameters Q_s and Z_s determined using the results from the additional capacitance tests, as described above, are compared with the values obtained at the same test conditions using the extending pipe-line tests carried out earlier. The two sets of results for the pump impedance Z_s are compared on Fig. 4.3 and those for the pump flow Q_s on Fig. 4.4.

418 The values for the pump impedance Z_s show good agreement for all bar the first two harmonics of the amplitude spectrum. The phases give reasonable agreement for all the harmonics. Similarly, the values for the pump flow Q_s show some disagreement in their amplitudes but give good agreement between their phases. These discrepancies on the flow amplitudes are evident in the plots for the synthesised pump flows as shown on Fig. 4.5. However, the changes are relatively small and the flow profile still shows the salient features of the mechanics of flow delivery.

419 From these results we can conclude that although the simplified test method provides values that are not as exact as those defined earlier, they are accurate enough to allow for comparisons to be made between different pumps or different test conditions. We can proceed, therefore, to examine the effects of swashplate angle upon the pump parameter values Z_s and Q_s.

ANALYSIS OF RESULTS

Effect of Swashplate Angle on the Pump Impedance

420 The pump impedance values determined from the additional capacitance tests at each of the four swashplate settings are shown in Fig. 4.6. The amplitude spectra, excluding for the moment the results for the first two harmonics, suggest that the swashplate angle has little or no effect on the impedance of the pump. This results was expected as we know that the volume of the pump V is not affected by the position of the swashplate. Thus, if the capacitance model, as given by equation 3.39, is correct then there will be no change in the pump impedance. This result is supported by the phase spectra as shown on Fig. 4.6. The large variation in the phases for the seventh harmonic are most likely due to a resonance condition occurring at this frequency in one of the two test circuits. This resonance also affects the pump flow values as illustrated on Fig. 4.7.

421 The variation in the impedance amplitudes at the first two harmonics are a result of inadequacies in the test method. It is clear that one or more of the assumptions made when establishing the theory in support of the test procedure, outlined above in Sections 403 to 414, do not hold true at these lower frequency levels. However, the test method provides a reasonable basis on which to establish a more accurate test procedure. Further work to determine the nature of these limitations at the lower frequency levels and to establish a more acceptable test procedure is in progress at the University of Bath.

Effect of Swashplate Angle on the Pump Flow

422 The pump flow values determined from the results for the additional capacitance tests at each of the four swashplate settings are shown on Fig. 4.7. This figure shows that there was a steady reduction in the amplitudes of Qs as the swashplate angle was decreased and this was accompanied by a slight shift in the phase. The synthesised pump flows, shown on Fig. 4.8 as a function of time, show that the change in swashplate angle has had little effect on the back flows into the cylinders.

423 The high levels of oscillation superimposed upon the flow profiles for the 3/4 and 1/4 swash conditions makes any comparisons between the different profiles difficult. These oscillations occur as a result of the errors in the phases for the seventh harmonic of the pump flow at these swashplate settings. Recomputing the synthesised flows using a phase value of -64^{o} for the seventh harmonic of both the 3/4 and 1/4 swash values produced a more realistic set of flow profiles as illustrated on Fig. 4.9. This modification has not affected the back flows which still show little variation with swashplate angle.

DISCUSSION OF RESULTS

424 The results obtained for the different swashplate settings are in line with the description of the performance of the pump given in Section 334. Since the pump impedance is predominately capacitive and the overall volume of the pump V does not change with the position of the swashplate then the pump impedance Z_s will not be effected by changes in the swashplate angle. The results for the pump flow Q_s are deceptive in that the minimal change in back flows that occur as the swashplate angle is reduced implies that there would be a similarly large back flow with zero swashplate angle. This appears to be a contradiction; if however we examine the variation in cylinder volume due to changes in swashplate angle we can show this to be correct.

425 Table 4.1 gives values for the volume of a cylinder V_c as it opens to the delivery line for each of the swashplate settings. If we neglect the effects of the system then the pressure rise in the cylinder due to compression of the oil is given by:-

$$\Delta P = \frac{\Delta V_c}{V_c} \beta$$

Using this expression, we find that for a cylinder opening at t.d.c. the reduction in volume required to give a pressure of 200 bar, ΔV_{c2}, decreases as the swashplate angle is reduced, as shown on Table 4.1. This volume must be made up by the flow into the cylinder as it opens to the delivery line, and so the values of V_{c2} must relate to the back flow levels. With the cylinder opening at t.d.c. we see that there is a 15 $^{o}/o$ reduction in the required compression ΔV_{c2} as the swashplate angle is decreased

to 1/4 full swash. If, however, the opening is delayed then there is a reduction in the cylinder volume, ΔV_{c1}, due to the angle of the swashplate which produces an initial rise in the cylinder pressure ΔP_c. Hence the change in volume needed to produce a pressure of 200 bar reduces. Table 4.1 shows that for a delay of 2^{o} after t.d.c. the change in volume ΔV_{c2} between full swash and 1/4 swash settings as fallen to 13 $^{o}/o$. However, for a delay of 4^{o} after t.d.c. there is little difference in the volume changes required for any swashplate angle.

426 We know from the high back flow values that the cylinder must open to the delivery line at or soon after the t.d.c. position. The geometrical tolerances for the port plate design give a nominal delay value of approximately 2^{o} of rotation after t.d.c. At this position there is an appreciable variation in the cylinder volumes for the different swashplate settings, as given by Table 4.1. However, if we consider the rotational speed of the pump 8.82 degree/mSec. we can see that these conditions change rapidly, the equal volume condition, approximately 4^{o} after t.d.c., is reached in under .3mSec. Thus given such conditions we would expect to find back flows of a similar value no matter what swashplate angle is used, even zero swashplate angle. In practice, however, we are unlikely to find many applications which have significant mean system pressure levels together with a pump swashplate set at zero since the mean flow from the pump is needed to provide the pressure level.

427 The combined additional capacitance and H.I.P. tests proved to be sufficiently accurate for the purpose of comparing the different pump conditions. Unfortunately, they are clearly not suitable for use

in defining component parameter values for use in system models. Further work is required before these techniques could be used to provide reliable results.

CHAPTER 5

Flow Ripple Measurement Applied to a Bent Axis Pump System

INTRODUCTION

501 A further system was available which contained a bent axis pump with a test circuit consisting of a pipeline and restrictor valve. In addition to the pressure transducers, a flowmeter capable of measuring transient flows at pressure ripple frequencies was included. Refer Section 211. This system provided the opportunity for further examination of the transmission line model, including flow as well as the pressure ripple. In addition, such results would provide additional information with regard to the component parameters.

502 This test arrangement was convenient rather than purpose built and as such has several limitations. The electric motor used as the prime mover was limited in power for the size of pump used, furthermore the control of the oil temperature was inadequate. These factors limited the pressure levels and flowrates that could be used. In addition, the space around the test rig was limited, restricting the overall length of the test pipeline to 3.5 meters. This, together with the fact that the Frequency Response Analyser was only available for limited periods at this time, restricted the number of test results that could be obtained. Nevertheless, the results provide an evaluation of the transmission line model and component parameters.

MEASUREMENT OF PRESSURE AND FLOW RIPPLE

Experimental Rig

503 A general arrangement of the test circuit is shown as a line diagram on Fig. 5.1.

Pump

504 The pump was a Dowmatic (Type 2) variable delivery unit of the axial piston tilting head design. This has 10 pistons and a maximum displacement of 203 cm^3/rev. The pump is designed for use in closed loop transmission systems, thus the test circuit was arranged as a closed loop system as illustrated on Fig. 5.1. The make up flow, provided by a small gear pump integrally mounted in the Dowmatic unit, is fed into the low pressure return line as shown on Fig. 5.2. This make up flow must be large enough to maintain a pressure of between 7 and 18 bar in the return line. A significant pressure head is required in the suction line to ensure that the piston slipper pads remain in contact with the swashplate under all conditions of operation. Finally, there is a connection from the high pressure line to the servo actuator mounted on the pump casing to provide control of the tilting head position.

Prime Mover

503 A 3 phase, 30 KW, electric motor running at a nominal speed of 1470 rev./min. was used to drive the pump through a flexible coupling. This available power level falls short of the maximum continuous power rating of the pump, 56 KW. So that we could use high pressure levels, 200 bar, the pump swashplate was set to give a flowrate of 1.57 l/s, which is equivalent to one third of its maximum displacement setting. However, it was discovered during the first few test runs that the oil cooler could not cope with this power level. As we are already using a low value of pump displacement it was

decided that the pressure level should be reduced to 104 bar (1500 p.s.i.) thus halving the power level. Adequate cooling was then available.

Pipeline

506 The test pipeline consisted of various lengths of rigid steel tubing with a nominal internal diameter of 25.4 mm (1"). The transient flowmeter contained a 90 degree bend and so this was positioned close to the pump, mounted vertically. This ensured that the pileline downstream of the flowmeter could be easily changed and also that the axis of this line was along the horizontal plane, as illustrated on Fig. 5.3. Changes in the overall length of the pipeline were obtained by using different sections of pipeline between the flowmeter and termination.

Termination

507 To load the system a 25.4 mm (1") variable restrictor valve was used.

Return Line

508 Flexible hose was used for the return line to allow for movement of the restrictor valve to accommodate the different lengths of test pipeline. The return flow was passed through a nominal 10 μm mesh size filter, turbine flowmeter and oil cooler before returning to the pump to complete the closed loop circuit.

Experimental Procedure

509 The test method is essentially the same as that used for the tests with the Reyrolle pump

described in Sections 345 and 346. The restrictor valve was adjusted to give a mean system pressure level of 104 bar. Once steady oil temperatures had been achieved the pressures at the pump and termination and the pressure and flow from the transient flowmeter were recorded for the first ten harmonics of piston frequency. This process was repeated several more times with different lengths of pipeline. This resulted in the overall length of the pipeline increased from 1 to 3 m using a total of 20 different pipe lengths.

ANALYSIS OF THE RESULTS

510 To analyse the test results we begin as before by eliminating the as yet unknown pump parameters Q_s and Z_s from the transmission line equation, as described in Sections 351 and 352. This is done by forming the pressure ratio P_T/P_P using the results obtained at each test condition. That is at each new pipeline length. In addition, this ratio P_T/P_P was computed using equation 3.42 with a termination impedance Z_T taken as the experimentally determined steady state value, Z_{Tss}.

511 Comparing the theoretical and experimental values of the pressure amplitude ratio on a basis of their variation with pipeline length we again found them to be out of phase. We know that these two sets of results can be brought into phase by reducing the value of the bulk modulus of the oil, B. It was decided, therefore, to use a bulk modulus value reduced by 3 $^{o}/_{o}$ in line with the results used for the previous tests. The theoretical values for the pressure amplitude ratios were recomputed, using this revised bulk modulus value, which when compared with the experimental ratios now gave good agreement as shown on Fig. 5.4.

512 We can see from Fig. 5.4 that the peaks formed by the experimental results exhibit a greater degree of attenuation than those predicted by the theoretical model. Similar results were obtained by Tilley (8) using a similar test arrangement. However, Tilley found that this error could be reduced if the value of the pipe friction factor R was increased to 2.5 times its original value. However, the use of such a large correction factor cannot be rationally explained. The prediction of both steady state and frequency dependant friction factors has received a considerable

amount of attention; see Sections 317 to 319. Furthermore, we have already obtained good agreement for the previous test results using the standard friction factor values. The results obtained for the pressure amplitude ratios derived using the frequency dependant impedance for the valve suggest that the error in peak amplitudes may be reduced if the frequency dependant rather than the steady state value was used. It was, therefore, decided to leave the friction factor at its theoretical value and proceed with the analysis starting with the impedance of the valve.

Prediction of the Termination Impedance

513 Using the method detailed above in Section 362 values for the valve impedance Z_T were predicted from the experimental results, for each harmonic of piston frequency. The results contained a large amount of scatter but showed no variation with pipeline length. Thus a weighted mean value was taken to give the impedance at each harmonic. The impedance spectra obtained is shown on Fig. 5.5.

514 It is clear from Fig. 5.5 that the impedance of this valve is also frequency dependant. In fact, this larger valve has a greater variation in both amplitude and phase with frequency than the smaller valve used earlier. This is illustrated using the plot of the non dimensional value Z_T/Z_{Tss} against frequency using the results for both valves obtained with a mean system pressure of around 100 bar, shown on Fig. 5.6. It is probable that the increased variation in the results for the larger valve at the higher harmonics is a result of the larger physical dimensions of the valve, which would allow resonances or standing wave effects to created within the valve body.

515 We can now recompute the values for the pressure ratio P_T/P_P using the valve impedance spectrum values given on Fig. 5.5. The revised plots for the amplitude ratio are shown on Fig. 5.7 along with the corresponding experimental results. These curves show that the change in the valve impedance has brought about the attenuation in the peak amplitudes of the theoretical curve which was needed to provide good agreement with the experimental values. It is clear, therefore, that the assumed friction factor is correct and the errors encountered by earlier investigators in their predictions of P_T/P_P were due to the use of a steady state value for the valve impedance Z_T. Good agreement was

also obtained using the phase values as shown on Fig. 5.8.

516 The pressure ratio P_T/P_ρ is a useful parameter for assessing the mathematical model for a pipeline and termination. However, we have in these experiments the additional values of pressure and flow at the same location along the pipeline, namely P_f and Q_f. The ratio of the pressure and flow at the same position gives the impedance at that position. That is:-

$$\frac{P_f}{Q_f} = Z_o \frac{\left(e^{-\gamma x_f} + \rho_T e^{-\gamma(2l-x_f)}\right)}{\left(e^{-\gamma x_f} - \rho_T e^{-\gamma(2l-x_f)}\right)} \qquad (5.1)$$

$= Z_f$ the impedance at the flowmeter.

If we let $l = x_f + d$, where d is the distance from the flowmeter to the restrictor valve, then we can rewrite equation (5.1) as:-

$$Z_f = Z_o \frac{\left(e^{\gamma d} + \rho_T e^{-\gamma d}\right)}{\left(e^{\gamma d} - \rho_T e^{-\gamma d}\right)} \qquad (5.2)$$

rearranging gives:-

$$Z_f = Z_o \frac{\left(1 + \rho_T e^{-2\gamma d}\right)}{\left(1 - \rho_T e^{-2\gamma d}\right)} \qquad (5.3)$$

which is the equation for the entry impedance of a line length d terminated by an impedance Z_T.

517 Values for the amplitude and phase of Z_f were computed using equation 5.1. The results plotted against line length l are shown on Figs. 5.9 and 5.10.

These curves demonstrate the large variation in amplitude and phase values for the entry impedance to a pipeline that can be brought about by changes to the length of the line, ℓ. This variation in entry impedance can be used to good effect when designing systems with low pressure ripple levels, as will be revealed in latter chapters. Values for Z_f determined using the results obtained for P_f and Q_f are also plotted on Figs. 5.9 and 5.10 which show good agreement between the theoretical and experimental impedance values.

Prediction of the Pump Impedance

518 We can predict the pump impedance Z_s from the results for the pressure close to the pump P_p using the method outlined in Sections 368 to 371. The impedance spectrum obtained in this way is shown on Fig. 5.11. This is a much more complex spectrum than the volumetric impedance spectra exhibited by the Reyrolle pump, shown on Fig. 3.19. This was expected as the Dowmatic pump has a more complicated design of delivery port.

519 The connections from the delivery line to the servo actuator and relief valves, as illustrated on Fig. 5.2, influence the impedance values, but the dominant feature of this arrangement is the long outlet line, as illustrated on Fig. 5.12. The tilting head method of varying the displacement of the pump necessitates the use of such a long port. This connects the port plate, which moves relative to the pump mounting, to the axis of rotation of the tilting head which is fixed. This allows for easier connection of the pump to a hydraulic circuit. The line is extended even further with this particular design by the addition of elbows to the inlet and outlet ports which effectively doubles the length of the delivery line, as shown in Fig. 5.12.

520 We have, in effect, determined the lumped impedance value of a system. This system consists of a pump and a length of pipeline of non uniform cross section with a number of side branches. If we ignore these side branches and assume that the system is formed by a pump and a length of pipeline then we can determine an impedance value for the 'pump' of this simplified system. Assuming that the delivery port forms a part of the test pipeline then we can redraw the circuit as illustrated on

Fig. 5.13. In this revised system we have placed the pump outlet at the port plate, position A on Fig. 5.12.

521 Values for the impedance of this 'pump', of the simplified system, were predicted from the results for the pressure P_p using an overall pipeline length and transducer position as given on Fig. 5.13. The impedance spectrum obtained Z_{sA} is illustrated on Fig. 5.14. As expected, this new impedance spectrum Z_{sA} differs greatly from the impedance predicted at the pump outlet Z_s. However, this revised impedance also has a complex form and cannot be represented by a capacitive model as suggested by the result for the axial piston pump obtained previously, section 372. It is clear, therefore, that the internal and external connections of the pump cannot be omitted from the impedance model. Unfortunately, we cannot incorporate these features in the impedance model as we lack details of these connections.

522 Although the impedance model has not provided a convenient representation for the pump we can still use the lumped parameter value Z_s in the model of the pressure standing wave. Thus we can again assess the reliability of the predicted impedance spectrum by comparing the theoretical and experimental values for the ratio P_p/P_{pmin} . as given by equation 3.50 and outlined in section 377. The pressure amplitude ratios $|P_p/P_{pmin}|$. are compared on Fig. 5.15 and their corresponding phase differences are shown on Fig. 5.16. We can see that there is reasonable agreement between the two sets of results for both the amplitude ratios and phase differences. This implies that we have a reliable value for the pump impedance Z_s. We can now consider the pump flow Q_s.

Prediction of the Pump Flow

523 Unlike the pump impedance Z_s the pump flow Q_s cannot be represented by a lumped parameter at the outlet of the pump. The source of the flow ripple, the pumping mechanism, is in this case situated at the upstream end of a length of pipeline in which pressure and flow standing waves are created. This suggests that the flow at the pump outlet will be given by the value of the flow standing wave at this point. In turn, the value of the flow standing wave at any position along this pipeline will depend upon the impedance of the system to which the pump is connected. If we, therefore, use the method outlined in section 381 above to predict a value for the pump flow Q_s at the pump outlet we should find that the values given for Q_s will vary with each value of P_p used.

524 Values for the pump flow Q_s, at the outlet of the pump, were predicted using the results for P_p obtained for each length of pipeline l as described in section 382. The results confirm that the value of Q_s depends upon the circuit configuration. This is illustrated on Fig. 5.17 which shows the variation in the predicted values for the first harmonic of Q_s as the line length l is increased. The overall pattern of the results is typical of a flow standing wave. It may be possible to obtain a more representative value for Q_s if we consider the source of the flow ripple isolated from the long delivery line of the pump. That is if we consider the 'pump' of the revised system model as illustrated on Fig. 5.13.

525 Values for the 'pump' flow at the port plate Q_{sA} were predicted using the revised theoretical model for the test circuit as used to predict the 'pump' impedance Z_{sA}. The results contained a large

amount of scatter but did not form any logical patterns as did the previous values of Q_s. Mean values were determined from the results and these form the impedance spectrum illustrated on Fig. 5.18. It can be seen that the fifth harmonic term predominates, which is emphasised by the synthesised flow shown as a function of time on Fig. 5.19. As with the 'pump' impedance Z_{SA} it is clear that the flow spectrum is affected by the internal and external connections of the pump. However, we can examine the value of this flow spectrum by using this and the pump impedance spectrum Z_{SA} to predict the levels of pressure and flow in the system.

Prediction of Pressure and Flow Levels at any Point in the System

526 The pressures at the outlet of the pump, P_p, for the revised test circuit illustrated on Fig. 5.13 were computed using the transmission line equation 3.17 and values for Q_{sA} and Z_{sA} as given on Figs. 5.18 and 5.19. When plotted against line length ℓ the amplitude of P_p shows the typical peaks and troughs associated with the variation in pressure ripple level at this position, as illustrated on Fig. 5.20. The pressure amplitudes recorded at P_p are also plotted on Fig. 5.20 which shows reasonable agreement between the theoretical and experimentally determined values. Likewise, the predicted and recorded values for the phase of P_p also give good agreement as shown on Fig. 5.21.

527 These results indicate that this revised circuit model can be used to give reliable values for the pressure ripple levels in a hydraulic system. In this experiment we can also evaluate the model for the flow ripple using the results obtained from the transient flowmeter. Thus the values for the flow Q_f and the pressure P_f were computed using the transmission line equations 3.18 and 3.17 applied to the revised circuit as shown on Fig. 5.13. The resulting amplitudes values are shown plotted against line length ℓ on Figs. 5.22 and 5.24, and similarly the phase values are shown on Figs. 5.23 and 5.25. The pressure and flow values recorded at the transient flowmeter are also plotted on these figures which show that there is good agreement between the theoretical and experimental results. With the values Q_f and P_f we have now defined all the parameters for this point in the circuit, the impedance at this point is given on Figs. 5.9 and 5.10.

528 The results obtained suggest that pumps of a more complex design can be represented by system models consisting of a 'pump' and associated circuit. It should prove possible, therefore, to be able to derive values for the flow and impedance of the pumping mechanism. However, to extend this model to provide a mathematical representation of the whole pump we need a detailed knowledge of the pump's design. Although we can derive a lumped impedance value at the outlet of the pump we cannot obtain a corresponding flow value as this depends upon the impedance of the system to which it is attached. Thus the model for such a pump would consist of the impedance and flow values for the pumping mechanism and an impedance model of the porting. Alternatively, it may prove possible to provide values of flow at the pump outlet for various values of entry impedance to the system. These could be computed for a wide range of possible system impedance values and presented graphically for easy reference.

DISCUSSION OF RESULTS

529 The results obtained, with this rather makeshift test arrangement, confirm the reliability of the transmission line model outlined in Chapter 3, when applied to a pipeline and termination. This is demonstrated by the accuracy of the results for the pressure ratio P_T/P_p and the flowmeter impedance Z_f, defined by equations 3.42 and 5.3 respectively, and illustrated on Figs. 5.7 to 5.10. The improved definition of the theoretical curves for the amplitude ratios shown on these figures, over those achieved by previous investigators, is due entirely to the use of a more accurate value for the termination impedance Z_T. We again demonstrated that the impedance of a simple variable restrictor valve is frequency dependent, as shown on Fig. 5.6.

530 The complex design of this particular pump makes it more difficult to establish the parameters Q_s and Z_s. Of the two parameters the impedance Z_s is more easily derived as we can represent the pump by a lumped impedance value at the pump outlet which can be predicted without reference to the design of the pump. Furthermore, this lumped impedance value can be used in the transmission line model as shown in Section 522. Unfortunately, it is not possible to derive a similar lumped value for the pump flow. This has to be referred to the pumping mechanism as a result more information regarding the detail design of the pump is needed. The attempt made here to incorporate the main feature of the pump design, the long outlet line, into the model for the pump was partially successful since by using the revised model for the pump reasonable predictions were obtained for the values of the pressures and flows in the test system, as given in Section 526. These results suggest, therefore, that a more accurate pump model could be

derived given more detailed information regarding the design of the pump and provided that we were able to model the various pipeline configurations involved.

531 With the work detailed in this and the previous two chapters we have shown that it is possible to determine the impedance spectra for hydraulic circuit components. Once established these component parameter values can be used in the impedance model for complete systems. Unfortunately, the simplified hydraulic system which was modelled so successfully above does not represent even the simplest of practical hydraulic circuits, given the single, straight, uniform length of pipeline employed. Before attempting to expand the mathematical model so that it may represent a practical hydraulic system it is necessary to examine the effect upon the pressure and flow ripple of various pipework configurations that are commonly employed.

532 In the formation of hydraulic pipe networks there are two basic arrangements which are used repeatedly in constructing a circuit. These are:-

i) branches, by which the pump flow is divided and directed towards two or more terminations

ii) sections of pipeline along which two or more components are spaced.

The latter arrangement can be termed impedances in series whereas the former, branch lines, represent impedances in parallel. It is the aim of the work in the next two chapters to evaluate the effects of these two circuit arrangements upon the generation of pressure ripple standing waves within a practical hydraulic circuit.

CHAPTER 6

Branch Line Systems

INTRODUCTION

601 The work so far has been confined to simple systems which consist of a straight length of pipeline connecting a source of flow ripple to a termination. We have derived accurate impedance models to represent the pressure and flow standing waves in this type of hydraulic system. However, although the system was operated under normal conditions of pressure, flow, speed and temperature such simple systems cannot be used for any practical purpose. To be able to represent mathematically systems of a more practical nature we need to be able to model pipeline networks.

602 A basic pipeline arrangement that occurs in the design of any hydraulic circuit is that of branched lines. All practical systems have at least two terminations, one of which will nearly always be a pressure relief valve.

603 Branch lines have been studied from the earliest investigations into pressure ripple propagation. Stewart (18) investigated the effect of closed ended side branches as a method for attenuating the pressure ripple at discrete frequencies. It is this aspect of the use of branch lines that has predominated all investigations into their influence on pressure ripple propagation. Much of this work, as with Stewart, has been concerned with systems which used air or other gases. However, more recent investigators such as Lewis et al (19), Sewall et al (20) have considered systems using oil and of these the results obtained by Sewall are of particular interest as the mean pressures and frequency range examined, 100 bar and 100 to 1000 Hz, are more relevant to the practical applications considered here.

604 In all previous investigations the performance of closed ended branch lines were evaluated both experimentally and theoretically using a form of transmission loss factor. Transmission loss can be expressed in different ways but fundamentally it is an expression which relates pressure ripple conditions downstream of the branch line or similar device to conditions upstream. The system conditions are commonly expressed in terms of pressure or energy levels. A typical performance curve for a closed ended branch line is given on Fig. 6.1. By using a ratio of system pressures or energy levels, the pump parameters have been eliminated from the evaluation. As a result the actual pressure levels within a system are not determined. This is a limitation if we are going to assess the performance of hydraulic systems which include branch lines. We have to be able to derive the pressures at any point in the system.

605 In the work detailed below we aim to show that simple circuit theory can be used, in conjunction with the impedance models derived earlier, to predict the pressure standing wave levels in all sections of the system. The theoretical analysis will be supported by a wide range of experimental testing. In order to keep the investigation as simple as possible, the test rig and experimental procedures are based upon those used in the earlier extending pipeline tests detailed in chapter 3. By using the same conditions of speed, pressure and flow with the same circuit components, we reduce the number of unknown parameters which would otherwise require evaluation.

MATHEMATICAL MODEL OF A BRANCHED SYSTEM

606 We can extend the model derived earlier for the

simple test circuit, (chapter 3) to include one or more branch lines by using simple network rules. We begin by considering a hydraulic system with a single branch line as shown diagrammatically on Fig. 6.2, with the corresponding impedance representation on Fig. 6.3. In this circuit the pressure at the junction P_2 is common to all three pipelines. That is P_2 is the pressure at the termination to line 1 and the pressure at the entrance to lines 2 and 3.

607 If we consider the flow at the junction then for continuity the algebraic sum of the flows around the junction must be zero. This is equivalent to Kirchoffs 1st law.

Hence $$Q_1 = Q_2 + Q_3 \qquad (6.1)$$

Now the flows entering lines 2 and 3 can be expressed in terms of the pressure and impedance at the entrance to each line.

Thus $$Q_2 = \frac{P_2}{Z_{e2}} \quad \text{and} \quad Q_3 = \frac{P_3}{Z_{e3}} \qquad (6.2)$$

If we let the impedance at the junction as 'seen' from line 1 be Z_J then similarly:-

$$Q_1 = \frac{P_2}{Z_J} \qquad (6.3)$$

If we now combine these equations and eliminate P_2 we get

$$\frac{1}{Z_J} = \frac{1}{Z_{e2}} + \frac{1}{Z_{e3}} \qquad (6.4)$$

Equation 6.4 is the standard expression for combining impedances in parallel which can be used to obtain the effective impedance at the junction Z_J.

Where

$$Z_J = \frac{Z_{e2} Z_{e3}}{Z_{e2} + Z_{e3}} \qquad (6.5)$$

608 In this way the system downstream of the junction can be represented by a single lumped impedance value Z_J located at the junction. This becomes the termination impedance for line 1 as illustrated on Fig. 6.4. In so doing we have reduced the branch line circuit to the simpler pump, pipeline and termination system. Using this simplified circuit we can now determine the pressure levels at any position along line 1, using the transmission line equation 3.17. In this case the reflection coefficient at the junction ρ_T will be given by:-

$$\rho_T = \frac{Z_J - Z_{o1}}{Z_J + Z_{o1}} \qquad (6.6)$$

609 Using the simplified circuit we can establish a value for the pressure at the junction P_2 which we can then use to determine the pressures along lines 2 and 3. We have already seen in chapter 3 how the influence of the pressure ripple source or, as in this case, the system upstream of a pipeline can be eliminated from the expression for pressure in a line by the formation of a ratio between pressures at different points along the line. If we form, therefore, a ratio between the pressure in line 2 at a distance x from the junction, P_{x2} and the pressure at the junction P_2 we see that the resulting expression is dependent on the parameters of the pipeline and its termination. That is:-

$$\frac{P_{x2}}{P_2} = \frac{e^{-\gamma_2 x} + \rho_{T2} e^{-\gamma_2 (2l_2 - x)}}{1 + \rho_{T2} e^{-2\gamma_2 l_2}} \qquad (6.7)$$

We can therefore evaluate the pressures along line 2 using equation 6.7 and values for P_2 evaluated previously. Likewise the pressures along line 3 are given by a revised equation 6.7.

610 This procedure can be applied to systems with more than one branch line by simply repeating the exercise of reducing each junction or 'node' in turn to its respective lumped impedance value. This process is repeated until the system representation has been simplified to a simple pump, pipeline and termination circuit, for which we can determine the pressure levels. The process is then reversed to predict the pressure levels throughout the remainder of the circuit. This approach is demonstrated diagrammatically on Fig. 6.5, which shows the step by step procedure required by multibranched systems.

EXPERIMENTAL INVESTIGATION OF A BRANCH CIRCUIT

611 To establish the suitability of the mathematical model in representing the pressure standing waves in a branch line system a large amount of experimentation was undertaken. To do this the test rig used for the extending pipeline tests described in Sections 337 to 343 was modified by the addition of a branch line 1.18m in length at right angles to a straight length of pipeline of 3.94m at a position .58m from the pump flange. This revised circuit is illustrated on Fig. 6.6. The added pipeline is terminated by a second 19mm restrictor valve.

612 As only one flowmeter was available at the time of testing the two return lines were arranged such that either the combined flow or the flow from line 3 only could be measured. It was necessary to be able to read the total flow so that the pump swashplate setting

could be adjusted and then monitored during the tests. The directional control valve used to achieve this was greatly oversized to ensure that only a negligible pressure rise was generated in either return line, and thus would not affect the response of either restrictor valve.

613 To monitor the pressure standing wave effects at the junction and along line 3, the branch line, two more piezo electric pressure transducers were inserted in the 'T' of the junction and close to valve 2. This is in addition to those transducers already in place at the pump flange and close to valve 1 as illustrated in Fig. 3.8.

614 Before commencing the investigation into the wave propagation in branch lines a short series of tests were carried out to ensure that the two restrictor valves used are identical in response as well as construction. To establish this a number of extending pipeline tests, described in detail in Sections 349 and 350, were repeated using the second restrictor valve. The results obtained were compared with those for the original tests using the same pipe lengths. These values showed no changes in the pressure levels for all the harmonics of the pumping frequency. We can conclude, therefore, that the valves have identical characteristics.

EFFECT OF FLOW DIVISION

615 Before evaluating the mathematical model for a branch line system derived above we must first examine the effect, if any, that the separation in the mean flow at the junction has upon the propagation of the pressure ripple. To do this we can use the test procedure outlined below.

616 Experimental Procedure:-

As for the earlier extending pipeline tests described in Section 345 the pump swashplate was set to give a mean flowrate of 0.7 l/s for a system pressure of 200 bar. This setting was maintained throughout this series of tests.

617 With the test circuit arranged as shown on Fig. 6.6 valve 2 was closed and valve 1 was adjusted to give a mean system pressure of 100 bar. The pressure amplitudes and phases were recorded at the four positions P_1, P_2, P_3 and P_4 once steady conditions had been established. As with the earlier extending pipeline tests the oil temperature was maintained at a steady 40°C. Following this valve 1 was readjusted to give a mean pressure of 150 bar. The four pressures were recorded and again with valve 1 set to give a mean pressure of 200 bar.

618 After this the two valves were adjusted so that 3/4 of the total pump flow passed along line 2 with the mean pressure set initially to 100 bar. The four pressures were recorded when steady conditions had been obtained. The valves were then readjusted to give a mean pressure of 150 bar whilst maintaining the 3 to 1 ratio for the flow division at the junction. The pressures were recorded at this condition and again with the valves adjusted to give a 200 bar mean pressure level for the same flow conditions.

619 This process was repeated using three more values for the flow division at the junction, as given in Table 6.1. Increasing the flow in line 3 and so decreasing the flow along line 2 with each new setting of the valves. The process was completed with valve 1 closed and all the flow passing through line 3.

620 In order to ascertain the effect upon the propagation of pressure waves of an abrupt change in the direction of a proportion of the mean flow, which occurs at the junction, pipelines 2 and 3 were interchanged, as illustrated on Fig. 6.7. In doing this we have interchanged the impedances at the entrance to lines 2 and 3 with regard to their location relative to the direction of the mean flow entering the junction. However, the total impedance at the junction remains the same. If, therefore, the separation of the mean flow at the junction has any effect upon the propagation of the pressure ripple then this should be evident in the results obtained using both of these circuit configurations.

621 The tests detailed above were repeated using this rearranged test circuit. However, it became obvious during testing that the pressure amplitudes and phases recorded for this second circuit differed from those obtained earlier using the original pipe configuration. Closer examination of the results after completing the tests showed that the largest differences occured at the second harmonic of piston frequency, as shown on Fig. 6.8. It *will be shown later* that these discrepancies were due in part to the large levels of pipe vibration observed during this latter set of tests. It is *apparent* that the movement of the pipes created sufficient interaction with the flow ripple as to directly effect the pressure levels.

622 The causes of this vibration and the mechanism by which it can interact with the propagation of the pressure ripple will be discussed later in Sections 666 to 674. It is sufficient at this point to understand that the vibration is induced by a force generated in line 3, the branch line, as a result of a pressure imbalance along the axis of the line which is a

consequence of the pressure standing wave along the line. Thus in order to reduce the amplitudes of the vibration a fairly large mass was clamped to the junction. The tests detailed above were repeated for both circuit configurations with the junction constrained by the large mass. The results obtained for these tests showed close agreement between the pressure amplitudes and phases for all four transducer locations. These values also compared favourably with the first set of results recorded using the original test circuit arrangements as illustrated on Fig. 6.9.

623 It is apparent, therefore, that the variations in the results for the first series of tests were due to the vibration of the pipework. There is also the implication that the separation of the mean flow at the junction does not disturb the propagation of the pressure ripple. However, more work is required before such a definite conclusion can be drawn. Before considering further experimental work we can extract some useful information from the results obtained so far.

624 Examination of the Results:-

It is clear from the results that, as expected, raising the mean system pressure level increases the pressure ripple amplitudes. This is illustrated on Fig. 6.9, which also demonstrates the high amplitudes obtained for the second harmonic of piston frequency. The magnitudes of these high amplitudes correspond to the maximum levels obtained during the extending pipeline tests and this implies that the system is close to or at a resonance condition at this frequency. Correspondingly the changes in the flow division ratio at the junction have the greatest effect on the pressure ripple amplitudes at the second and third harmonics of

piston frequency as shown on Fig. 6.10. The two frequencies at which the largest pressure levels were recorded. This variation in the flows along lines 2 and 3 had little effect upon the results for the remaining harmonics as shown on Fig. 6.10.

625 These results are in agreement with the theory so far considered. The only parameters affected by the variation in the flows along lines 2 and 3 are the impedances of the valves. These have, in the form of reflection coefficients, a large influence upon the amplitude and phase of the pressure ripple standing wave. The amplitude of the reflection coefficient changes the magnitude of the standing wave whereas the phase governs the position of the standing wave relative to the termination and hence relative to the fixed pressure transducer locations where the pressure levels are monitored. The degree by which the recorded pressure levels are affected depends upon whether the system is close to a resonance or anti-resonance condition for the harmonic of piston frequency considered. Hence the larger changes in the pressure levels recorded for the second and third harmonics.

626 So far the results imply that the separation of the mean flow at the junction does not introduce any obvious variations in the generation of a pressure ripple standing wave within the circuit. A more stringent examination of this inference could be made by applying the theoretical model derived in Sections 606 to 610. However, as such comparisons would only apply to this particular configuration the results would be of limited value. Many more results for different system configurations, on the lines of the extending pipeline tests, are therefore needed.

EFFECT OF JUNCTION IMPEDANCE

627 The simplest method of changing the impedance at the junction is to alter the entry impedance Z_e of one or both downstream pipelines. The easiest practical method of achieving such a variation is to change the length of the pipeline between the junction and the valve.

628 The variation in the entry impedance Z_e with line length l is given by equation 4.2. The complex nature of this expression means that the relationship is cyclical. This can be seen from the plots for the amplitude and phase of Z_f given on Figs. 5.9 and 5.10. There are, therefore, maximum and minimum impedance values which give the limiting values that can be achieved by solely changing the pipeline length. The pipeline lengths at which these maxima and minima occur can be determined by considering equation 4.2.

629 If we substitute for ζ_T in equation 4.2 using equation 3.11 then we can obtain the expression:-

$$Z_e = \frac{Z_T + Z_o \, Tanh \, \gamma l}{1 + Z_T/Z_o \, Tanh \, \gamma l} \qquad (6.8)$$

If we assume a lossless line then $\gamma = \frac{j\omega}{a}$

we then obtain:-

$$Z_e = \frac{Z_T + j Z_o \, Tan \frac{\omega l}{a}}{1 + Z_T/Z_o \, Tan \frac{\omega l}{a}} \qquad (6.9)$$

which has a maximum value of $Z_e = Z_T$ when

$$\frac{\omega l}{a} = 0, \pi, 2\pi \text{ - - - } n\pi.$$

This corresponds to pipeline lengths ℓ of

$$\ell = \frac{an\pi}{\omega} = \frac{n\lambda}{2}$$ an integer number of half wavelengths.

Similarly the minimum value occurs when $Tan \frac{\omega\ell}{a} = \infty$ that is $$\frac{\omega\ell}{a} = \frac{\pi}{2}, \frac{3\pi}{2}, \frac{5\pi}{2} --- \frac{(2n-1)\pi}{2}$$ which corresponds to pipeline lengths ℓ of

$$\ell = \frac{a\pi}{\omega 2} = \frac{(2n-1)\lambda}{4}$$ an odd integer number of quarter wavelengths.

at which point $$Z_e = \frac{Z_o^2}{Z_T}$$

Thus the greatest possible variation in the impedance at the entrance to either pipeline will be obtained if the length of the line ℓ is increased or decreased in stages over a length corresponding to one quarter of the wavelength of the pressure ripple frequency considered.

Test Procedure to Determine the Effect of Junction Impedance

630 Using the branch line test circuit shown on Fig. 6.6 as the basis line 2 was reduced in length from 3.63 to 1.8m. With the circuit so arranged the series of tests described above in sections 616 to 619 were repeated; that is the pressures at P_1 to P_4 were recorded for various values of flow in lines 2 and 3; but for only one mean pressure level, 200 bar. Following these tests the length of line 2 was increased by a few centimetres and the tests were repeated. The whole process was repeated several times, resulting in the use of 20 different lengths for line 2 from 1.8m to

4.0m. This ensured that we had obtained the maximum variation in the entry impedance to line 2, Z_{e2}.

631 On completion of this series of tests line 2 was restored to the original length of 3.63m. The test procedure described above using line 2 was then repeated using line 3. This time the line length was increased in length from 1.3m up to 2.1m using a total of 10 different line lengths. Although this range of line lengths does not create the maximum variation in the entry impedance to line 3, Z_{e3}, they complement those for line 2 as these two sets of line lengths overlap for a proportion of their ranges.

Discussion of the Results Obtained with Various Junction Impedances

632 To begin with we can examine the effect of the impedance at the junction upon the pressure ripple standing wave by considering the conditions downstream of the junction along lines 2 and 3. In so doing we also examine the variation in the termination impedance of the valve with mean flowrate and its effect upon the pressure levels.

633 The conditions upstream of the junction can be eliminated by the formation of ratios between pressures at any two points along the pipeline. To do this we assume the circuit upstream of the junction to be a lumped flow ripple source. Using this assumption, the analysis then follows the procedure employed previously in sections 352 to 354 to examine the termination impedance values for the extending pipeline tests. Using equation 3.17 to give the pressures at P_2, P_3 and P_4 we obtain the ratios

$$\frac{P_3}{P_2} = \frac{e^{-\gamma_2(\ell_2 - x_2)} + \varsigma_{T2}\, e^{-\gamma_2(\ell_2 + x_2)}}{1 + \varsigma_{T2}\, e^{-2\gamma_2 \ell_2}} \qquad (6.10)$$

and

$$\frac{P_4}{P_2} = \frac{e^{-\gamma_3(\ell_3 - x_3)} + \varsigma_{T3}\, e^{-\gamma_3(\ell_3 + x_3)}}{1 + \varsigma_{T3}\, e^{-2\gamma_3 \ell_3}} \qquad (6.11)$$

634 Now given that the transducers for P_3 and P_4 are located the same distance from their respective valves, as shown on Fig. 3.8, then x_2 equals x_3. Furthermore, the valves have identical impedance spectra for the same pressure and flow settings. Thus for conditions in which the mean pressures and flowrates were the same in each line then the reflection coefficients ς_{T2} and ς_{T3} are the same and hence the pressure ratios P_3/P_2 and P_4/P_2 will be equal when the pipeline lengths ℓ_2 and ℓ_3 are the same.

That is $$\frac{P_3}{P_2} = \frac{P_4}{P_2} \quad \text{when} \quad \ell_2 = \ell_3$$

635 We can examine the pressure ripple in lines 2 and 3 by determining the values for the pressure ratios P_3/P_2 and P_4/P_2 using the test results obtained above. The results for both lines can be considered together by using the results for those tests for which the flows along the lines were the same. That is the valve impedances were the same. To begin with we can examine the results obtained for test conditions at which the component impedances are known.

636 The results recorded with the full pump flow, .7 l/s, in line 2 are considered along with those obtained with the same full flow along line 3. The amplitude ratios $\left|P_3/P_2\right|$ and $\left|P_4/P_2\right|$ determined from

the two sets of test results are plotted against pipeline length on Fig. 6.11. The two sets of results clearly coincide and in so doing form the now familiar curves previously established for the extending pipeline tests in chapter 3. Similarly, the values for the phase difference when plotted against line length show the same coincidence, producing the characteristic set of curves shown on Fig. 6.12. These results indicate that the same conditions, in terms of the pressure ripple standing wave, exist in each line and as such appear unaffected by the flow separation at the junction.

637 We have a value for the impedance of the valve at this maximum flow condition so we can determine theoretical values for the pressure ratio using equation 6.10 or 6.11. In this way values for the pressure amplitude ratio were computed for pipeline lengths from 0 to 4m and the results are plotted on Fig. 6.11 in comparison to the corresponding experimental values. The figure shows good agreement between the theoretical and experimental results which implies that the mathematical model for a pipeline and termination downstream of a junction is correct. Similarly, the values computed for the phase difference also give good agreement with the experimental results as shown on Fig. 6.12.

638 Repeating this process with the results obtained with no mean flow in the lines; with the valves closed; produced the theoretical and experimental values for the pressure amplitude as shown on Fig. 6.13 and for the phase differences as shown on Fig. 6.14. The theoretical values were determined using equation 6.10, but in order to do this the termination impedance for a closed restrictor valve was assumed to be infinite which gives the reflection coefficient a

value of +1. The good agreement obtained between the theoretical and experimental results as shown by Figs. 6.13 and 6.14 endorses the use of an infinite value for the termination impedance as well as the overall impedance model for pipelines with closed ends.

639 The two test conditions considered correspond to the limiting system flow values, it is reasonable to assume therefore that the mathematical model can be applied with equal confidence at any intermediate flow condition. Unfortunately, we cannot determine theoretical values for the three remaining test conditions, which cover these intervening mean flow levels, as we do not have the valve impedance spectra corresponding to these conditions. However, as we have established that the model provides an accurate representation of the pressure ratios P_3/P_2 and P_4/P_2 then we can derive values for the valve impedances at these remaining test conditions from the experimental results.

VARIATION OF THE TERMINATION IMPEDANCE WITH FLOWRATE

640 To determine the impedance of the valve at the three intermediate flow settings the method used to obtain the impedance spectra from the results for the extending pipeline tests, described in detail in Sections 362 to 364, was again employed. Briefly values for the impedance of the valve are derived using the pressure ratio equation 3.42 with values for the two pressures P_T and P_P determined experimentally. In this case $P_T = P_3$ or P_4 and $P_P = P_2$. Values of Z_T are predicted from the results for the pressures recorded for each pipeline length used and the arithmetic mean of these values gives the impedance value at each harmonic.

641 The valve impedance spectra obtained in this way are illustrated on Fig. 6.15 and are also compared as non dimensional plots for $Z_T/Z_{T_{ss}}$ on Fig. 6.16. The change in the impedance characteristic with decreasing flowrate follows a similar pattern to the change induced by an increase in the mean system pressure level as can be seen by comparing Figs. 6.16 and 3.16. This result could be expected as both involve closing the valve, introducing similar changes to the steady state characteristics and to the geometrical configuration of the valve.

642 Using the valve impedance spectra derived above values for the pressure amplitude ratios and phase differences were computed for the three test conditions. The results when plotted against pipeline length and alongside their respective experimental values gave good agreement with these experimental results. This is illustrated using the results obtained with a mean flow of .5 l/s on Figs. 6.17 and 6.18.

643 Having successfully demonstrated that the impedance model for the pressure ratio is valid downstream of the junction then we can now expand the analysis to include the circuit upstream of the junction. Ultimately predicting the pressure levels at any location within the system.

MODELLING THE COMPLETE SYSTEM

644 To continue with the analysis of the results upstream of the junction, in line 1, the impedance representation for the circuit is reduced to one consisting simply of a pump, pipeline and termination using the method outlined earlier in sections 606 to 610.

645 The validity of the impedance model for lines 2 and 3 has been well proven in the previous sections and so the entry impedances to these lines, Z_{e2} and Z_{e3}, can be evaluated with confidence. These two impedances are combined in parallel using equation 6.5 to give the impedance at the junction, Z_J. This junction impedance now becomes the termination impedance for the simplified theoretical model. Thus the pressures at any point along line 1 can be determined using the pump and pipeline parameters already established in chapter 3 in the transmission line equation 3.17.

646 In this way the pressures at P_1 and P_2 were computed using parameter values which correspond to the pressure and flow settings used for the experimental tests described in sections 630 and 631, in which the length of line 2 was varied. This involved the computation of the entry impedance to line 2, Z_{e2}, using values of line length ℓ_2 increased in small increments from 0 to 4.0m. Each value for Z_{e2} is combined with the impedance for line 3, Z_{e3}, to give values for the impedance at the junction Z_J. Finally, the pressures at P_1 and P_2 are evaluated using each of the values for the junction impedance.

647 The resulting pressure amplitudes for P_1 predicted using the system parameters which correspond to the test condition with line 3 closed are shown plotted against line length ℓ_2 on Fig. 6.19. The figure shows the typical peaks and troughs, previously obtained for the extending pipeline tests in Chapter 3. One notable feature is the high resonance pressures, greater than 40 bar, obtained for the second harmonic. In addition to these theoretical values for the pressures recorded at P_1 are also plotted on Fig. 6.19 which shows good agreement between the mathematically predicted amplitudes

and these experimentally determined levels. Similarly good agreement was obtained for the pressure phases as illustrated on Fig. 6.20 using the pressure phases for P_1 that correspond to the pressure amplitudes of fig.6.19.

648 The results obtained for P_1 show that the impedance model derived above provides an accurate representation of this simplified circuit model. This implies that the pressures at any point in the system can also be predicted with equal reliability. To support this suggestion we need to predict the pressures at the remaining transducer positions.

649 Values computed for the pressure amplitude at P_2 for the test condition with valve 2 closed are shown plotted against line length l_2 on Fig. 6.21. This illustration shows good agreement with the experimental values recorded at P_2 which are also plotted on this figure. Similarly, good agreement was obtained for the phases of P_2 as shown on Fig. 6.22. The pressures at P_2 provide the basis for the computation of the pressures in lines 2 and 3. Using the values computed for P_2 the pressures P_3 and P_4 were determined, using equation 6.7, for the test conditions with valve 2 closed. The results for the pressure amplitudes of P_3 and P_4 are shown plotted against pipeline length l_2 on Figs. 6.23 and 6.25 and the results for the pressure phases are shown on Figs. 6.24 and 6.26. The pressure amplitudes and phases recorded at P_3 and P_4 are plotted alongside their corresponding theoretical predictions. Once again these figures show good agreement between the mathematically predicted values and the results obtained experimentally.

650 In addition to the test condition considered here, valve 2 closed, good agreement was also obtained between the theoretically derived values for the four pressures P_1 to P_4 and the results determined by

experiment for the four remaining test conditions. We can conclude, therefore, that the impedance model derived above provides an accurate representation of a branched line system.

EFFECT OF JUNCTION POSITION

651 The changes in the pressure standing wave pattern that results when a second pipeline or circuit is added to an existing system depends upon the value of the lumped impedance for this additional line or circuit and upon the position at which it is connected to the original system. The point of connection dictates the impedance value for the portion of the original circuit which now lies downstream of this newly formed junction. In turn, this impedance value determines the impedance for the junction, thus the magnitude and position of the standing waves upstream and downstream of this position. To demonstrate the effects that such an addition can have on an established hydraulic system a short series of tests were carried out as described below.

652 The test circuit used above was rearranged as shown on Fig. 6.27. This new circuit represents an addition of a pipeline of 1.15m to an existing system consisting simply of a pump, pipeline and termination. Using this revised circuit a reduced form of the test procedure detailed above in Sections 630 and 631 was undertaken. This time the pressure amplitudes and phases were recorded at the four transducer positions P_1 , P_2 , P_3 and P_4 once steady conditions had been achieved with the mean system pressure set at 200 bar firstly with valve 2 closed and then with valves 1 and 2 adjusted to give equal flows along lines 2 and 3. Following this the circuit was rearranged with the junction positioned closer to valve 1 by a few centi-

metres whilst the lengths of line 3, l_3, and from the pump to valve 1, $l_1 + l_2$, were kept the same. The tests given above were repeated using this revised circuit. This whole process was repeated several more times with the junction repositioned closer to valve 1 before each set of tests. In all a total of 12 different positions for the junction were used.

653 The pressure amplitudes recorded with valve 2 closed at the four positions P_1 to P_4 are shown plotted against the position of the junction on Figs. 6.28 to 6.31. The large variation in the amplitudes of each harmonic created by the different locations for the junction are clearly illustrated. It is evident from these plots that there are certain positions in a given circuit where it would be better to connect an additional line than others. We can demonstrate this using the first set of pressure values recorded for this last set of tests. The test circuit for which they were obtained is the same as that used for the original branch line tests described in Sections 611 to 614. That is with the junction positioned .58m from the pump flange. If we examine the results for the test configuration on Figs. 6.28 to 6.31 we see that this choice of pipeline lengths was not a good one. They confirm that the system was close to resonance for the second harmonic of piston frequency. Clearly positioning the junction closer to the pump or close to valve 1 would have had the effect of reducing the recorded pressure levels for the lower harmonics. Indeed the narrowness of the resonant peaks for the amplitude of the second harmonic as shown on Figs. 6.28 to 6.31 implies that a significant reduction in the recorded pressure levels would have been obtained by relocating the junction only a few centimetres from its original position.

654 Values for the four pressures P_1 to P_4 were computed using values for the junction position moved in small increments from a position close to the pump to a position close to valve 1. The results obtained for the pressure amplitudes are plotted alongside their corresponding experimental values on Figs. 6.28 to 6.31. Again good agreement has been achieved between the theoretical and experimental results. Similarly good agreement was also obtained with the values for the pressure phases for these test conditions as illustrated on Figs. 6.32 to 6.35.

655 These results suggest that it may be possible to determine an optimum position or range of suitable locations for the connection of an additional branch line to an existing system or in designing the pipe-work for a system which incorporates branched lines. Furthermore, this position can be determined using the mathematical model for the system, although the criterion upon which such an optimisation could be based has yet to be established. It is clear, however, that any evaluation of system performance will require a complete model for the system. If we again consider the first test circuit the line lengths used of 3.36, 1.18 and .58m are close to resonant pipe lengths for the 1st, 3rd and 5th harmonics respectively whereas we have already seen that the strongest resonance for the system is that of the second harmonic.

USE OF STUB LINES FOR PRESSURE RIPPLE ATTENUATION

656 As mentioned in the introduction to this chapter, the study of closed ended branch lines represents the largest proportion of the work previously undertaken on the study of the transmission of pressure ripple through circuits with branch lines. This level of interest is due to the fact that closed ended branch lines (stub lines) can be used as a simple form of

pressure ripple attenuator.

Theoretical Considerations on Stub Lines

657 It has been shown earlier in Sections 628 and 629 that the impedance at the entrance to a pipeline Z_e varies with the length of the line ℓ, as given by equation 4.2. Furthermore, if the line is assumed to be loss-less then the minimum value for Z_e is given by Z_o^2/Z_T, when the line length is one quarter of a wavelength for the frequency considered. If we now consider a line which has a closed end then the termination impedance Z_T will be infinite. In this case the minimum value for the entry impedance Z_e will be zero.

658 If we add, therefore, a closed ended line to an existing system, with its length equivalent to one quarter the wavelength of any ripple frequency present within the system, then the pressure at the point of connection and hence downstream of this position would be zero for the ripple frequency concerned. This simple device appears to offer a means of eliminating individual troublesome pressure ripple frequencies from a hydraulic system. Ideally a stub line would perform as, in electrical terms, a notch filter. Such a filter attenuates single frequencies whilst leaving all other frequencies unchanged, as illustrated on Fig. 6.36. Unfortunately, this ideal state cannot be achieved in practice. The pipelines are not loss-less and so the impedance at the entrance to a pipeline will always have a finite value. Nevertheless, the minimum value for Z_e will be very low and thus will give low pressure levels when tuned to a particular frequency. However, the remaining ripple frequencies will also be affected by the addition of a stub line which may lead to a worsening of conditions at these frequencies.

Discussion of Results Obtained using Stub Lines

659 For the pump used the first harmonic of pressure ripple, when loaded at a pressure of 200 bar, has a wavelength λ of 8.2m. If we wish to attenuate the pressure ripple at this frequency we require a stub line 2.05m in length. Two such stub lines with this line length were used on the simple circuit as shown on Fig. 6.6.

660 One of these was used during the tests described above in which line 2 was extended between each recording of the four pressures P_1 to P_4. In this case line 2 was the stub line and the combined lengths of lines 1 and 3 was 1.76m. The pressures recorded for this circuit at P_1 and P_4 are shown on Fig. 6.37. These values are shown in comparison to pressures recorded at these positions but with the stub line removed. By comparing the pressures downstream of the stub line P_4 we demonstrate the effectiveness of the stub line as an attenuator. Fig. 6.37 shows that the addition of the stub line has reduced the amplitude of the first harmonic and of the other harmonic frequencies except the second. Conversely, the amplitude for this second harmonic has been greatly increased.

661 The second circuit was investigated during the range of tests in which line 3 was extended between each test. In this instance line 3 was the stub line and the combined lengths of lines 1 and 2 was 3.94m. The pressures recorded for this circuit at P_1 and P_3 are shown on Fig. 6.38. The results are again shown in comparison to values recorded without the stub line in the circuit. This time the reduction in the amplitude of the first harmonic is much greater. Furthermore, the amplitudes of the remaining harmonic frequencies have also been attenuated.

662 These results show that the degree of attenuation is a function of the interaction between the original circuit and the attenuating stub line. The results are in line with the theory detailed above and they show how the practical conditions differ from the ideal lossless line case. An ideal lossless stub line would reduce the pressure ripple downstream of the junction to zero, irrespective of the state of the original circuit or the position of the junction.

663 An important aspect of using a stub line length equivalent to one quarter wavelength for a particular frequency is that this is also an odd number of quarter wavelengths for the odd harmonics of this frequency. Thus a degree of attenuation should be obtained at all the odd harmonics of the pressure ripple. The pressures recorded at the junction P_2 show that such a reduction in the pressure amplitudes for all the odd harmonics of the pressure ripple were obtained, for both circuit configurations, as illustrated on Fig. 6.39. This implies that the pressure ripple in a system could be attenuated using two stub lines. One with a length equivalent to one quarter wavelength for the first harmonic and the other with a length equivalent to one quarter wavelength for the second harmonic. Thus providing a simple method of attenuating the pressure ripple in any hydraulic system. There are, however, drawbacks to using this method.

664 Pressure ripple frequencies are not normally constant even for system which have nominally fixed speed prime movers such as electric motors. The speed of such devices does vary with load. Furthermore, we know that the sonic velocity and hence the wavelength of the pressure ripple is affected by the Bulk Modulus of the oil which in turn is influenced by changes in pressure, temperature and air entrainment as outlined in Sections 320 to 323. Although the variation in

the ripple wavelength created by the changes in the circuit parameters are only small they are sufficient to cause large scale variations in the pressure ripple levels. This can be demonstrated using the results for the first harmonic of the pressure amplitude $|P_4|$ as it varies with the length of the stub line l_2, illustrated on Fig. 6.25. The figure shows a sharp dip in the amplitude levels around the quarter wavelength, 2.05m, condition showing that any small changes in the wavelength around this value will create large variations in the pressure amplitude levels. Such a result was also noted by Lewis et al (19) and Sewall et al (20).

665 In conclusion, therefore, it is clear that stub lines provide a useful means of attenuating specific pressure ripple frequencies. In general, however, we must concur with Sewall and say that in-line pressure ripple attenuators, such as described by Whitson (21), which cover a much broader frequency band provide the most useful method of reducing fluid borne noise levels.

EFFECTS OF PIPE VIBRATION

666 In deriving the impedance model to represent the transmission of pressure waves in a simple hydraulic system it was assumed that the component bodies remained stationary. This is valid in the majority of cases as the components are securely mounted either directly on the structure or with the pipes firmly supported at regular intervals. However, this is not the case if the bends or branch lines are present in a system in which the pipes are free to move. As a result, the motions of the pipes, which are a result of the pressure forces acting within the system, can influence the response of the system to the propagation of pressure transients.

667 The effect of longitudinal pipe motion upon the pressure and flow ripple has been examined by authors such as Blade et al (22). Blade used what was essentially a pump, pipeline and termination system. This had a long (21m) length of pipeline containing a 90^{o} elbow at its mid-point. The line was supported in such a way that only the downstream half was free to move and this only longitudinally. It was found that the movement of the pipe, excited by the unbalanced pressure forces acting upon the elbow and termination, had a significant effect upon the resulting pressure levels.

668 Such effects are evident in the results for the first tests carried out with an unrestrained branched line test system as described above in Sections 615 to 622. In this case the pipe movement was excited by the unbalanced pressure forces acting on the 'T' of the junction and the termination to line 3; valve 2; as shown on Fig. 6.6, or on the junction and the termination to line 2; valve 1; as shown on Fig. 6.7, when the pipes 2 and 3 were interchanged.

669 In order to establish the levels of vibration generated in the pipes these tests were repeated. On this occasion only the highest value of mean system pressure, 200 bar, was used. This corresponded to the conditions which provided the highest vibration levels. The tests were carried out using both circuit configurations, given on Figs. 6.6 and 6.7, with the pipes free to move and again with the large mass clamped to the junction. In addition to the four piezo electric pressure transducers two accelerometers were attached to the junction and termination of the branch line, orientated to measure the longitudinal motion of this line. The F.R.A. was used to record the pressures and the two velocities in terms of their amplitudes and phases for the first ten harmonics of piston frequency.

670 Examination of the results showed that the pressure amplitudes and phases were in agreement with those for the original set of tests. Thus, the differences in the pressure amplitude values obtained using both test circuits with the pipes free to move are again significant, as illustrated on Fig. 6.40. Similarly, the results obtained when the movement of the pipes was restrained do not possess this discrepancy. This indicates that the variation is due entirely to the motion of the pipes.

671 The high levels of vibration observed when the pipes were free to move are confirmed by the velocity levels recorded. The results obtained for both test circuits are illustrated on Figs. 6.41 and 6.42. These show the large amplitude for the second harmonic of piston frequency obtained using the second test circuit. Likewise, the reduction in the levels of vibration brought about by the addition of a large mass clamped securely to the junction is demonstrated using the results obtained for this test configuration illustrated on Fig. 6.43.

672 We know that the vibration is a result of the difference in dynamic pressure levels at the junction and the termination of the branch line. These unbalanced pressures provide the oscillatory force necessary to create and maintain the vibration of the pipework. However, for a given force value the level of the vibration will depend upon the mechanical response of the system. The pressure forces are easily determined using pressure values measured at, or predicted for the two pipeline discontinuities. The mechanical response, however, is too complex to derive theoretically and much more difficult to obtain experimentally.

673 The pressure force is given by the product of pressure and cross sectional area. If we consider a

length of line of cross sectional area A connecting two bends, or as in this case a 'T' junction and termination, at which the pressures are P_1 and P_2 then the pressure force is given by:-

$$F_p = A(P_1 - P_2) \qquad (6.12)$$

If we now apply this to the two test circuits, shown on Figs. 6.6 and 6.7, then the pressure forces generated by the branch line will be F_{P_1} and F_{P_2} for each circuit respectively. We can use the pressure levels recorded at the junction, P_2 and the branch line termination, P_3 or P_4, to calculate these pressure forces. There is an obvious error introduced using the experimental values recorded at P_3 and P_4 as these are not the pressures at the termination since the end of the line lies inside the body of the valve. However, such errors should be small, especially at the lower harmonics.

674 The pressure forces evaluated in this way for the two test circuits are shown on Fig. 6.44 which shows the relatively high magnitudes for the forces generated by the unbalanced pressures. In addition, the figure also demonstrates how the vibration levels are governed by the mechanical response of the system. If we compare these force values with the corresponding vibration velocities shown on Fig. 6.41 we see that the highest velocities do not coincide with the largest forces. The figures show that the high level of vibration at the second harmonic of piston frequency obtained using the second test circuit is a result of a relatively small oscillatory force acting on a system which must have a natural mode of vibration close to this disturbing frequency.

SYSTEM MODELLING INCORPORATING MECHANICAL VIBRATION

675 Ideally it should be possible to incorporate the motion of the pipes into the mathematical model to provide a comprehensive theoretical description of the response of a hydraulic system to excitation by an oscillatory flow source. Such a method was applied successfully by Blade, et al (22). However, in their case the circuit under test was constructed such that only one mode of vibration was possible. For most systems, unfortunately, the mechanical response cannot be easily defined.

676 A more practical approach is to measure the actual vibration velocities generated within a hydraulic system when in operation. The results can be used to amend the theoretically predicted values for the pressure ripple standing waves. Such a method was employed by Regetz (23) to correct for discrepancies, between predicted and experimentally obtained pressure levels, which were a result of longitudinal pipe vibration.

677 The test circuit used by Regetz was again essentially a pump, pipeline and termination. Now although the pipeline was straight its length, 21m, gave it a natural longitudinal frequency of 68 Hz. This was within the frequency range used by Regetz of 0.5 to 90 Hz. With such an uncomplicated arrangement, it may have been possible to incorporate the mechanical and fluidic responses in the mathematical model as achieved by Blade. However, Regetz used the more practical approach, correcting the predictions for the pressure levels at the frequencies affected by the vibration using the values for the pipe velocities measured during the tests.

678 To obtain the correction for the predicted pressure levels the pipe velocity, measured at the

termination, was divided by the pressure also measured at this point for each frequency considered. This produced a range of impedance values which when added vectorially to the impedance for the termination at the same frequency gave an effective impedance value for the termination. That is an effective impedance value for the termination is given by:-

$$Z_{Tv} = \left(\frac{V_p}{P_T}\right) \cdot A + Z_T \qquad (6.13)$$

A, the cross sectional area of the pipe, is included in this expression to correct the units of impedance from a velocity/pressure relationship as used by Regetz to a flow/pressure ratio as used in this thesis.

679 This method was successfully applied by Regetz to his simple system. However, this model requires a knowledge of both the vibration velocity and the pressure ripple value at the termination. Furthermore, it is felt that the alteration of a known coefficient in order to achieve the necessary correction tc the mathematical prediction may not model the mechanism by which the pipe motion interacts with the pressure or flow ripple.

680 The longitudinal motion of a pipe changes the value of the instantaneous flow at any point along the line measured with respect to a fixed point on the pipeline. It should be possible, therefore, to amend the analysis by considering this as an additional flow component rather than an impedance factor. If we consider a closed ended pipeline subjected to longitudinal sinusoidal vibration then the displacement of the closed end of the line creates a sinusoidal variation in the flow value at this position. This is analogous to the action of a piston producing a

sinusoidal flow pattern. A value for such a flow variation, as illustrated on Fig. 6.45, is given by:-

$$Q_v = A \cdot v \cdot \sin(\omega t - \phi) \qquad (6.14)$$

681 If we consider the test circuit as illustrated on Fig. 6.7 then the vibration of the branch line 3 will create a flow at Valve 2. This can be considered as a secondary source of flow, Q_{sv} with its associated 'source' impedance Z_{sv}. The impedance will be infinity for the closed line or Z_{T2} with the valve open. We can now consider this to be the pump for a second system supplying a circuit along line 3 before branching along lines 1 and 2 which are terminated by impedances Z_s and Z_{T1} respectively. The impedance representation for such a circuit is given on Fig. 6.46.

682 Using these rearranged impedances we can compute values for the pressures that would occur at the four transducer positions given such a system. If we let these pressures be P_{1v}, P_{2v}, P_{3v} and P_{4v} then we now have two values of pressure at each position. One for the original system without vibration P and the other for the assumed secondary system P_v. The overall results for the pressure at each position for the system, including vibration, are determined by superimposing these two sets of results. This is directly analogous to the superposition theorem used in electrical circuit theory. Thus the final pressure values are obtained by the vectorial addition of the two pressures P and P_v

That is the combined pressure at for example P_1 is

$$P_{1\,Combined} = P_1 + P_{1v} \qquad (6.15)$$

We can assess the suitability of this method by analysing the results obtained above in Sections 615 to 621.

GENERAL ANALYSIS

683 To analyse the pressure standing wave levels in a branched line circuit with pipe vibration we can use the results obtained with the circuit as shown on Fig. 6.7, as this configuration gave the highest levels of vibration. If we consider this circuit with valve 1 closed then the secondary 'source' impedance Z_{sv} will be infinite. Thus the reflection coefficient at this point will be unity.

684 In order to determine a value for the secondary 'source' flow Q_{sv}, produced by the motion of valve 1, we must assume that:-

i) line 2 is rigid
ii) the vibration takes place solely along the axis of line 2.

With these assumptions we can use the vibration velocity measured at valve 1, given on Fig. 6.41 to evaluate the secondary flow Q_{sv}.

685 The secondary flow spectrum Q_{sv} derived using the vibration velocity of valve 1 in equation 6.14 is given on Fig. 6.47. The figure shows only one significant amplitude which predictably is at the second harmonic of piston frequency. This has a value that is comparable to the amplitude of the tenth harmonic of the pump flow spectrum Q_s. Using these values for Q_{sv} and Z_{sv} the pressures P_{1v} to P_{4v} were computed for the revised circuit model as illustrated on Fig. 6.46. The pressure levels at each of the transducer positions can now be obtained by adding vectorially these secondary pressure values to those predicted earlier for the basic circuit.

686 The results determined for the pressure amplitude at the pump flange $|(P_1 + P_{1v})|$ are shown on Fig. 6.48

along with the values computed for the basic circuit P_1. These results show that the superposition of the pressure levels for the secondary circuit has brought about a reduction in the amplitude of the second harmonic. However, if we compare these values with the corresponding experimental results given on Fig. 6.49 we see that the reduction in the amplitude of the second harmonic is less than was obtained in practice. The comparison also shows that further reductions in the values for the first and third harmonics could have been expected.

687 The most likely cause of this error lies in the assumption that the branch line vibrates as a uniform rigid body solely along its axis. We know that this is incorrect from the results of the vibration levels recorded at the junction and the valve given on Figs. 6.41 and 6.42. Ideally, for a rigid line these should be identical. However, the approximation to a purely axial mode of vibration is necessary to simplify the analysis. If we assume that the line between the pump and valve 1 vibrates as a simple beam with fixed ends then we know that this can only be in one of several fixed modes. Some of these modes are illustrated on Fig. 6.50. It can be seen from this figure that unless the junction is situated at any anti-node for the particular mode of vibration encountered then the change in the attitude of the junction will impart a bending moment upon the branch line, as illustrated on Fig. 6.51. Clearly, the vibration velocity measured at the valve is only a component of the motion of the valve. More information is needed, therefore, before we can evaluate the full effect of the pipe vibration on the pressure ripple levels.

688 These results imply that there is no practical method by which the vibration effects on the pressure ripple in a typical hydraulic circuit can be represented.

Fortunately, this does not limit the application of the impedance model for pressure ripple standing waves in a system since it is desirable for any motion of the pipelines to be restricted in order to reduce the noise levels. The results do suggest, however, that the superposition theory, applied here, can be used to model systems which have more than one source of flow ripple.

DISCUSSION OF RESULTS

689 The results have shown that the impedance model can be used to define the pressure and flow ripple standing waves generated in a hydraulic system containing a single branch line. Furthermore, this successful application of the mathematical model for a single branch line implies that systems with more than one branch can be modelled with equal confidence.

690 Using the large amount of data obtained we have been able to show how, by careful selection of the length and position of the branch line, it is possible to bring about a useful reduction in the pressure ripple levels for specific frequencies. This applies to branch lines which are terminated by a component as well as those with closed ends.

691 In modelling the branched line circuit we used values for the valve impedance that were derived from the results for the extending pipeline tests. Hence, we have confirmed the reliability of these values. In addition, we have expanded the range of valve operating conditions for which we have impedance spectra. These spectra obtained for the different mean flow levels have again showed the complex nature of this simple type of valve.

692 Finally, we have seen how the pressure forces

in the system can give rise to significant levels of vibration and that this vibration of the pipelines can influence the pressure ripple levels. Although the attempt to incorporate the effects of the vibration of the pipelines into the impedance model was not an unqualified success, the theory of superposition outlined for this purpose can be usefully employed to model other systems which have more than one source of flow ripple. For example, systems with a pump and motor.

CHAPTER 7

A Series Pipe System

INTRODUCTION

701 The techniques developed in the previous chapters can be used to model the majority of hydraulic systems, including many with pipelines and components connected in series. That is systems which have changes in pipe section or those containing devices such as filters or attenuators, as these can be modelled using existing theory. Problems arise, however, when smaller, high impedance components, such as valves, are considered. These devices are energy dissipators, creating large pressure drops and very high flow velocities over short distances. This chapter is concerned with the detailed examination of the case of pressure wave transmission across these high impedance, highly turbulent regions.

702 Unlike branch lines, little or no work has been done which relates directly to this type of circuit configuration except for those concerned with the performance of various types of pressure ripple attenuators or silencers. Most of these attenuators are of the form of pipeline or chamber resonators as shown by Whitson (21) which are designed to attenuate the pressure ripple whilst introducing the minimum of pressure loss into the system. The length and/or volume of such devices is sufficient to allow standing wave effects to be created within them. Because they behave in this way we can model their effect upon the pressure ripple using straight forward adaptations of the transmission line theory already covered in this thesis. Filters have similar physical properties which, coupled with their low pressure drop, suggests that these too may be modelled in this way or as simple capacitive devices.

703 A large pressure drop across a valve results in very high flow velocities through the orifice which creates a region of turbulent flow immediately downstream of the orifice. In the worst cases where the high flow velocities cause the static pressure to fall below the vapour pressure of the fluid cavitation can occur. In addition, valves are normally small in length and volume which eliminates the possibility of standing wave effects being generated within them. However, the mean pressure levels downstream of a valve need not be negligible and it is feasible that significant pressure standing wave levels can be generated in this region.

704 In the work detailed below we aim to show that simple electrical circuit theory can be used in conjunction with the impedance model to predict the pressure standing wave levels both upstream and downstream of a valve. In order to do this we have to establish:-

i) the effect on the pressure wave of its passage through the valve orifice and the region of turbulence or even cavitation immediately after.

ii) the influence on the pressure standing wave upstream of the valve of the conditions downstream.

Once again the theoretical appraisal is supported by a wide range of experimental testing.

705 As with the branch line investigation, detailed in the previous chapter, we can simplify the investigation by using a test rig and test procedures based upon those used for the extending pipeline tests detailed in Chapter 3. Furthermore, by using the same circuit components operating under the same test conditions of speed, pressure and flow we reduce the number of conditions for which we do not have the required parameter values.

MATHEMATICAL MODEL OF A SERIES SYSTEM

706 The derivation of a mathematical representation for a hydraulic system with loads located along a single pipeline can be developed along similar lines to those used to establish the model for branched systems.

707 A simplified hydraulic system with a second loading device positioned downstream of an existing load is illustrated on Fig. 7.1. The first step in modelling this circuit is to represent the circuit in terms of its component impedances, as presented on Fig. 7.2. Now in order to model this arrangement we must assume that the first load Z_{T1} has no length, or more practically its length must be insignificant when compared to the wavelength of the flow ripple. This is true for the majority of valves used as in-line components. Exceptions may arise in cases where the pumps are run at high speed or when harmonics of an unusually high order are to be considered.

708 Assuming then that Z_{T1} has no length then no standing wave effects can be created within the component and so the flows at the entry and exit of this load are equal.

That is $Q_{in} = Q_{out} = Q_z$ the flow through Z_{T1}.

709 If we consider line 2 then the impedance of the pipeline and its termination Z_{T2} is given by the lumped impedance Z_{e2}, the impedance at the entrance to the line given by equation 4.2. Now the pressure at the entrance to line 2 is the pressure at the exit of valve 1, P_{out}, which is given by the product of the flow and impedance at this point. That is

$$P_{out} = Q_z Z_{e2} \qquad (7.1)$$

Similarly the pressure at the entrance to valve 1, P_{in}, is given by

$$P_{in} = Q_z Z_{in} \qquad (7.2)$$

where Z_{in} is the impedance at valve 1 as 'seen' from line 1.

If we assume that the impedance/flow relationship for the valve is as for steady state conditions then

$$(P_{in} - P_{out}) = Q_z Z_{T1} \qquad (7.3)$$

Substituting for equations 7.1 and 7.2, and eliminating Q_z we obtain

$$Z_{in} = Z_{T1} + Z_{e2} \qquad (7.4)$$

Hence the total impedance at the termination of line 1 is given by the vector addition of the impedances of the valve Z_{T1} and the lumped impedance Z_{e2} for line 2 and its termination.

710 By obtaining a single lumped impedance value for the termination of line 1 we have reduced the theoretical circuit model to one consisting of a pump, pipeline and termination as illustrated on Fig. 7.3. As with previous circuits of this kind, the pressure at any location can be determined using the transmission line equation 3.17. In like manner the flow at any point can be obtained using equation 3.18. We can therefore use these impedance models to determine the pressure and flow at valve 1, P_{in} and Q_z. Either of these parameters can be used as a reference level for evaluation of conditions in line 2.

711 If we assume that the system centred upon line 2 can be considered to be another simple pump, pipeline

and termination circuit then the system upstream of line 2 can be represented by a source flow Q_s' and a source impedance Z_s'. In this case we could use the transmission line equation 3.17 to determine the pressure levels within this system, provided that we had values for Q_s' and Z_s'. We can, however, obtain values for the pressure at any point along line 2, P_{x_2}, by forming a ratio between this pressure and the pressure at valve 1, P_{out}, as given by equation 3.17. That is P_{x_2} is given by:-

$$P_{x_2} = P_{out} \frac{\left(e^{-\gamma_2 x_2} + \varsigma_{T_2} e^{-\gamma_2 (2l_2 - x_2)}\right)}{\left(1 + \varsigma_{T_2} e^{-2\gamma_2 l_2}\right)} \qquad (7.5)$$

By combining equations 7.1 and 7.2 we can obtain a value for P_{out} from the value for P_{in} already obtained. Thus

$$P_{out} = P_{in} \frac{Z_{e_2}}{Z_{in}} \qquad (7.6)$$

Alternatively if we substitute for Z_{in} we get

$$P_{out} = P_{in} \frac{Z_{e_2}}{Z_{T_1} + Z_{e_2}} \qquad (7.7)$$

712 As an alternative to using this pressure/impedance relationship for valve 1 we can use the flow through the value Q_2 as the reference value for the analysis of the pressure levels in line 2. The pressure at the entrance to line 2 is given by equation 7.1, if we expand this expression by substituting for Z_{e_2} using equation 4.2 we get:-

$$P_{out} = Q_2 Z_{o_2} \frac{\left(1 + \varsigma_{T_2} e^{-2\gamma_2 l_2}\right)}{\left(1 - \varsigma_{T_2} e^{-2\gamma_2 l_2}\right)} \qquad (7.8)$$

To obtain the pressure at any point along line 2 we can again use the pressure ratio P_{x_2}/P_{out} as given by equation 7.5. If we substitute for P_{out} in this expression using equation 7.8 we obtain an expression for P_{x_2} based upon the flow through the valve Q_2. That is

$$P_{x_2} = Q_2 Z_{o_2} \frac{\left(e^{-\gamma_2 x_2} + \rho_{T_2} e^{-\gamma_2 (2l_2 - x_2)}\right)}{\left(1 - \rho_{T_2} e^{-2\gamma_2 l_2}\right)} \qquad (7.9)$$

713 We can see that the expression 7.9 is equivalent to the transmission line equation 3.17, where the source flow $Q_S = Q_2$ and the source impedance Z_S is infinite. This gives a reflection coefficient ρ_S of unity.

EXPERIMENTAL INVESTIGATION OF IMPEDANCES IN SERIES

Experimental Rig

714 To provide a practical evaluation of the pressure standing waves generated in a hydraulic system with impedances in series a suitable test rig was constructed. The test circuit used for the extending pipeline tests, described in detail in Sections 337 to 343, was constructed with a line 1.2m long. To this arrangement an additional straight section of pipeline, .72m in length, was attached to the outlet of the restricter valve. This second section of pipeline was also terminated by an identical 19mm. restricter valve as illustrated on Fig. 7.4. These two valves were previously shown to be identical in response during the testing of the branched line system in chapter 6.

715 To obtain the mean pressure level in line 2 a pressure gauge was attached just downstream of valve 1. As with the pressure gauge for line 1 precautions were taken to ensure that no standing wave effects were created in the gauge line. These are described in Sections 207 to 209. As there will be a pressure drop

across valve 1 then the oil temperature in line 2 will be higher than the oil temperature in line 1. This arises because the pressure drop is achieved by dissipating energy at the valve, the majority of which is picked up by the oil. This results in the oil temperature increasing by approximately $5^{o}C$ for every 100 bar drop in pressure across the valve. In order to monitor the mean temperature of the oil in line 2, a thermocouple was attached to the pipeline. This was taken to be the temperature of the oil once steady conditions were established.

716 The overall control of the oil temperature level has been simplified for this test arrangement by the addition of an automatic temperature control system. Control of the oil temperature for previous test circuits depended upon the expertise of the operator in controlling the flow of cooling water.

717 Lastly to moniter the pressure standing wave effects in line 2 two piezo electric pressure transducers were mounted in line 2, one close to each valve as illustrated on Fig. 7.4. The mounting blocks for these transducers are as shown on Fig. 2.2.

Test Procedures

718 Before turning our attention to the pressure standing waves generated within the system we must first examine and understand the nature of the pressure and flow regime present in or close to the first restricter valve. It is at this point that any interference with the straight forward transmission of the flow ripple across the valve, as proposed by the impedance model outlined above, would occur.

Pressure and Flow Across Restrictor Valve 1

719 The very high flow velocity produced as the oil

passes through valve 1 generates turbulence immediately downstream of the restriction. The degree of turbulence produced depends upon the magnitude of the flow velocity, the fluid viscosity and to some extend the geometry of the valve. In many cases the high flow velocity creates a large fall in the static pressure level and under these conditions cavitation will occur. The presence of cavitation greatly increases the magnitude of the flow disturbance.

720 If the impedance model derived above is to have any validity then the portion of any incident wave which is not reflected at valve 1 back towards the pump must pass freely through the valve. That is the wave must not be affected by the variations in the pressure levels and flow velocities or by the localised changes in the oil and pipeline characteristics which those variations produce, including changes in the pipe friction and bulk modulus of the oil. The possibility of interference to the transmitted wave will increase as the flow velocity and hence the turbulence increases. The worst case occurs when the flow velocity is high enough to cause the pressure to fall to the vapour pressure of the oil and cavitation can occur.

721 The violent process of cavitation, the alternate formation and collapse of vapour bubbles, gives rise to very high local pressures upto 1 GN/m^2 which can occur thousands of times a second. This continuous action results in considerable vibration and noise which may possibly interfere with the transmitted pressure waves. The causes and effects of cavitation and its influence on the performance of system components such as valves has been investigated extensively by, for example, McCloy (24). However, none of this work considered the effect, if any, of cavitation upon the propagation of pressure ripple through such a region. Several researchers showed that cavitation can be

eliminated by raising the pressure level downstream of the orifice, an effect that is illustrated on Fig. 7.5 which is taken from (24). In the test application considered here the restriction is located between two distinct pressure levels, with the lower downstream pressure set at a value which is a significant proportion of the upstream level. The mean pressure levels proposed for the system tests are given on table 7.1. It is possible, therefore, that no cavitation will occur during these tests.

722 To establish whether cavitation will be present for any of the proposed test conditions the pressure and flow characteristics for valve 1 were investigated using the test circuit shown on Fig. 7.4. The position rather than the frequency range of the piezo electric pressure transducer means that the pressure disturbance due to cavitation cannot be detected using this arrangement, another method of detection is required. A simple and yet effective method of detecting the presence of cavitation, which has been used to great effect by Tullis (25), is to mount an accelerometer onto the body of the valve. This picks up the vibration induced by turbulent flow and cavitation. This method was adopted and an accelerometer was attached to the valve body and the output was displayed on an oscilloscope.

723 To try out this test method the system was set up to give conditions in which valve 1 should cavitate. To achieve such a condition valve 2 was opened fully and valve 1 was adjusted to give a mean system pressure of 100 bar in line 1. With valve 1 set at this value, it is possible to increase the back pressure on valve 1 up to 100 bar without raising the pressure in line 1 above the 200 bar working limit.

724 The acceleration signal obtained at this condition was of a typically noisy form, rich in frequencies with fluctuating amplitude levels of large magnitude. This

type of vibration response is generally accepted as being consistant with the presence of cavitation. Slowly closing valve 2 to increase the back pressure on valve 1 did not produce any discernable change in the accelerometer signal until a pressure of 55 bar was reached. Continuing to increase the back pressure produced further reductions in the acceleration levels, which reached a minimum value when the back pressure had risen to 65 bar. Further increases in the back pressure up to 100 bar did not produce any further changes to the acceleration signal. The changes in the acceleration levels over this range of back pressures are shown on Fig. 7.6. Although these traces clearly illustrate the change from cavitating to non cavitating conditions, they lack definition, due to limitations of the recording equipment employed. Better defined traces obtained later clearly show the large variation in acceleration levels between cavitating and non cavitating conditions as shown on Fig. 7.7. These results confirm the effectiveness of this test method in detecting cavitation. Furthermore, it is possible, with careful control of the test conditions, to detect not only the presence of cavitation but also the various phases of cavitation, as was shown to great effect by Tullis.

725 The technique was used to examine the system with the valves adjusted to give each of the four proposed test conditions as listed on Table 7.1. However, rather than confirming the results to a simple yes or no indication of the presence of cavitation for each test condition the examination was incorporated into an overall evaluation of the pressure and flow characteristics for valve 1 at each setting. In this way a more detailed picture of the state of the system at each setting was obtained.

726 To determine these pressure/flow characteristics valves 1 and 2 were adjusted to give the required mean

pressure levels in lines 1 and 2 with the pump swash-plate set to give a flow of 0.7 l/s at 200 bar. Once steady conditions had been achieved the pump swash was reduced to give a flowrate of around .05 l/s, valve 2 was then readjusted to regain the required back pressure level. From this point the flowrate was increased over several incremental stages up to its original value. At each flow setting the back pressure was reset to the desired level and once steady conditions were established the pressure and flowrate were recorded. In addition, the accelerometer signals were observed so that the point at which cavitation occurred could be noted. This process was repeated for each of the proposed test conditions and also for an additional condition using a back pressure of 10 bar. This latter test was included to provide a more complete profile of the variation in the valve characteristics with setting and back pressure. 10 bar was the minimum pressure level that could be maintained easily by adjustment of valve 2 throughout the full range of pump flow. The pressure and flow characteristics obtained are shown on Fig. 7.8 which shows that cavitation is present when the system is set with a 50 bar pressure level in line 2. A further illustration of this is given on Fig. 7.9 which shows the valve acceleration levels for each test condition.

727 Now that we have established the nature of the flow regimes present at valve 1 for each of the test conditions we can turn over attention to the transient pressures either side of the valve. To begin with the pressures at P_3 and P_4 were monitored and recorded with the system operating at each of the four test conditions using a spectrum analyser. Details of the analyser are given in chapter 2. The pressure amplitude spectra obtained for P_2 and P_3 are shown on Fig. 7.10. It was observed during the testing that a reduction in the back pressure below 50 bar did not produce any discernable

changes in the spectra of either P_2 or P_3.

728 It is evident from these traces that a significant proportion of each incident wave reaching valve 1 is able to pass freely through the valve. Furthermore, these transmitted waves are of sufficient magnitude to be able to generate pressure standing waves in line 2. It is also significant that the results obtained with cavitation present do not show any obvious deviation from those for the other conditions. What cannot be ascertained from these results, however, is the affect upon the magnitude and phase of these transmitted waves of their passage through the valve. To investigate these effects we need to examine the pressure ripple standing waves in lines 1 and 2.

EXAMINATION OF THE PRESSURE RIPPLE STANDING WAVES IN LINES 1 AND 2

729 To investigate the pressure ripple standing waves generated either side of valve 1 the extending pipeline technique used successfully in the previous tests was again employed. In this application the length of line 2 was varied whilst that of line 1 remained the same. This creates the minimum of change in the system conditions whilst ensuring the maximum variation in the impedance at valve 1.

730 The variation in the entry impedance to line 2, Z_{e2}, effects the pressure ripple in each line in different ways. In line 1 only the impedance at the termination (valve 1) is affected, and this will be reflected by the pressure levels recorded at P_1 and P_2. The ripple in line 2 on the other hand is affected directly by the change in line length. As for the extending pipeline tests in Chapter 3. Secondly,

the changing conditions in line 1 give rise to different values for the flow entering line 2 for each new line length l_2 and so changing the amplitude and phase of the pressure ripple.

731 To obtain a reasonable degree of variation in the standing wave levels the magnitude of the entry impedance Z_{e2} needs to change by the maximum possible amount. We know from the analysis of equation 4.2 that this is achieved when the line length is altered by a value equivalent to one quarter the wavelength of the frequency considered. Thus l_2 will have to be increased or decreased over a distance of approximately 2.0m in this case.

Test Procedure

732 The experimental work was conducted as follows:- With reference to the circuit diagram given on Fig. 7.4 line 2 was reduced in length giving a value for l_2 of .37m. Valves 1 and 2 were then adjusted to give pressure levels of 50 bar in line 2 and 200 bar in line 1. Once steady conditions had been achieved, the pressure amplitudes and phases were recorded at each of the four transducer positions, P_1 to P_4. Further results were obtained using this circuit configuration with the valves readjusted to give mean system pressure levels in lines 1 and 2 respectively of 200/100, 200/150 and finally 206/200 bar, as listed on Table 7.1. In all cases the pressure levels were only recorded once the temperature levels had stabilized. The temperature values obtained for each test condition are given in Table 7.2.

733 This whole procedure was repeated several more times with line 2 extended by a small amount between each set of tests. A total of 32 different line lengths

were used which increased ℓ_2 from .37m upto 3.7m, approximately one half wavelength for the fundamental piston frequency. Thus the entry impedance to line 2, Z_{e_2}, will have undergone its maximum variation in magnitude.

Analysis of the Results

734 An initial examination of the test results reveals that the pressure amplitudes are lower than those obtained for any of the previous tests using the same mean pressure levels. However, the variations in the pressures in lines 1 and 2 appear superficially to support the proposed mathematical model. The pressure recorded in line 2 show a variation with line length similar to those obtained for the extending line tests described in Chapter 3. Furthermore, the pressure in line 1 exhibit less variation with line length although the degree of variation increases as the mean pressure in line 2 is increased.

735 To analyse the results in more detail we again begin with the section of the system furthest from the source of the flow ripple. Hence we start by analysing the pressure standing wave levels in line 2.

Standing Wave Effects in Line 2

736 To analyse the results obtained in line 2 we need to eliminate the effects introduced by the system upstream of line 2. We can do this by forming a ratio between pressures at any two points along line 2. If we assume that the system upstream of line 2 can be considered as a flow ripple source, as implied by the theoretical analysis given in Section 712, then the pressures at P_3 and P_4 can be derived using equation 7.9. If we now form a ratio using the expressions

for P_3 and P_4 we get:-

$$\frac{P_4}{P_3} = \frac{e^{-\gamma_2(l_2-x_4)} + \rho_{T2}\, e^{-\gamma_2(l_2+x_4)}}{e^{-\gamma_2 x_3} + \rho_{T2}\, e^{-\gamma_2(2l_2-x_3)}} \qquad (7.10)$$

Thus the, as yet, unknown quantity Q_L is eliminated and only the properties of the pipeline and termination are required.

737 The pressure amplitude ratio $|P_4/P_3|$ determined from the experimental results obtained for the test with 200 bar mean pressure in line 2 are shown plotted against line length l_2 on Fig. 7.11. This figure shows the familiar set of curves which were first derived for the extending pipeline tests described in chapter 3. In addition to the experimental values the figure also shows the theoretically derived amplitude ratios which were computed using equation 7.10 with the known pipeline parameter values and the valve impedance spectra previously determined in chapter 3.

738 As expected, good agreement was obtained between the theoretical and experimental pressure ratio values. The pressure ratio impedance model for a pipeline and termination has proved to be reliable for all circuit configurations. The accuracy of the model in this case is further emphasised by the results for the phase differences $(\angle P_4 - \angle P_3)$ which are shown on Fig. 7.12. In addition, the values predicted for the test conditions with 100 and 150 bar mean pressure in line 2 also produced good agreement with their corresponding experimental results. We may note that the valve impedance spectra used for these latter test conditions are not quite correct. An error arises because the constant pressure of 200 bar maintained in line 1 has

the effect of fixing the flowrate through the system to 0.7 l/s. Thus as the pressure in line 2 is decreased from 200 bar the greater the discrepancy in the impedance values. However, such errors can be regarded as insignificant when compared to the variations obtained for the valve impedance predictions.

739 It is clear that the basic fluid mechanics of the generation of pressure standing waves within a pipeline are unaffected by the presence of a highly turbulent region at one of its terminal regions. We are able, therefore, to predict with accuracy the pressure ratio P_4/P_3 which implies that we can obtain accurate values for the entry impedance, Z_{e2}. The accuracy of any predictions for the actual pressure levels in line 2 will depend upon the accuracy with which we can determine the value for the flow entering the system. In section 708 above we assumed that the flow entering line 2 is the same flow that entered valve 1, which is unaffected by its passage through the valve. We must, therefore, be able to obtain reliable values for the flows in line 1. However, before proceeding with the analysis of the conditions in line 1 we can derive the impedance for the additional valve setting with a system pressure of 50 bar.

Prediction of the Valve Impedance

740 Having established the validity of the impedance model for the pipeline and termination of line 2 then we can use the experimental results obtained with a mean pressure in line 2 of 50 bar to predict the impedance of the valve at this setting. As on previous occasions, the valve impedance was determined using the method outlined in detail in Sections 362 to 364. Briefly this consists of rearranging equation 7.10 so that the reflection coefficient ζ_{T2} can be determined using values for the pressure ratio P_4/P_3

obtained from the experimental results. Values for the valve impedance Z_{T2} can then be derived from these values of S_{T2} using equation 3.11.

741 The valve impedance spectrum obtained is given on Fig. 7.13. This spectrum is similar to those derived for the valve at the previous pressure levels as given on Fig. 3.16, as illustrated using the non dimensional plot of Z_T/Z_{Tss} on Fig. 7.14. It is clear that this latter spectrum is in harmony with the earlier valve spectra and again demonstrates the complex nature of the valve impedance.

742 As a final evaluation of the predicted valve impedance the pressure amplitude ratio $|P_4/P_3|$ and phase difference $(\angle P_4 - \angle P_3)$ were computed for values of line length ℓ_2 from 0 to 4m. These values gave good agreement when compared to their corresponding experimentally determined values.

Standing Wave Effects in Line 1

743 As expected the results for the pressure amplitudes and phases recorded at P_1 and P_2 in line 1 vary with the length of line 2. Furthermore, the degree of variation is dependent upon the mean system pressure in line 2. This is demonstrated on Fig. 7.15 which shows the results obtained for the first and second harmonics of piston frequency at P_1 for the 50, 100 and 150 bar mean pressure settings in line 2. It is clear from this figure that there is little effect on the standing wave in line 1 as a result of changes to line 2 with low pressure levels. However, as the back pressure is increased the change in the length of line 2 is reflected in the pressure levels recorded in line 1 as shown on Fig. 7.15.

744 As mentioned earlier the only parameter involved in the generation of the pressure ripple standing wave in line 1 that is affected by changes in conditions in line 2 is the impedance at the termination of line 1. Therefore, the variation in the pressure amplitudes and phases at P_1 and P_2 occur as a result of changes to the impedance encountered at valve 1 by the incident travelling waves. This termination impedance is provided by the combination of the impedance of the valve Z_{T1} and the impedance of the system downstream of the valve. That is line 2 and its termination, Z_{e2}.

745 If we consider the mathematical model proposed in Sections 706 to 713 we see that the first stage in the modelling process is to reduce the circuit to a simple pump, pipeline and termination as illustrated on Fig. 7.3. The termination impedance for this simplified circuit Z_{in} is given by the vector addition of the valve impedance Z_{T1} and the entry impedance to line 2, Z_{e2}, as given by equation 7.4. We know that the entry impedance Z_{e2} varies with line length l_2 and has a minimum value of Z_{o2}^2/Z_{T2} and a maximum value of Z_{T2}. Thus for a given flowrate the maximum value Z_{T2} and the maximum variation $(Z_{T2} - Z_{o2}^2/Z_{T2})$ increases with mean pressure level. This variation in Z_{e2} is mirrored by the pressure levels recorded at P_3 as shown on Fig. 7.16. The variation in the pressure levels in line 2 are not, however, repeated by the pressures recorded in line 1 over the same change in the length of line 2, as illustrated on Fig. 7.15. This difference arises because the effect of Z_{e2} upon the value of the lumped impedance Z_{in} is reduced by the addition of the constant impedance term Z_{T1}. This can best be demonstrated using a polar plot for the addition of the two complex quantities.

746 The graphical evaluation of the lumped impedance

Z_{in} is illustrated on Fig. 7.17, which uses the impedance values for the first harmonic of piston frequency applicable to the 100 bar test condition. The figure snows the vector Z_{T1} and the vector locus for the entry impedance Z_{e2} which is generated at the length of line ℓ_2 is increased from zero. The latter gives a clear indication of the change in phase and amplitude of Z_{e2} with increasing line length. The effect of pipe friction is also shown, as a loss-less line would produce a circular locus. For the test conditions used, and this will be discussed later, it is assumed that the valve impedances Z_{T1} and Z_{T2} are the same. Thus the maximum value for the lumped impedance Z_{in} will be $2Z_T$, where $Z_T = Z_{T1} = Z_{T2}$, which occurs when ℓ_2 is zero. This maximum value is shown as the starting point for the resultant vector locus of Z_{in}. Examination of this new locus shows that the total variation in the phase of Z_{in} due to changes in the pipeline length has been reduced when compared to the locus of Z_{e2}. Furthermore, the change in the amplitude of Z_{in} for different pipeline lengths has been diminished. It is clear, therefore, that for this system a larger value for the constant term Z_{T1} will further reduce the influence of the variable element Z_{e2} as the resultant vector locus of Z_{in} is moved away from the axis of the polar plot. Alternatively, similar changes in the values for Z_{in} can be brought about by reducing the spread of the locus of Z_{e2}, which is achieved by reducing the value of its termination impedance Z_{T2}.

747 If we consider the test conditions employed we see that as the impedance of valve 2, Z_{T2}, is increased, to raise the mean pressure in line 2, then the impedance of valve 1, Z_{T1}, has to be reduced, to maintain a pressure in line 1 of 200 bar. Thus for each change in test conditions the increase in Z_{T2} and decrease in

Z_{T1} both contribute to an increase in the amount by which Z_{in} is affected by changes in the length of line 2. The results for the pressure amplitudes at P_1 given on Fig. 7.15 follow these proposed changes in the termination impedance Z_{in} and so support this lumped parameter model.

Examination of the Values Predicted for the Lumped Termination Impedance Z_{in}

748 To validate the impedance model for the termination impedance to line 1, Z_{in}, we can employ the pressure ratio technique as used for previous evaluations of predicted termination impedance spectra, as described above in Sections 352 to 354. The formation of a ratio between pressures at any two points on the line eliminates the pump parameters from the transmission line equation as given, for example, by equation 7.10.

749 The pressure amplitude ratios for P_2/P_1 determined from the experimental results obtained with back pressure levels, in line 2, of 50, 100 and 150 bar are shown plotted against line length l_2 on Figs. 7.18, 7.19, 7.20. The variation in the values of P_2/P_1, shown by these figures demonstrates the influence of the entry impedance Z_{e2} on the overall termination impedance value Z_{in}, as suggested by the mathematical model. The increase in the degree of variation with the back pressure level in line 2 is clearly shown.

750 To compute values for the pressure ratio $|P_2/P_1|$ we need to predict values for the lumped termination impedance Z_{in}, for each value of line length l_2 used. The variable term Z_{e2} can be evaluated using the entry impedance equation 4.2. Unfortunately, the impedance spectra for valve 1 is not known for these precise

conditions. Although the pressure drops and flows for the valve settings are the same as those for which the valve impedance spectra have been determined, Figs. 3.15 and 7.13, the actual valve settings differ because of the different back pressure levels. However, the results for the pressure and flow characteristics obtained earlier for the valve at these settings produced steady state impedance values similar to those obtained previously with zero back pressure. This, in conjunction with the known pattern of variation for the valve impedance spectra with both mean pressure and flow as given by Figs. 6.16 and 7.14, suggests that little error will be introduced if these established impedance spectra are used.

751 Values computed for the pressure amplitude ratio $|P_2/P_1|$ are shown, plotted against line length ℓ_2, alongside their corresponding experimental values on Figs. 7.18, 7.19 and 7.20. We can see that these theoretical values gave good agreement with the experimental results. If we are very critical then we could say that the agreement between the theoretical and experimental values is not as precise, in some instances, as that obtained with earlier pressure ratio values. This implies that the lumped termination impedance model is inaccurate. However, considering the nature of the problem it is felt that the accuracy achieved is acceptable. Nevertheless, we will reassess this result when we consider the predictions for the individual pressure levels in line 1.

752 Similarly, the results obtained for the pressure phase differences $(\angle P_2 - \angle P_1)$ gave the same variation with line length ℓ_2 and back pressure level, as shown by Figs. 7.21, 7.22 and 7.23. In addition, these figures show the good agreement that was obtained between the theoretical values computed for $(\angle P_2 - \angle P_1)$ and their corresponding experimental values.

MODELLING THE PRESSURE LEVELS IN LINE 1

753 Now that we have a suitable model for the termination impedance Z_{in} for the theoretically simplified test circuit we can consider the individual pressure levels in line 1. The pressures at any point along the line can be derived using the transmission line equation 3.17 with a reflection coefficient ρ_T given by:-

$$\rho_T = \frac{Z_{in} - Z_{o1}}{Z_{in} + Z_{o1}} \qquad (7.11)$$

The pump parameter values of Q_s and Z_s are known for this test condition and these are given on Figs. 3.19 and 3.25.

754 The pressure amplitude and phase were computed for the pressure at P_2 for the test condition with 150 bar mean pressure in line 2. These values were derived using values for the line length ℓ_2 increased in small increments from 0 to 4m in determining the termination impedance Z_{in}. The results, plotted against line length ℓ_2, are shown on Figs. 7.24 and 7.25. The corresponding experimental results are also shown on these figures, which show good agreement with the theoretically predicted levels.

755 Good agreement was also obtained for the pressures predicted at P_1 at this condition and also for pressures P_1 and P_2 for the tests with 100 and 50 bar mean pressure in line 2. The discrepancies found with the pressure ratio predictions, discussed above, were not reflected in these results. Any errors in the predicted termination impedance Z_{in} indicated by the pressure ratio results do not appear to have introduced any significant errors in the evaluation of the individual pressure levels. These results suggest,

therefore, that we have a valid model for the termination impedance Z_{in}.

MODELLING OF THE PRESSURE LEVELS IN LINE 2

756 The final stage of this investigation is the mathematical evaluation of the pressure ripple standing wave that is generated in line 2. To evaluate the pressure levels we must first determine the pressure or flow at valve 1. That is P_{in} or Q_z. Either of these values can be used as a reference level from which the pressures along line 2 can be derived, as described in Sections 711 and 712 above. We know from the analysis of line 1 given above that both the pressure and flow at valve 1 can be predicted with a reasonable degree of confidence. For this analysis of line 2, however, we will use the flow through the valve Q_z as the parameter more readily associated with the transmission of the fluid ripple from line 1 to line 2.

757 The flow through the valve Q_z is given by the transmission line equation 3.18 with $x = \ell_1$. Once the flow has been established for a given test condition then the pressure at any position along line 2 can be determined using equation 7.9. Using these two expressions the amplitudes and phases for the pressure at P_3 and P_4 were computed using values for the line length ℓ_2 increased in small increments from 0 to 4m for each of the test conditions. The results for the pressure amplitude and phase at P_3 for the test with 150 bar mean pressure in line 2 are shown plotted against line length ℓ_2 on Figs. 7.26 and 7.27. The corresponding experimental results are also plotted on these figures, which show good agreement with the theoretical values. Good agreement between theoretically predicted pressures and their corresponding experimentally obtained values was also

obtained for the other results at P_3 and for the results at P_4.

758 We have already established that the system centred upon line 2 behaves in a predictable manner with regard to the generation of the pressure ripple standing wave using the pressure ratio P_4/P_3 as shown in sections 736 to 739 above. Clearly, the accuracy achieved for the predictions of the pressures at P_3 and P_4 is a measure of the 'source flow' and 'source impedance' values employed. The results obtained here, therefore, confirm the validity of the impedance models for the series pipeline circuit, in particular those represented by equations 7.4 and 7.9. It follows that the flow ripple Q_z passed through the valve without hindrance, even with cavitation present.

SYSTEMS WITH LOW IMPEDANCE LEVELS - VALVE 1 FULLY OPEN

759 Apart from confirming the effectiveness of the pipeline impedance model for line 2, as outlined in Sections 736 to 739 we have so far ignored the results for the tests carried out with valve 1 fully open. Discussion of this particular test condition has been left until now as it represents a limited range of system conditions. For many in-line system components a significant pressure drop is intrinsic to their method of operation. There are, however, components such as non-return valves which are designed so as to cause the minimum of restriction to the oil flow. There are also many applications where components such as directional control or restrictor valves will encounter such operating conditions.

760 Initial examination of the results reveals that there are much larger variations in the pressure levels

recorded in both lines as the length of line 2 is increased. This is to be expected due to the increased mean pressure level in line 2 which raises the value of the valve impedance Z_{T2} whilst reducing the impedance of valve 1, Z_{T1}. As Z_{T1} is reduced to these minimal levels the lumped impedance value Z_{in} approaches the value of the entry impedance Z_{e2}. Thus, the standing wave patterns will approach those for a single uninterrupted length of pipeline. We can look for such a convergence in the standing wave patterns by comparing the values for the pressure amplitudes recorded at P_1 and P_4 with those recorded at the corresponding positions P_p and P_T for the extending pipeline tests described in Chapter 3. These comparisons are shown on Figs. 7.28 and 7.29. Note that in order to compare these two sets of results the line lengths for the series impedance tests are the total lengths from the pump to valve 2, given by $(l_1 + l_2)$.

761 We can see from these figures that, as predicted by the mathematical model, the addition of a low impedance component to an existing circuit does not create any large scale variation in the standing wave patterns. This does not mean, however, that its effect is insignificant. The results show that there has been a distinct attenuation in the peak amplitude levels which could have a significant effect on the noise levels generated by a system.

762 As with the previous test conditions, we can predict the pressure levels in the system provided that we have a value for the impedance of valve 1. With such a low impedance level, $Z_{T1ss} = 1{\cdot}5 \times 10^{10}$ N.s.m.$^{-5}$, any small variations with frequency will become insignificant when it is combined with Z_{e2} to give the termination impedance for line 1, Z_{in}. Values for the pressures were computed, therefore,

using the steady state value $Z_{T_1 ss}$, which when compared with their corresponding experimental results gave good agreement. This is demonstrated using the values for the pressure at P_3 on Figs. 7.30 and 7.31.

DISCUSSION OF RESULTS

763 The results have shown that the impedance model can be used, with minimal additional theory, to define the pressure and flow ripple standing waves generated in a hydraulic system with two valves situated along a single pipeline. In proving the mathematical model we used conditions of mean pressure and flow that are applicable to practical hydraulic systems. The success of the model for this circuit implies that systems with more than two valves positioned along a single pipeline can be modelled with equal confidence.

764 We showed how conditions downstream of the first value can affect the pressure ripple levels upstream of the valve. The degree by which the pressure levels are affected depends upon the relative impedances of valve 1 and the entry impedance to line 2. Where the interaction is significant, it is possible to reduce the pressure ripple levels at specific frequencies by careful positioning of the valves relative to the pump and to each other. This aspect of circuit design can be usefully employed along with tuned length branch lines to reduce the pressure ripple levels at specific frequencies.

765 In the course of computing the pressure ripple values for the circuit we used values for the pump and valve impedances which were determined earlier from the results of the extending pipeline tests given in Chapter 3. We have once again, therefore, confirmed the accuracy of these impedance values.

In addition, we also extended the range of operating conditions covered by valve impedance spectra by predicting values for the 50 bar mean pressure condition.

CHAPTER 8

Reducing Fluid Borne Noise at the Design Stage

INTRODUCTION

801 With the work undertaken so far we have shown that the pressure and flow standing wave values can be modelled reliably for most hydraulic systems, operating with steady conditions of speed, pressure, flow and temperature, provided that the impedance values of all the components in the system are known. There are obviously a number of areas which require further investigation. These areas of uncertainty, many of which are under consideration at this time, are outlined in sections 807 to 829 below as suggestions for future work. This does not prevent us, however, from looking ahead to the uses of such a comprehensive system model.

802 The major benefit of having the ability to predict pressure ripple, or to use the more relevant expression fluid borne noise (FBN), levels in a hydraulic system lies in its use as an aid to designing quieter systems.

803 The total airborne noise level produced by a hydraulic system results from the mechanical vibrations present in all parts of the system. The vibration originates in those components which put power into or take power from the hydraulic system. Thus the main sources are the prime mover, pump, motor and valves. These vibrations are transmitted from their component sources to all other components to which they are mechanically connected. This transmission of vibration throughout the system is known as structure borne noise (SBN). Hence the reduction of noise made by a hydraulic system is fundamently a vibration problem, with FBN as a major source of vibration. Furthermore, the fluid provides a transmission path which ensures that this FBN is present in all parts of the circuit. It is the reduction in this source

of vibration that we are concerned with here.

804 A number of investigators have produced work outlining methods for reducing the noise levels of hydraulic systems. Some of these relate to individual components whilst others such as (26), (27), (28) and (29) are presented in the form of guidelines to assist designers of hydraulic equipment. The guidelines outline in detail methods for reducing the vibration or noise from each component in a system. However, the basic approach to noise reduction can be divided into three categories.

1) Insulate the system. Totally enclose the system in an acoustic encloser or insulate sections of the system with cladding.

2) Eliminate the sources of vibration. Select components which produce lower levels of vibration or improve the design or construction of existing components.

3) Restrict the transmission of the vibration through the system. Use anti-vibration mounts, flexible hose, pipe clamps with a high damping factor and FBN attenuators.

805 Although these guidelines deal comprehensively with ways of reducing airborne and structure borne noise the suggestions for reducing FBN levels are limited. It is the aim of the work detailed below to suggest and discuss methods of reducing the FBN levels in any hydraulic system.

806 The predominant factor governing the level of FBN in any hydraulic system is the magnitude of the flow ripple generated by the pump. This flow ripple can be reduced but not eliminated. There will, therefore, always be a degree of FBN in any hydraulic system. For a given pump the magnitude of the FBN will depend upon the impedance of each of the components

in the system and the design of the pipe network. It is possible, therefore, to minimise the levels of FBN generated in any system by paying particular attention to the selection of suitable components and to the design of the pipe network. In the sections that follow the criteria for selecting each system component are examined. In addition, the work shows how the ability to represent mathematically the FBN in a hydraulic system can be used to design the pipe network so that the FBN levels are kept to a minimum or at least the worst possibilities are avoided.

SUGGESTIONS FOR FUTURE WORK

807 The main areas which require further investigation can be sub-divided as follows:-

1) Component impedances.
2) Systems with more than one source of pressure ripple.
3) Pressure ripple in low pressure lines.
4) Component parameter values which vary with time.

Component impedances

808 To be able to predict FBN levels in a hydraulic system the impedance values of all the circuit components must be known, under all conditions of operation. Ideally, these values would be given by mathematical models based upon the detail design and steady state operating characteristics of the components. An accurate mathematical representation of the impedance of a component is a useful tool for evaluating changes in design. If these individual component models are used in the evaluation of the overall system model then the amount of data required can be greatly reduced.

809 Assuming that the FBN levels can be defined using values for ten harmonics of the fundamental pumping frequency (Gear, vane or piston frequency) then ten values of amplitude and phase are needed to define the impedance of a component at a single operating condition. Thus a large amount of data would be required even for a simple system with few components. Furthermore, the impedance of a simple component, such as a variable restrictor valve, varies with pressure, flow and frequency, as shown on Figs. 3.17 and 6.16. Thus for systems operating over a range of pressures and flows it is clear that the amount of data required would be unacceptably large. With individual component models, however, only the values of the mean system pressures and flows at each operating condition would be required. The relevant component impedance values would be computed prior to the evaluation of the FBN levels.

810 The majority of the work undertaken to date has been concerned with modelling the impedance and flow of various types of pump. For example, Kelsey (16), Bowns (12), Davidson (13) and Edge (30). This concentration of effort around the pump impedance, and more specifically the pump flow, is to be expected. Minimising the pump flow ripple is the most effective method of reducing the FBN levels in any system. However, it is evident from the work done that the flow ripple can be reduced but not eliminated. It is clear, therefore, that a similar amount of attention will have to be devoted to establishing impedance models for the remaining circuit components.

811 Before such mathematical representations become available the impedance and flow values for each component will have to be derived experimentally. The test procedures developed for this purpose will

also be needed to verify the various mathematical models as they are derived. A simple practical method of establishing the impedance values for any component and in the case of pumps and motors the flow ripple values is therefore required.

812 The extending pipeline test, used for the majority of the experimental work described in this thesis, can be used for this purpose. The large number of results that can be obtained using this method serves to improve the reliability of the impedance and flow valves. Unfortunately, both the experimental procedure and the processing of the data to give the impedance or flow values are very time consuming. A more practical procedure is required.

813 As with the theoretical investigations into component parameters the work undertaken to find an acceptable test method has concentrated on pumps. The high impedance pipeline and expansion chamber tests, outlined in Chapter 4, are representative of the type of test method required. These particular test methods lacked the accuracy of the extending pipeline test and it may be necessary, due to the nature of pressure ripple generation and measurement, that some loss of accuracy will have to be accepted in order to obtain a simple test method.

814 At present the most promising test method appears to be the 'hydraulic trombone' as described in Wing (31). This is essentially a simplified form of the extending pipeline test. The 'trombone' arrangement provides a simple means of varying the length of the pipeline. This, together with the use of a number of transducers positioned along the line, enables a large number of values to be obtained in a

relatively short period of time. The data can be rapidly processed by a computer to give reliable values for Q_s and Z_s. It is also possible to adopt this method to determine impedance values for other circuit components.

Systems with more than one flow source

815 These include:-

1) Pump and motor transmission circuits.
2) Boosted suction line circuits.
3) Multiple pump systems.

816 Pump/motor and boosted suction line circuits are similar systems when considered as impedance models. Both contain two sources of flow ripple positioned at opposite ends of a length of pipeline. Consider a simple pump/motor circuit as illustrated on Fig. 8.1. This shows the two sources of flow ripple, the pump Q_{sp} and the motor Q_{sm}. To analyse this type of system it is considered as two separate circuits. In one circuit the pump is the source of flow ripple Q_{sp} and the motor is the termination Z_{tm}. In the other circuit the roles are reversed, as illustrated on Fig. 8.2. To determine the pressure levels for the complete system the values derived for each of these separate circuits are combined using the principle of superposition as outlined in Sections 681 and 682.

817 Thus the pressure at any point x along the pipeline may be determined for each system using equations 8.1 and 8.2.

For the pump as flow source

$$P_{px} = \frac{Q_{sp} Z_{sp} Z_o}{Z_{sp} + Z_o} \frac{\left(e^{-\gamma x} + \varsigma_{tm} e^{-\gamma(2l-x)}\right)}{\left(1 - \varsigma_{sp} \varsigma_{tm} e^{-2\gamma l}\right)} \qquad (8.1)$$

and for the motor as flow source

$$P_{mx} = -\frac{Q_{sm} Z_{sm} Z_o}{Z_{sm} + Z_o} \frac{\left(e^{-\gamma x} + \varsigma_{tp} e^{-\gamma(2l-x)}\right)}{\left(1 - \varsigma_{sm} \varsigma_{tp} e^{-2\gamma l}\right)} \qquad (8.2)$$

and the total pressure at any point x is given by the vector sum of the two separate pressure valves.

That is $$P_x = P_{px} + P_{mx} \qquad (8.3)$$

818 Unfortunately, this simple pump/motor transmission circuit does not represent a practical system. A pressure relief valve would normally be included to limit the pressure level between the pump and the motor, as shown on Fig. 8.3. Nevertheless, the analysis remains the same except that a branch line and relief valve must be included in the circuit model in accordance with the method outlined in chapter 6.

819 The same analysis can be used to describe boosted suction lines. In this case the flow sources are the boost pump Q_{sbp} and the main system pump Q_{sp}. A typical boost circuit is illustrated on Fig. 8.4. Tests performed on such a system, Freitas (32), showed that the pressure ripple downstream of the main pump contained components at the harmonic frequencies associated with the boost pump. The

amplitudes of these components were below 1 bar when the boost pressure was 3.5 bar but they increased dramatically as the boost pressure was increased. This suggests that the lowest possible boost pressure levels should be used. The reverse did not apply. Changes to the main system pressure did not affect conditions in the suction line.

820 It is probable, therefore, that the same effects would occur with pump/motor systems in which conditions downstream of the motor could be affected by those between the pump and motor. This is particularly relevant when the pump/motor system is in the form of a closed loop as illustrated on Fig. 8.5. In this circuit we have all the possible system configurations, branch lines, impedances in series, pump/motor circuits and boosted suction line. It is the interaction between the different sections in this type of circuit that needs to be examined further.

821 Systems using two or more pumps to provide a variable flow source can be dealt with in a similar manner to pump/motor or boosted suction line circuits. A typical multipump system is shown on Fig. 8.6, in this type of circuit each pump is considered in turn to be supplying a system in which the other pumps are regarded as terminations. The pressure levels for the complete system are obtained by the superposition of the pressures determined for each of the individual circuit models.

Low Pressure Lines

822 These are either:-

1) Unboosted suction lines.
2) Return lines.

823 Pressure ripple standing waves are generated

in unboosted suction lines as a result of the flow ripple created at the pump inlet. It is important that we avoid large amplitudes in this line. If a large amplitude pressure ripple is superimposed upon a mean pressure level that is normally at a below atmospheric pressure it is possible to create conditions, at the inlet to the pump, in which cavitation can occur.

824 Initial tests, Tilley *et al* (33), have indicated that the transmission line equations 3.17 and 3.18 can be applied to suction lines, provided that air release and cavitation do not occur. Further tests are needed to extend the analysis to cover the effects of air release and cavitation. In addition, further work is required to establish the impedance and flow values for the inlet side of pumps, Q_{sin} and Z_{sin}.

825 Return lines do not present the same problems as suction lines. Cavitation and air release are common occurances in these lines and, although such conditions are not desirable, they can be accommodated without causing loss of system performance. This problem has, to some extend, already been considered during the investigation into systems with impedances in series, Chapter 7. The results obtained with a low mean pressure level downstream of the first valve are indicative of the pressure ripple levels that can occur in return lines. Fig. 7.11 shows the pressure ripple amplitudes generated in this low pressure line.

826 From the work on impedances in series we know that the pressure ripple levels generated in a return line will depend upon the levels created in the main system. It should be possible, therefore, to predict the pressure ripple levels in the return line once the pressures at the termination to the main system have been established. Furthermore, in many systems the return lines from each individual termination are

brought together into a single pipeline connected to the reservoir. With this type of circuit configuration the theory of superposition, as outlined above in Section 816, can be used to obtain the final pressure levels.

Component Parameter Values which Vary with Time

827 Any changes that occur in the system parameters of pressure and flow are brought about by changes to one or more of the component impedances. For example closing a valve, changing the position of an actuator, altering the angle of the pump swashplate. Except for changes in the pump speed, in which case the pump impedance remains constant but the frequency and value of the flow ripple are altered. The effect upon the FBN which may result from changes in frequency, flow or impedance during the operation of a hydraulic system will depend upon:-

1) the rate of change of the frequency, flow or impedance with time.
2) whether the variation is continuous or at discrete intervals.
3) the frequency of the variation.

828 If the rate of change is slow or occurs at discrete, infrequent intervals of time then the FBN levels can be considered at each stage, where the conditions are steady. However, when the changes are continuous or occur at frequent time intervals then the influence on the FBN will depend upon the frequency of the variation. If the variation is continuous but at a low frequency then the FBN can be considered at a number of discrete operating conditions. When the variation is at a higher frequency, significant when compared to the fundamental pumping frequency, then the variation will

have to be accounted for in the mathematical model.

829 It may be possible to incorporate the variation in the impedance model of the component or alternatively present it in the form of a secondary flow source, depending upon the type of component. Ultimately, however, it may be necessary to revert to first principles and re-establish the standing wave equations incorporating time as an additional system parameter.

ASPECTS OF CIRCUIT DESIGN

830 When designing systems to give low levels of FBN the designer begins by selecting the most suitable components. The criteria on which to base the selection of a component differs for each type of component. However, they can be grouped together under three headings.

i) Sources of flow ripple
ii) Pipelines
iii) Circuit components.

Sources of Flow Ripple

831 Pumps and motors as the sources of flow ripple are the most important components in any hydraulic circuit. The values of source flow Q_s and source impedance Z_s have the greatest influence on the pressure and flow ripple standing wave generated in any system, as given by equations 3.17 and 3.18. It is preferable, therefore, to use pumps or motors which have low values of Q_s and Z_s . Selection of a pump or motor on the basis that it does not have a large variation in flow delivery, a low value of Q_s, will often provide an additional benefit of reduced vibration levels, as a more even flow delivery provides a more even loading of the pumping mechanism, as

described by Helgestad et al (1). The same will also apply to motors.

832 The application often dictates the type of pump or motor to be used. Pumps are selected on the basis of pressure, flow and speed whereas motors are selected on a basis of torque and speed requirements. However, where it is possible to use different types of pump or motor significant benefits, in terms of reduced FBN levels, can be obtained by selecting the best type of unit. For example it is known that, in general, internal gear pumps have the lowest values for Q_s, next come external gear pumps and vane pumps and finally piston pumps. As detailed in Bowns et at (12). This would suggest that whenever low FBN levels are required it would be preferable to use internal gear pumps.

Pipelines

833 The first choice to be made is whether to use rigid pipelines or flexible hoses. Flexible hose has to be used where there is relative movement between components. In other parts of the circuit flexible hoses are primarily used to reduce the transmission of SBN. They can be used to isolate the sources of vibration (pumps, motors, valves, etc.) from the rest of the circuit. In the remainder of the circuit it is normal to use rigid pipelines as these radiate less noise than flexible hoses of the same length, as demonstrated by Crook et al (34).

834 The effectiveness of a flexible hose as an attenuator of SBN increases with frequency and length (34). Furthermore, the degree of attenuation varies with the type of hose used. The stiffer types of hose, steel braided or wire wound, give less attenuation than the more flexible textile or nylon braided types

as noted by Hughes et al (35).

835 Flexible hoses can be used to attenuate FBN levels, however, the degree of attenuation obtained is less than that for SBN. Much longer lengths of hose are needed to produce significant reductions in FBN levels (34). As with SBN the attenuation increases with frequency and length, and the degree of attenuation varies with hose construction (35). It is no surprise, therefore, to find that the greatest reduction in FBN is obtained when using nylon braided hoses. Such hoses are limited in use by their low pressure rating, but they can be usefully employed in suction or return lines to reduce both SBN and FBN. In general, however, it is clear that flexible hoses do not provide a satisfactory method of reducing FBN.

836 Selection of the pipe sizes is based upon the pressure drops created at the maximum flow conditions. The pressure losses due to the pipelines, bends and charges in section are part of the total load of the system. It is normal to try to limit these losses to less than 10 $^{o}/_{o}$ of the total load value. The pipe diameter has a large influence on the pressure loss values, as indicated by Poiseuille's equation 3.26. The larger the diameter of the pipe the lower the pressure loss. There are, however, practical limitations such as size and expense which suggest that there is an optimum pipe size for each application.

837 The generation of pressure ripple standing waves is also influenced by changes in the diameter of the pipeline. Variations in the cross sectional area A and friction factor R effect both the characteristic impedance Z_o and propagation constant γ as defined by equations 3.8 and 3.5. The sensitivity of these parameters to changes in pipe diameter are illustrated on Figs. 8.6 and 8.7.

838 The real part of the complex propagation constant, $R_e(\gamma)$, represents the degree of attenuation imposed on the pressure ripple as it passes along the pipeline. In terms of decreasing the FBN levels an increase in this attenuation is desirable. However, this attenuation would be achieved at the expense of increased pressure losses, adding to the total system load. This, in turn, would necessitate a higher pressure level at the pump, increasing the flow Q_s and impedance Z_s and hence the pressure ripple in the system.

839 The effect of changes in the characteristic impedance, Z_o, is not so clearly defined. Its influence on the FBN levels depends upon the changes that occur in the values of the various reflection coefficients, as defined by equations 3.11 and 3.14. Since these are complex values variations in both magnitude and phase have to be considered. A reduction in the amplitude of Z_o will not necessarily result in a reduction in the amplitude of the reflection coefficient. Furthermore, even if such a reduction was achieved it is unlikely to create any significant reductions in the FBN levels. This suggests, therefore, that the influence of the pipe diameter on the FBN levels need not be taken into consideration when sizing the pipelines for a system.

840 The selection of the lengths for each pipeline is much more important. It is also the most difficult. Changes in the lengths of pipelines or the positions of junctions or valves can have considerable effect on the pressure ripple levels in a system, as was shown in the work presented in the earlier chapters. To be able to determine the most beneficial lengths of pipeline and component positions it is necessary to consider the total system. Thus before any discussion of the arrangement of a system pipe network can commence the criteria for selecting the remaining circuit components need to be examined.

Circuit Components

841 When choosing the remaining circuit components the designer must avoid those components that have impedance values which would create resonance conditions. The type of component is dictated by the application. For example, pressure relief, flow control, etc. Thus the selection of a component on a FBN level basis can only be made from different makes of the same unit.

842 In many cases there will be no benefit in selecting a different component. Consider a simple component such as a restrictor valve. It has been shown, Chapter 3, that the impedance of such valves varies with setting and frequency. However, the impedance spectra does not include any resonant peaks. As such valves tend to be of a similar design and construction, it is unlikely that different valves, designed to operate at the same conditions of pressure and flow, would have differing impedance spectra. This also applies to larger components such as actuators, the size of which is dictated by the operational requirements of load, length of stroke and velocity. As it is the volume and/or length of an actuator that governs its impedance value then any actuator chosen for a particular application will have similar impedance values.

843 Components that are more complex in operation, such as pressure relief or flow control valves, can exhibit resonant peaks in their impedance spectra. These often coincide with the mechanical response of a component such as the first stage of a two stage pressure relief valve. In this way modular valve packs, commonly used in hydraulic systems for their compactness, which incorporate a number of different valves fed from a common manifold can contain several resonances. It should be possible, however, to represent such units using a lumped impedance model enabling

selection in the same way as for a single component.

844 It is clear that the selection of the circuit components does not demand the same degree of attention as did the selection of a 'quiet' pump. However, when we consider valves we have the additional problem of cavitation which is also a significant source of noise. It is probably better to select a valve on a basis of cavitation noise levels rather than on its impedance value.

845 For a given pump the FBN levels in a system depend upon the configuration of the pipe network. By paying careful attention to the design of the pipework, it may be possible to keep these FBN levels to a minimum. However, a reduction in the FBN levels can also be achieved by using a circuit component not mentioned so far, namely a FBN attenuator or silencer.

Fluid Borne Noise Attenuators

846 A more direct method of reducing the pressure ripple levels in a hydraulic system is to use a FBN attenuator or silencer. There are many different forms of silencer. Perhaps the simplest is the closed ended branch line which acts as a notch filter, as described earlier in Sections 657 and 658. After this come pipe resonators and expansion chambers which act over a broader frequency band. All these units are simple to design and construct to suit particular circuit requirements. At the top of the range of silencers are the more complex, hybrid types of silencer, designed to attenuate ripple frequencies over a much larger frequency range - typically from 200 to 2000 Hz. Whitson (21) details and compares the commonest forms of FBN silencers.

847 Selection of a suitable silencer is based upon:-

i) the frequencies to be removed.
ii) the amount of pressure drop that can be accepted.
iii) the space available.

848 The frequency content of the FBN in a system will depend upon the pump used and whether the drive is fixed or variable speed. Clearly the frequency content of a system can vary between a few harmonic frequencies covering a narrow frequency range to many, 15 or more, harmonics over a wide range of frequencies. There are, therefore, as many possible applications as there are types of silencer. However, the majority of systems will require a silencer that covers a broad frequency band.

849 The pressure drop created by the majority of silencers is relatively small. Some have no pressure drop as the main flow path is geometrically continuous. The highest pressure drops are created by the hybrid type silencers. This can be as high as 10 bar, but most create significantly lower levels. In those silencers which do create a pressure drop there is a relationship between the performance of the silencer, its size and the pressure drop. If a larger pressure drop can be accepted then a greater attenuation or a reduction in size can be achieved.

850 The amount of space needed to accommodate a silencer is often the factor limiting its use. The hybrid types of silencer are, in particular, relatively large. Typically these are cylindrical, 10 to 15 cm. in diameter and 0.5 to 1.0 m. in length. The dimensions of the silencer are dictated by the value of the lowest frequency to be attenuated and to a lesser degree the mean pressure level. The mean flowrate does not affect the size of the silencer. It is clear, therefore, that such a silencer can only be accommodated in the larger hydraulic circuits.

851 Silencers provide a simple solution to a large number of FBN problems. By attenuating the pressure ripple a silencer provides a relatively ripple free flow to the circuit downstream of its location. This can be particularly effective when the circuit is susceptible to the pressure forces created by the pressure ripple. However, the pressure ripple levels upstream of the silencer are not reduced and in some cases can be increased. The effectiveness of a FBN attenuator, in reducing the noise levels generated by a system, will depend upon whether the major source of noise is the circuit or the pump and prime mover. If the latter is the case the addition of a silencer will not cause any significant reduction in the overall noise levels, and in some instances may increase them. Thus the circuits most suited to using FBN attenuators are those in which the power pack, pump and prime mover, is positioned away from the main operation area.

852 Having selected the most suitable circuit components, the designer can now turn his attention to the arrangement of the pipe network. The layout of any system is normally dictated by the positions of the circuit components. However, even with fixed locations for the circuit components, different lengths of pipeline and different positions for junctions and bends can usually be used to achieve the same system configuration.

Circuit Configuration

853 In the work described earlier, it was shown how small changes in the arrangement of pipelines in a simple hydraulic circuit could produce large variations in the pressure ripple levels. In this way the pressure ripple could be attenuated at discrete frequencies. For example, a closed ended branch line could be used, which had a length equivalent to one quarter the wave-

length of the ripple frequency to be attenuated. Although such stub lines provide the highest levels of attenuation, any branch line that has a reasonably high termination impedance could be used with little reduction in the attenuation achieved. In the same way, judicious positioning of in-line components could produce similar benefits.

854 Attenuation of discrete frequencies could be advantageous for fixed speed systems. At best, a single tuned line will attenuate all the odd harmonics of the selected frequency. Although such tuned lines can only be designed for one operating condition, it may be possible to use a number of tuned lengths distributed throughout a system to provide a degree of attenuation for the predominant ripple frequencies. Mathematical derivations for the tuned lengths required, using rigid pipeline, are detailed in Appendix.

855 Although only rigid pipelines have been considered so far, flexible hose can be used in the same way. The transmission of pressure ripple through flexible hose is a more complex process, due to the flexibility of the hose wall. This interaction between the pressure ripple and motion of the pipe wall has been successfully represented by Longmore et al (36). It is possible, given the properties of the hose as defined by Longmore, to predict the pressure ripple levels in a flexible hose. The study of flexible hoses has shown that a degree of attenuation can be achieved using significant lengths of hose (35). Furthermore, tuned lengths of hose can be used to attenuate discrete ripple frequencies, although this is not in general a satisfactory method, as shown by Longmore (36).

856 In fixed speed systems operating with reasonably constant conditions of pressure and temperature tuned lines can be very helpful. If, as is more usual, the

system is variable speed or the operating conditions vary with time then these simple solutions become less effective. Nevertheless, as the FBN levels can be predicted for any system, it should be possible to determine the most suitable circuit configurations in order to reduce the FBN levels or at least avoid the worst conditions. An interactive computer program would enable a system designer to evaluate, quickly and efficiently, FBN levels for different circuit configurations or for the same circuit under different operating conditions. A problem arises when different circuits or system operating conditions are compared on a basis of their FBN levels. Some form of FBN factor is required which would allow an evaluation to be made of the relative merits of each system or operating condition.

POSSIBLE PARAMETERS FOR USE AS A FBN LEVEL FACTOR

857 Ideally a numerical or graphical representation of the fluid borne noise (FBN) within a hydraulic system should present the circuit designer with a measure of the potential noisiness of the system. This would enable objective comparisons to be made between different system configurations. In addition to this FBN factor a more detailed breakdown of the FBN levels throughout the system would identify the worst areas of the circuit. This would highlight, for the circuit designer, sections of the circuit where improvements may be possible. There are a number of parameters which could be used as measures of the noisiness of a system in terms of its FBN levels. These are:-

i) the entry impedance to the system,
ii) the maximum pressure levels
iii) the pressure standing wave ratio
iv) the mean pressure or root mean square of the pressure levels
v) the pressure forces

Entry Impedance to the System

858 It can be shown that the pressure at the outlet of a pump P_o, which is also the pressure at the entrance to the system, is given by:-

$$P_o = \frac{Q_s Z_s Z_{se}}{Z_s + Z_{se}} \qquad (8.4)$$

Where Z_{se} is the impedance for the system at that point. Thus for any given pump with parameters Q_s and Z_s the lowest value of pressure, P_o, would occur with the lowest value for Z_{se}. Furthermore, a low pressure level at the entrance to a system ensures low pressure levels throughout the system.

859 This single system impedance value can be computed knowing the system component parameters and pipework arrangements. Once determined, it provides a simple numerical value for at a glance comparisons between rival circuit designs. However, it is possible for two systems to have similar system impedance spectra yet differ greatly when considering their overall FBN levels. Furthermore, no specific information, regarding the worst areas of the system, can be derived.

860 Z_{se} is a convenient form of FBN factor, provided it is used only as a rough guide to system selection and design. To obtain a more detailed picture of the FBN levels, the pressure levels within the circuit will have to be considered. In this case, a more general term, rather than individual pressures at specific points, will be required.

Maximum Pressure Level

861 Maximum pressure levels predicted for each section of the circuit would provide some indication as to

possible problem areas. A mean of all the individual maximum pressure values would give a measure of the overall FBN level. However, if some form of pressure value is to be used as an indicator of system performance, it would be preferable to use a value that relates in some way to the vibration or noise levels created.

862 Unfortunabely, there is no simple, direct, mathematical link between FBN, vibration and airborne noise (sound) levels. Although unbalanced pressure forces have been shown to be a cause of vibration on a more general level, all that can be stated is that the vibration and airborne noise are related in some way to the magnitude of the pressure disturbance.

863 The pressure standing wave pattern is itself an envelope formed by the variation in magnitude of the disturbing frequency. Thus a single pressure amplitude value cannot represent the overall disturbance level. As an example, Fig. 8.8 shows two possible amplitude plots for systems A and B. Both have the same maximum pressure amplitudes but plot A represents the noisier system.

Pressure Standing Wave Ratio

864 The Pressure Standing Wave Ratio (PSWR) is the ratio of the maximum pressure level to the minimum pressure level, P_{max}/P_{min} . This improves the definition of the pressure disturbance, but as a ratio it does not give a true guide to the magnitude of the disturbance. For example, Fig. 8.9 shows two amplitude plots each with the same PSWR but plot A has the higher amplitudes and so represents the more noisy system. However, in both of the above examples, Figs. 8.8 and 8.9, the noisier system is that with the higher mean pressure level.

Mean Pressure or Root Mean Square Value

865 The mean pressure is given by:-

$$|P_{mean}| = \int_0^{\ell} \frac{|P|}{\ell} \cdot d\ell \qquad (8.5)$$

Although this is a single amplitude valve, it is more representative of the FBN levels than the maximum value, as shown on Fig. 8.8. However, when considering the generation of vibration or noise it is better to use a root mean square value. Since a RMS value is more representative of the energy of the pressure disturbance. The RMS value is given by:-

$$|P_{RMS}| = \sqrt{\int_0^{\ell} \frac{|P|^2}{\ell} \cdot d\ell} \qquad (8.6)$$

866 Values for $|P_{RMS}|$ in each section of the circuit would give a clear indication of the FBN levels. In addition, an overall measure, if required, of the FBN in a system could be derived by obtaining a mean value of all the individual $|P_{RMS}|$ values obtained.

Pressure Forces

867 Interaction between the pressure ripple and airborne noise levels in a system is via the motion of the pipelines. This occurs in two ways:-

i) through radial expansion and contraction of the pipe walls in response to the pressure fluctuations.

ii) through transverse vibration of the pipelines often generated by the unbalanced pressure forces created in each length of

pipeline.

868 The noise created by the radial expansion and contraction, or breathing mode, of a pipe is small in comparison to that produced by transverse vibration, as demonstrated by Kuhn et al (37). Furthermore, the pressure forces can be of sufficient magnitude as to cause vibration in the structure supporting the system. Values for all the pressure forces present in a system would, therefore, provide an extremely detailed representation of the probable noise level for the system.

869 The pressure force generated in a straight section of pipeline connecting two bends is given by:-

$$F_p = (P_2 - P_1)\, A \qquad (8.7)$$

where P_1 and P_2 are the pressures at each bend. Computation of the pressure forces for each straight section of pipeline in a circuit clearly requires a large amount of data regarding the pipework for the proposed circuit. In addition to the component impedances and pipe sizes required in the evaluation of Z_{se} or $|P_{RMS}|$ details of the position of every bend and junction in the circuit are also needed.

Choise of FBN factor

870 Of the parameters described above, the RMS value of pressure ripple provides the most convenient measure of FBN levels in a hydraulic system. These can be used as individual values derived for each section of pipeline or as a mean value to provide an overall FBN factor for a given circuit.

871 Pressure force values provide a more detailed picture of the noise potential of a hydraulic circuit.

However, the greater amount of information needed in the evaluation of these factors is an obvious limitation to their use. Especially when dealing with large and more complex system designs.

OTHER ASPECTS OF NOISE GENERATION

872 Measures of system performance based upon the FBN levels provide an indication of the potential vibration (SBN) levels generated in the system. These in turn indicate possible noise levels created by the system. Although the FBN, SBN and airborne noise levels are related, their interaction is very complex and cannot be represented mathematically. Nevertheless, in order to present a more representative measure of the noise potential of a particular system, some account should be taken of these various interactions. That is between FBN and SBN, SBN and airborne noise and, not forgetting, the relationship between the noise generated and the listener.

873 To obtain a better assessment of the noise potential of a hydraulic system, it may be possible to bias the FBN factors using expressions or values which take account of the major aspects of the generation and perception of noise associated with a mechanical system. The major aspects are the:-

i) mechanical response of the system to excitation
ii) generation of airborne noise (sound) due to vibrations of pipes or surfaces.
iii) response of the listener.

Mechanical Response

874 Due to the complex nature of most practical hydraulic circuits, the mechanical response of a system will include many resonant frequencies. A possible response curve is shown on Fig. 8.10. Such a system

can be said to have a high modal density.

$$\text{Modal Density} = \frac{\text{Number of Resonances}}{\text{Frequency Band}}$$

These resonances would include several fundamental natural frequencies and their harmonics.

875 It can be shown that the peak heights given by the displacement curve do not alter with frequency, for a given disturbing force. Even hysteretic damping has no effect on these peak values. It does, however, produce a small reduction in the widths of these peaks, as shown on Fig. 8.11.

876 If a system has a high modal density value then there would be a high probability that one or more of the resonant frequencies would coincide with one or more of the harmonics of the pressure ripple.

$$\text{Probability of resonant and ripple frequencies coinciding} = \frac{\Sigma \text{Peak Widths}}{\text{Frequency Band}}$$

Thus the probability depends upon the modal density and the hysteretic damping. Now for the majority of mechanical systems the modal density does not vary, and damping has little effect. Thus for a single disturbing frequency the probability will remain constant with frequency. If, however, the disturbance is created by pressure ripple there will be several harmonic frequencies to consider. In this case the probability will depend upon the number of harmonics in the frequency band considered.

$$\text{Probability} = \frac{\Sigma \text{Peak Widths}}{\text{Frequency Band}} \times \text{Number of Harmonics}$$

877 The number of harmonics in a given frequency band

will depend upon the fundamental frequency of the pressure ripple. Thus the probability will decrease, for a given frequency range, if the fundamental ripple frequency is increased.

$$\text{Probability} \propto \frac{1}{\omega}$$

It may be necessary, therefore, to apply a correction factor proportional to the inverse of the fundamental frequency, $1/\omega$, to any overall FBN factor when comparing systems. To take account of different pump speeds or number of pumping elements (Pistons, gears or vanes).

Generation of Airborne Noise

878 The relationship between vibration and airborne noise is often expressed in terms of Radiation Efficiency, σ. This is defined as the ratio of the actual acoustic power, W_A , to the ideal acoustic power, W_I.

$$\text{That is} \quad \sigma = \frac{W_A}{W_I} \qquad (8.8)$$

Although actual values of Radiation Efficiency, σ, cannot be derived for such complex systems, variations in its value with changes in the system conditions can be examined.

879 Fagerlund (38) showed that for a pipeline the radiation efficiency, σ , was directly proportional to the disturbing frequency when this frequency was below the coincidence frequency, ω_c . Where the coincidence frequency, ω_c , is defined as the frequency at which the propagation velocity of a flexural wave in the pipe surface is equal to the velocity of sound in the acoustic medium.

$$\text{That is} \quad \omega_c = \frac{\sqrt{3}\ a_o^2}{k\ a_s} \qquad (8.9)$$

where a_o = Velocity of sound in air
a_s = Velocity of sound in steel
k = wall thickness of the pipe

Given the pipewall thickness for pipelines used in high pressure oil hydraulic system the frequency range of the vibration due to FBN will always be below the coincidence frequency, ω_c . For example, with the 19mm. pipeline used in the work described earlier, with a

wall thickness of 2.05 mm, the coincidence frequency would be

$$\omega_c = 63 \text{ KHz.}$$

880 A correction factor proportional to the fundamental frequency, ω , of the FBN would, when applied to the FBN factors, take into account the increased noise levels associated with the vibration of pipelines in systems with higher pressure ripple frequencies. This does not, unfortunately, include the vibrating faces of the pump and valve bodies, etc. and the surfaces on which the components are mounted. It is known that the radiation efficiencies for these components will increase with frequency. However, the increase need not be proportional to the frequency but to some power of the frequency.

That is $\sigma \propto \omega^n$

Nevertheless, a correction factor that is proportional to frequency would provide a degree of adjustment. So allowing for more realistic appraisals of systems with different FBN frequencies.

Response of the Listener

881 A predominant factor in any evaluation of a noisy system is the effect of the noise generated on the person operating the system, or persons working in close proximity to the system. It would be useful, therefore, to consider the response of the human ear to different frequencies and sound levels. There would be no point in considering frequencies or sound levels which cannot be perceived by the human ear.

882 Although the vibration levels cannot be related directly to the value of the noise level produced by a system the frequency content will be the same. Some form of correction factor could, therefore, be applied

which would take into account the frequency response of the human ear. In common with the standard forms of noise measurement, one of the standardised weighting curves could be applied. These have been agreed internationally and are referred to as A, B and C curves. The weighting curves, illustrated on Fig. 8.12, are an attempt to match the frequency response characteristics of the human ear at different loudness levels. Comparing these curves with the equal loudness contours, depicting the average response of the human ear, shown on Fig. 8.13, it is clear that there is a resemblence between the loudness contours and inverted weighting curves. Though the human perception of sound is too complex to be completely accounted for by a simple frequency weighting these curves, A, B and C, provide a guide to the noise level as detected by a listener.

883 Applying the more generally used A weighting to the noise potential values for the system will provide a more realistic evaluation of the noise potential of the system. Values determined for the pressure forces or RMS pressure levels can be factored in line with curve A as given on Fig. 8.12 or using the attenuation factors given on Table 8.1.

Correction Factors

884 The correction factors implied by the mechanical response of the system and its radiation efficiency appear to cancel each other out. Since the latter varies with frequency whilst the former varies with the inverse of frequency. However, neither factor can be ruled out on the basis of these brief discussions. The need for one or both of these factors can only be ascertained through practical investigation.

885 The 'A' weighting, on the other hand, should be applied in all cases. By eliminating or attenuating frequencies which are not perceived by the listener, a more realistic appraisal of the noisiness of a system

can be obtained.

CONCLUSION

886 The ability to represent mathematically the FBN levels in a hydraulic system provides the system designer with a useful tool for those systems where noise is a major consideration. At this time, however, the application of the mathematical model to system design is limited by the availability of reliable component impedance values or models. Its future as an aid to developing quiet hydraulic systems will remain limited until such time as these component impedance values are defined.

887 Nevertheless, many of these circuit components are large and complex and are themselves miniature systems. In addition to these, there are many groups of components, such as modular valve packs, which form sub-systems for which lumped impedance models are required. The ability to model complete systems can also be applied to these smaller systems, as demonstrated in Chapter 5. The main application of the mathematical models appears, therefore, to be in the derivation of lumped impedance values for the larger components and sub-systems.

CHAPTER 9

DISCUSSION and CONCLUSIONS

DISCUSSION AND CONCLUSIONS

Hydraulic Systems

901 We have demonstrated that the mathematical model can provide a precise representation of the pressure and flow ripple in simple hydraulic systems operating with typical mean pressures, upto 200 bar, and flows, 42 l/min. The model can be applied with equal confidence to large or small systems. The latter may include models for larger complex components such as pumps or modular valve packs.

902 The accuracy of the mathematical model depends upon the reliability of the individual component models. In order to obtain accurate values for each component parameter and also to provide a clear evaluation of the system model close attention has had to be paid to the experimental procedures.

Test Procedures

903 The nature of the pressure ripple propagation in a hydraulic system is such that no single pressure or flow measurement is sufficient to describe the conditions in the system. A large amount of test data is needed which can be analysed statistically to provide consistent values for each component parameter and to ensure that mathematical model is examined over the widest possible range of system conditions. The test procedure used by some researchers in which the speed of the pump is varied to obtain the necessary changes in the system conditions does not provide sufficient data for reliable results to be obtained. The extending pipeline test method, described in Chapter 3 and employed extensively in the work described above, does provide the necessary

data for deriving component parameters or assessment of the system model. The reliability of the results obtained over a wide range of system conditions and different circuit configurations is testimony to the usefulness of this test method. The one disadvantage to this procedure is that it is time consuming.

904 The shortened test methods, the High Impedance Pipeline and Additional Capacitance tests, evaluated in Chapter 4 only gave reliable values for the pump flow and impedance at specific test conditions. These tests provided few experimental values so no mathematical techniques could be employed to enhance their reliability. It is clear that any successful procedure will have to provide a reasonable amount of data in a short period of time. A possible solution may be a revised extending pipeline test procedure in which fewer pipeline lengths are employed but each line will contain many pressure transducers.

Component Parameters

905 Axial Piston Pump:-

We established that the impedance of an axial piston pump of simple design can be represented by the impedance value for a volume of a size equivalent to the mean volume of the pump as 'seen' from the delivery line. A mean value is used because the pump volume varies with shaft position as illustrated on Fig. 3.22. Furthermore, we have shown that the impedance of the pump is not affected by changes in the mean system pressure level or in the angle of the swashplate.

906 Similarly, the instantaneous pump flow was shown to follow the theoretical model suggested by Helgestad et al(1). The results obtained demonstrated the

predominant effect of the back flow on the pump flow profile, as shown on Fig. 3.27. The instantaneous flow profile is not affected by the angle of the swashplate, however, the mean system pressure does have a large influence on the pump flow spectra. The back flow into the cylinder, which is primarily an effect due to the compressibility of the oil, decreases as the system pressure is reduced.

907 We can use this simple pump design to represent the basic pumping mechanism which is at the heart of any axial piston pump. Thus the impedance and flow values for this basic pumping mechanism forms the basis of the model for any design of axial piston pump. This was demonstrated in Chapter 4 in which we showed that the impedance of a pump of complex design can be represented by a lumped impedance value at the pump flange. The pump flow on the other hand is more difficult to model as the flow entering the delivery line depends upon the impedance of the system as well as the effects of the sub-system within the pump. Hence, the model for pumps of a complex design will contain the parameter values for the basic pumping mechanism and an impedance representation of the pipe system within the pump.

908 Restrictor Valve:-

We have shown that the impedance of a simple variable restrictor valve is complex. The valve impedance varies with frequency and with opening. The results showed how the use of the incorrect steady state value gave rise to significant errors in the predicted pressure ripple values.

System Design

909 The ability to model with accuracy FBN levels within a hydraulic system provides the means by which

systems or circuit configurations can be compared. Appraisal can be based upon RMS valves for the pressure ripple in sections of the system or when greater detail is needed the pressure forces created in each length of pipeline.

910 Of the two factors the RMS valves of pressure ripple are more easily evaluated and provide an adequate representation of system performance. The evaluation of pressure forces, on the other hand, requires a large amount of detail regarding the circuit design which makes them very time consuming to use. However, in extreme cases they can be very beneficial, as specific problem areas can be pinpointed.

911 Unfortunately, the use of the mathematical model of FBN levels as a design tool is, at present, limited by the number of component impedance valves or models available.

CONCLUSION

912 The result of the work detailed here has been to provide an accurate method of predicting mathematically the pressure ripple levels generated in hydraulic systems under normal conditions of operation. In order to achieve this we have had to examine and develop the impedance models of axial piston pumps and variable restrictor valves.

913 On the experimental side the results obtained have not only provided the practical verification for the mathematical models but also demonstrated the extent, in both magnitude and frequency range, of the pressure variations created in high pressure hydraulic circuits.

914 The use of this work as an aid to the design of quiet hydraulic systems is limited by the lack of component impedance models. However, the concepts involved can also be applied to these component models. The larger, more complex components or groups of components are miniature sub-systems in themselves. It is probable, therefore, that future applications of this work will be concerned with the modelling of these component or sub-system impedances.

APPENDIX

EVALUATION OF OPTIMUM PIPE LENGTHS

A01 Consider the simple circuit illustrated here.

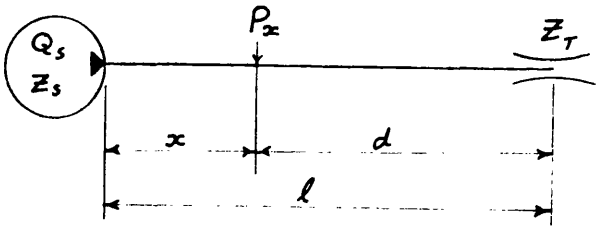

FIG A·1

The pressure at any position along the pipeline a distance d from the termination can be obtained by substituting for $x = \ell - d$ in equation 3·17. Thus

$$P_x = \frac{Q_s Z_s Z_o}{(Z_s + Z_o)} \cdot \frac{e^{-\gamma\ell}\left(e^{\gamma d} + \rho_T e^{-\gamma d}\right)}{\left(1 - \rho_s \rho_T e^{-2\gamma\ell}\right)} \qquad (A\cdot1)$$

Alternatively this can be written as:-

$$P_x = \frac{Q Z_s Z_o}{(Z_s + Z_o)} \cdot P_\ell \cdot P_d \qquad (A\cdot2)$$

where

$$P_\ell = \frac{e^{-\gamma\ell}}{\left(1 - \rho_s \rho_T e^{-2\gamma\ell}\right)} \qquad (A\cdot3)$$

Expression (A.3) defines the variation in the pressure level at point x which results from changes to the pipe length ℓ.

Also

$$P_d = \left(e^{\gamma d} + \rho_T e^{-\gamma d}\right) \qquad (A\cdot4)$$

Expression (A.4) defines the variation in the pressure level with distance along the pipeline for any given length of line.

Hence the PSWR will be given by

$$PSWR = \frac{P_{dmax}}{P_{dmin}} \qquad (A\cdot5)$$

A02 Consider the variation in pressure level along the pipeline.

ρ_T can be written as $\rho_T = |\rho_T| e^{j\phi_T}$ (A.6)

Let $\rho_T = e^{-2(p+jq)}$ (A.7)

Taking logs

$$\ln \rho_T = \ln|\rho_T| + j\phi_T$$

$$= -2(p + jq)$$

Separating terms gives

$$p = -\frac{1}{2}\ln|\rho_T| = \ln\frac{1}{\sqrt{|\rho_T|}} \qquad (A\cdot8)$$

and $$q = -\frac{1}{2}\phi_T \qquad (A\cdot9)$$

Substituting for equation (A.7) in equation (A.4)

$$P_d = \sqrt{\rho_T}\left(e^{(p+jq)}e^{\gamma d} + e^{-(p+jq)}e^{-\gamma d}\right) \qquad (A\cdot10)$$

Substituting for $\gamma = \alpha + j\beta$ in equation (A.10)

$$P_d = \sqrt{S_T}\left(e^{(p+jq)}e^{(\alpha+j\beta)d} + e^{-(p+jq)}e^{-(\alpha+j\beta)d}\right) \qquad (A\cdot 11)$$

Regrouping

$$P_d = \sqrt{S_T}\left(e^{(\alpha d+p)+j(\beta d+q)} + e^{-(\alpha d+p)-j(\beta d+q)}\right) \qquad (A\cdot 12)$$

Now

$\cosh\theta = \dfrac{e^{\theta}+e^{-\theta}}{2}$ therefore equation (A.12)

can be rewritten as

$$P_d = \sqrt{S_T}\cdot 2\cdot \cosh\left[(\alpha d+p) + j(\beta d+q)\right] \qquad (A\cdot 13)$$

A03 The hyperbolic cosine can be expanded using the identity:-

$$\cosh(a+jb) = \cosh a \cos b + j \sinh a \sin b$$

The magnitude of this expression is given by

$$\left|\cosh(a+jb)\right| = \left(\sinh^2 a + \cos^2 b\right)^{1/2}$$

and the phase angle

$$\angle\left(\cosh(a+jb)\right) = \tan^{-1}\left(\frac{\sinh a \sin b}{\cosh a \cos b}\right)$$

Applying the above identities to equation (A.13) gives

$$|P_d| = 2\sqrt{|\rho_T|}\left[\sinh^2(\alpha d+p) + \cos^2(\beta d+q)\right]^{1/2} \qquad (A\cdot14)$$

and

$$\angle P_d = \tan^{-1}\left[\tanh(\alpha d+p)\,\tan(\beta d+q)\right] \qquad (A\cdot15)$$

A04 Consider the case for a loss less line.

That is $R = 0$ Hence $\alpha = 0$

Thus equation (A.14) becomes

$$|P_d| = 2\sqrt{|\rho_T|}\left[\sinh^2 p + \cos^2(\beta d+q)\right]^{1/2} \qquad (A\cdot16)$$

and equation (A.15) becomes

$$\angle P_d = \tan^{-1}\left[\tanh p\,\tan(\beta d+q)\right] \qquad (A\cdot17)$$

Now the maximum pressure must occur when
$\cos^2(\beta d+q) = 1$ Thus:-

$$|P_d|_{max} = 2\sqrt{|\rho_T|}\,(\sinh^2 p + 1)^{1/2}$$

Similarly the minimum pressure occurs when
$\cos^2(\beta d+q) = 0$. Hence:-

$$|P_d|_{min} = 2\sqrt{|\rho_T|}\,(\sinh^2 p)^{1/2}$$

Combining these expressions then

$$\frac{|P_d|_{max}}{|P_d|_{min}} = PSWR = \left[\frac{(\sinh^2 p + 1)}{\sinh^2 p}\right]^{1/2} = \coth p \qquad (A\cdot18)$$

The exponential form of this hyperbolic cotangent gives:-

$$PSWR = \frac{1 + e^{-2\rho}}{1 - e^{-2\rho}}$$

Substituting for equation (A.8) gives

$$PSWR = \frac{1 + |\rho_T|}{1 - |\rho_T|} \qquad (A\cdot19)$$

Similarly the position of the standing wave is determined by the value of the reflection coefficient,

If $|P_d|_{max}$ occurs when $\cos^2(\beta d + q) = 1$

Then $\beta d_{max} + q = n\pi$ where n is an integer value.

Now $\beta = \frac{2\pi}{\lambda}$ and $q = -\frac{\phi_T}{2}$

Therefore

$$d_{max} = \frac{\phi_T}{\pi}\frac{\lambda}{4} + \frac{n\lambda}{2} \qquad (A\cdot20)$$

In the same way $|P_d|_{min}$ occurs when $\cos^2(\beta d + q) = 0$

Thus $d_{min} = \left(\frac{\phi_T}{\pi} - 1\right)\frac{\lambda}{4} + \frac{n\lambda}{2}$ (A·21)

That is

$|P_d|_{min}$ is $\frac{\lambda}{4}$ from $|P_d|_{max}$

A05 The derivation above shows that the magnitude of the PSWR is dependent solely upon the amplitude of the reflection coefficient, $|\rho_T|$. Furthermore the position of the standing wave is fixed relative to the termination and is independent, therefore, of the length of the line. The actual locations of the maxima and minima are governed by the phase of the reflection coefficient, ϕ_T . However, in order to examine the variation in the amplitudes of the pressure ripple with the length the pressure term, P_ℓ , has to be considered.

A06 Rearranging equation (A.3) gives

$$P_\ell = \frac{1}{(e^{\gamma\ell} - \rho_s \rho_T e^{-\gamma\ell})} \qquad (A.22)$$

Now $$\rho_s = |\rho_s| e^{-j\phi_s} \qquad (A.23)$$

Combining (A.6) and (A.23) then

$$\rho_s \rho_T = |\rho_s \rho_T| e^{j(\phi_s + \phi_T)} \qquad (A.24)$$

Let $$\rho_s \rho_T = e^{-2(u+jv)} \qquad (A.25)$$

Taking logs

$$\ln(\rho_s \rho_T) = \ln|\rho_s \rho_T| + j(\phi_s + \phi_T)$$

$$= -2(u + jv)$$

Thus $$u = \ln \frac{1}{\sqrt{|\rho_s \rho_T|}} \qquad (A.26)$$

and $$v = -\frac{1}{2}(\phi_s + \phi_T) \qquad (A.27)$$

Substituting for equation (A.25) in (A.22) gives

$$P_\ell = \frac{1}{\sqrt{|S_s S_T|}} \cdot \frac{1}{\left(e^{(u+\alpha\ell)+j(v+\beta\ell)} - e^{-(u+\alpha\ell)-j(v+\beta\ell)}\right)} \qquad (A\cdot28)$$

Now $\quad \sinh\theta = \frac{e^{\theta} - e^{-\theta}}{2}$

Thus

$$P_\ell = \frac{1}{\sqrt{|S_s S_T|}\ 2\sinh\left[(u+\alpha\ell) + j(v+\beta\ell)\right]} \qquad (A\cdot29)$$

A07 The hyperbolic sine term can be expanded using the identity

$$\sinh(a+jb) = \sinh a \cos b + j \cosh a \sin b$$

Or more appropriately in an inverted form:-

$$\frac{1}{\sinh(a+jb)} = \frac{\sinh a \cos b - j \cosh a \sin b}{\sinh^2 a + \sin^2 b}$$

The magnitude of this expression is given by:-

$$\left|\frac{1}{\sinh(a+jb)}\right| = \frac{1}{(\sinh^2 a + \sin^2 b)^{1/2}}$$

and the phase angle by:-

$$\angle\left(\frac{1}{\sinh(a+jb)}\right) = \tan^{-1}\left(\frac{-\tan b}{\tanh a}\right)$$

Applying these identities to equation (A.29) then

$$|P_\ell| = \frac{1}{2\sqrt{|S_s S_T|}\,\left[\mathrm{Sinh}^2(u+\alpha\ell) + \mathrm{Sin}^2(v+\beta\ell)\right]} \qquad (A\cdot 30)$$

and

$$\angle P_\ell = \mathrm{Tan}^{-1}\left[\frac{-\mathrm{Tan}(v+\beta\ell)}{\mathrm{Tanh}(u+\alpha\ell)}\right] \qquad (A\cdot 31)$$

A08 Now consider the case for the loss less line then.

$$|P_\ell| = \frac{1}{2\sqrt{|S_s S_T|}\,\left[\mathrm{Sinh}^2 u + \mathrm{Sin}^2(v+\beta\ell)\right]^{1/2}} \qquad (A\cdot 32)$$

and

$$\angle P_\ell = \mathrm{Tan}^{-1}\left[\frac{-\mathrm{Tan}(v+\beta\ell)}{\mathrm{Tanh}\,u}\right] \qquad (A\cdot 33)$$

The maximum pressure level must occur when $\mathrm{Sin}^2(v+\beta\ell) = 0$

Thus $$|P_\ell|_{max} = \frac{1}{2\sqrt{|S_s S_T|}\;(\mathrm{Sinh}^2 u)^{1/2}} \qquad (A\cdot 34)$$

Similarly the minimum pressure level occurs when $\mathrm{Sin}^2(v+\beta\ell) = 1$

Hence $$|P_\ell|_{min} = \frac{1}{2\sqrt{|S_s S_T|}\;(\mathrm{Sinh}^2 u + 1)^{1/2}} \qquad (A\cdot 35)$$

A09 Thus the maximum variation in the pressure level that can be brought about by a change in the length of the line is:-

$$\frac{|P_\ell|_{max}}{|P_\ell|_{min}} = \frac{(\sinh^2 u + 1)}{(\sinh^2 u)} = \coth u \qquad (A.36)$$

Applying the exponential form of $\coth u$, then equation (A.36) can be written as

$$\frac{|P_\ell|_{max}}{|P_\ell|_{min}} = \frac{1 + |S_s S_T|}{1 - |S_s S_T|} \qquad (A.37)$$

A10 The analysis has shown that the maximum variation in pressure levels that can be achieved by changes in the line length is a function of the amplitude of the product of the reflection coefficients, $|S_s S_T|$, given by equation (A.37). In the same way that the PSWR was a function of the amplitude of the reflection coefficient $|S_T|$ as given by equation (A.19) Likewise the line lengths which produce the maximum and minimum pressure levels are functions of the phases for the two reflection coefficients.

From equation (A.31) $|P_\ell|_{max}$ occurs when $\sin(\gamma + \beta\ell) = 0$

In which case it can be shown that

$$\ell_{max} = \frac{(\phi_s + \phi_T)}{\pi}\frac{\lambda}{4} + \frac{n\lambda}{2} \qquad (A.38)$$

Similarly, as $|P_\ell|_{min}$ occurs when $\sin(\gamma + \beta\ell) = 1$

Then

$$\ell_{min} = \left(\frac{(\phi_s + \phi_T)}{\pi} - 1\right)\frac{\lambda}{4} + \frac{n\lambda}{2} \qquad (A.39)$$

A11 This analysis shows that for a simple circuit, as illustrated on Fig. A.1, the lowest pressure levels at a given frequency will be obtained when the line length $l = l_{min.}$, as defined by equation A.39. It can be seen that much information regarding optimum line lengths and possible variations in pressure levels, together with values for the PSWR and the relative position of the standing wave, can be derived from knowledge of the reflection coefficients at the pump and termination, ρ_s and ρ_T.

A12 Unfortunately this simple analysis is only applicable to single ripple frequencies, hence its use on practical hydraulic systems is limited. Nevertheless an initial evaluation of the relevant parameters of pressure ratios and optimum line lengths for each of the predominant ripple frequencies in a system would provide a circuit designer with an initial indication of suitable pipe lengths.

REFERENCES

REFERENCES

1. Helgestad, B.O., Foster, K. & Bannister, F.K.
'Pressure transients in an axial piston pump'
Proc. I. Mech.E., Vol. 188, 17/74, 1974

2. Stewart, G.W.
'Acoustic Wave filters'
Phys. Rev. *20*, *528-551*, *1922*

3. Joukowsky, N.
'Water Hammer'
Proceedings American Water Works Association,
pp. 341, 1914

4. Waller, E.J.
'Problems in pressure surge analysis of positive displacement pump systems'
Oklahoma Engineering Experiment Station Publication,
No. 107, 1959

5. Constantinesco, G.
'Theory of wave transmission, a treatise on transmission of power by vibration'
Walter Haddon, 1922

6. Foster, K. & Parker, G.A.
'Transmission of power by sinusoidal wave motion through hydraulic oil in a uniform pipe'
Proc.I.Mech.E., Vol. 179, Part 1, No.19, 1964-65

7. Willekens, F.A.M.
'Fluid borne noise in hydraulic systems'
1st European Fluid Power Conference, National Engineering Laboratory, Sept. 10-12, 1973

8. Tilley, D.G.
'The measurement of transient flows in high pressure hydraulic systems'
Ph.D. Thesis, University of Bath, 1976

9. Chipman, R.A.
'Theory and problems of transmission lines'
Schaum's Outline Series, McGraw-Hill,

10. Uchida, S.
'The pulsating viscous flow superposed on the steady laminar motion of incompressible fluid in a pipe'
Z. Angew, Math. Phys. 1956-57.

11. Hayward, A.T.J.
'How to estimate the bulk modulus of hydraulic fluids'
Hydraulic Pneumatic Power, January, 1970.

12. Bowns, D.E., Edge, K.A. & Tilley, D.G.
'The assessment of pump fluid borne noise'
I.Mech.E. Seminar 'Quiet Oil Hydraulic systems - Where are we now?' London, 1977.

13. Davidson, L.C. & Taylor, D.W.
'The internal impedance of positive displacement pumps: experimental determination and effects on system noise'
National Conference on Fluid Power, Cleveland, October 26-28, 1976.

14. Isdale, J.D., Branton, W.C. & Spence, C.M.
'Bulk modulus measurement and prediction'
National Engineering Laboratory, No. 591.

15. Thurston, G.B., Hargrove, L.E. & Cook, B.D.
'Non linear properties of circular orifices'.
Journal of the Acoustical Society of ANEE America, 29(9), 992-1001, Sept. 1957.

16. Kelsey, J.S., Taylor, R. & Wood, K.
'The practical benefits of optimising the port plate timing for an axial piston pump.'
I.Mech.E. Seminar 'Quieter Oil Hydraulics', London 1980

17. Bowns, D.E., Edge, K.A. & McCandlish, D.
'Factors affecting the choice of a standard method for the determination of pump pressure ripple'
I.Mech.E. Seminar 'Quieter Oil Hydraulics', London, 1980.

18. Stewart, G.W.
'Influence of a branch line upon acoustic transmission of a conduct'
Phys. Rev. 26, 688-690, 1925

19. Lewis, W., Blade, R.J. & Dorsch, R.G.
'Study of the effect of a closed-end side branch on sinusoidally perturbed flow of liquid in a line'
NASA technical note D-1876, 1963.

20. Sewall, J.L., Wineman, D.A. & Herr. R.W.
'An investigation of hydraulic-line resonance and its attenuation'
NASA - TH-X-2787, 1972.

21. Whitson, R.J.
'The measured transmission loss characteristics of some hydraulic attenuators'.
I.Mech.E. Seminar 'Quieter Oil Hydraulics', London, Oct. 1980.

22. Blade, R.J., Lewis, W. & Goodykoontz, J.H.
'Study of a sinusoidally perturbed flow in a line including a 90° Elbow with flexible supports'.
NASA technical note D-1216, 1962.

23. Regetz, J.D.
'An experimental determination of the dynamic response of a long hydraulic line'.
NASA technical note D-576, 1960.

24. McCloy, D.
'Cavitation and aeration - the effect on valves and systems'
Hydraulic Pneumatic Power, January, 1966.

25. Tullis, J.P.
'Testing valves for cavitation'
I.Mech.E. Conference. 'Cavitation' Heriot-Watt University, Edinburgh, Sept. 1974.

26. Becker, R.J.
'Techniques for reducing hydraulic system noise'
Control Engineering, December 1973.

27. Szabo, M.
'Stop noise in hydraulic systems'
Hydraulic and Pneumatics, March 1975.

28. Becker, R.J. & Skaistis, S.J.
'How to quiet hydraulically-operated machinery and equipment'
Hydraulics and Pneumatics, October 1974.

29. Association of Hydraulic Equipment Manufacturers.
'Guidelines for the design of quiet hydraulic fluid Power Systems'.

30. Edge, K.A.
'The theoretical prediction of the impedance of positive displacement pumps'
I.Mech.E. Seminar 'Quieter Oil Hydraulics,'
London, 1980.

31. Wing, T.J.
'The fluid borne noise characteristics of hydraulic components and their measurement'
Ph.D. Thesis, University of Bath, 1982.

32. Freitas, F.J.T.
'A study of pressure fluctuations in the boost line of a piston pump'
M.Sc. Thesis, University of Bath, 1980.

33. Tilley, D.G. & Butler, M.D.
'The generation and transmission of fluid borne pressure ripple in hydraulic systems'
I.Mech.E. Seminar 'Quieter Oil Hydraulics', London, 1980.

34. Crook, A. & Heron, R.A.
'An investigation into the effects of circuit interactions on the noise emitted by hydraulic pumps and its influence on the selection of a standard test circuit.'
BHRA, RR 1322, Dec. 1975.

35. Hughes, M.L. & Sanders, B.C.G.
'The attenuation properties of hydraulic hose'
I.Mech.E. Seminar 'Quieter Oil Hydraulics,' London, 1980.

36. Longmore, D.K. & Tuc, B.
'Reduction of fluid borne noise in hydraulic circuits by means of flexible hoses'
I.Mech.E. Seminar 'Quieter Oil Hydraulics', London, 1980.

37. Kuhn, G.F. & Morfey, C.L.
'Transmission of low-frequency internal sound through pipe walls'
Journal of Sound and Vibration, 47(2), P.147-161, 1976.

38. Fagerlund, A.C.
'Transmission of sound through a cylindrical pipewall'
ASME Paper 73 WA/PID -4, Nov.12, 1973.

TABLES

TABLES:

TABLE 3.1 Properties of the Pipeline

Internal Diameter = 14.93 mm.
Wall Thickness = 2.05 mm.
Youngs Modulus for Steel = 206.8 GN/m

TABLE 3.2 Restrictor Valve Operating Conditions

Oil Temperature 40°C.

System Pressure (bar)	System Flow (l/s)	Valve Exponent (n)	Termination Impedance ($N.s.m.^{-5}$)
100	.73	1.88	.26 10
150	.715	1.93	.41 10
200	.7	1.97	.56 10

TABLE 4.1 Effect of Swashplate Angle on Cylinder Pressures and Volumes

a) Conditions at t.d.c.

Swashplate Angle	Cylinder Volume on Opening V_c mm.^{3}	Change in Volume due to Swash Angle ΔV_{c1} mm.^{3}	Pressure Rise due to change in Volume ΔP_c bar.	Reduction in Volume to obtain 200 bar ΔV_{c2} mm.^{3}
Full	11345	-	-	133
3/4	10753	-	-	127
1/2	10162	-	-	120
1/4	9570	-	-	113
0	8978	-	-	106

b) Conditions 2° after t.d.c.

Swash	V_c mm.^{3}	ΔV_{c1} mm.^{3}	ΔP_c bar.	ΔV_{c2} mm.^{3}
Full	11339	6	8.7	128
3/4	10748	4.5	6.7	122
1/2	10159	3	4.8	117
1/4	9579	1.5	2.6	111
0	8978	0	0	106

c) Conditions 4° after t.d.c.

Swash	V_c mm.^{3}	ΔV_{c1} mm.^{3}	ΔP_c bar.	ΔV_{c2} mm.^{3}
Full	11322	23	34.5	110
3/4	10735	17.5	27.5	109
1/2	10151	11.5	19.5	108
1/4	9564	6	10.5	107
0	8978	0	0	106

TABLE 6.1 Flows Through the Branch Line Circuit
Fig. 6·6

Mean System Pressure = 200 bar
Mean Pump Flow = 0.7 l/s

Test Condition	Flow Line 1 (l/s)	Flow Line 2 (l/s)	Ratio $Q_{l_1} : Q_{l_2}$
1	0.7	0	-
2	0.525	0.175	3 : 1
3	0.35	0.35	1 : 1
4	0.175	0.525	1 : 3
5	0	0.7	-

TABLE 7.1 Proposed Test Pressure Levels - Valves in Series Test Fig. 7.4

Pump Flowrate 0.7 l/s

Test No.	Pressure in Line 1 (bar)	Pressure in Line 2 (bar)
1	200	50
2	200	100
3	200	150
4	206	200

TABLE 7.2 Oil Temperature Levels

Test No.	Pressure		Temperature	
	Line 1 (bar)	Line 2 (bar)	Line 1 (°C)	Line 2 (°C)
1	200	50	40	49
2	200	100	40	46
3	200	150	40	43
4	206	200	40	40

TABLE 8.1 Attenuation Factors for the Standard Weighting Networks

Frequency Hz.	A dB	B dB	C dB	A	B	C
10	-70.4	-38.2	-14.3	.0003	.012	.193
12.5	-63.4	-33.2	-11.2	.0007	.022	.275
16	-56.7	-28.5	- 8.5	.0015	.037	.376
12.5	-50.5	-24.2	- 6.2	.003	.062	.49
25	-44.7	-20.4	- 4.4	.0058	.077	.603
31.5	-39.4	-17.1	- 3.0	.011	.139	.704
40	-34.6	-14.2	- 2.0	.019	.195	.794
50	-30.2	-11.6	- 1.3	.031	.263	.862
63	-26.2	- 9.3	- .8	.049	.342	.912
80	-22.5	- 7.4	- .5	.075	.426	.944
100	-19.1	- 5.6	- .3	.111	.525	.966
125	-16.1	- 4.2	- .2	.157	.616	.977
160	-13.4	- 3.0	- .1	.214	.704	.988
200	-10.9	- 2.0	0	.285	.794	1.0
250	- 8.6	- 1.3	0	.372	.862	1.0
315	- 6.6	- .8	0	.468	.912	1.0
400	- 4.8	- .5	0	.575	.944	1.0
500	- 3.2	- .3	0	.692	.966	1.0
630	- 1.9	- .1	0	.804	.988	1.0
800	- .8	0	0	.912	1.0	1.0
1000	0	0	0	1.0	1.0	1.0
1250	.6	0	0	1.072	1.0	1.0
1600	1.0	0	- .1	1.122	1.0	.988
2000	1.2	- .1	- .2	1.148	.988	.977
2500	1.3	- .2	- .3	1.161	.977	.966
3150	1.2	- .4	- .5	1.148	.955	.944
4000	1.0	- .7	- .8	1.122	.922	.912
5000	.5	- 1.2	- 1.3	1.059	.871	.862
6300	- .1	- 1.9	- 2.0	.989	.804	.794
8000	- 1.1	- 2.9	- 3.0	.881	.716	.704
10000	- 2.5	- 4.3	- 4.4	.75	.61	.603
12500	- 4.3	- 6.1	- 6.2	.61	.495	.49
16000	- 6.6	- 8.4	- 8.5	.468	.38	.376
20000	- 9.3	-11.1	-11.2	.343	.279	.275

FIGURES

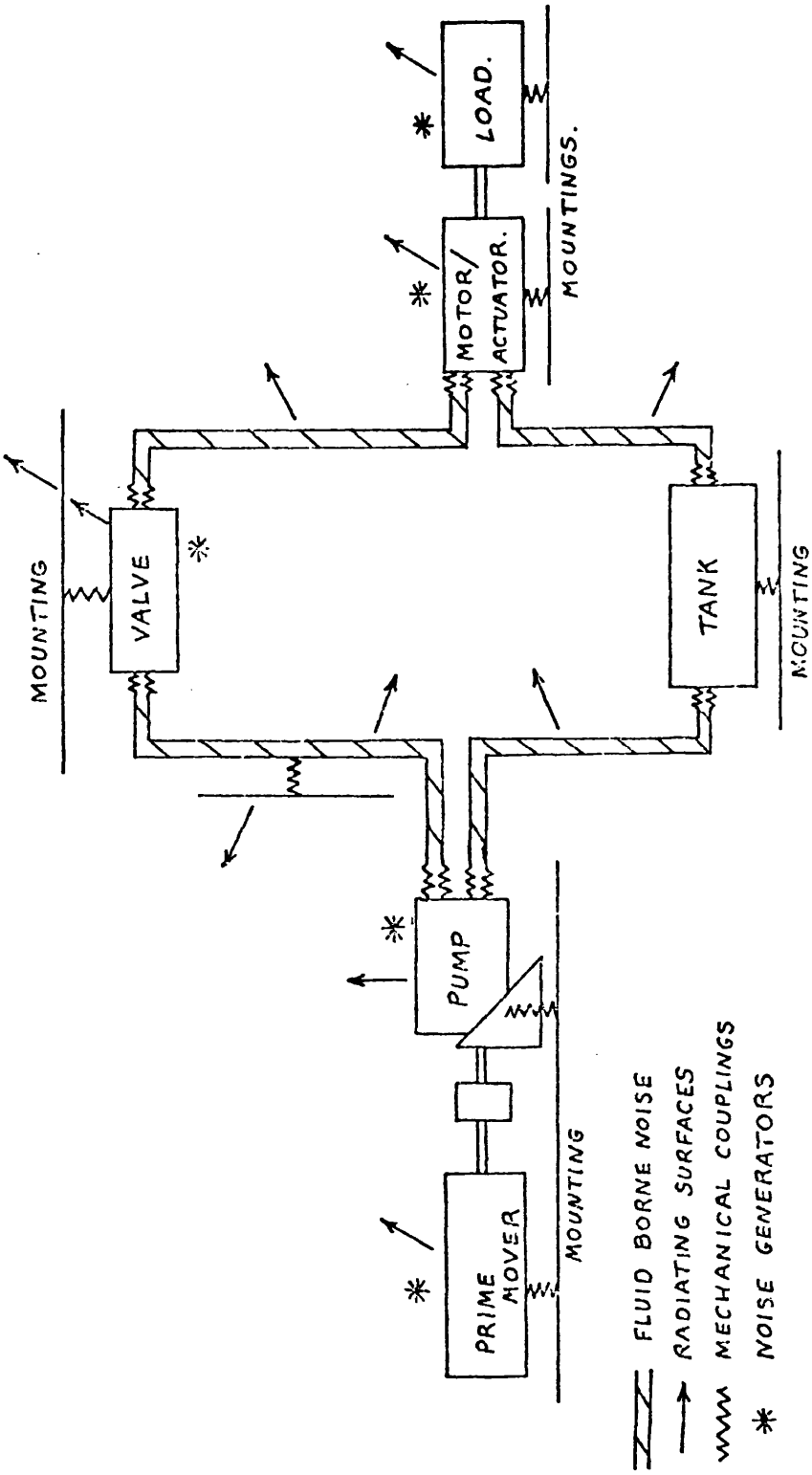

FIG 1·1 Sources of noise and noise transmission paths in a typical hydraulic system.

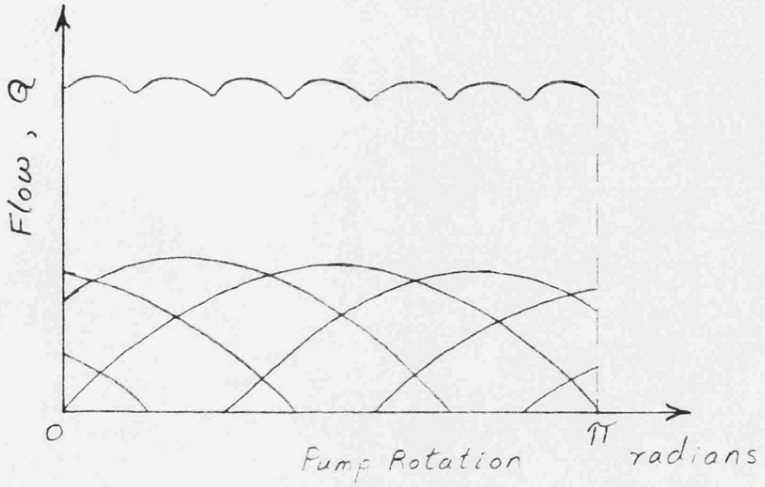

FIG 1·2 Idealised flow from a 7 piston pump.

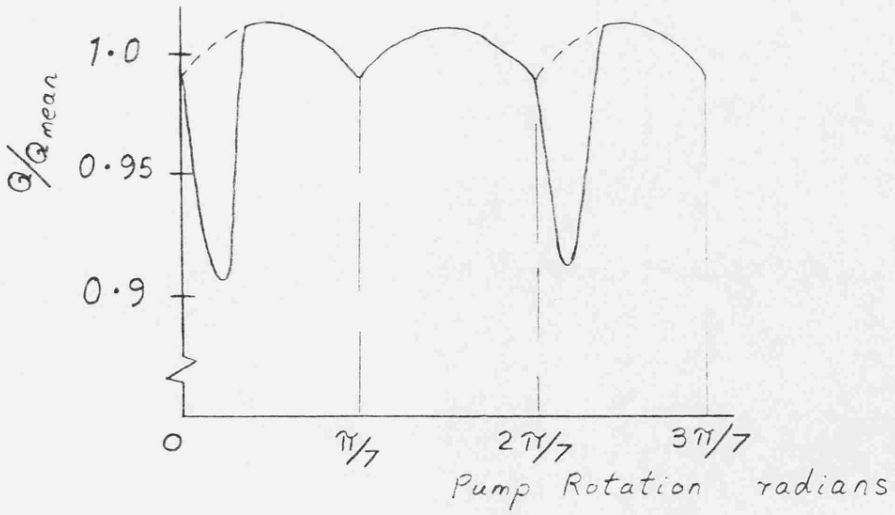

FIG 1·3 Effect of system pressure on the idealised pump flow.

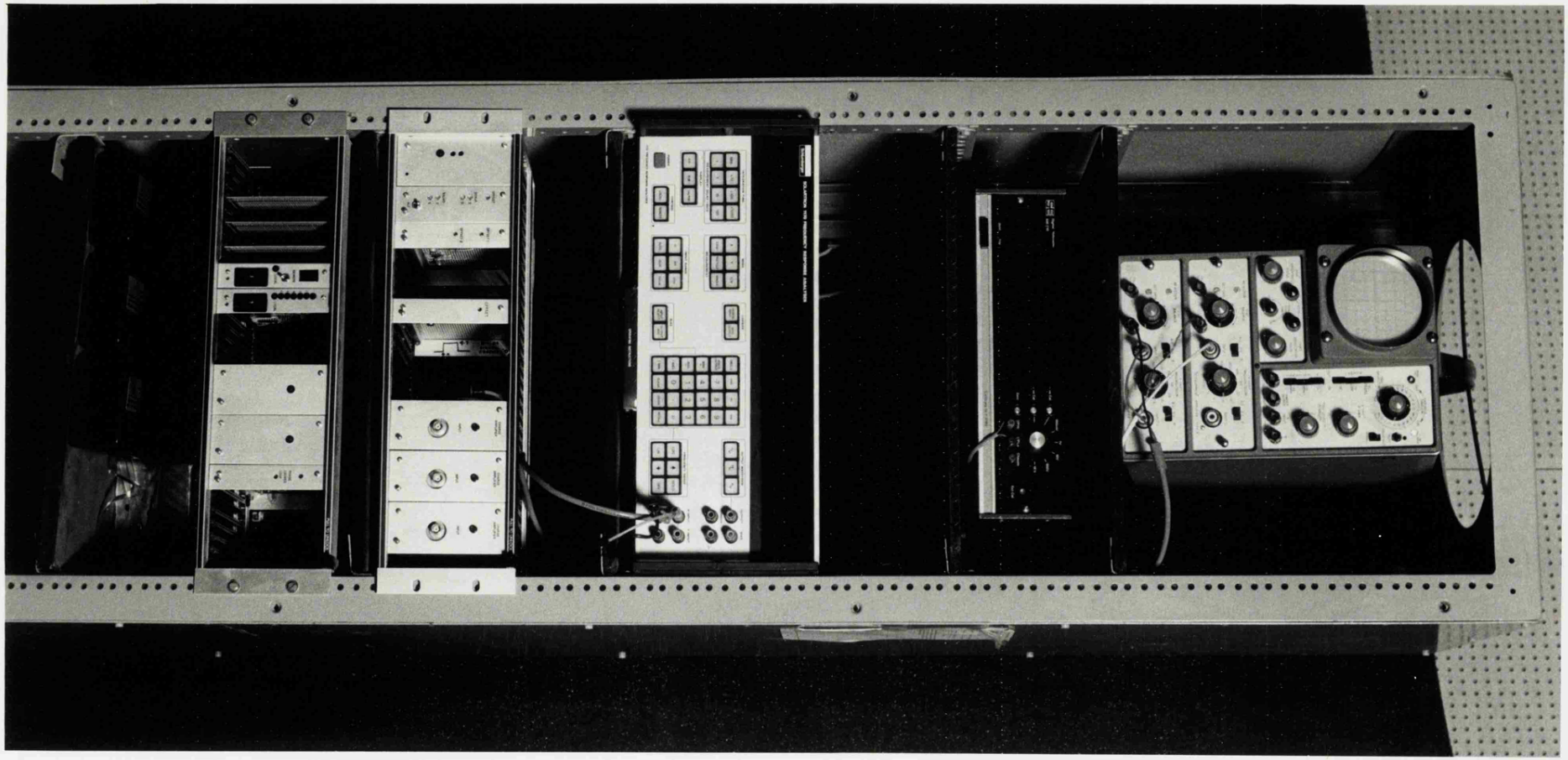

FIG 2·1 Rig Instrumentation

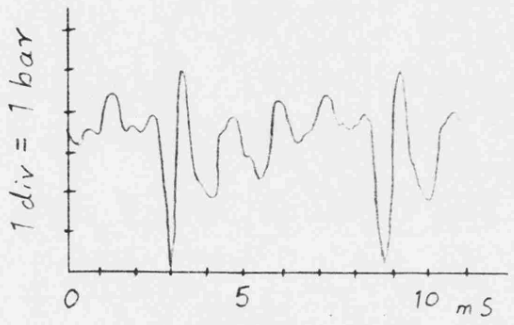

FIG 2·2 A Typical Pressure Transducer Trace

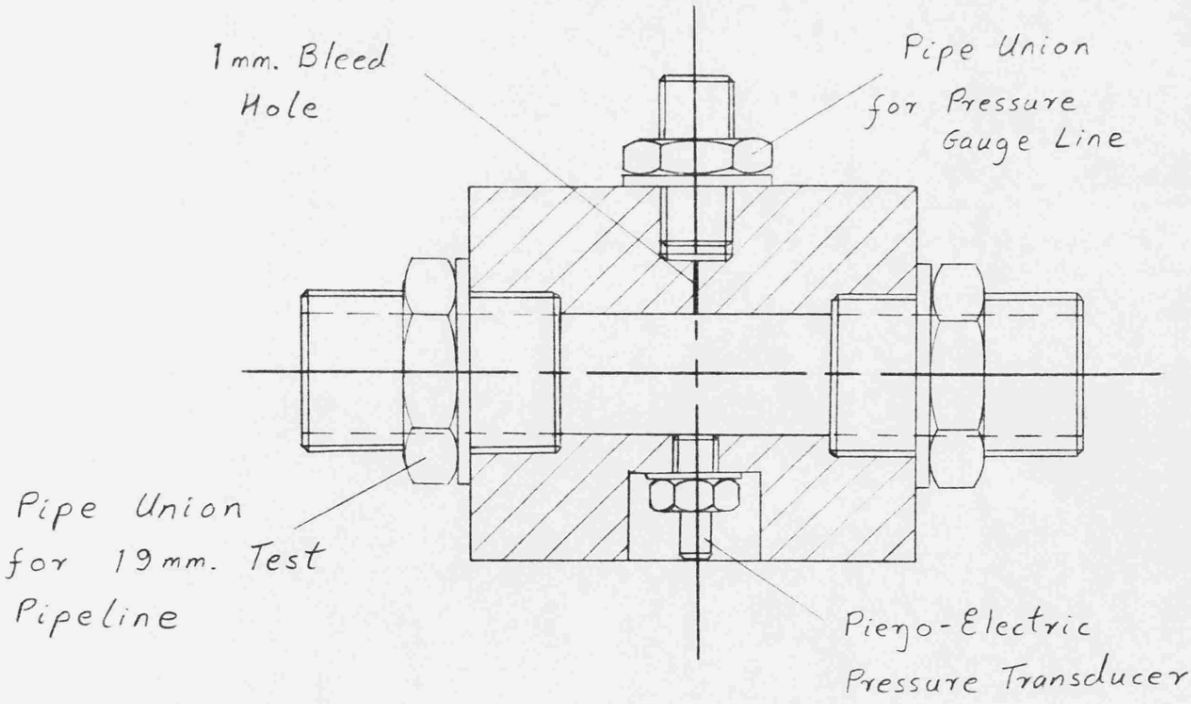

FIG 2·3 Pressure Gauge and Pieyo-Electric Transducer Connecting Block

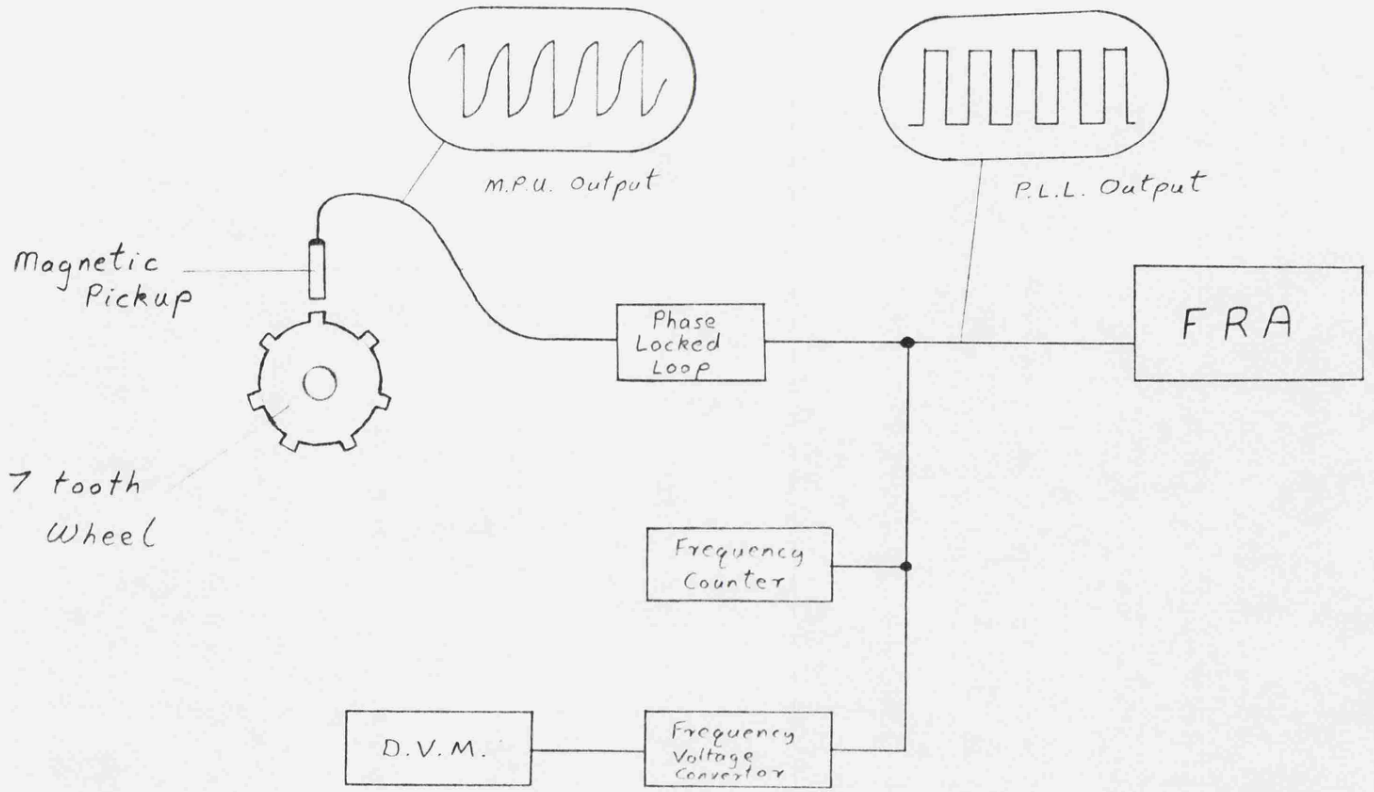

FIG 2·4 Block Diagram of the Shaft Speed Measuring System

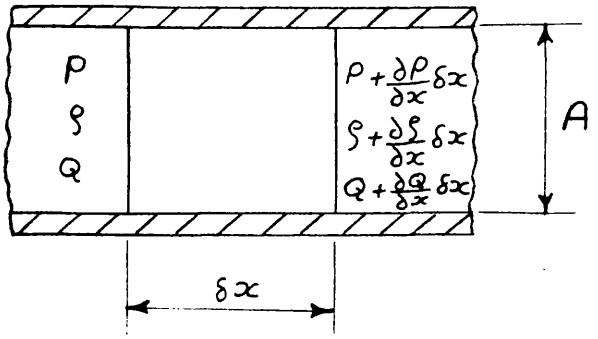

FIG 3·1 Elemental section of a pipeline containing a pressurised fluid

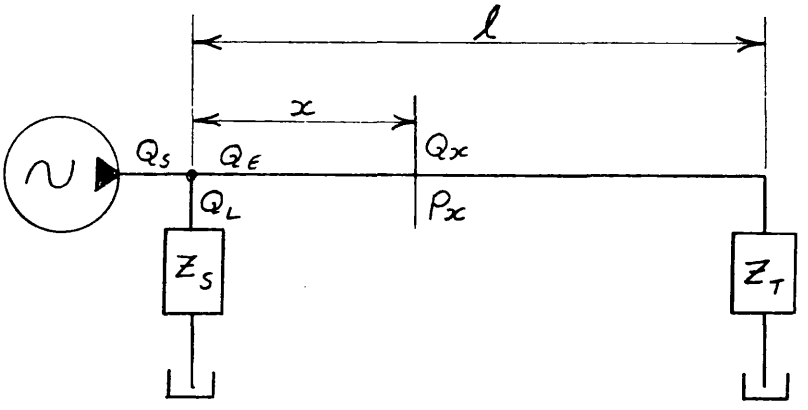

FIG 3·2 Impedance representation of a simple hydraulic system

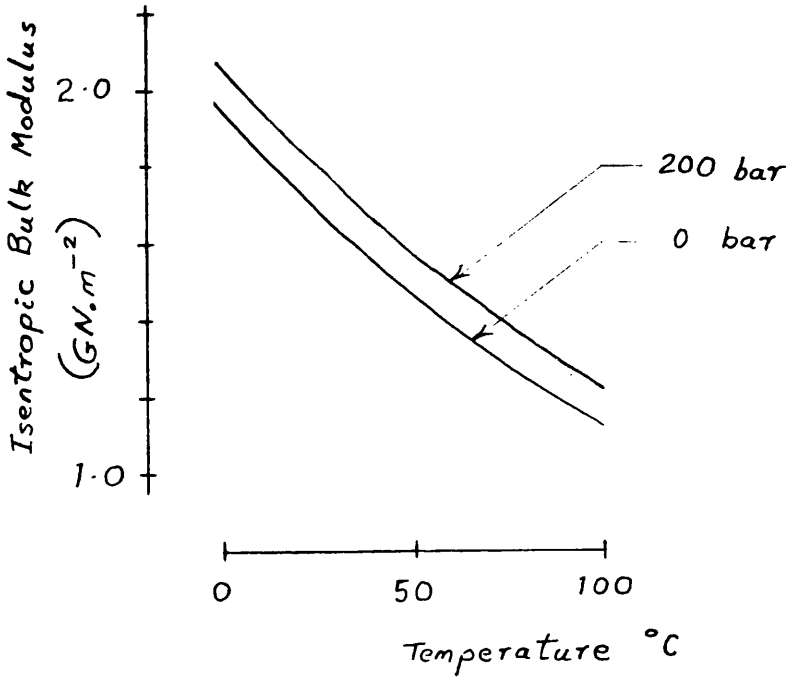

FIG 3·3 Bulk Modulus

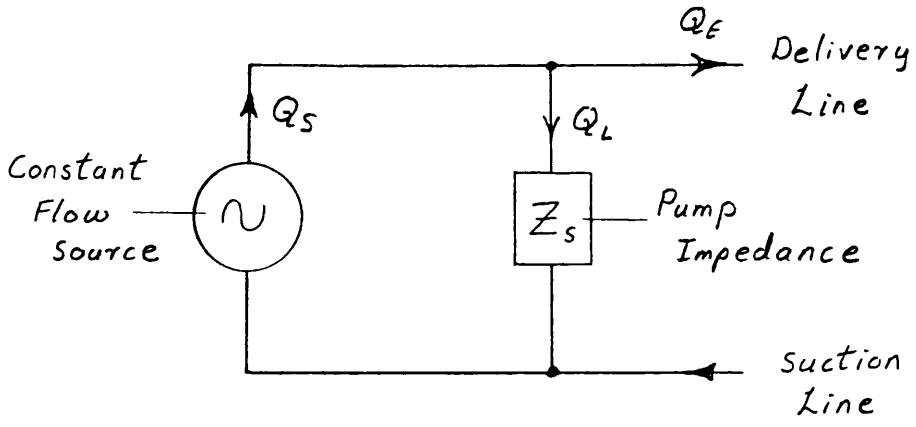

FIG 3·4 Impedance model of a positive displacement pump

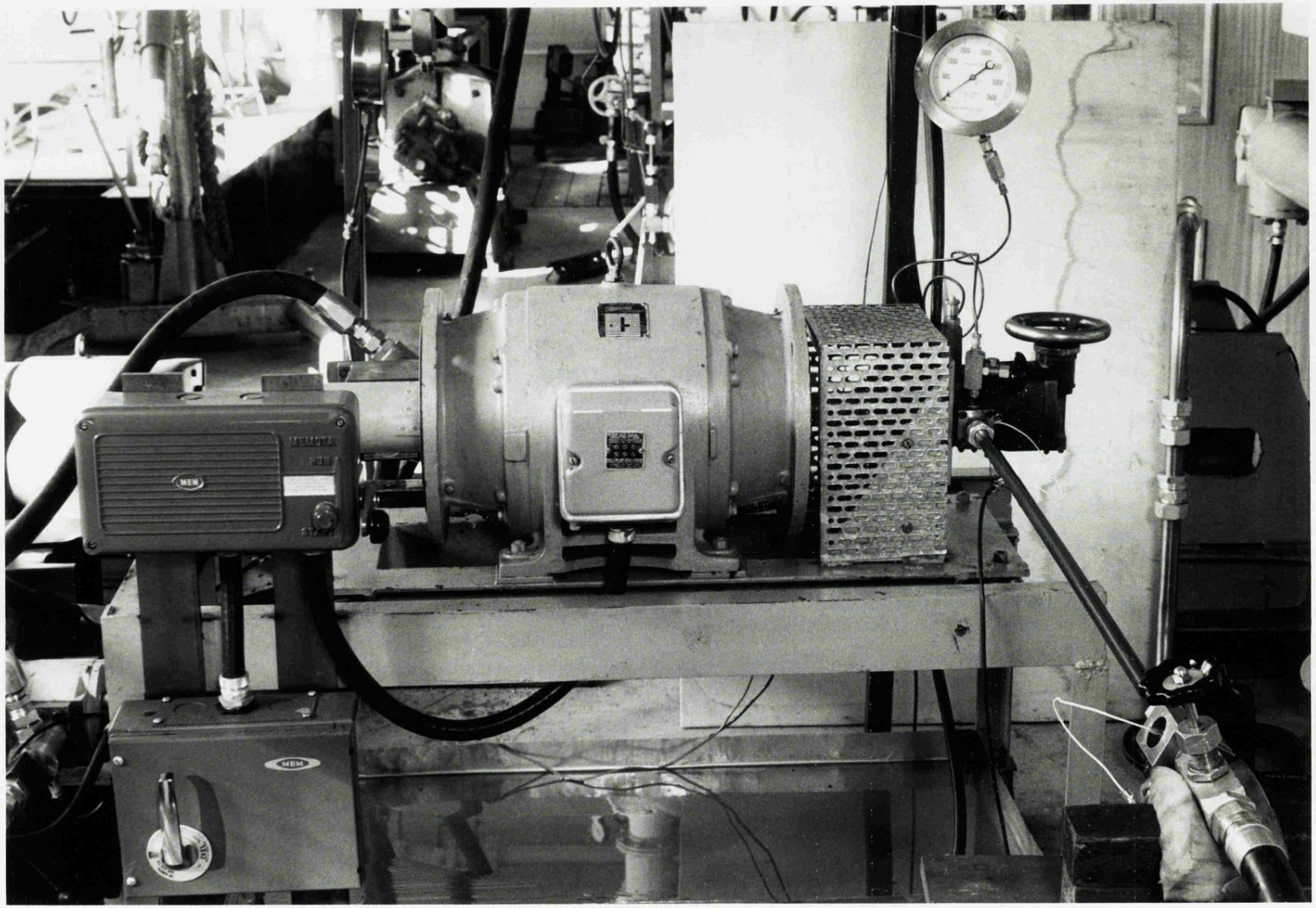

FIG 3·5 Test Rig

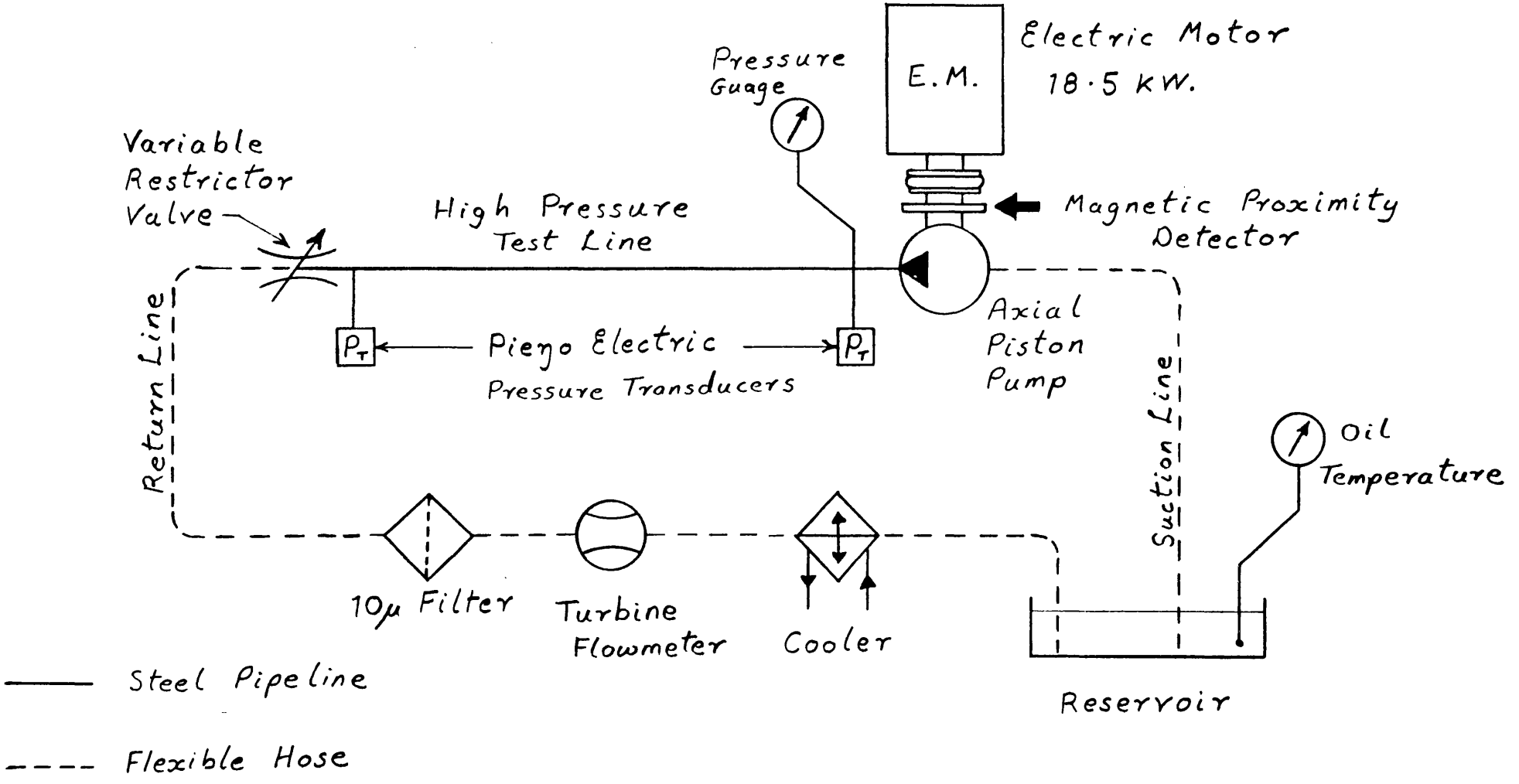

FIG 3·6 Line diagram of the experimental rig

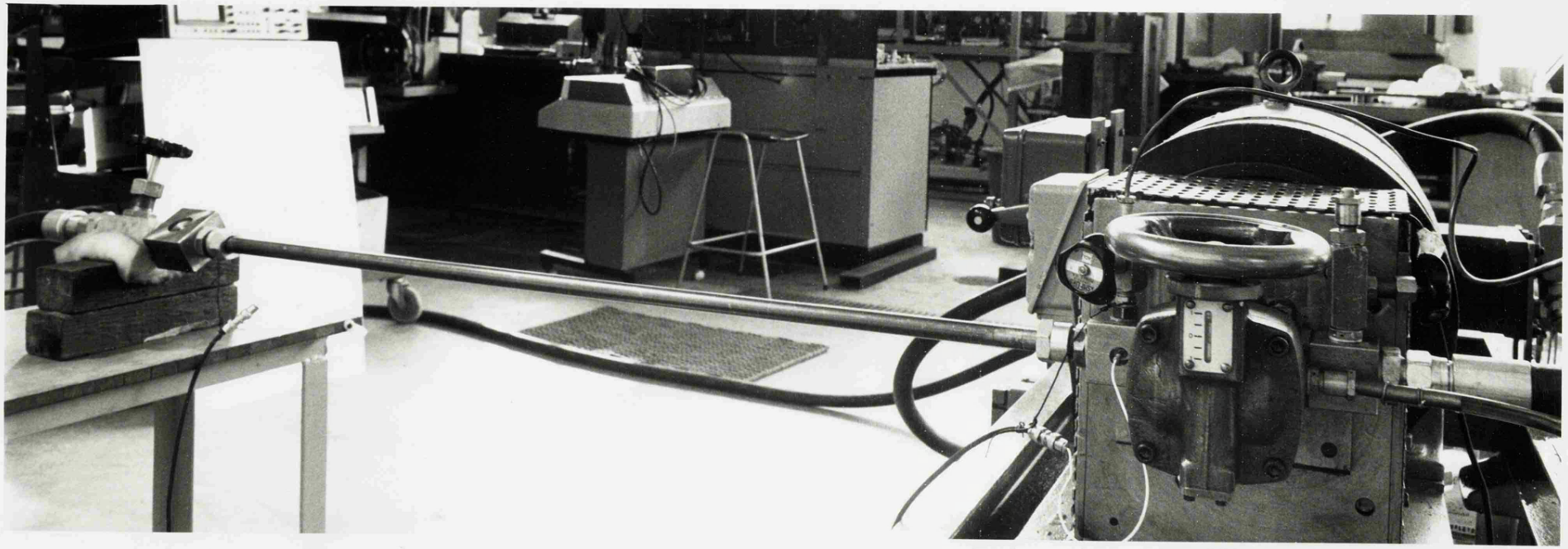

FIG 3·7 Test Pipeline

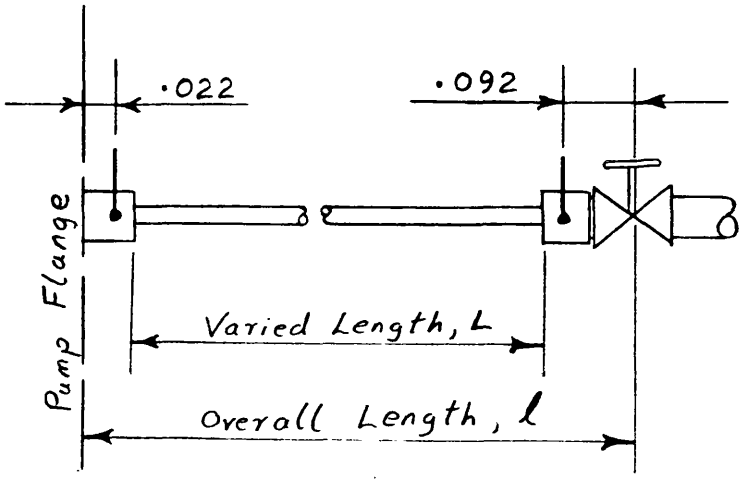

Overall Length $l = L + \cdot 709$ m.

| Pressure Transducers

FIG 3·8 Test Pipeline Transducer Positions.

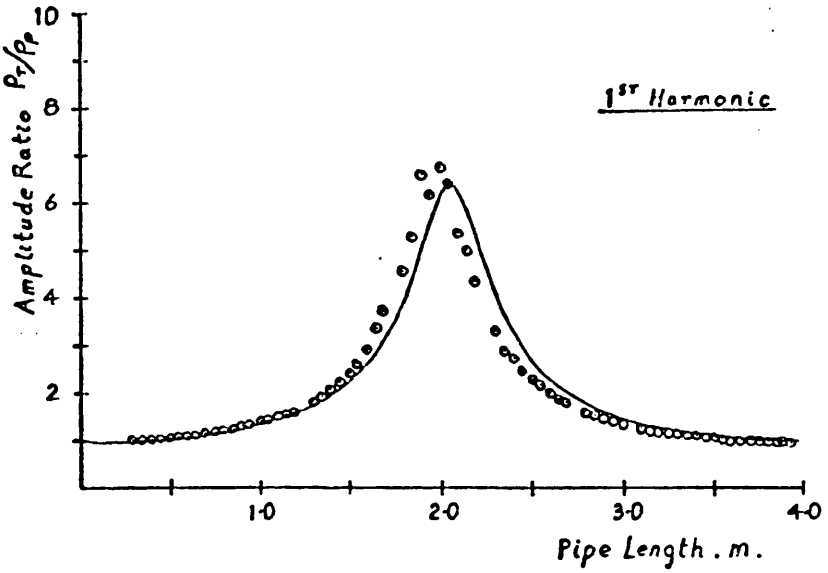

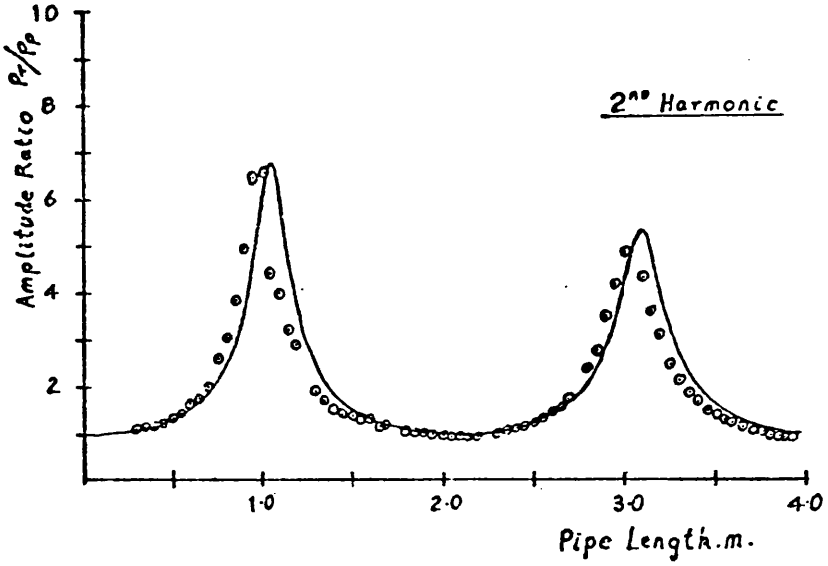

FIG 3·9 Pressure amplitude ratio $|P_T/P_p|$ Variation with pipeline length (System pressure 200 bar)

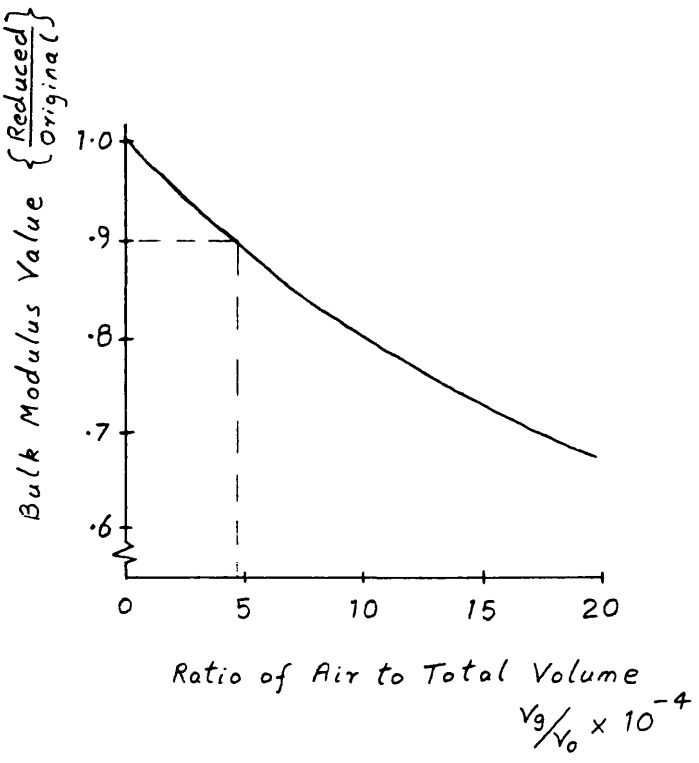

FIG 3·10 Reduction in the Bulk Modulus of the Hydraulic Fluid with increasing Air Entrainment

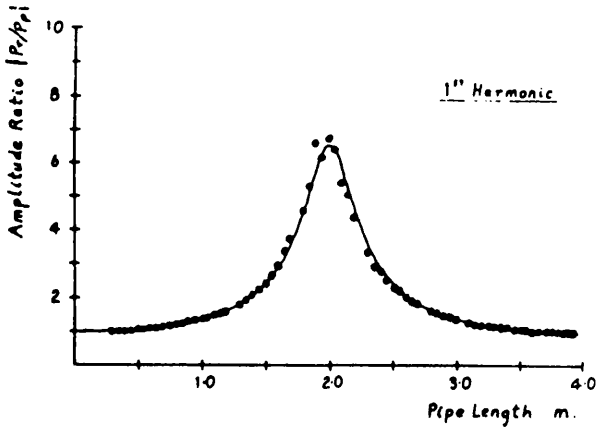

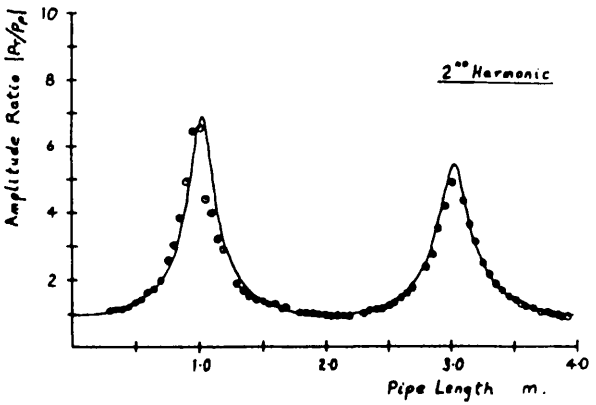

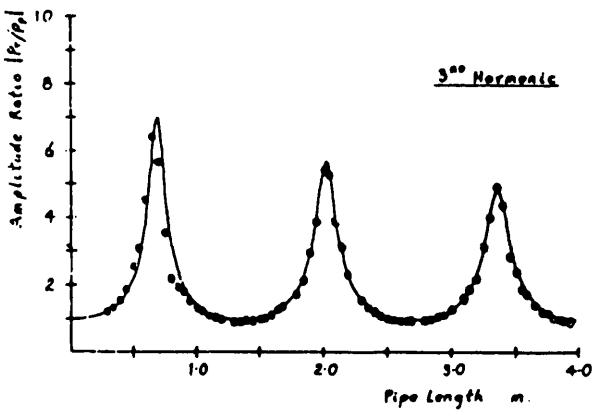

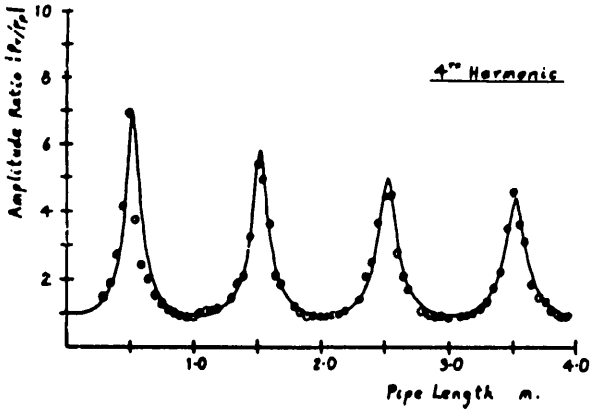

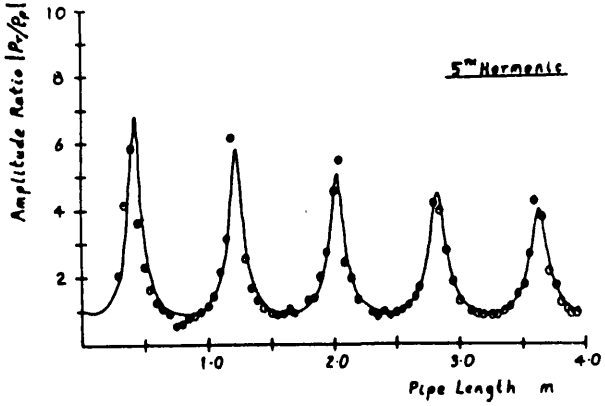

FIG 3·11

Pressure Amplitude Ratio $|P_T/P_p|$, computed using a corrected Bulk Modulus value, β.

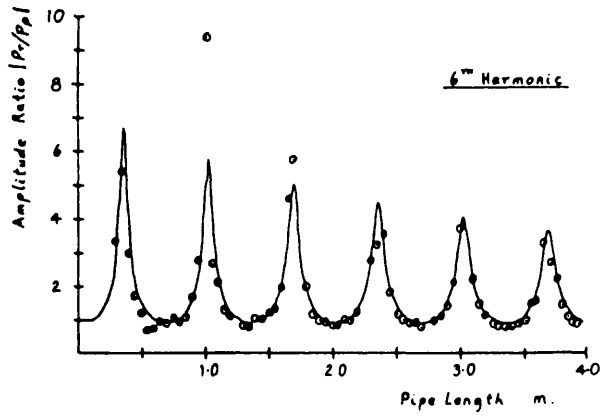

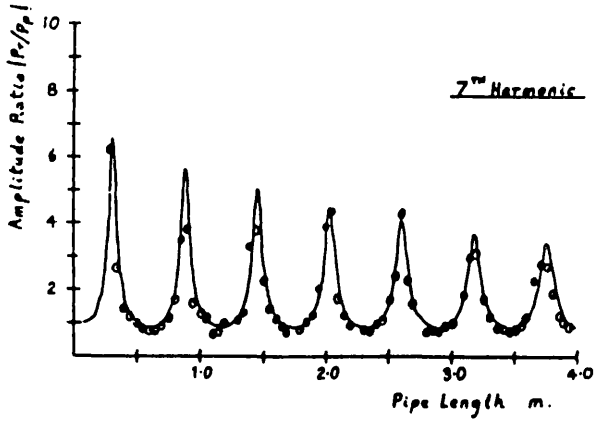

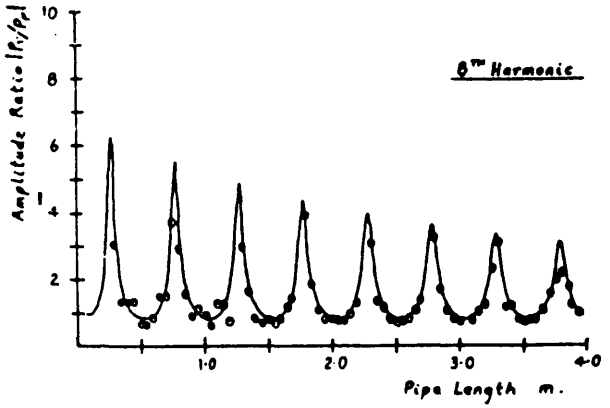

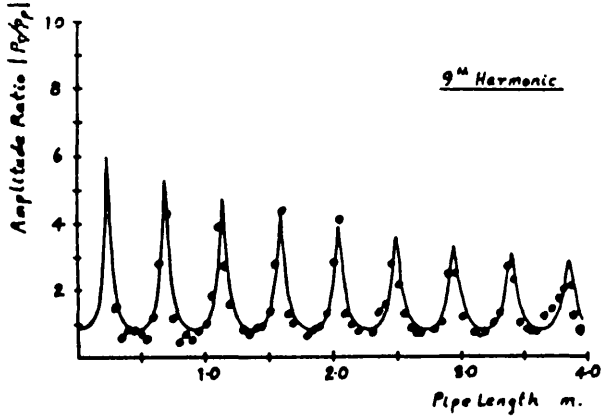

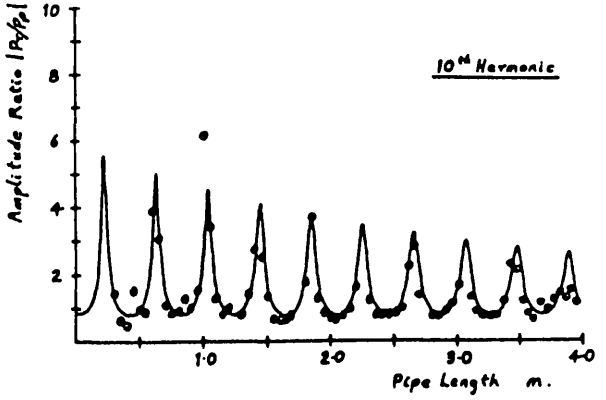

FIG 3·11 continued.

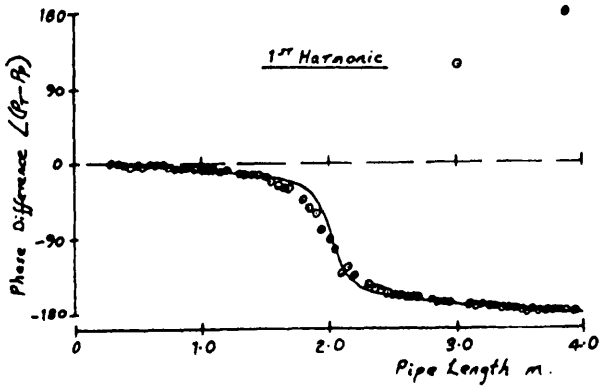

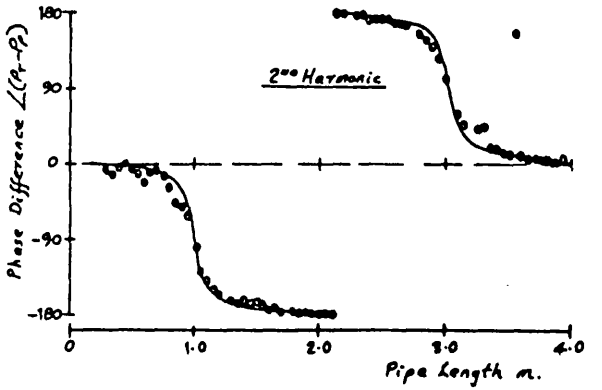

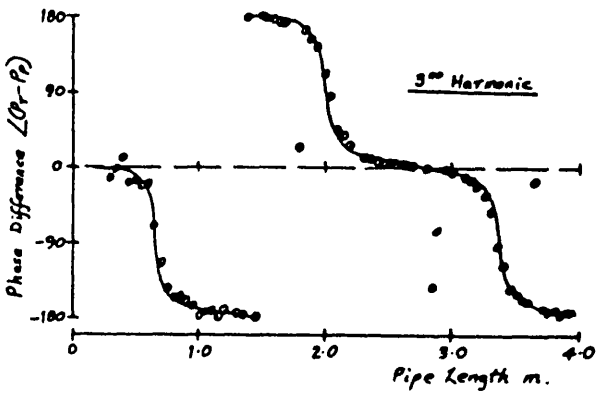

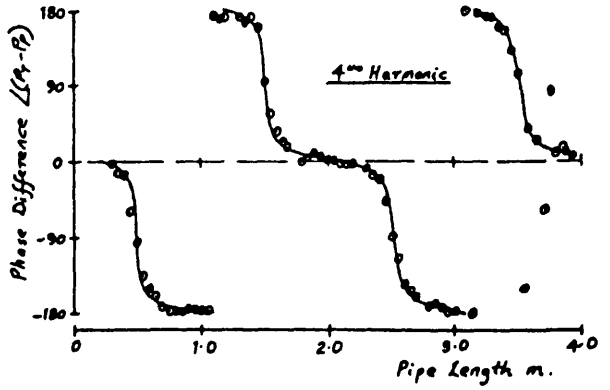

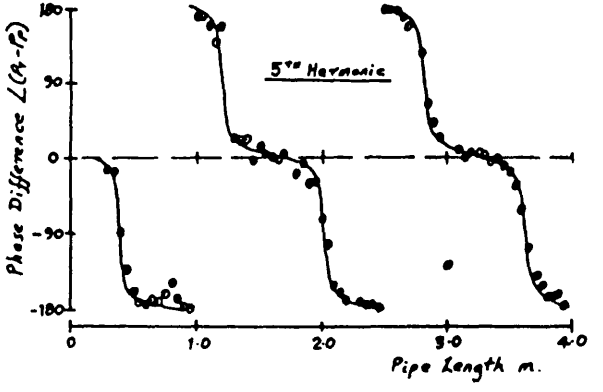

FIG 3·12

Pressure Phase Difference $\angle(P_T - P_P)$, computed using a corrected Bulk Modulus value.

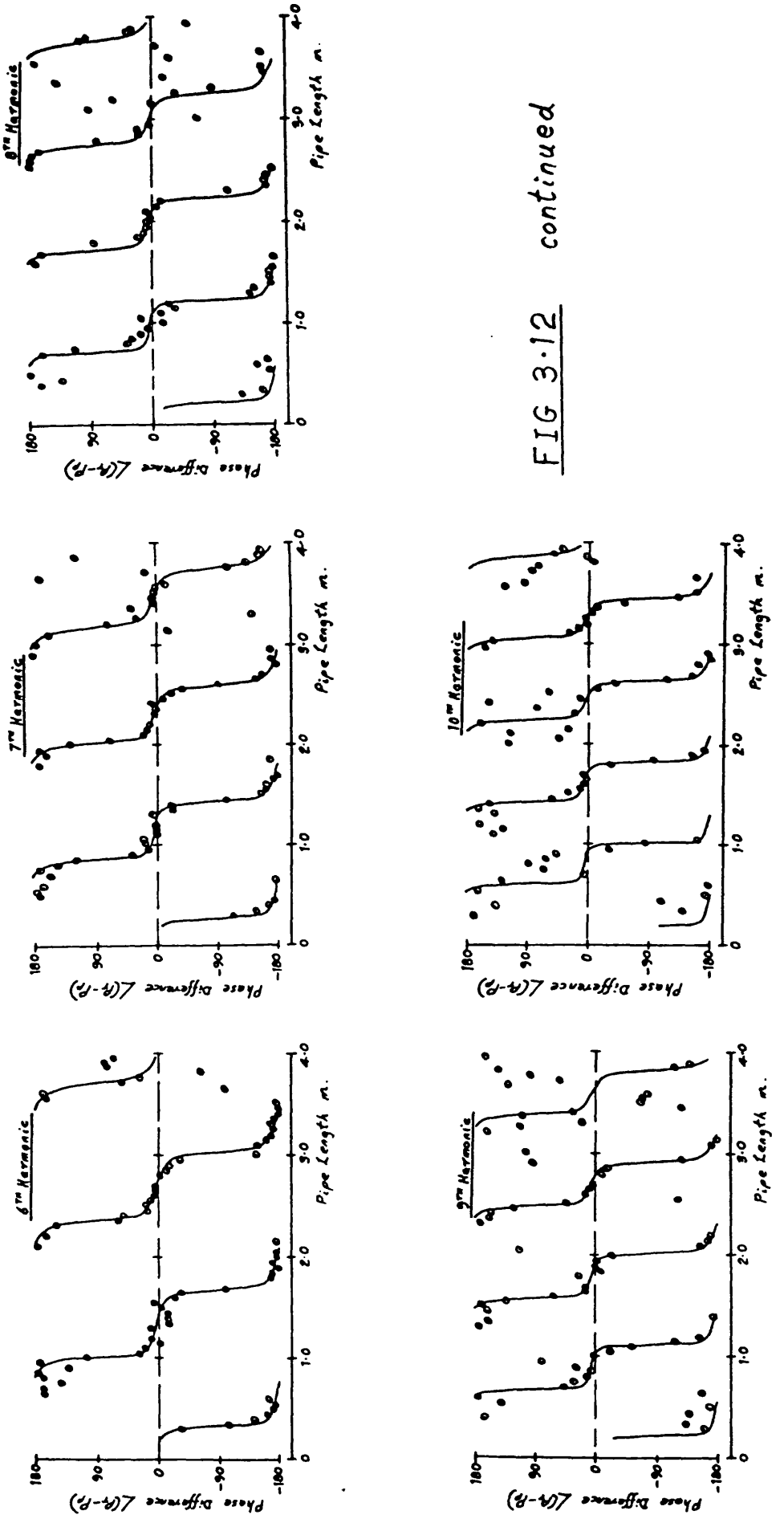

FIG 3.12 continued

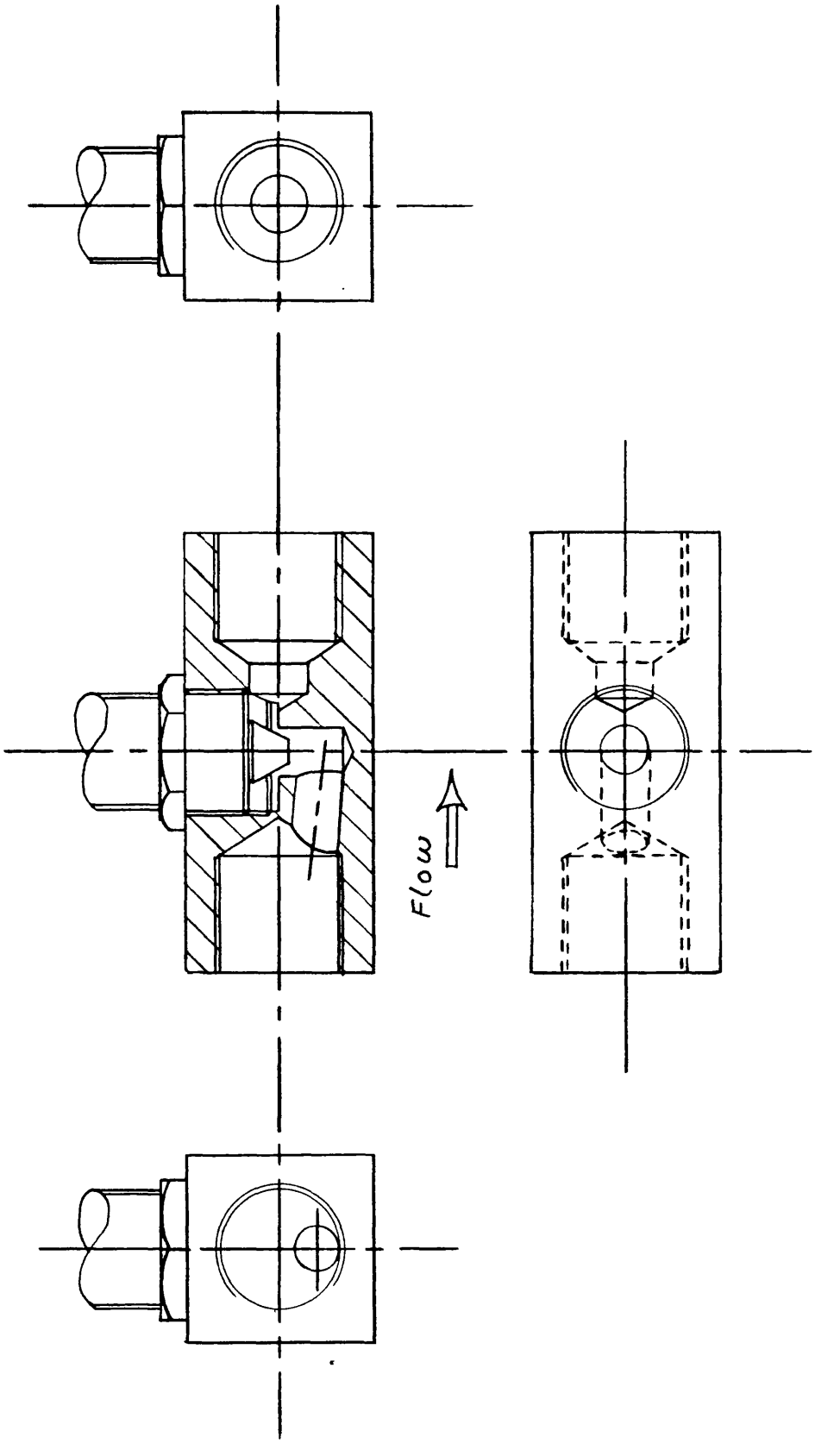

FIG 3·13 19 mm (3/4") Variable restrictor valve

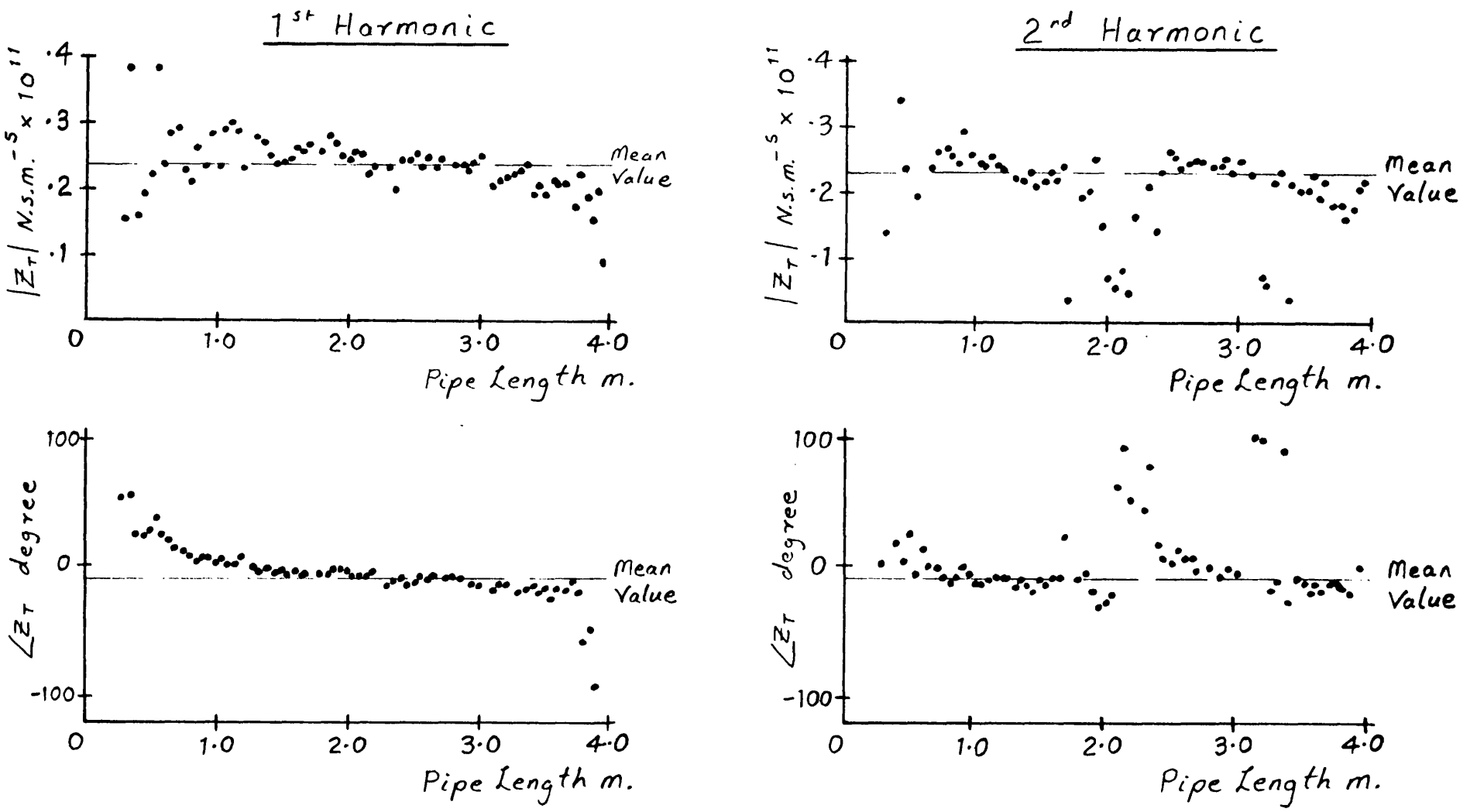

FIG 3·14 Valve impedance values predicted at each line length

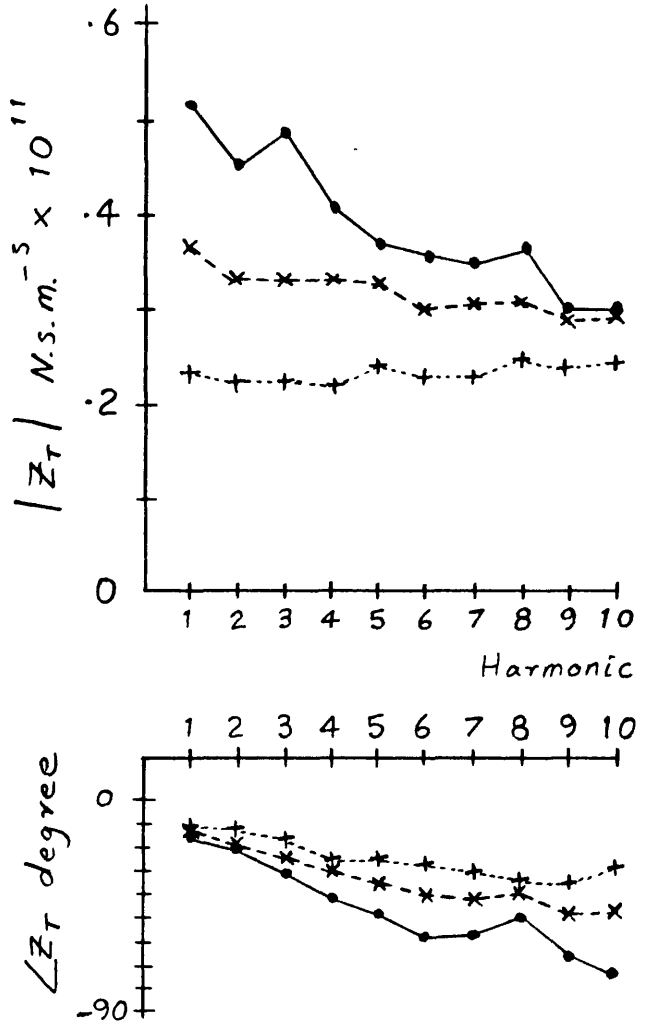

FIG 3·15 Valve impedance spectra.

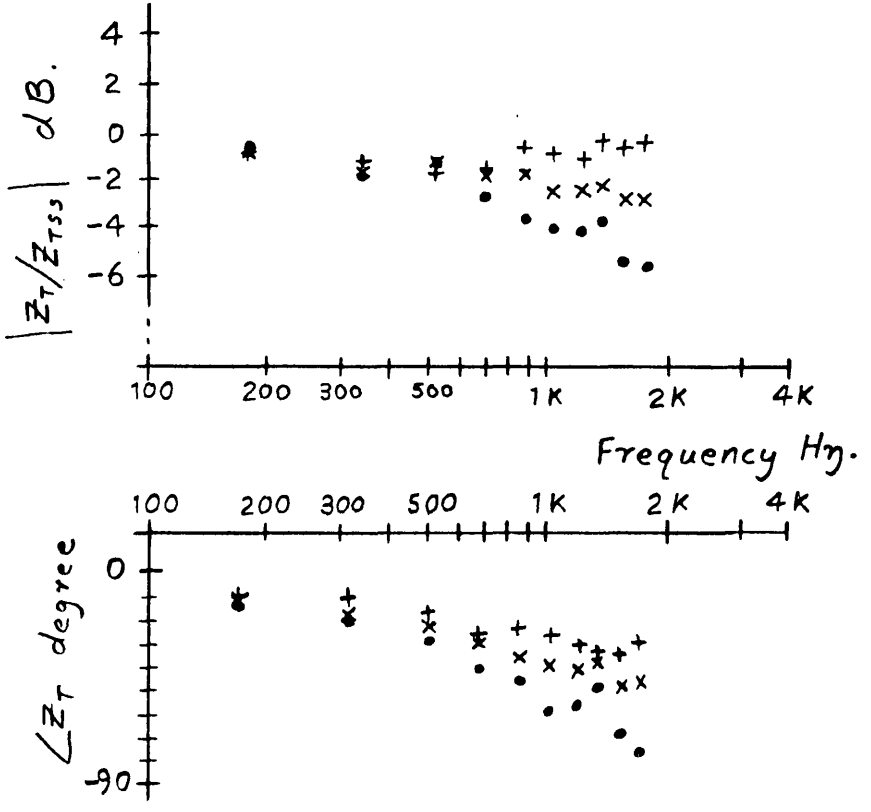

FIG 3·16 Valve impedance variation with frequency and setting.

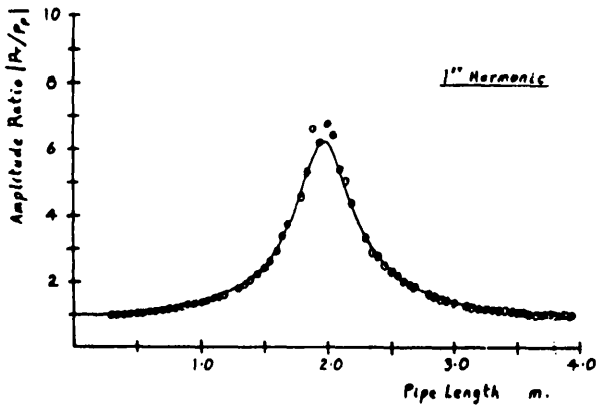

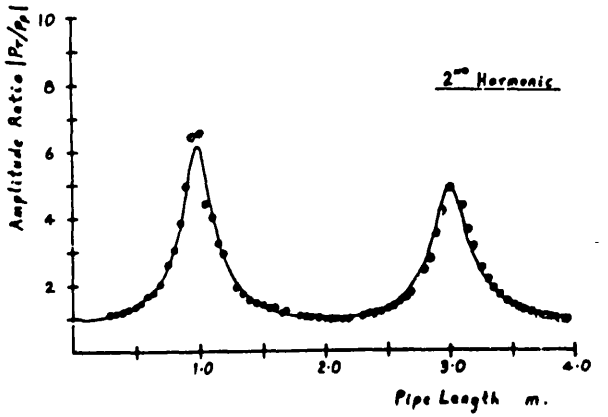

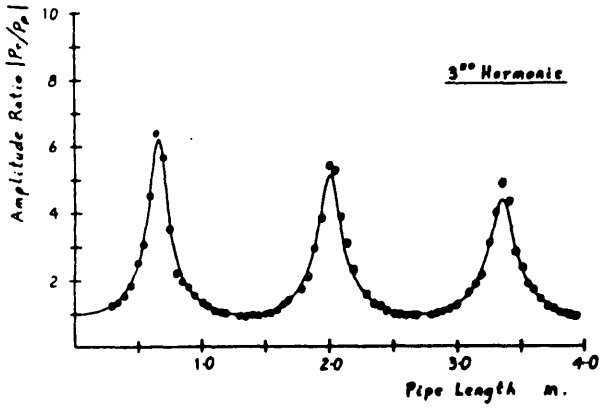

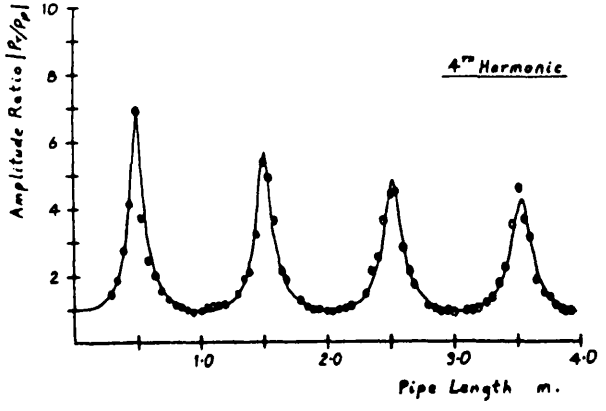

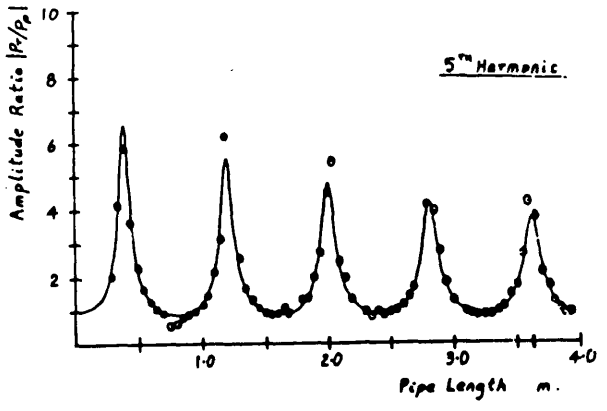

FIG 3·17

Pressure Amplitude Ratio $|P_T/P_p|$, computed using the predicted Valve Impedance Spectrum; Z_T, Fig 3·15.

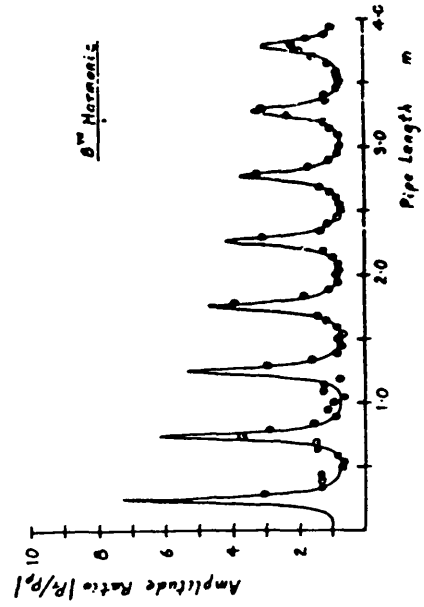

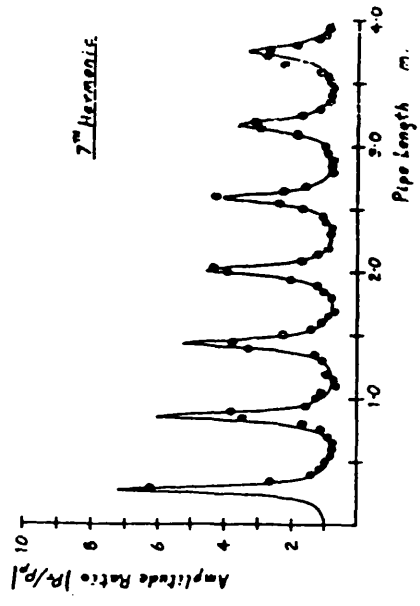

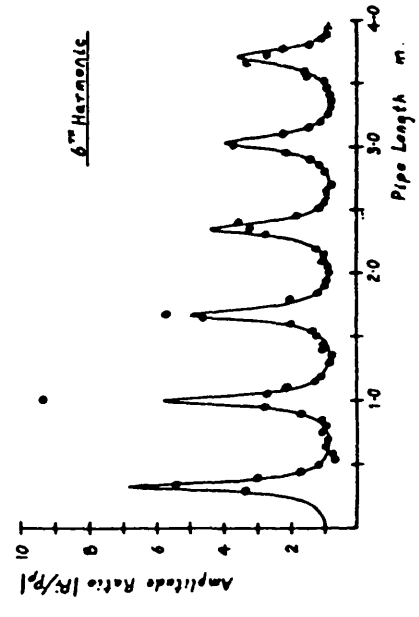

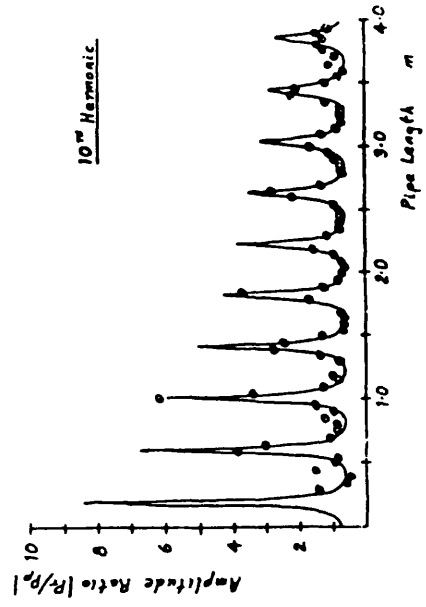

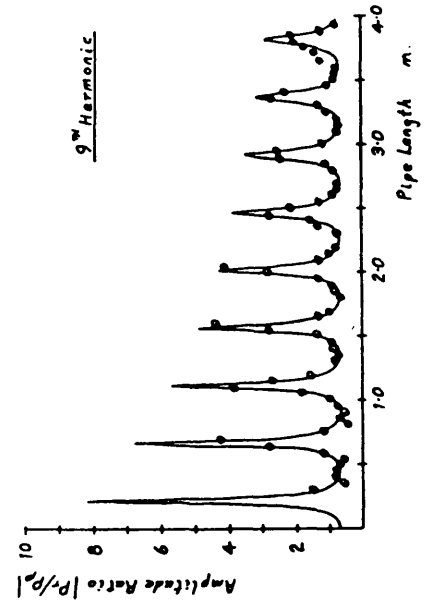

FIG 3·17 continued.

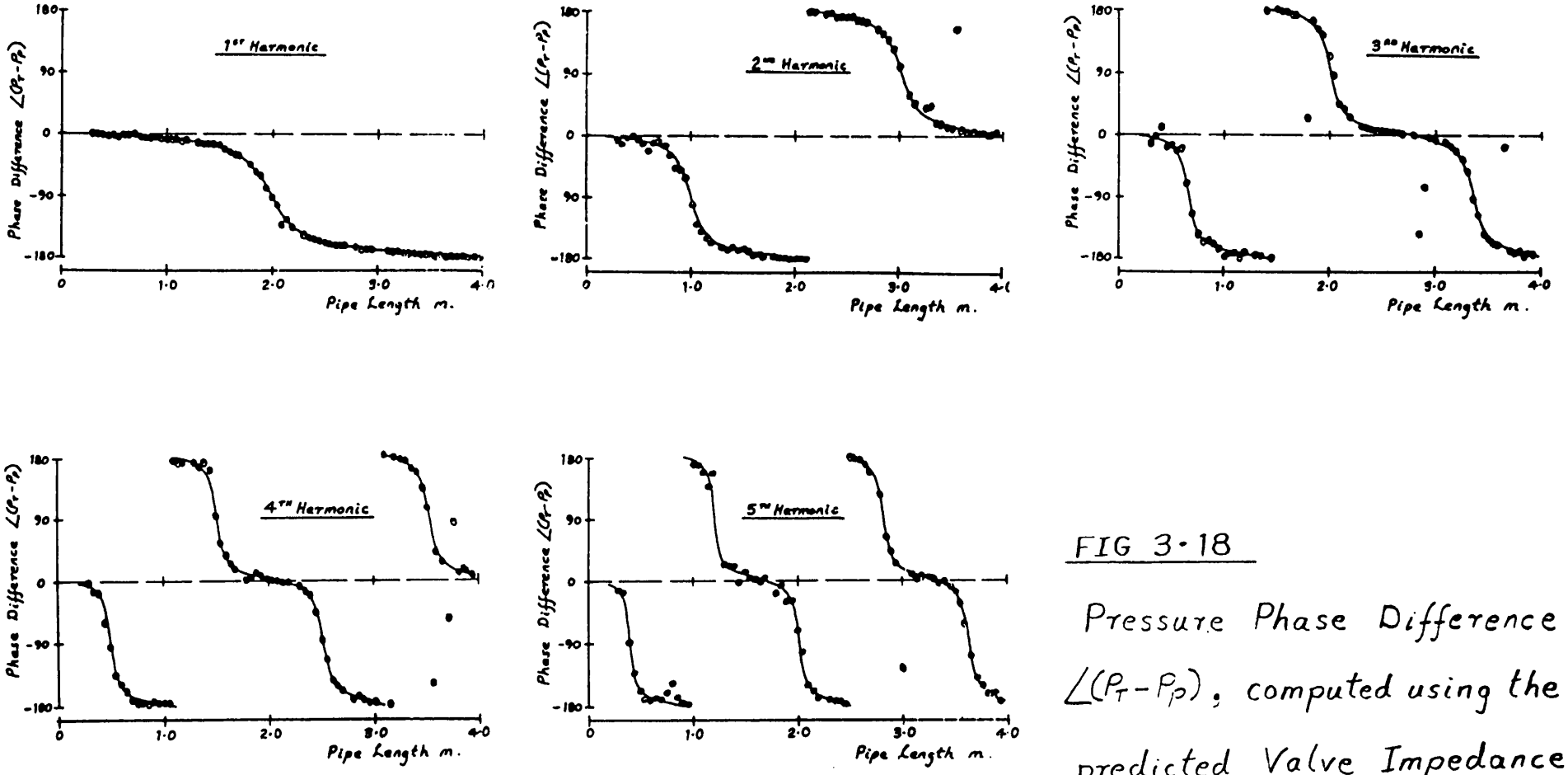

FIG 3·18

Pressure Phase Difference $\angle(P_T - P_p)$, computed using the predicted Valve Impedance Spectrum, Z_T, Fig 3·15.

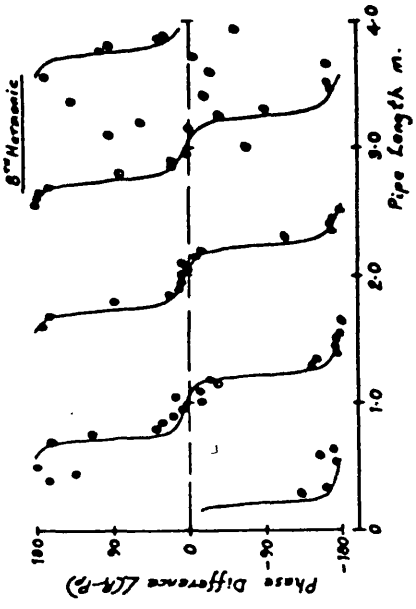

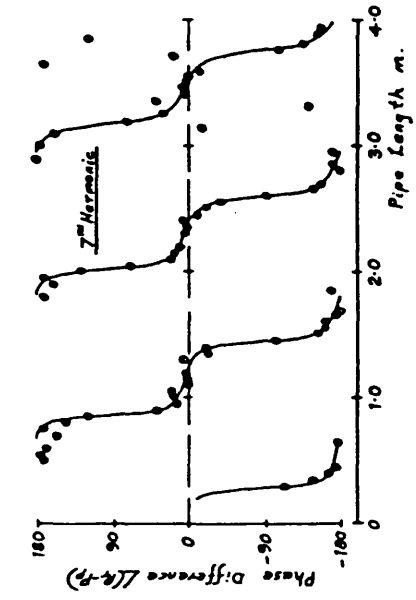

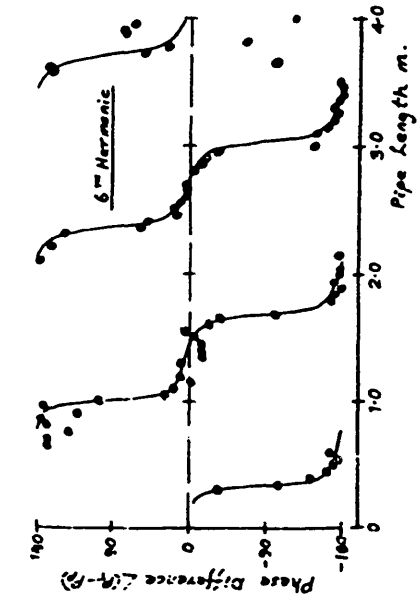

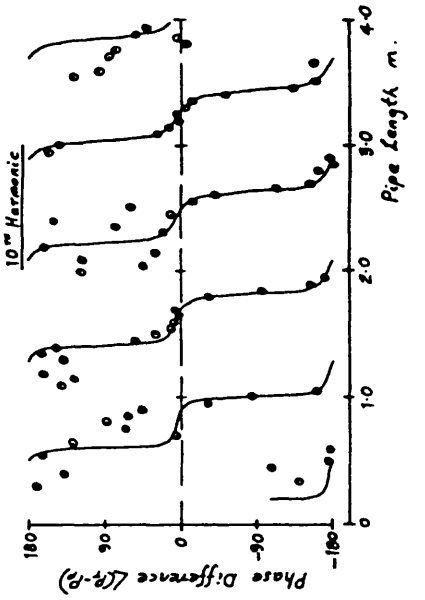

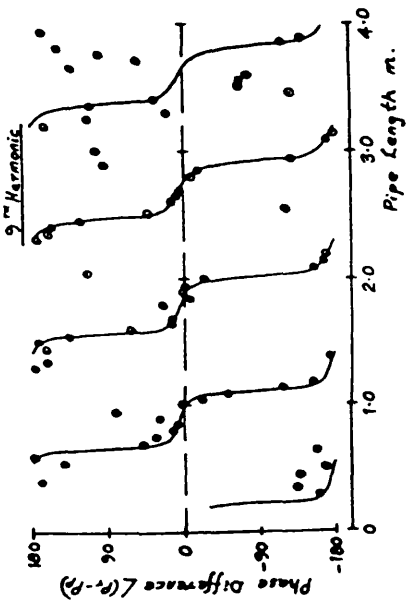

FIG 3·18 continued.

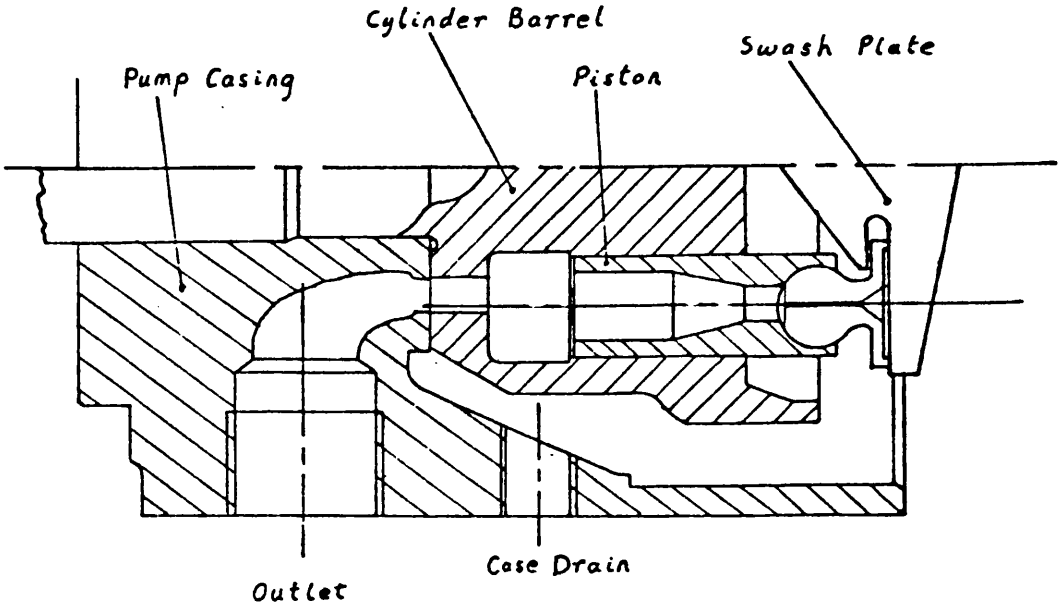

FIG 3·20 A section through the delivery side of the Reyrolle pump with the piston in mid-stroke.

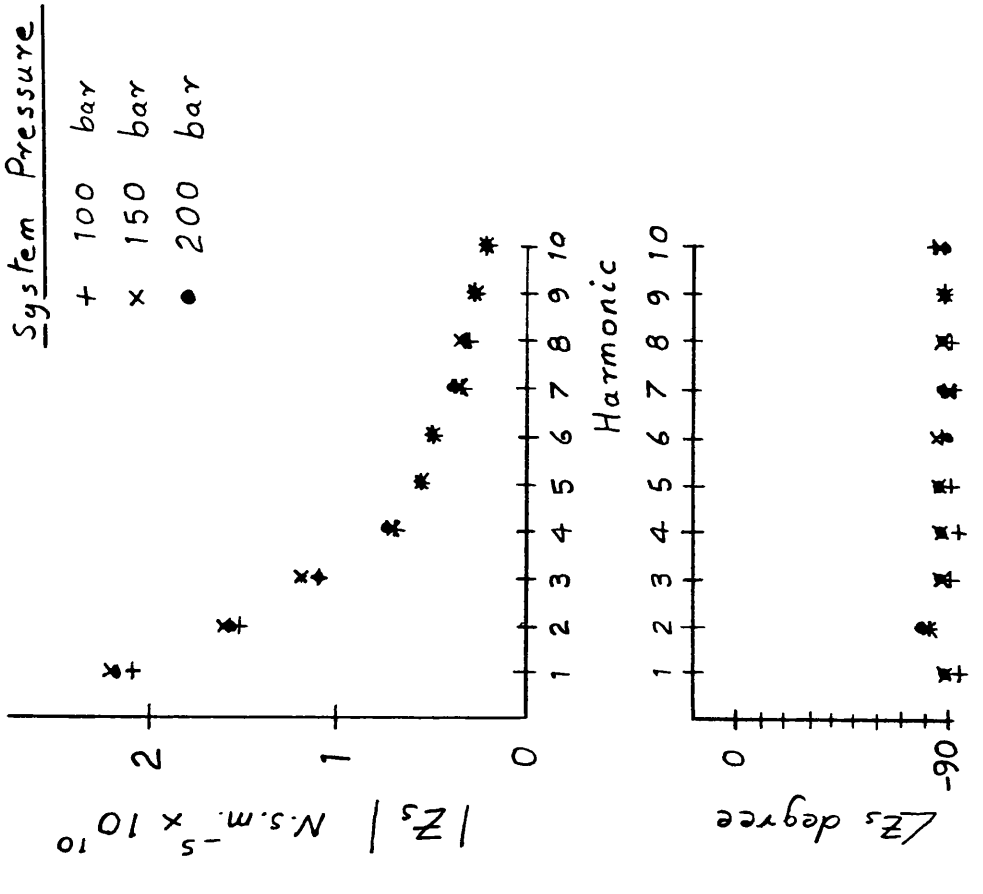

FIG 3·19 Pump impedance spectra.

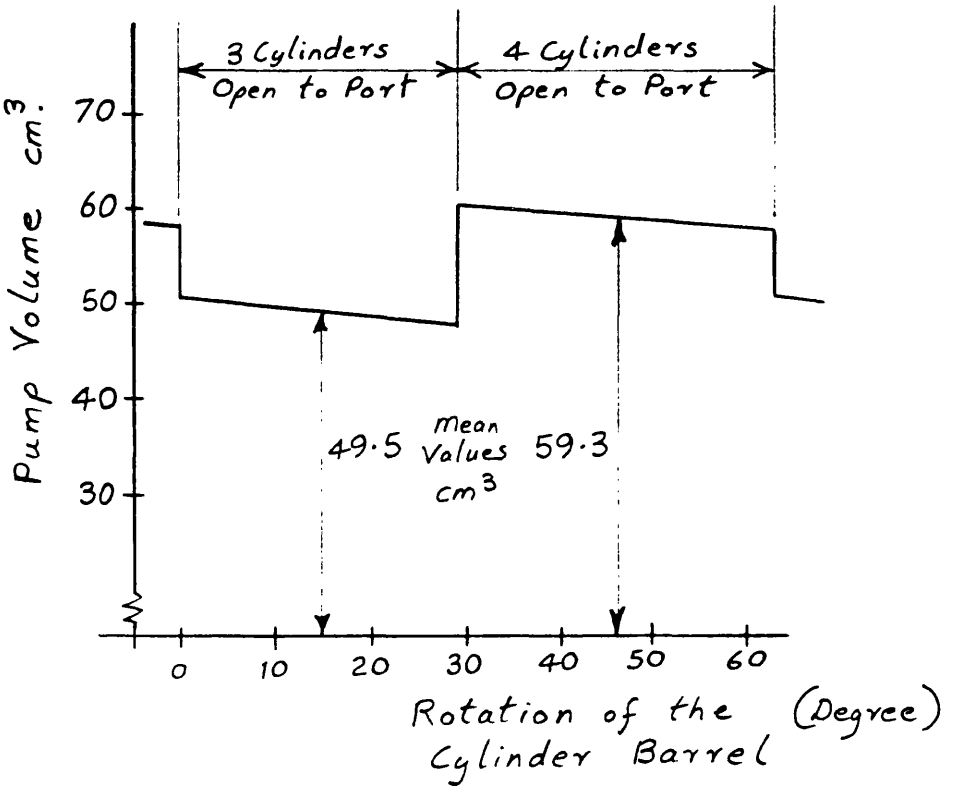

FIG 3·21 Variation in the 'pump volume' with cylinder barrel position.

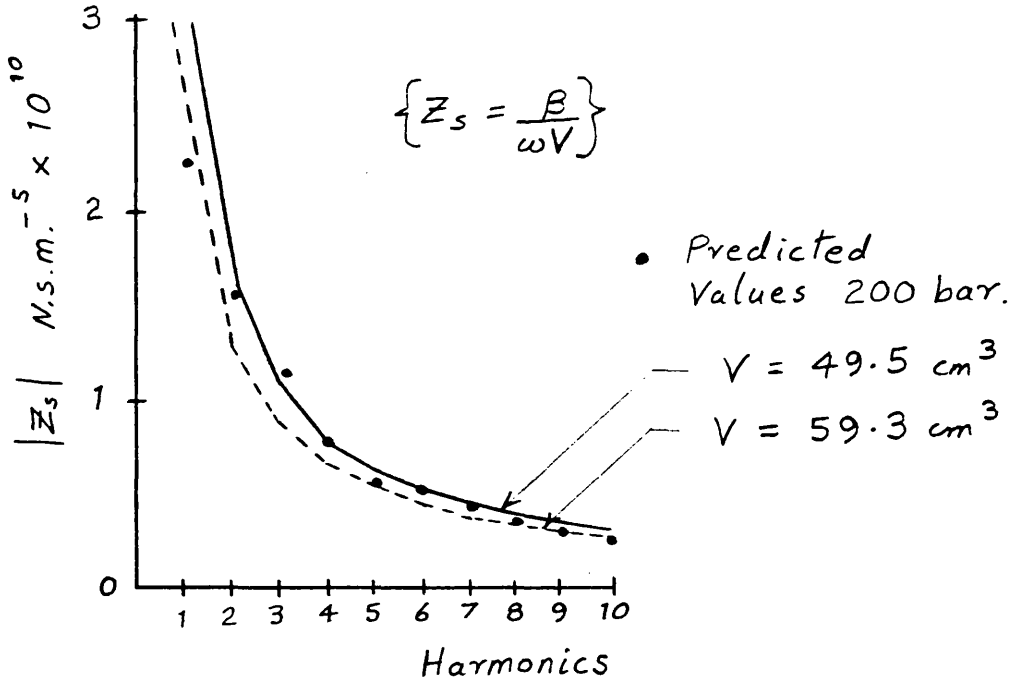

FIG 3·22 Comparing the predicted pump impedance with that of a simple volume, V.

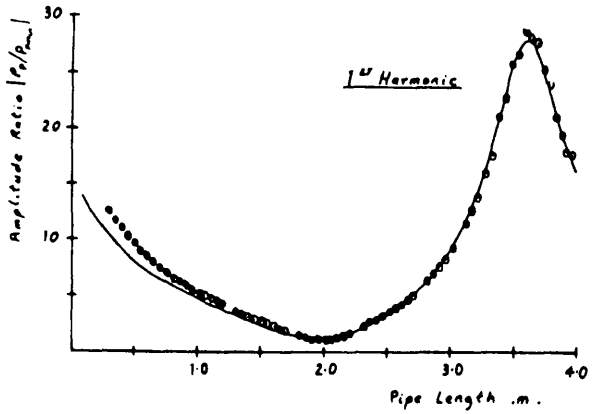

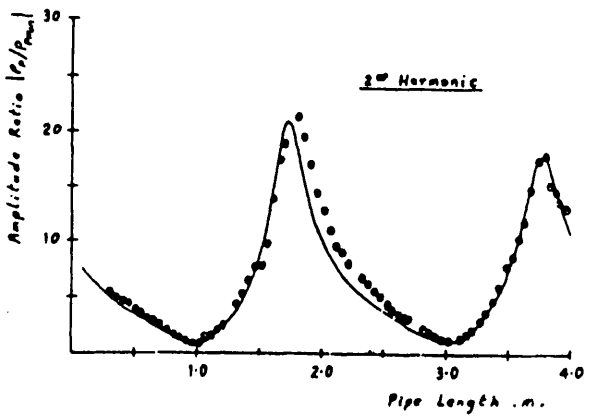

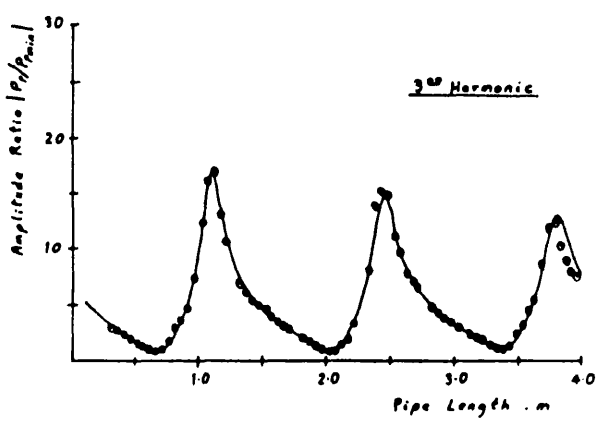

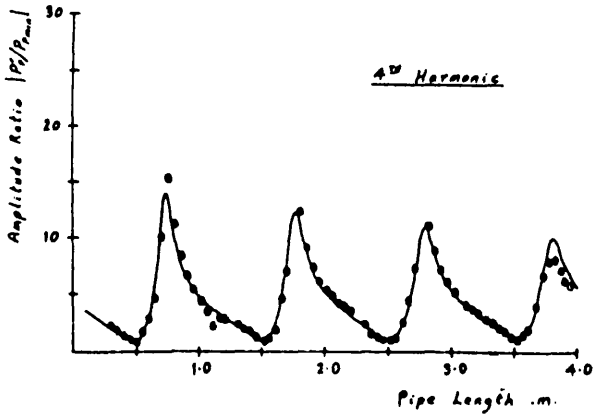

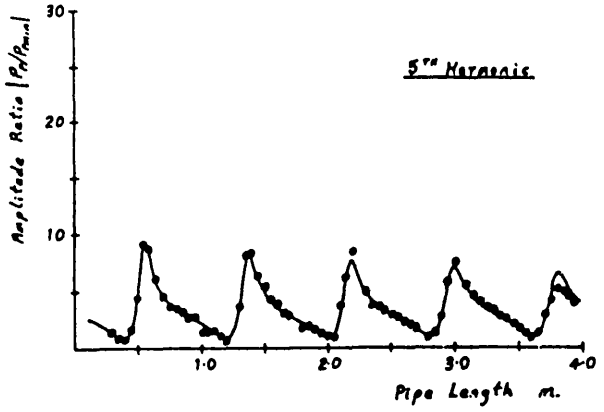

FIG 3·23

Pressure Amplitude Ratio

$|P_p/P_{pmin}|$

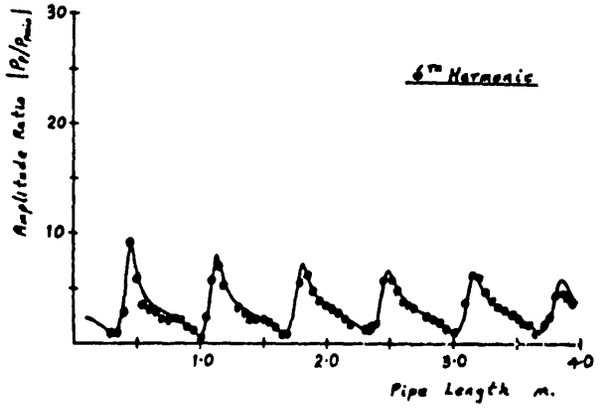

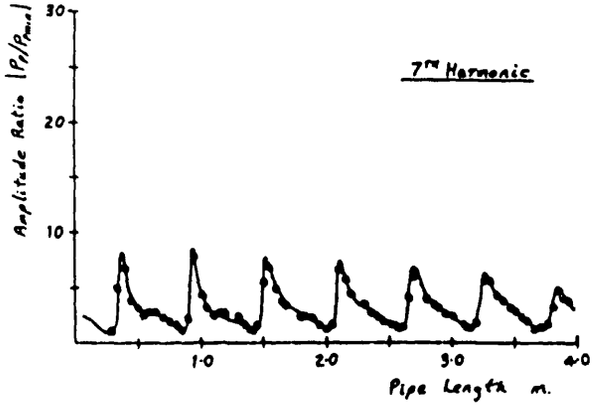

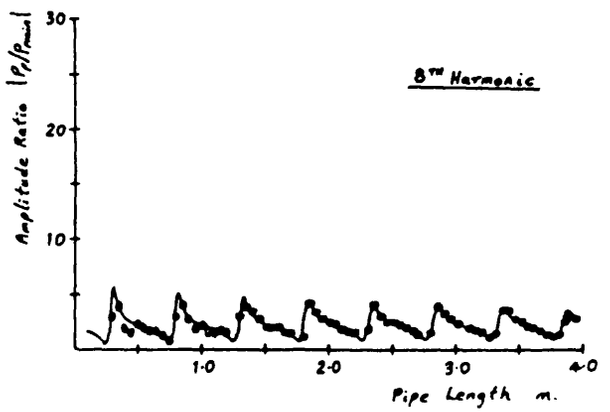

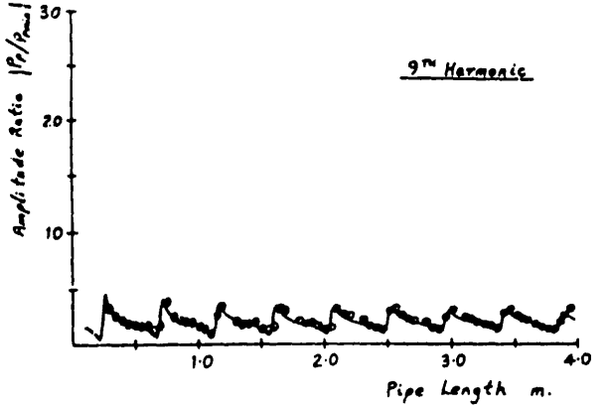

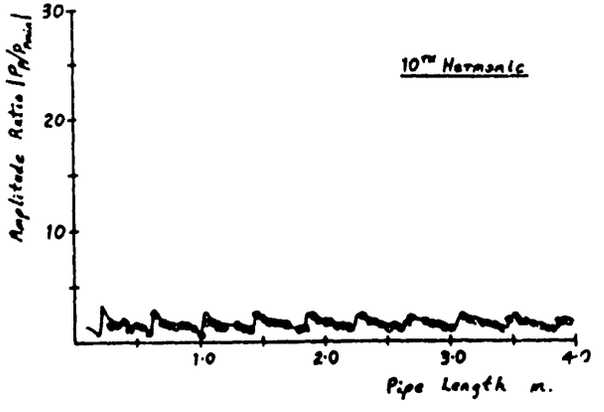

FIG 3·23 continued.

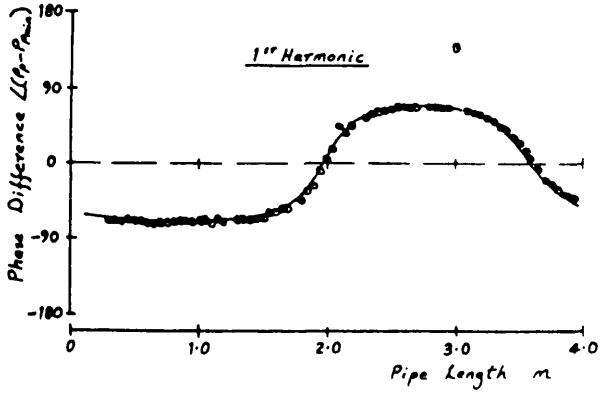

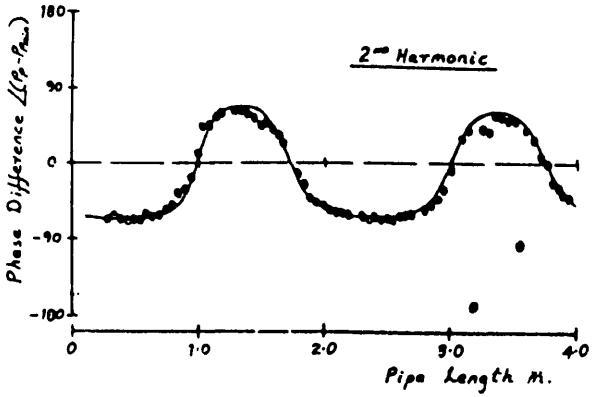

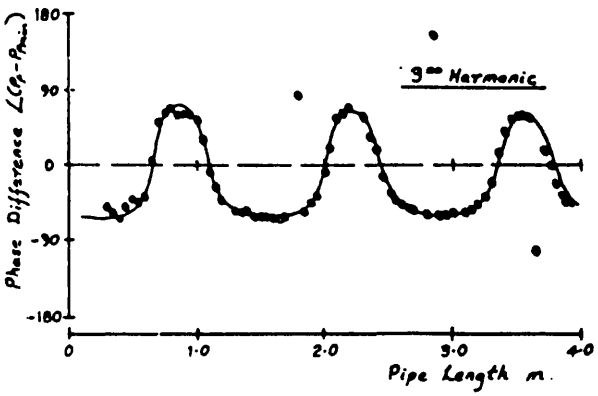

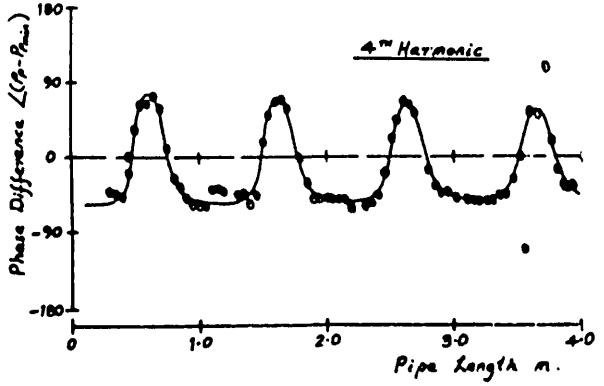

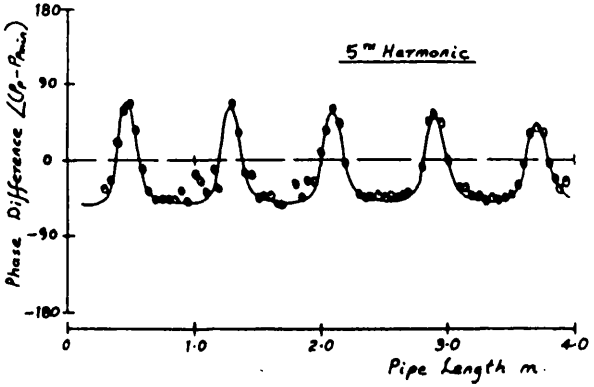

FIG 3·24

Pressure Phase Difference

$\angle(P_p - P_{pmin})$

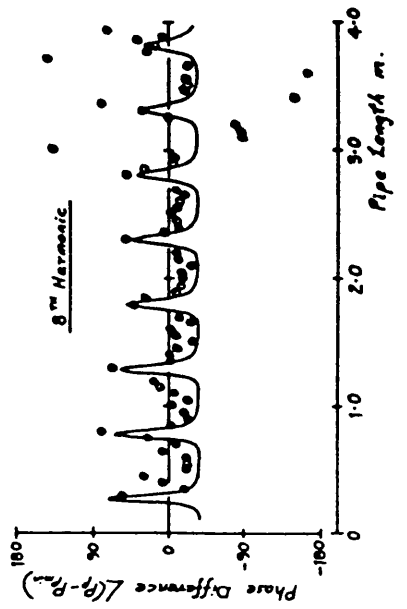

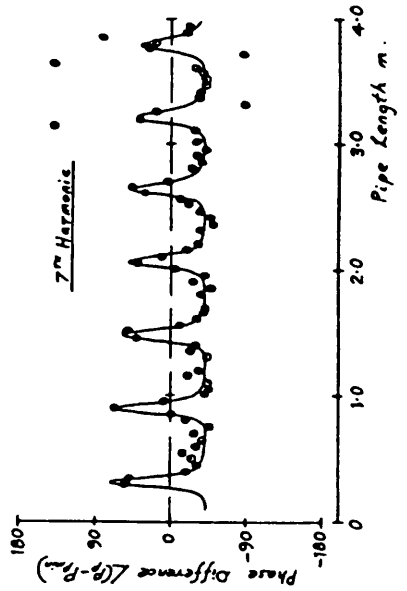

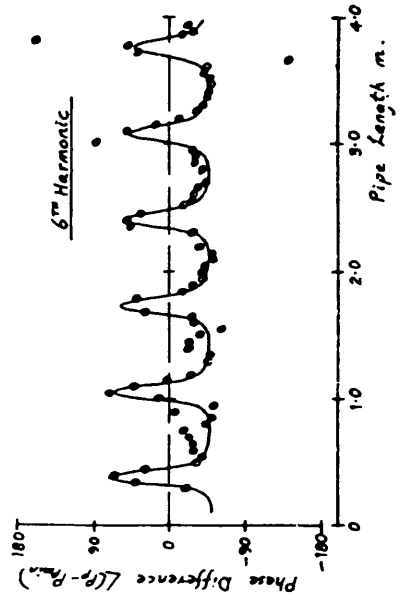

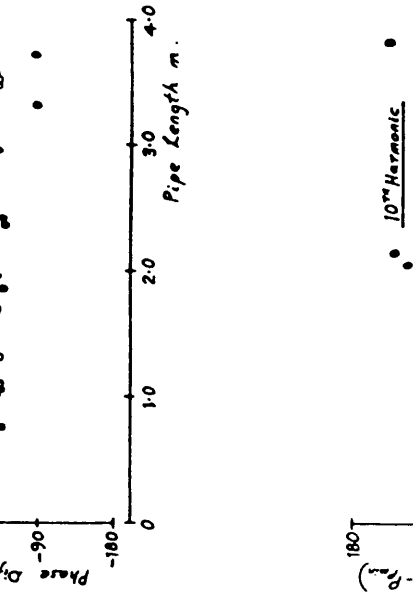

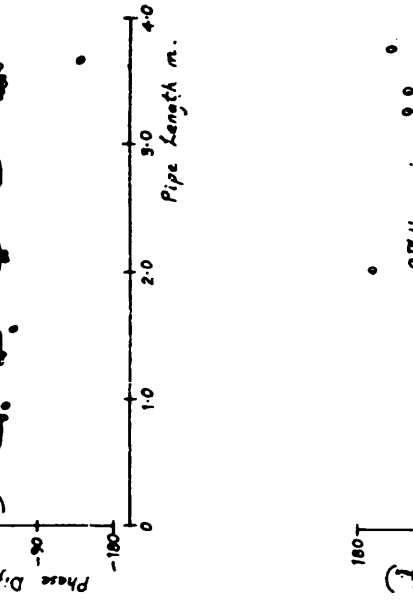

FIG 3·24 continued.

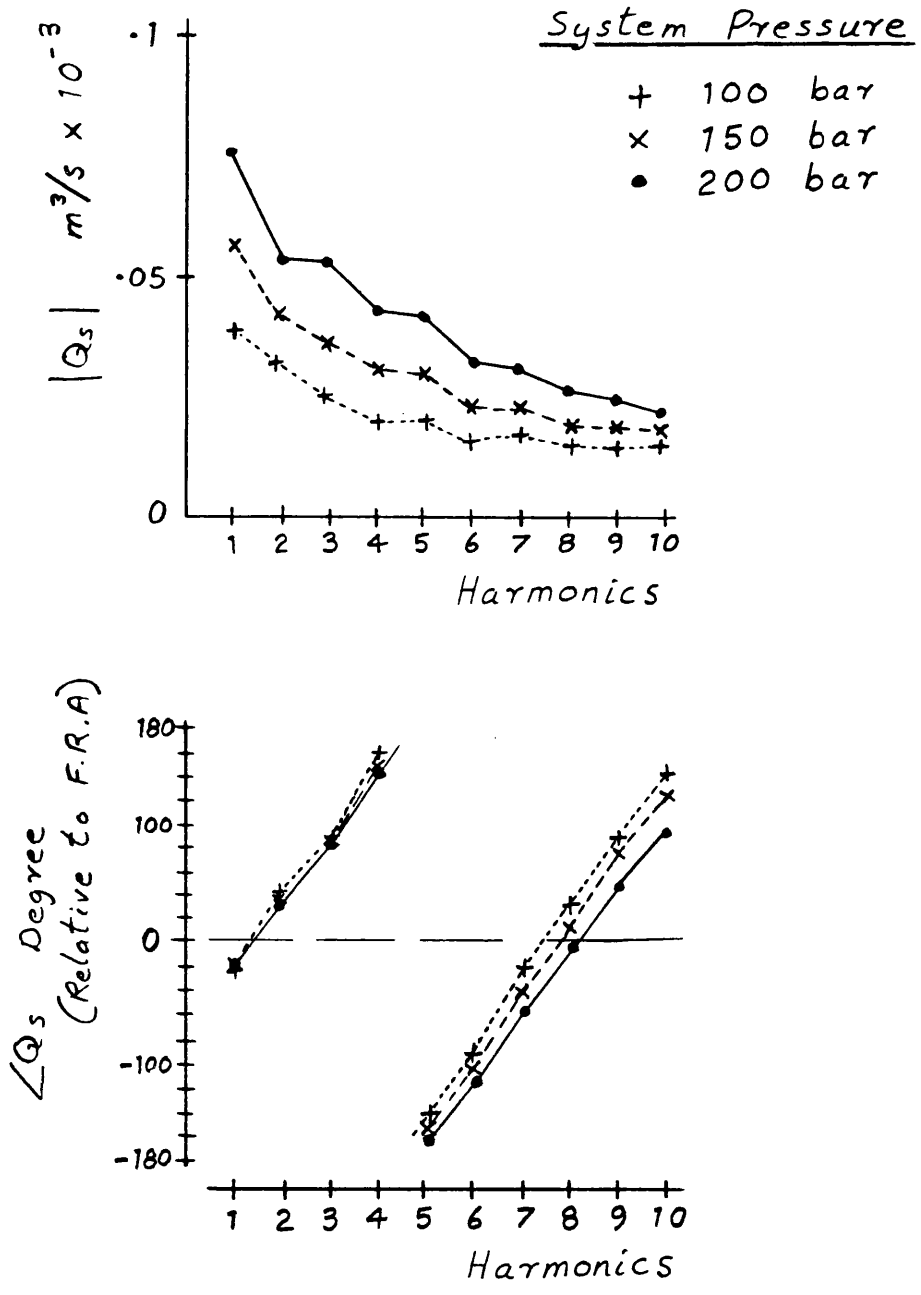

FIG 3·25 Pump flow spectra

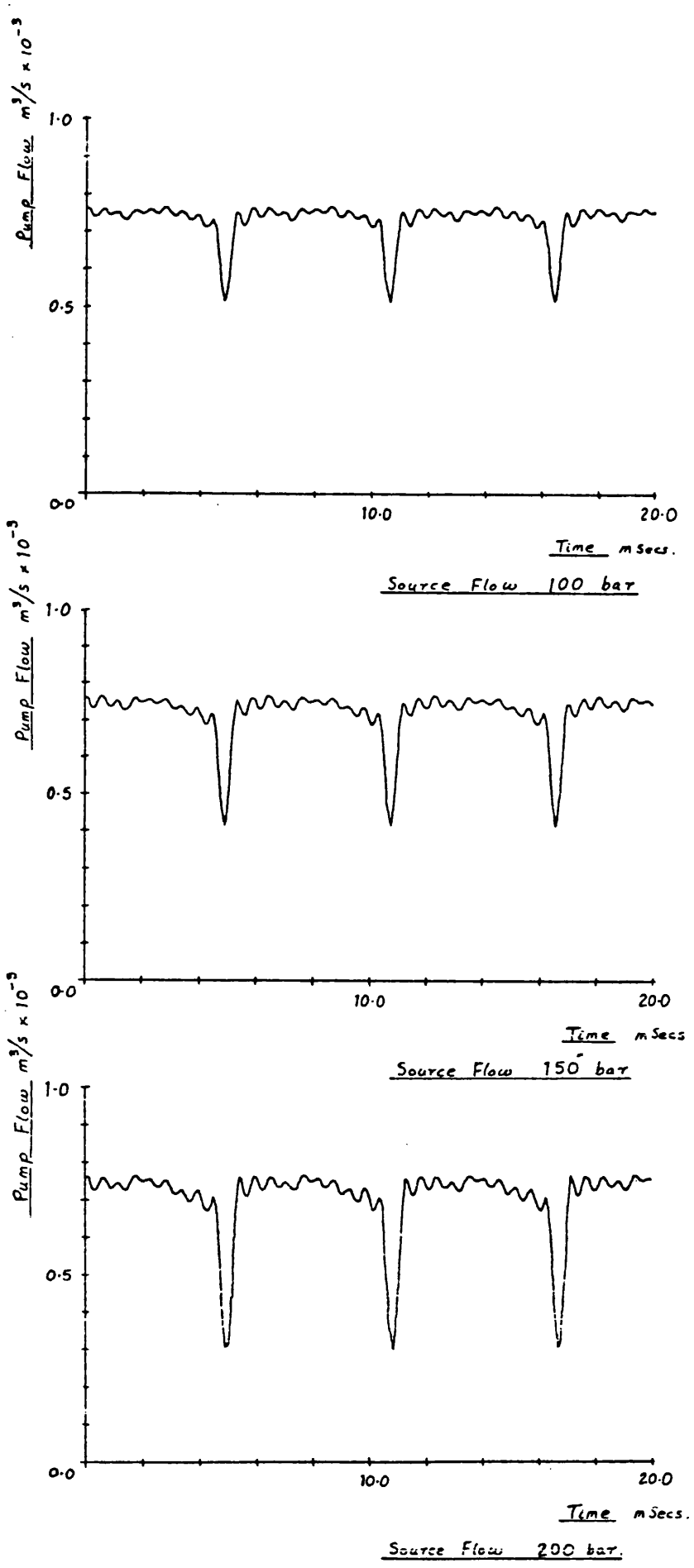

FIG 3·26 Synthesised pump flows

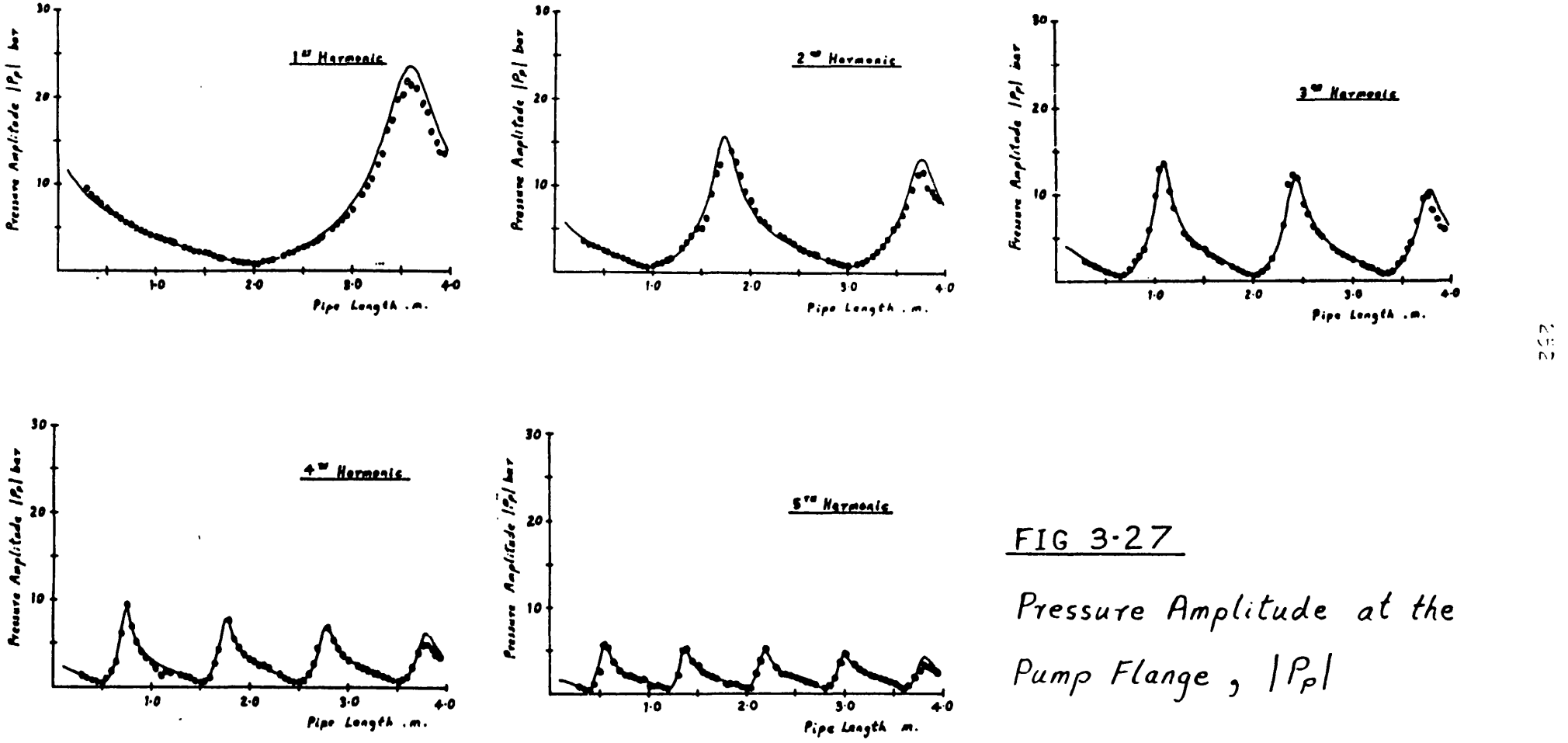

FIG 3·27

Pressure Amplitude at the Pump Flange, $|P_p|$

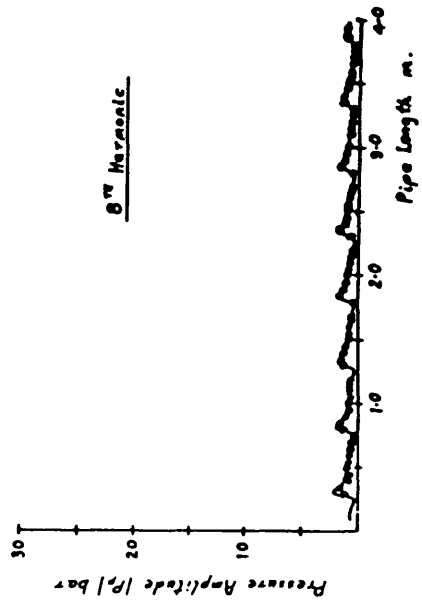

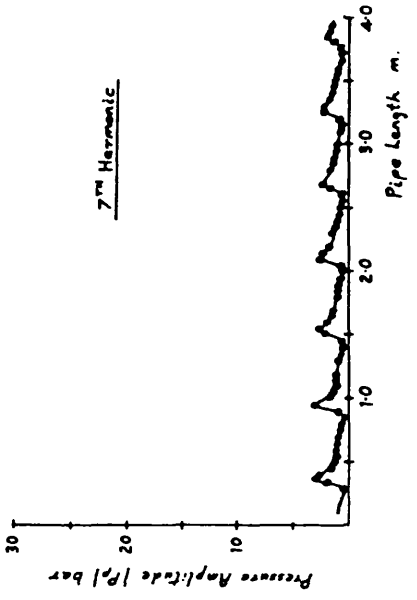

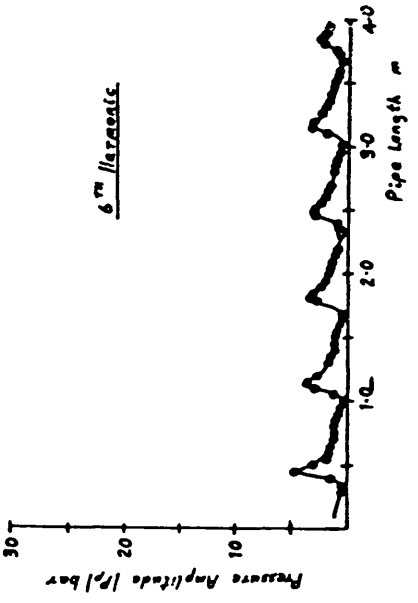

FIG 3·27 continued.

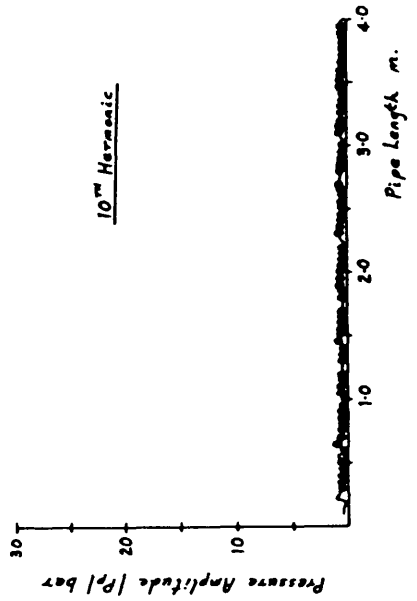

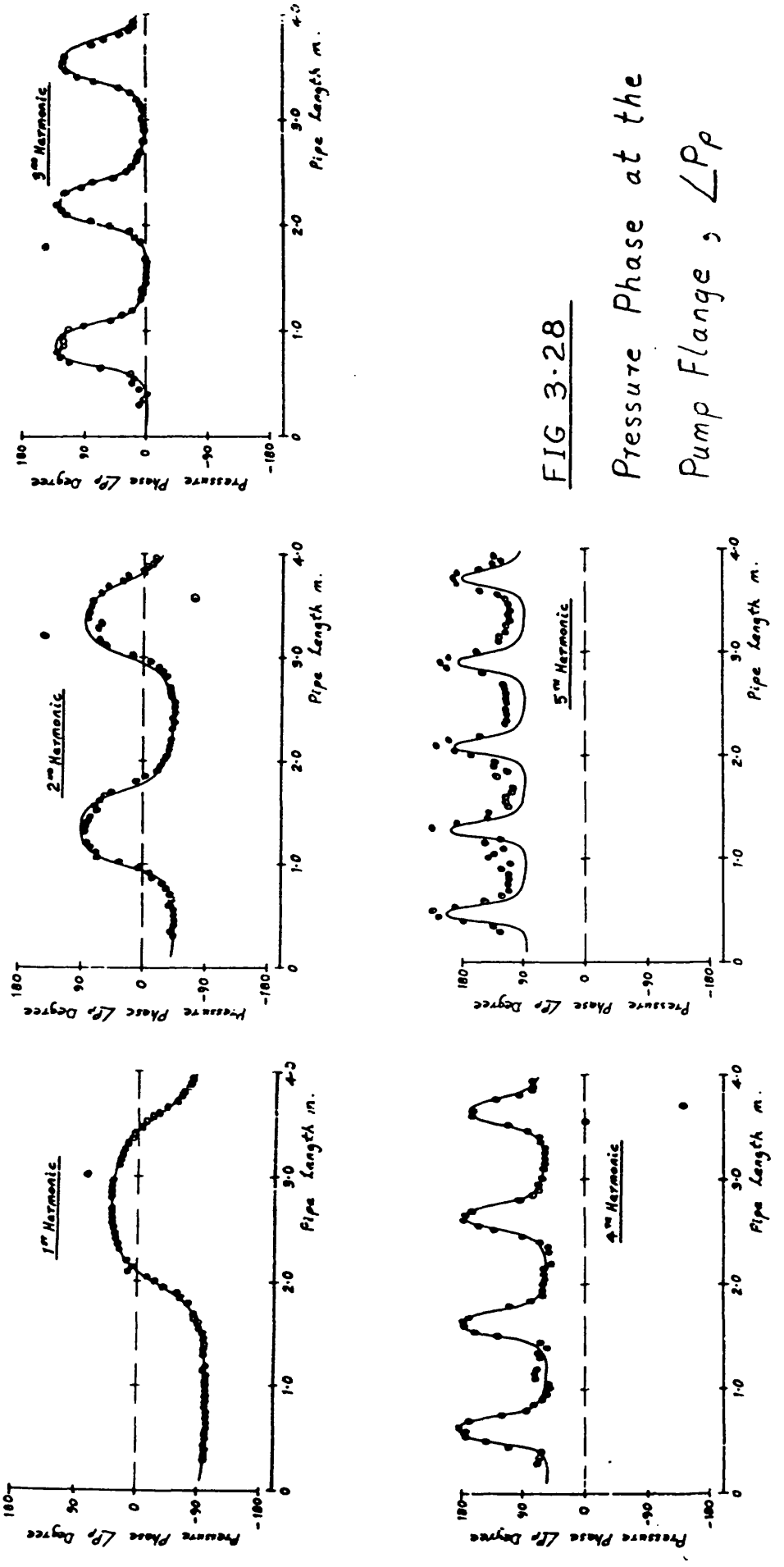

FIG 3.28

Pressure Phase at the Pump Flange ; $\angle P_p$

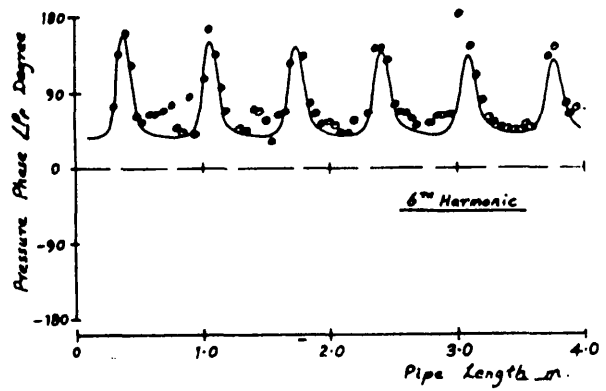

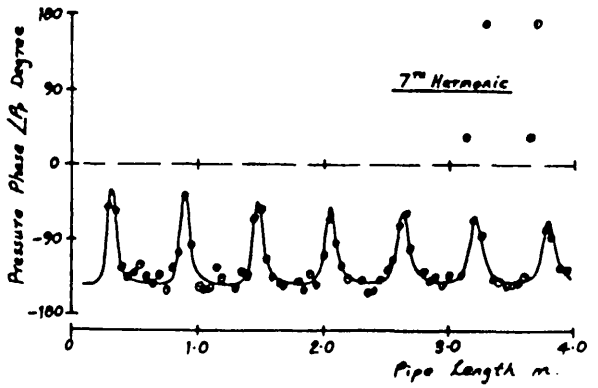

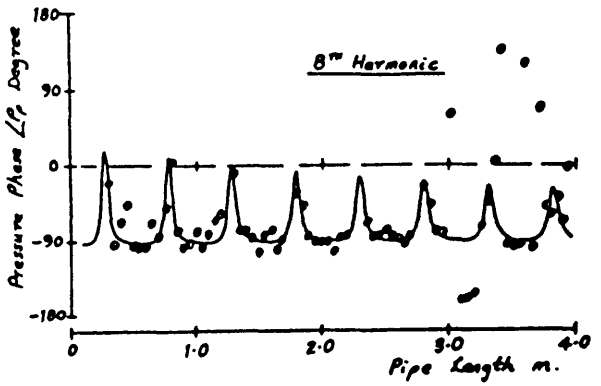

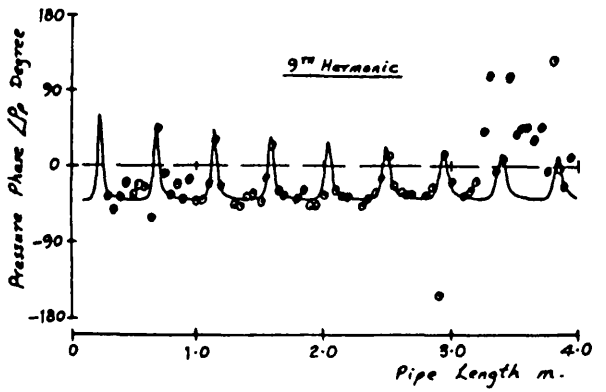

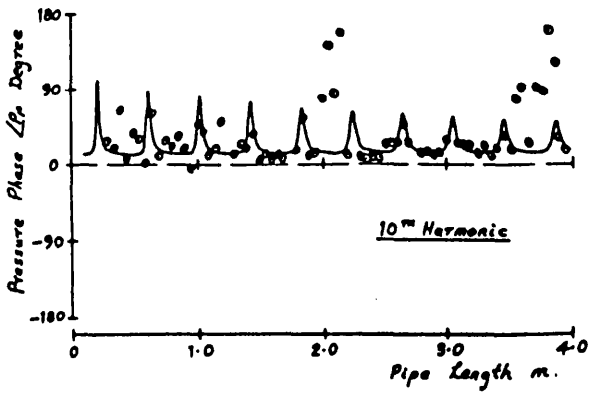

FIG 3·28 continued.

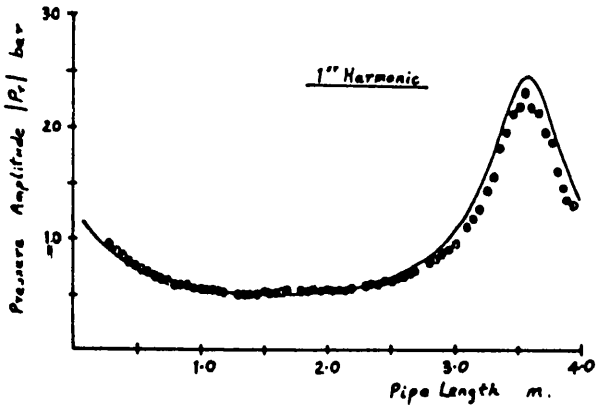

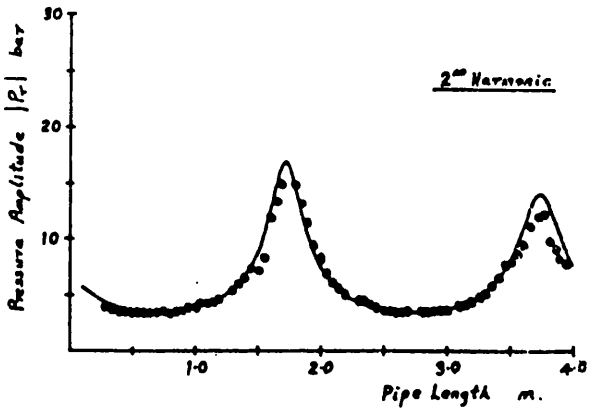

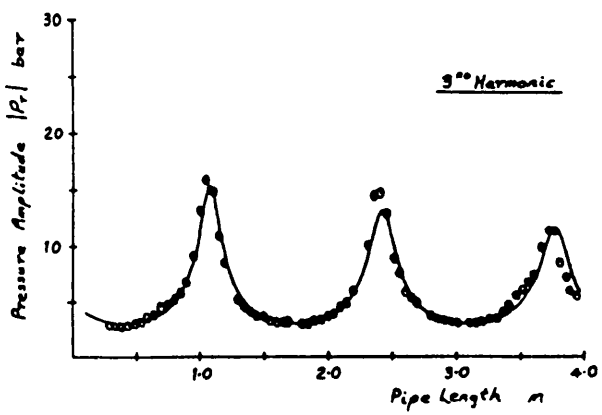

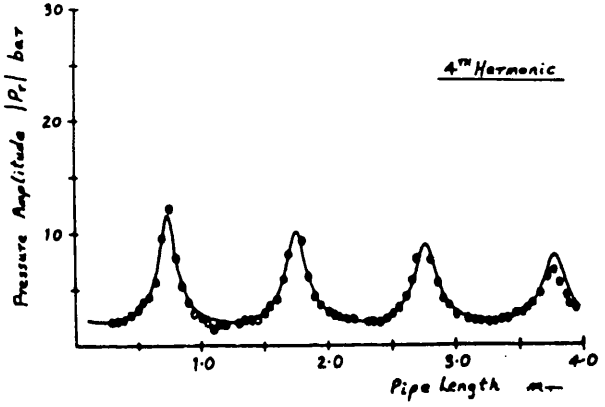

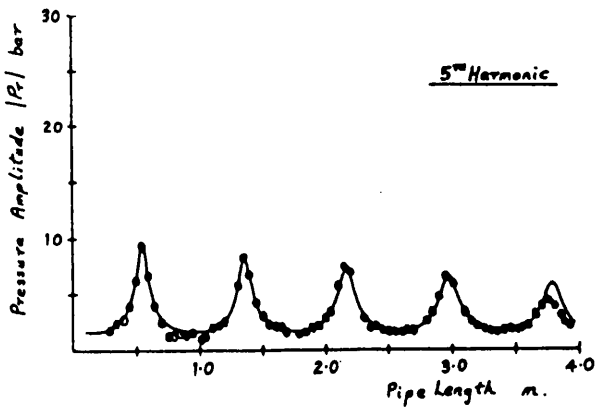

FIG 3·29

Pressure Amplitude at the Valve ; $|P_T|$

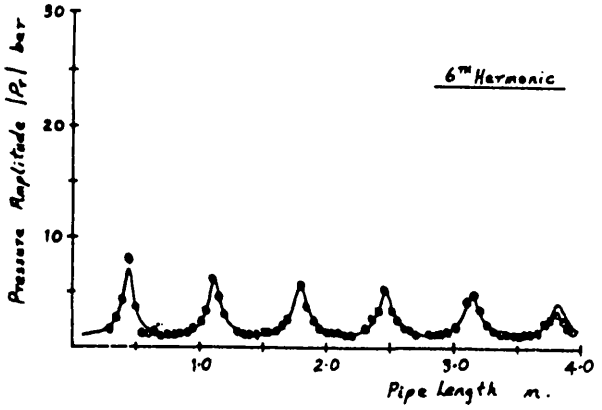

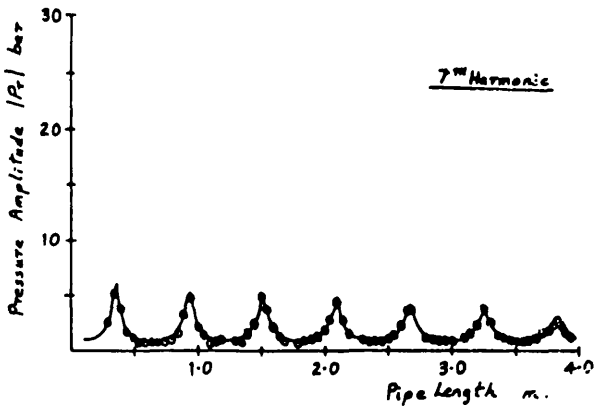

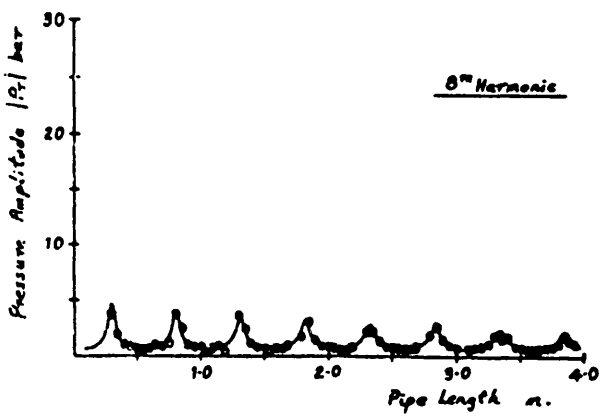

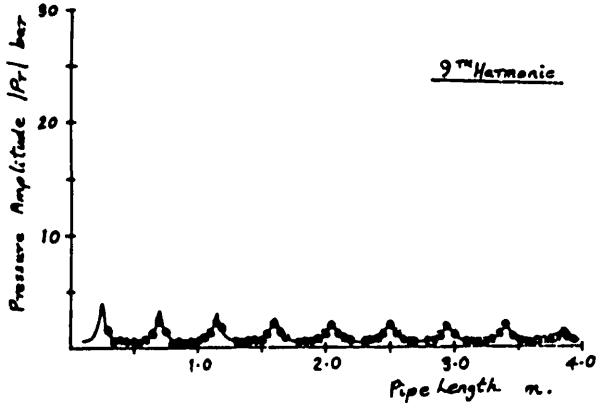

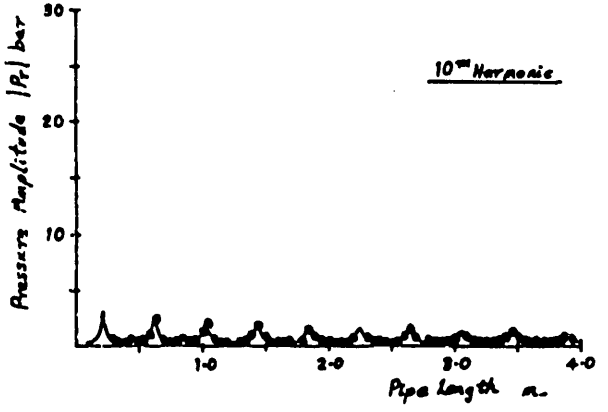

FIG 3·29 continued.

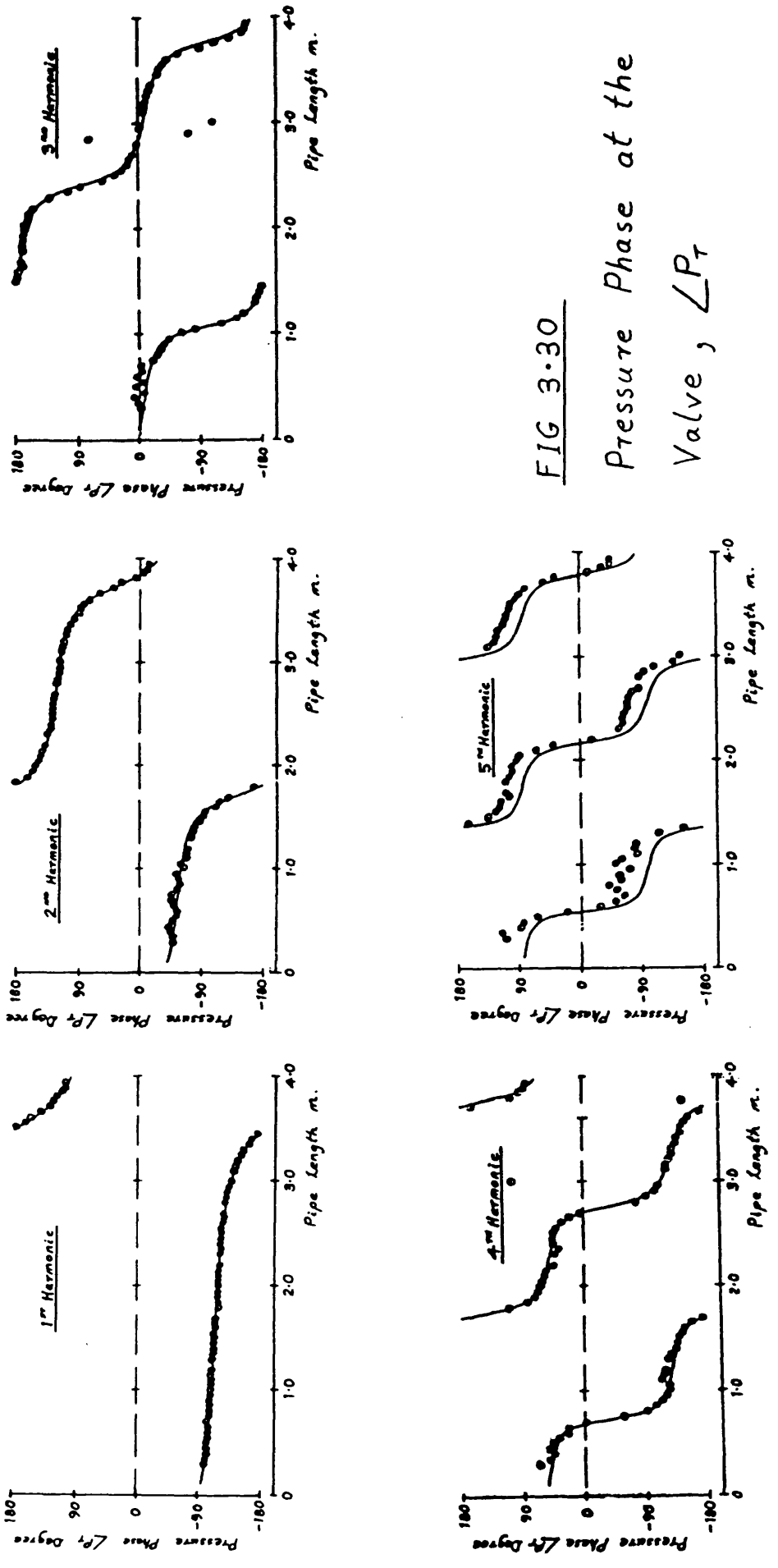

FIG 3·30

Pressure Phase at the Valve, $\angle P_T$

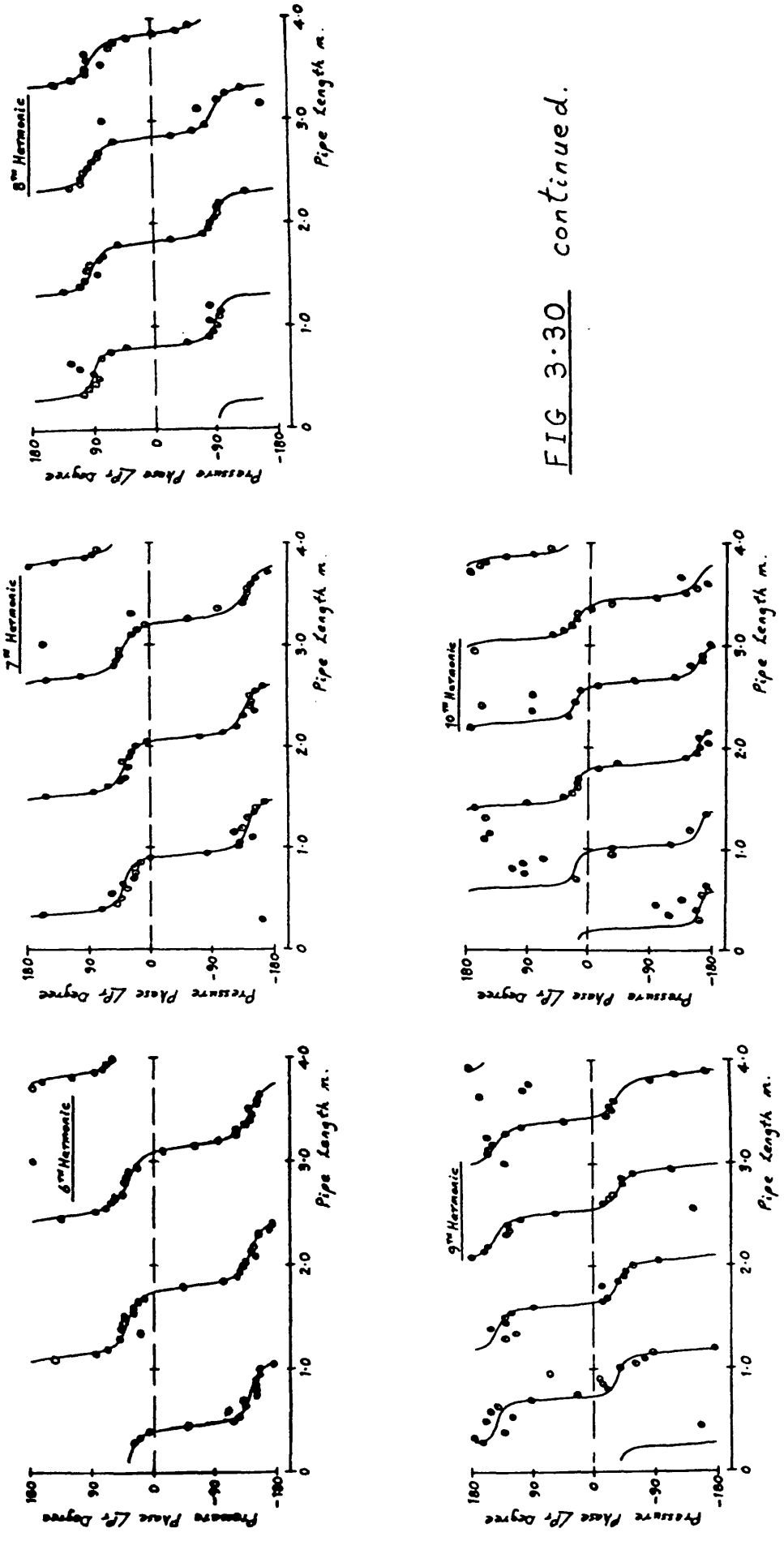

FIG 3·30 continued.

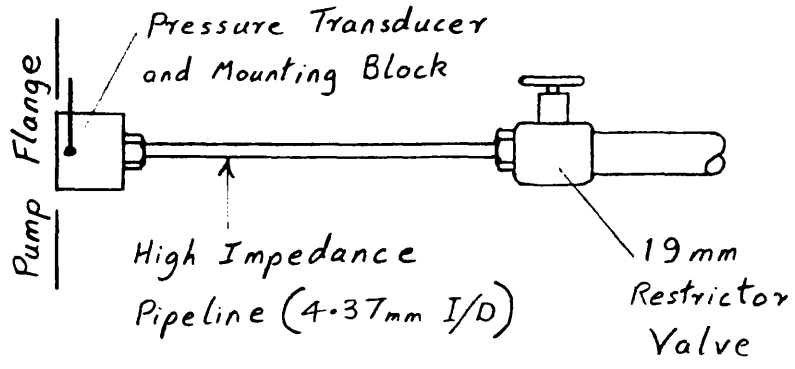

FIG 4·1 High Impedance Pipeline Test Circuit.

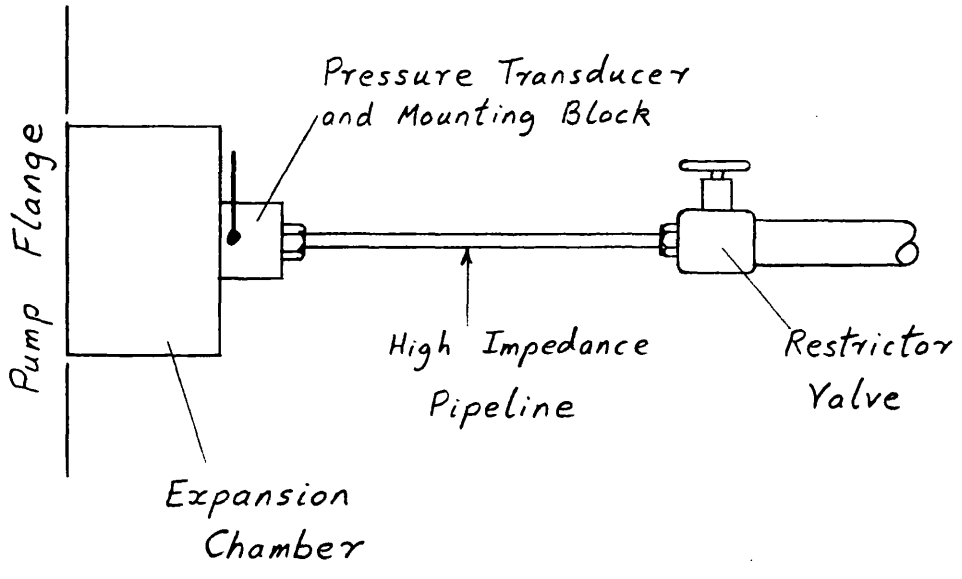

FIG 4·2 Additional Capacitance Test Circuit.

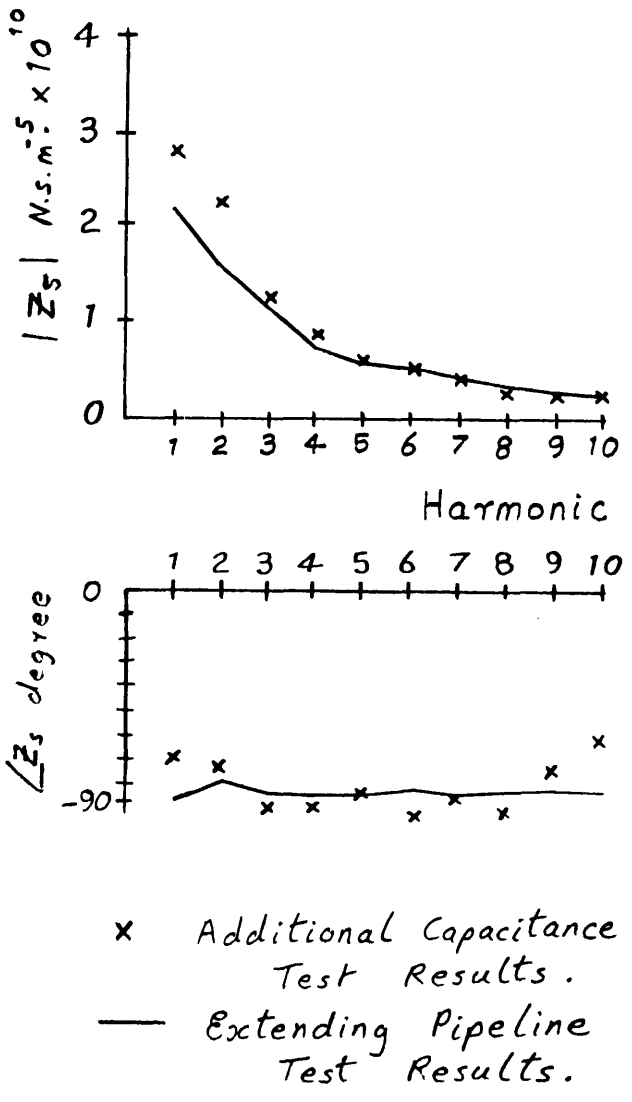

FIG 4·3 Comparing the pump impedance predictions.

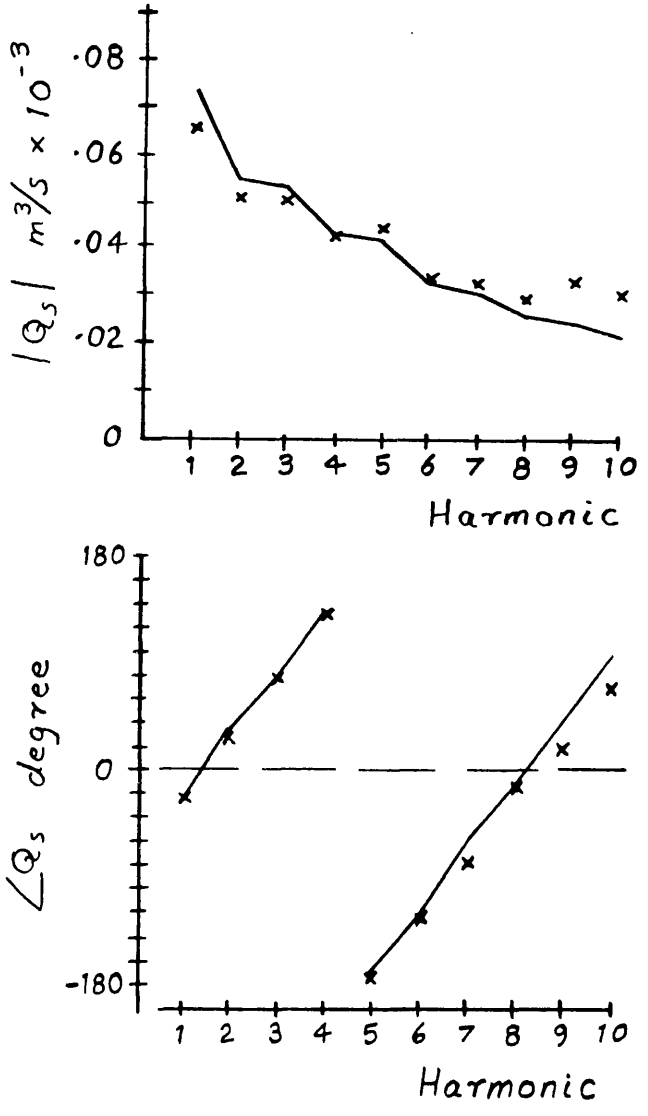

FIG 4·4 Comparing the pump flow predictions.

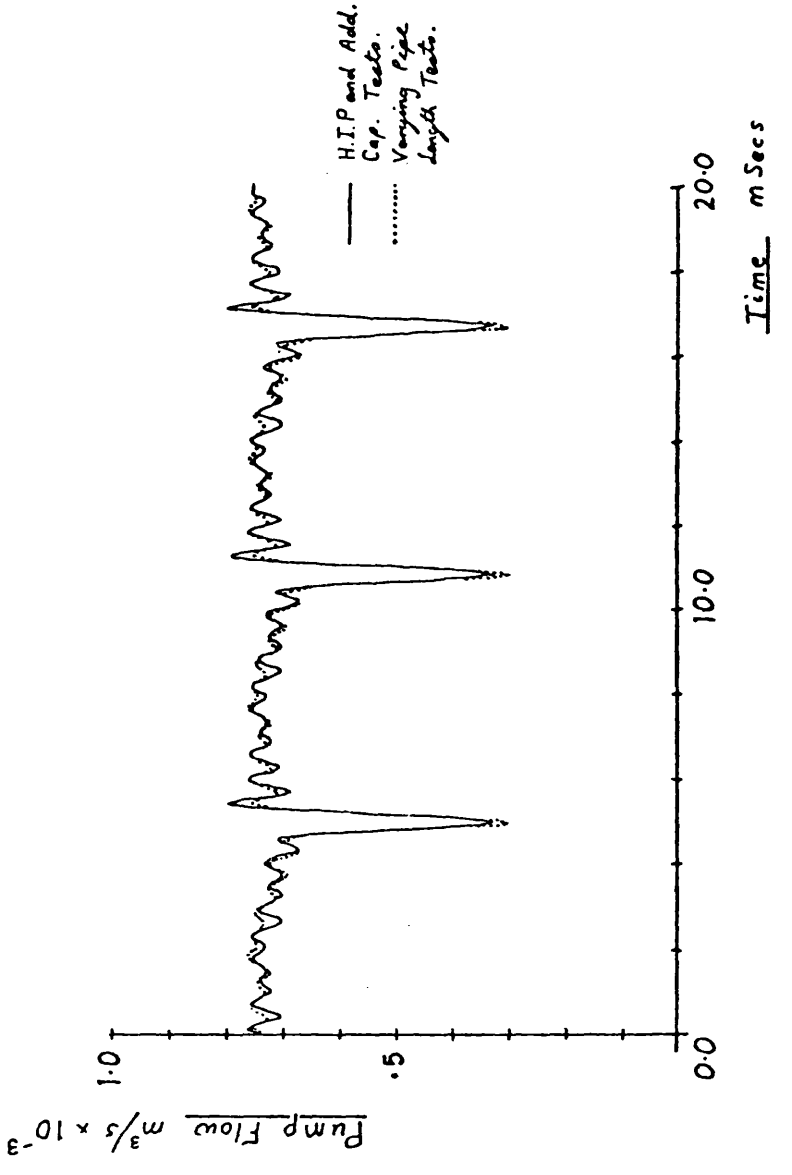

FIG 4·5 Comparing the synthesised pump flows.

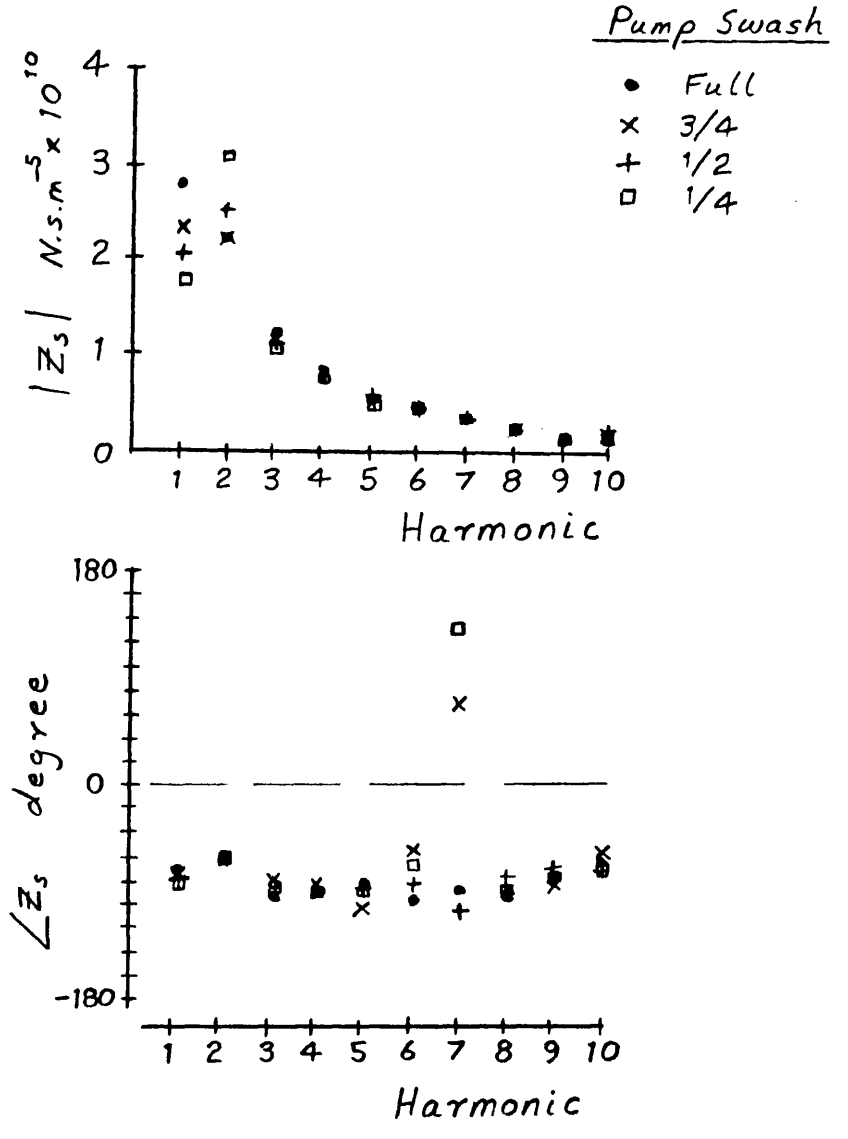

FIG 4·6 Effect of swashplate angle on the pump impedance.

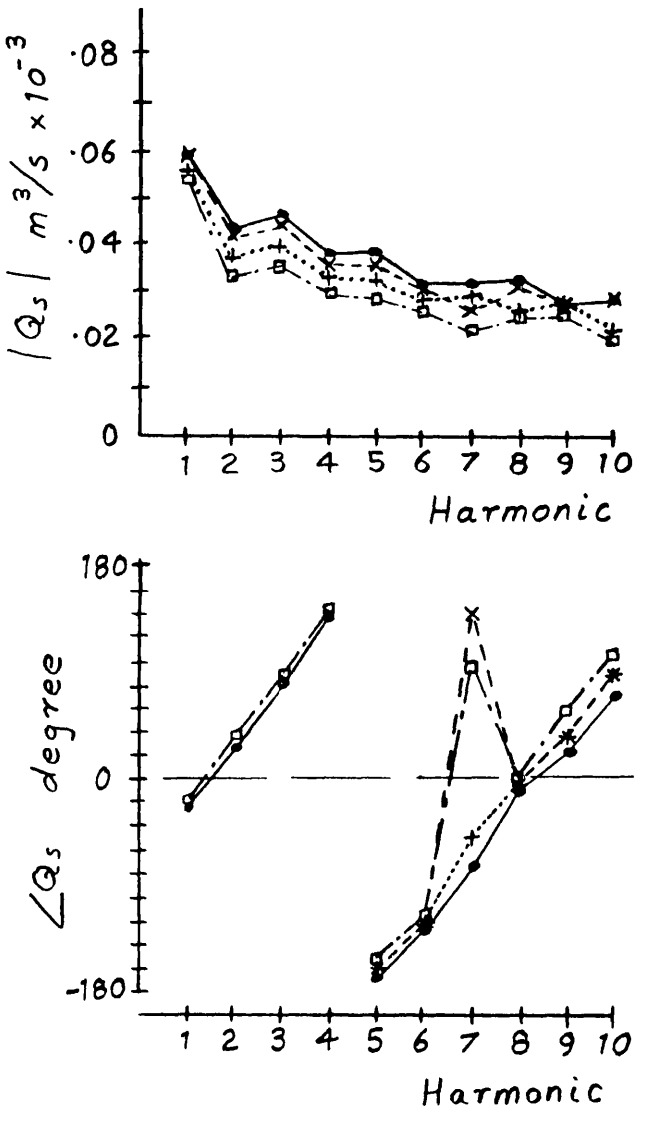

FIG 4·7 Effect of swashplate angle on pump flows.

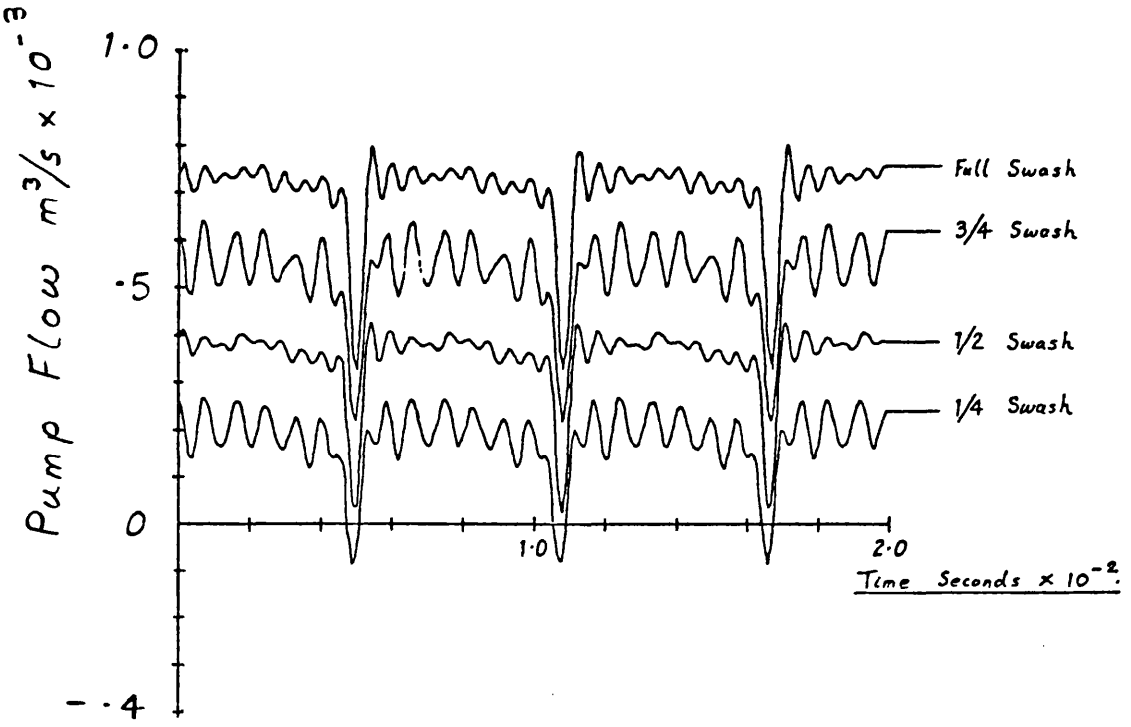

FIG 4·8 Effect of swashplate angle on the synthesised pump flow.

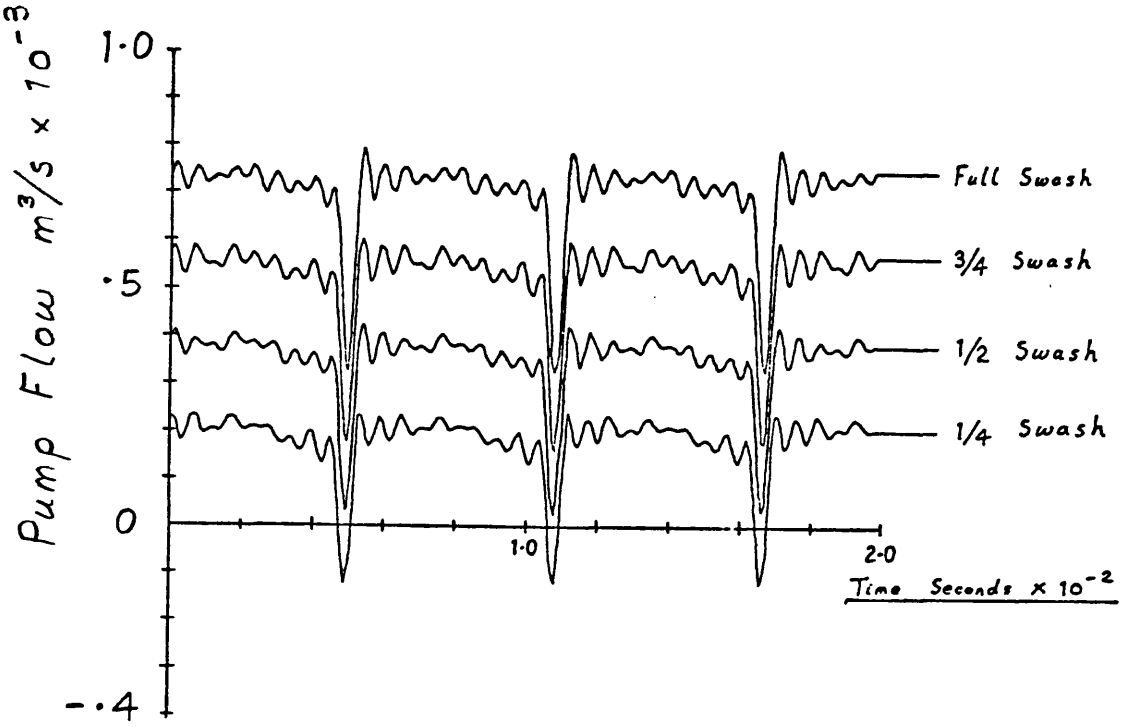

FIG 4·9 'Corrected' synthesised pump flows.

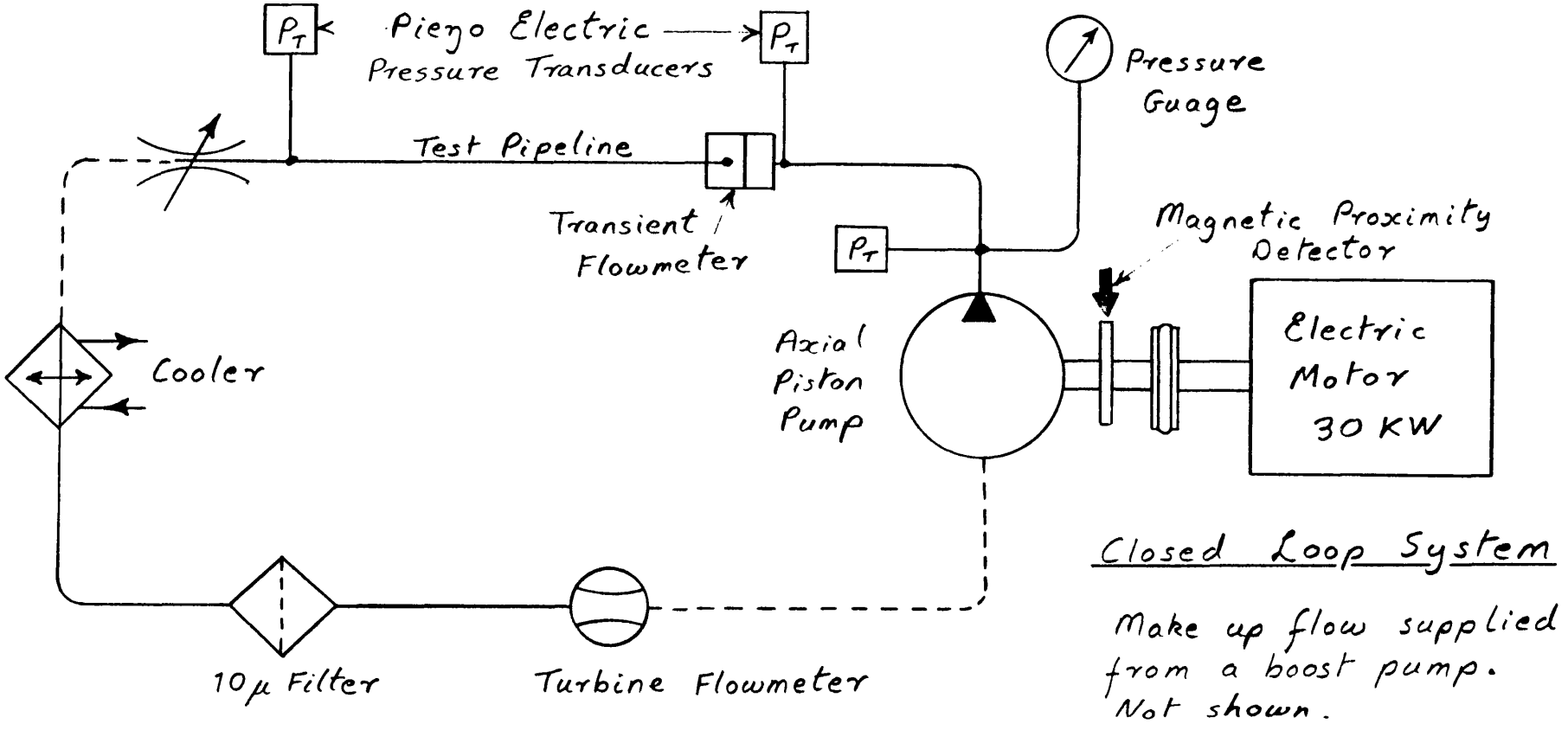

FIG 5·1 Line diagram of the test rig

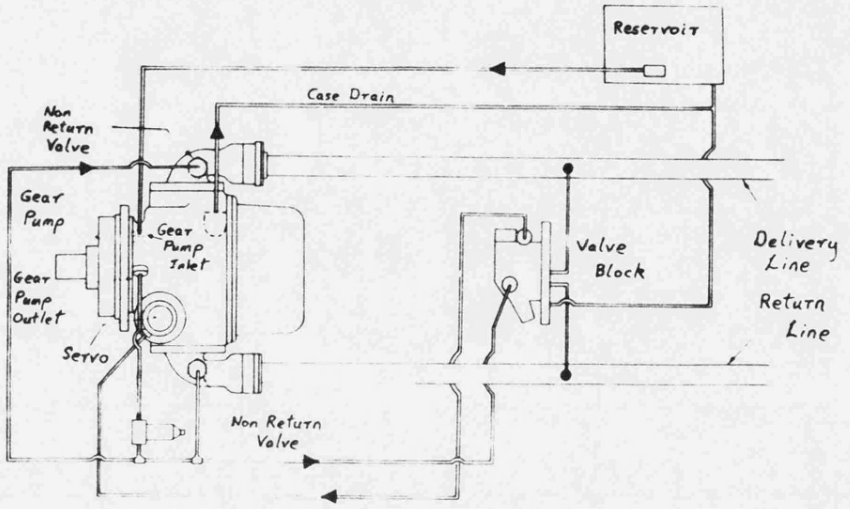

FIG 5·2 External Pump Connections

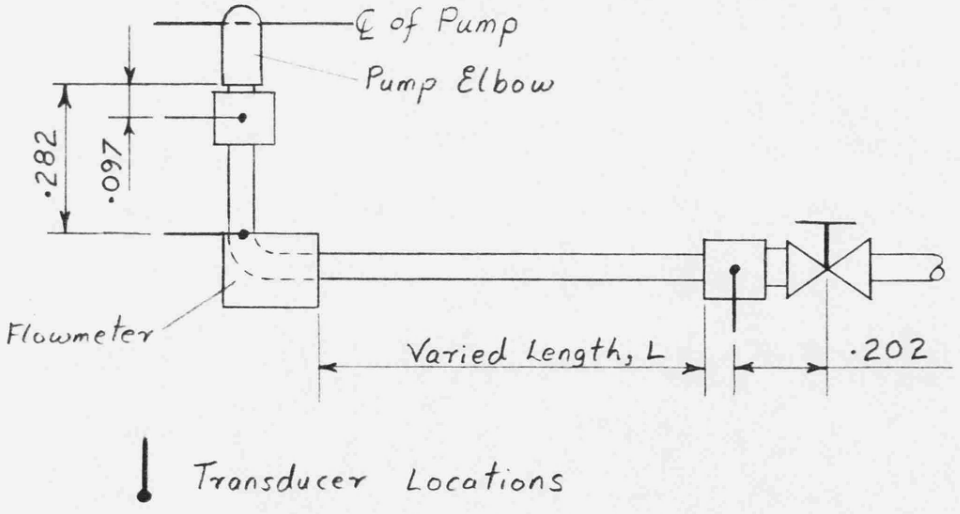

FIG 5·3 Test Pipeline and Transducer Positions.

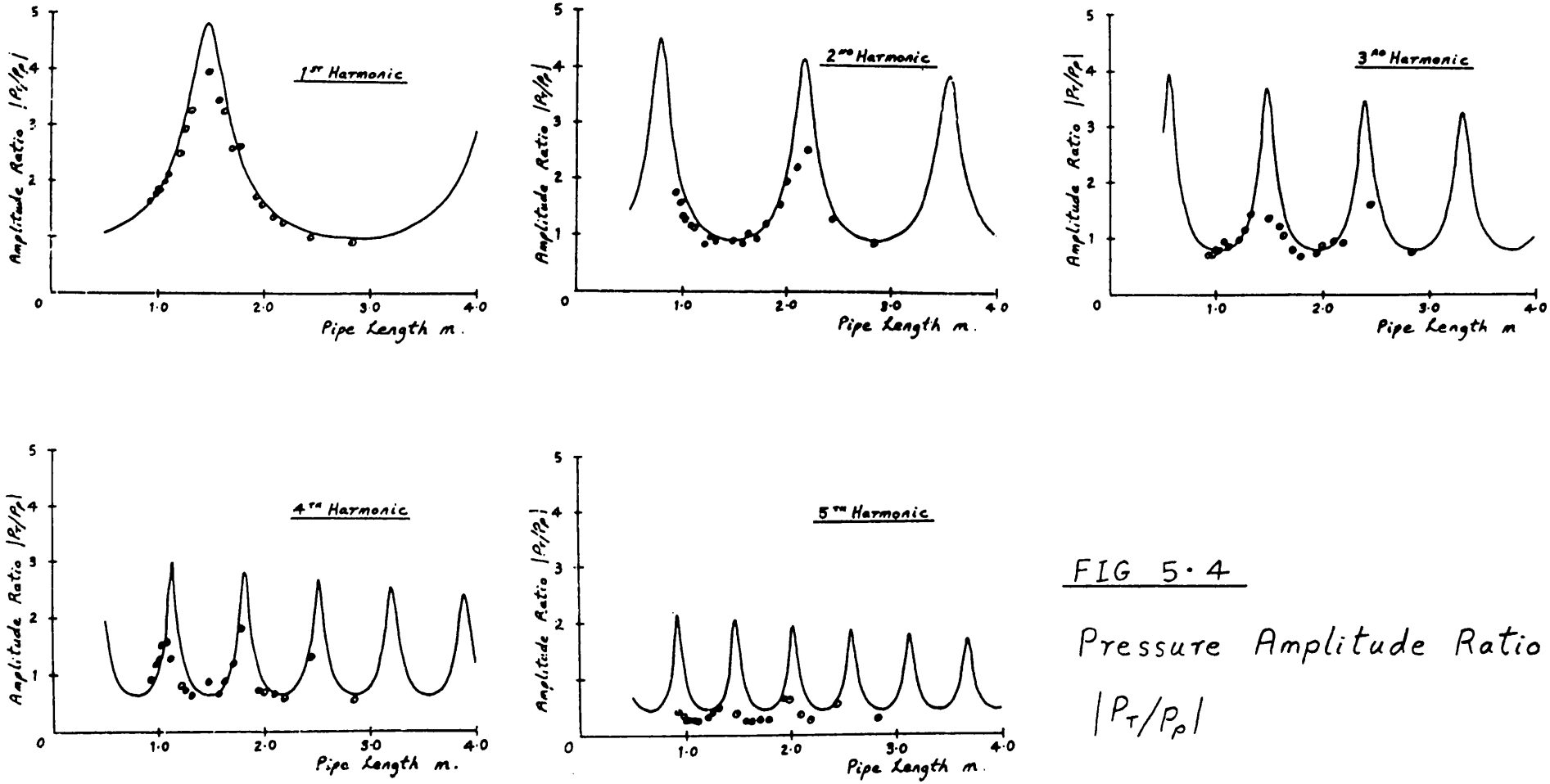

FIG 5·4

Pressure Amplitude Ratio

$|P_T/P_p|$

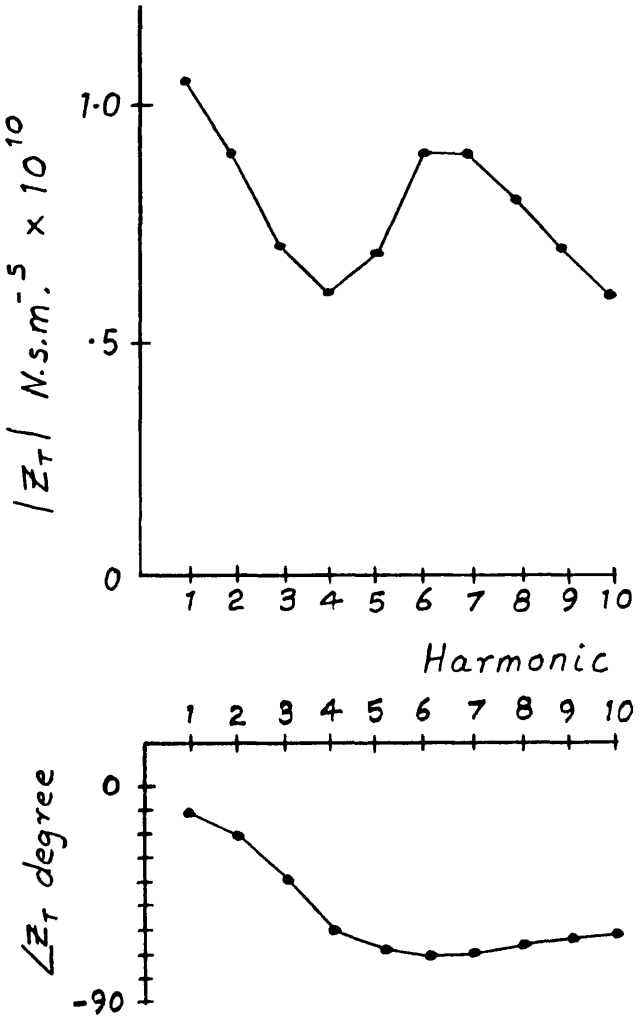

FIG 5·5 Valve impedance spectrum.

Results for :- • 25·4mm. Valve
× 19mm. Valve
(ref. Fig 3·16)

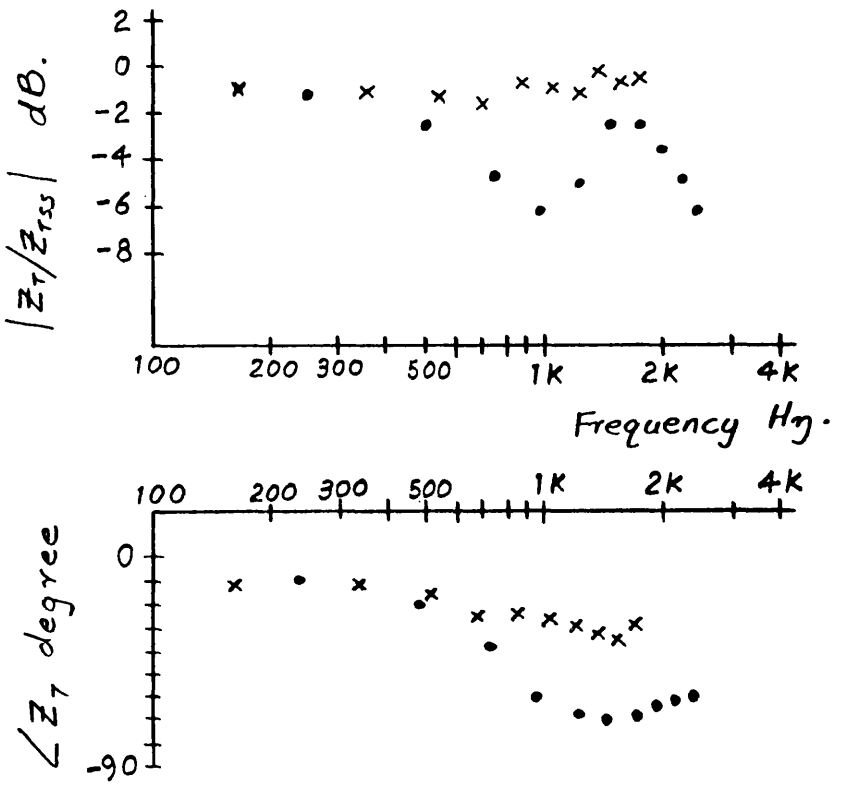

FIG 5·6 Valve impedance, variation with frequency.

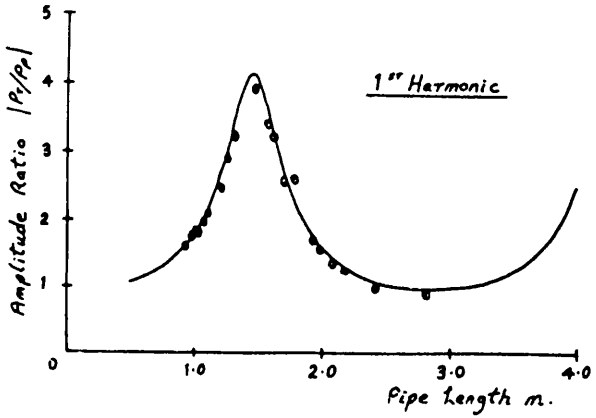

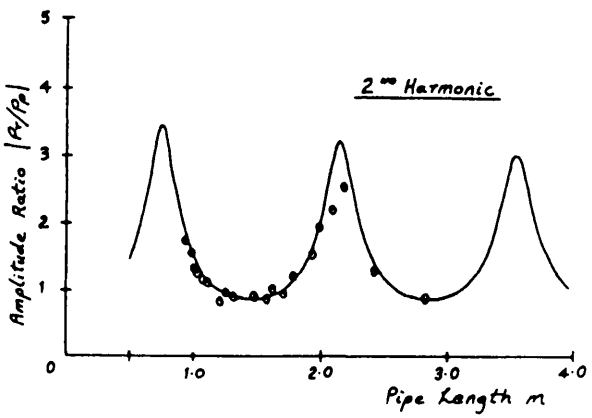

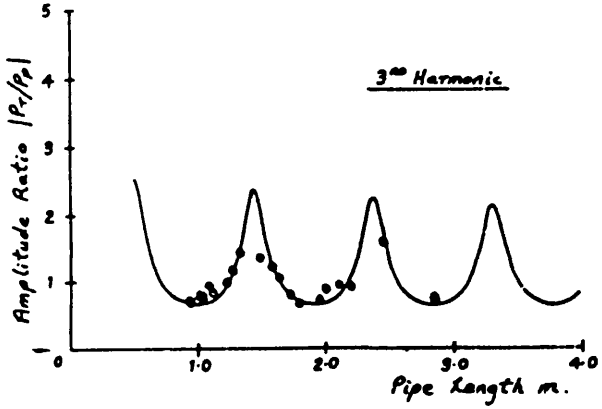

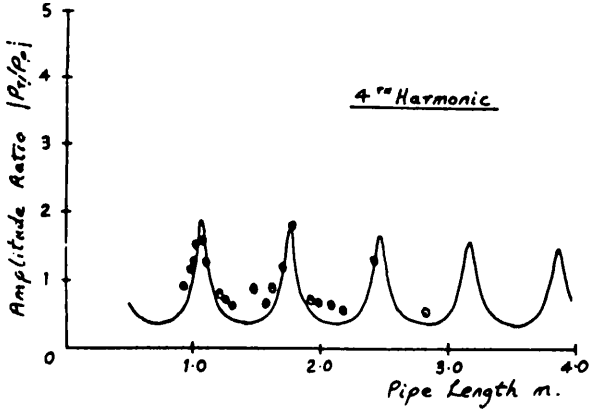

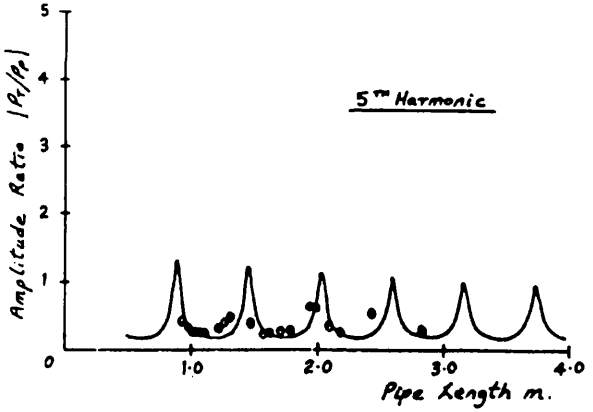

FIG 5·7

Pressure Amplitude Ratio $|P_T/P_p|$, computed using the predicted Valve Impedance Spectrum, Z_T, Fig 5·5

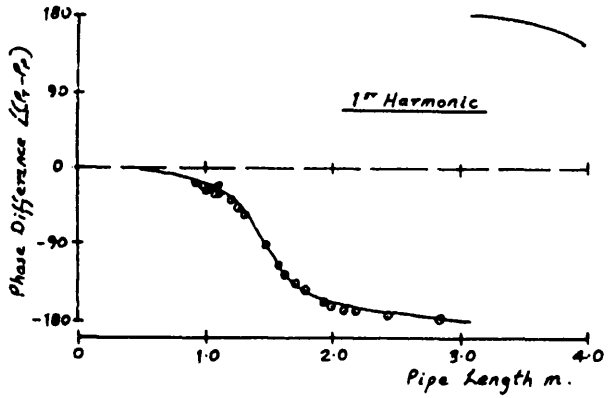

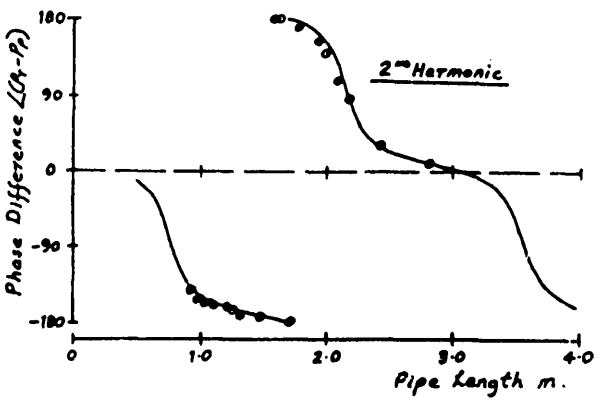

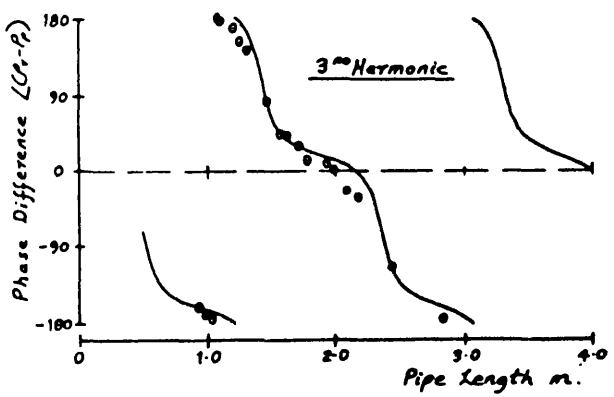

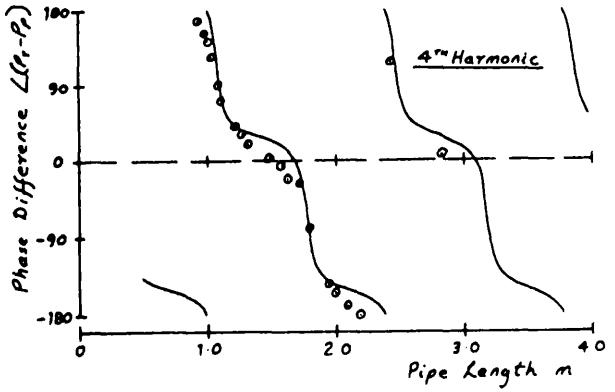

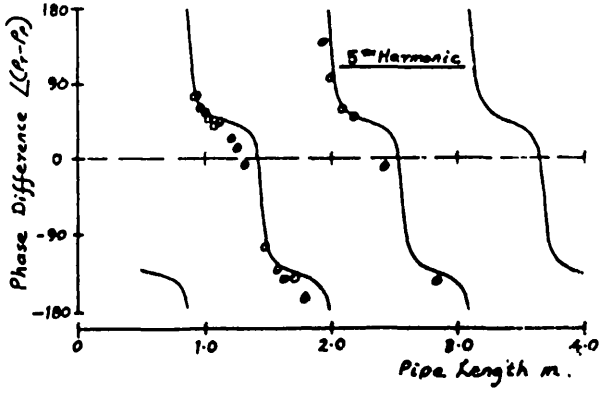

FIG 5·8

Pressure Phase Difference $\angle(P_T - P_p)$, computed using the predicted Valve Impedance Spectrum, Z_T, Fig 5·5

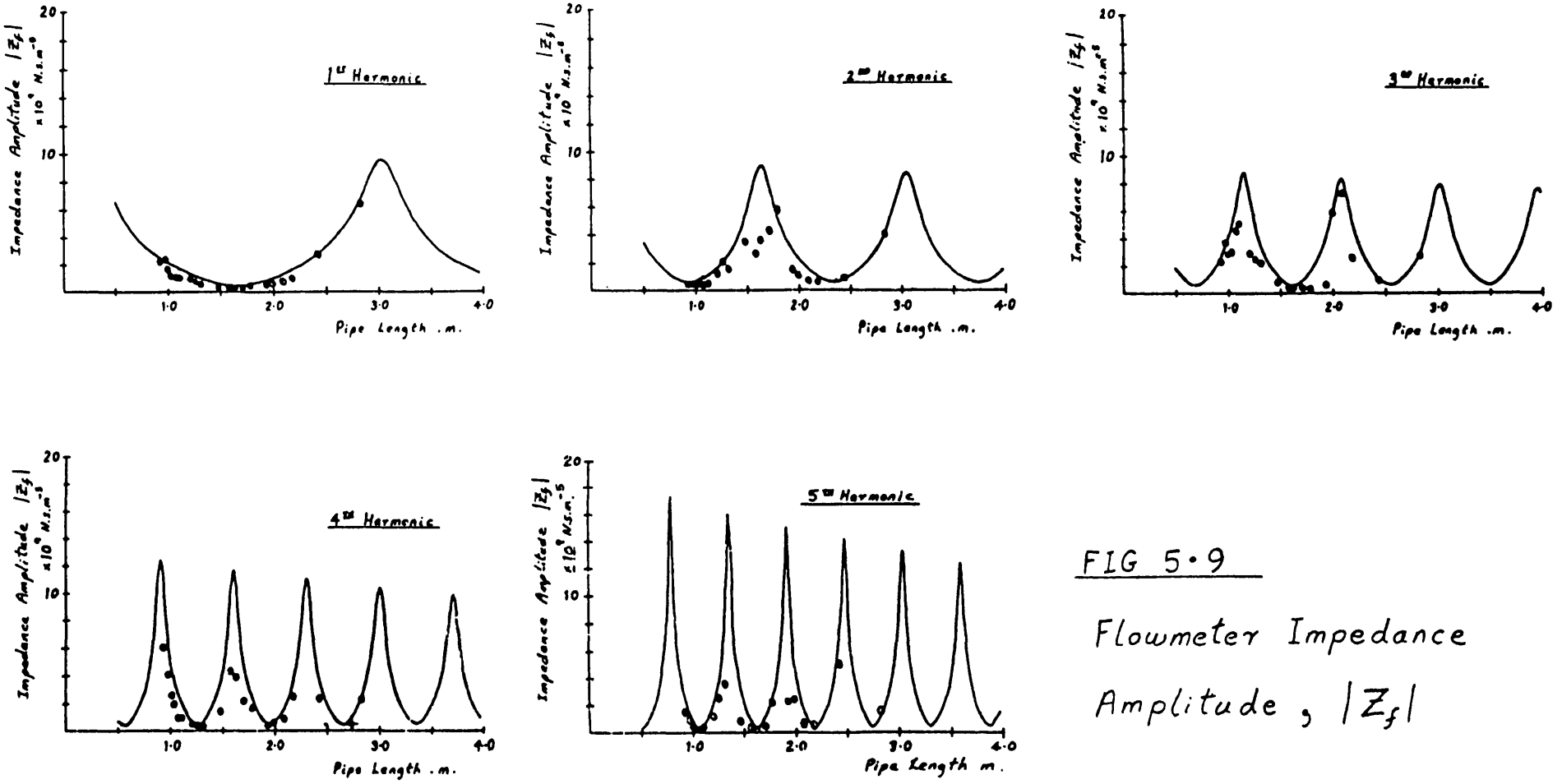

FIG 5·9

Flowmeter Impedance Amplitude, $|Z_f|$

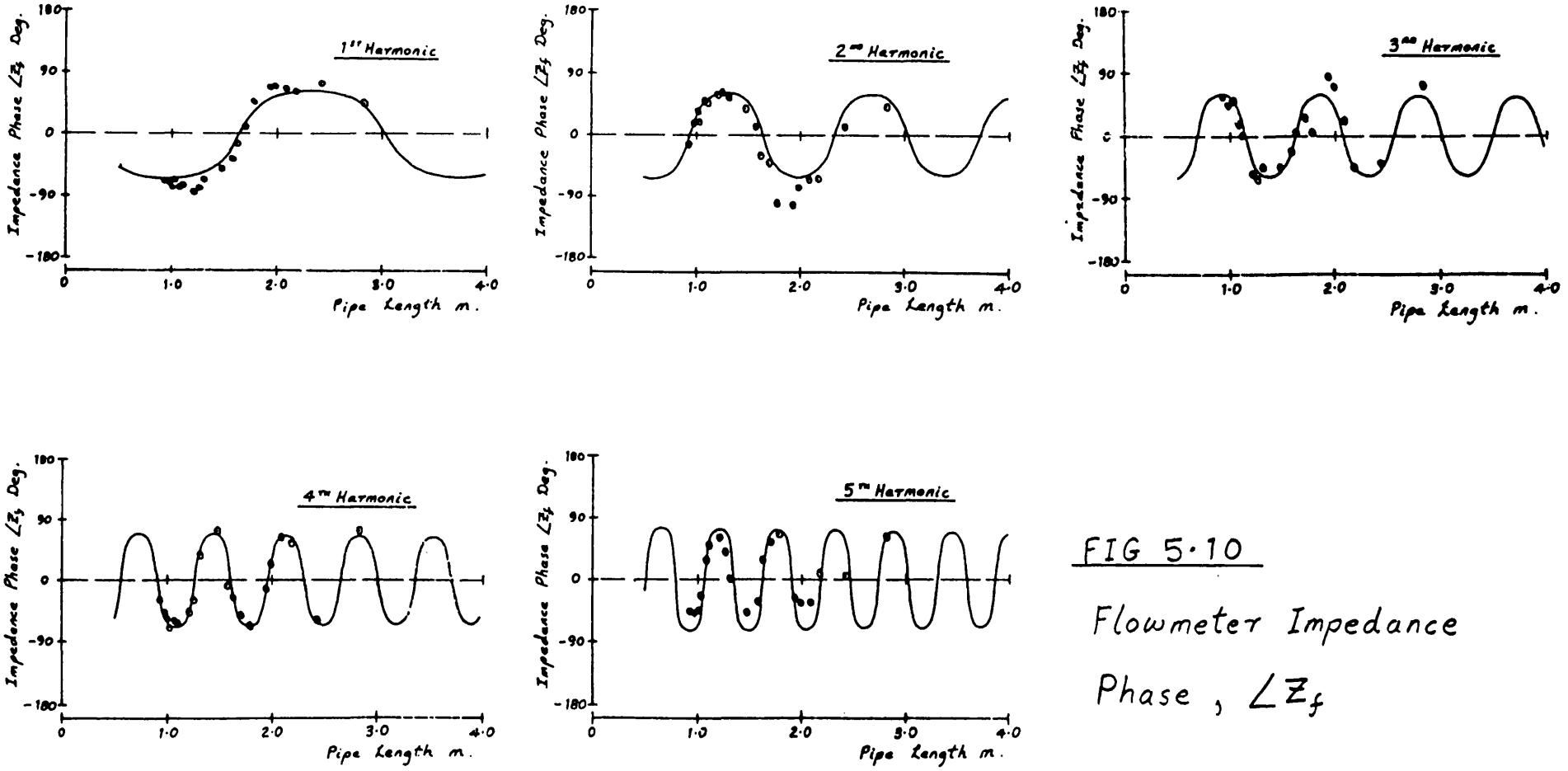

FIG 5·10

Flowmeter Impedance Phase, $\angle Z_f$

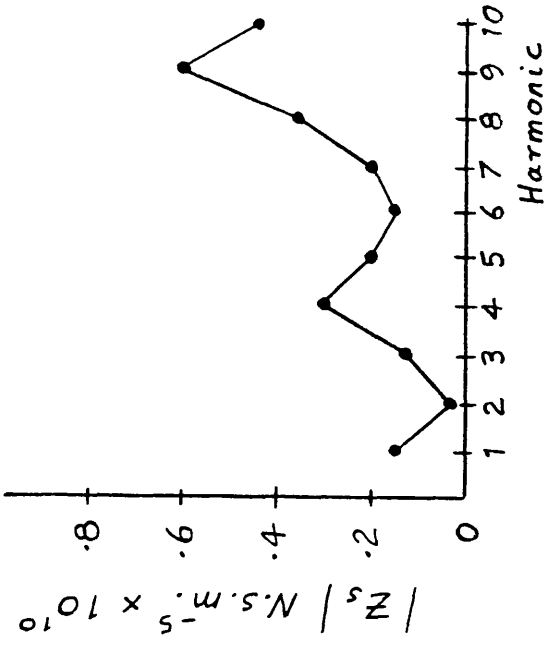

FIG 5·11 Pump impedance spectrum

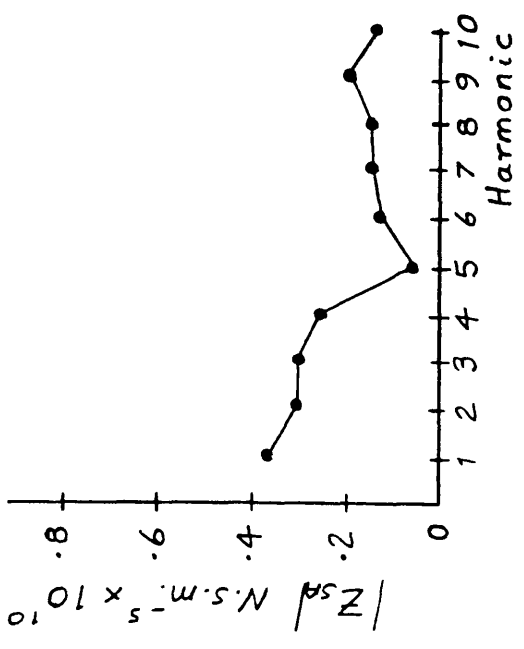

FIG 5·14 Pump impedance at the port plate.

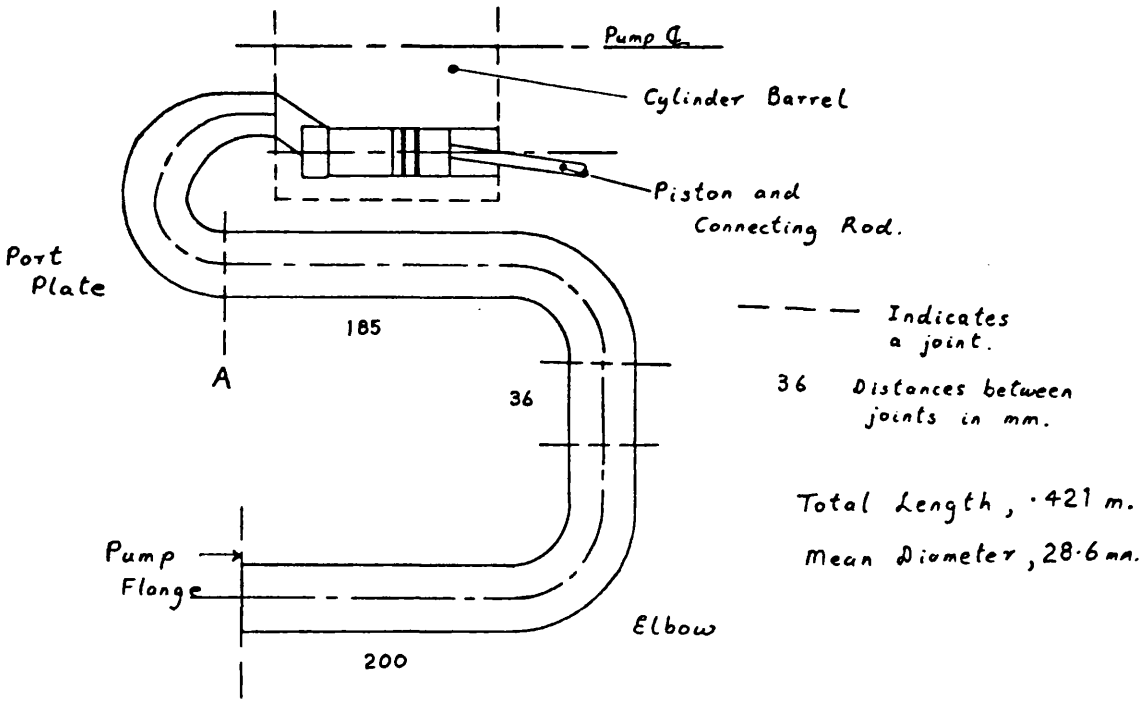

FIG 5·12 Simplified diagram of the pump delivery line.

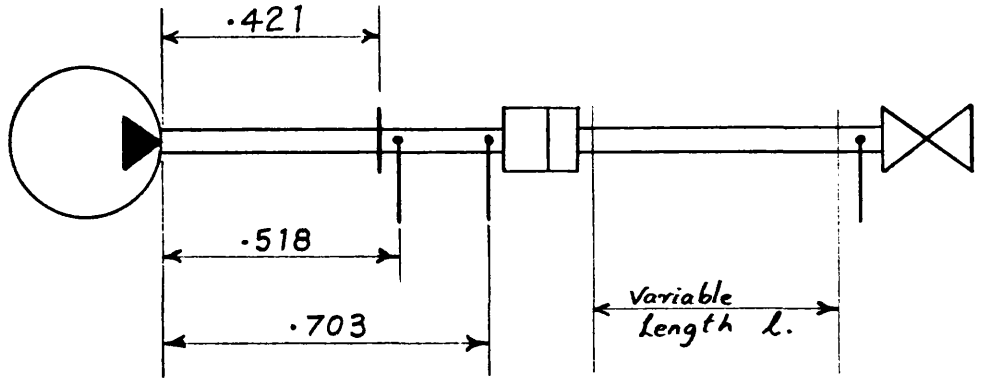

Overall line length $L = l + 1{\cdot}13$ m.

Pressure Transducers.

FIG 5·13 Revised test pipeline.

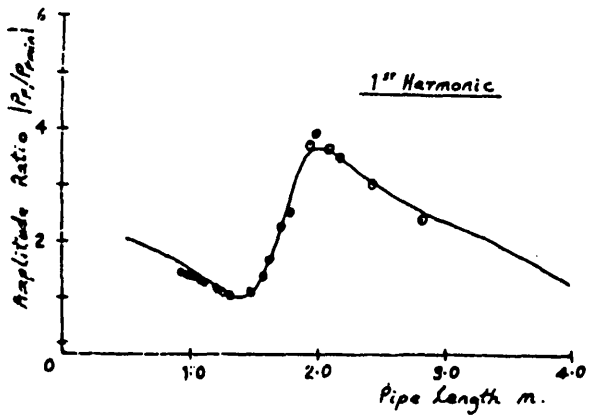

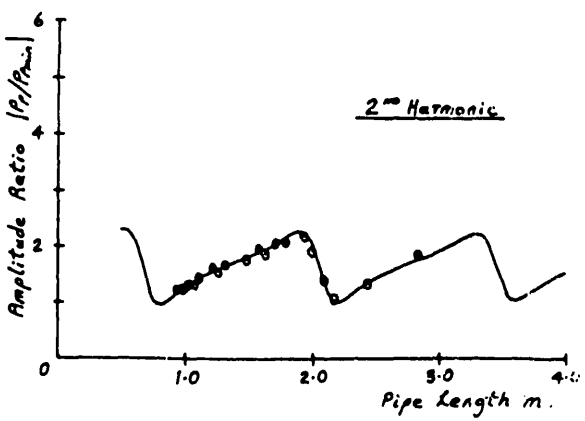

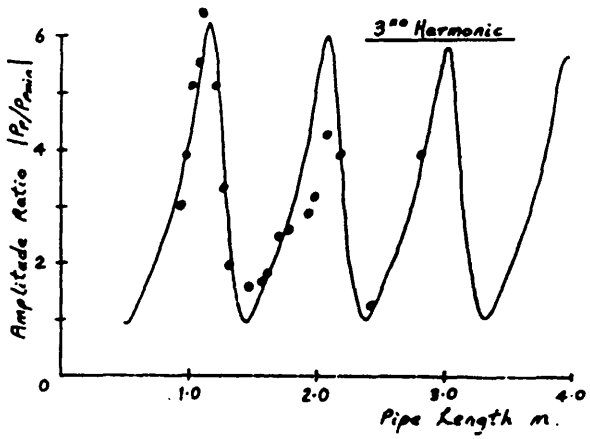

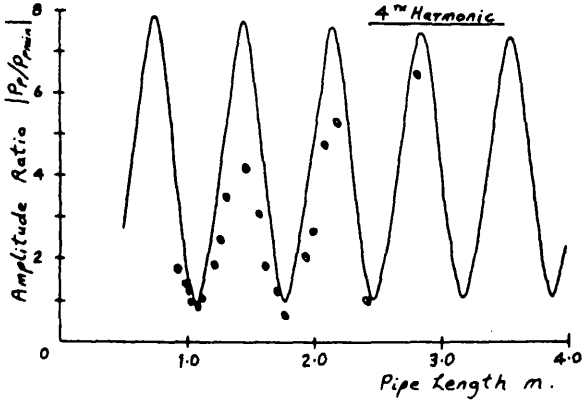

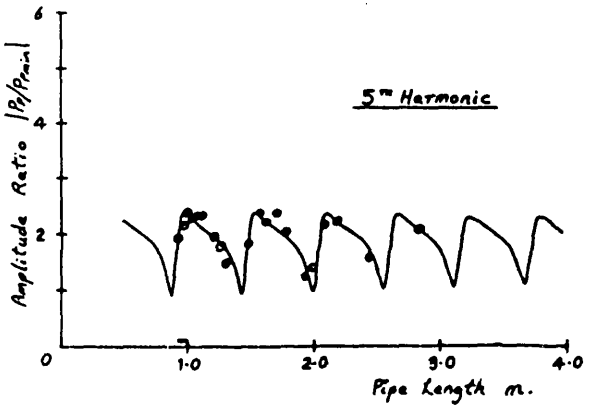

FIG 5·15

Pressure Amplitude Ratio

$|P_p/P_{pmin}|$

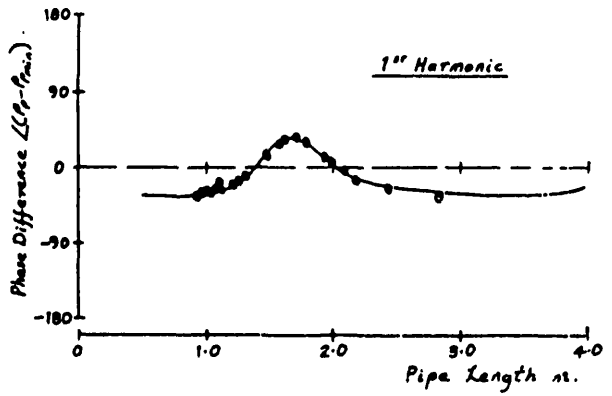

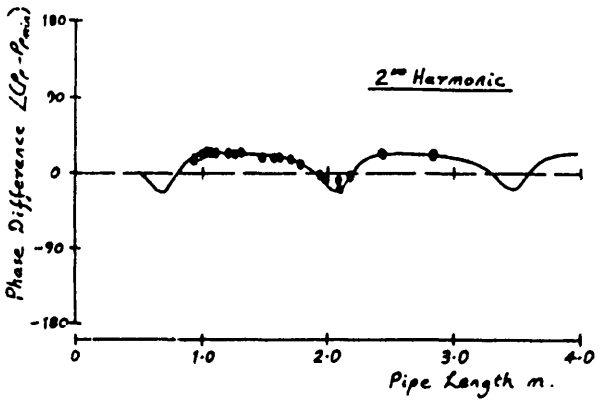

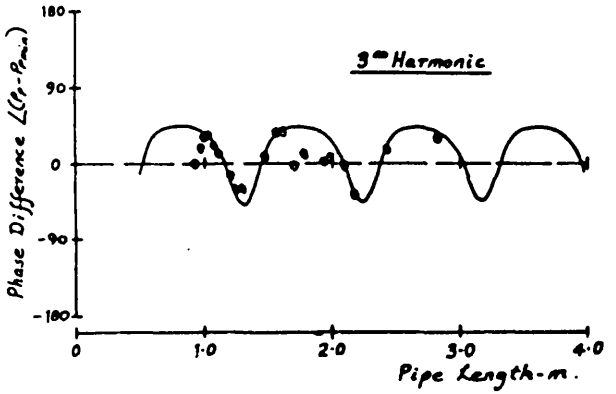

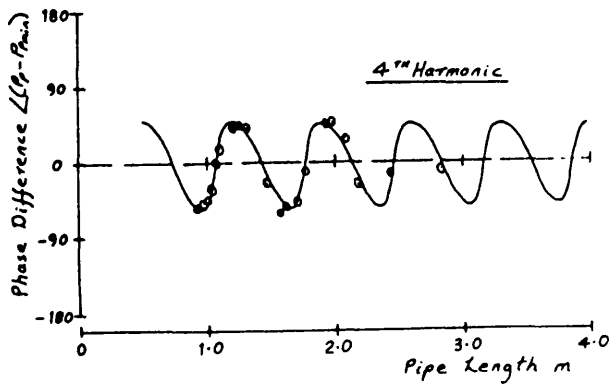

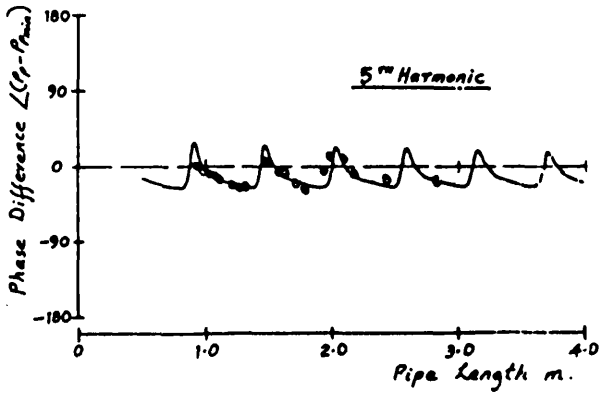

FIG 5·16

Pressure Phase Difference

$\angle(P_p - P_{pmin})$

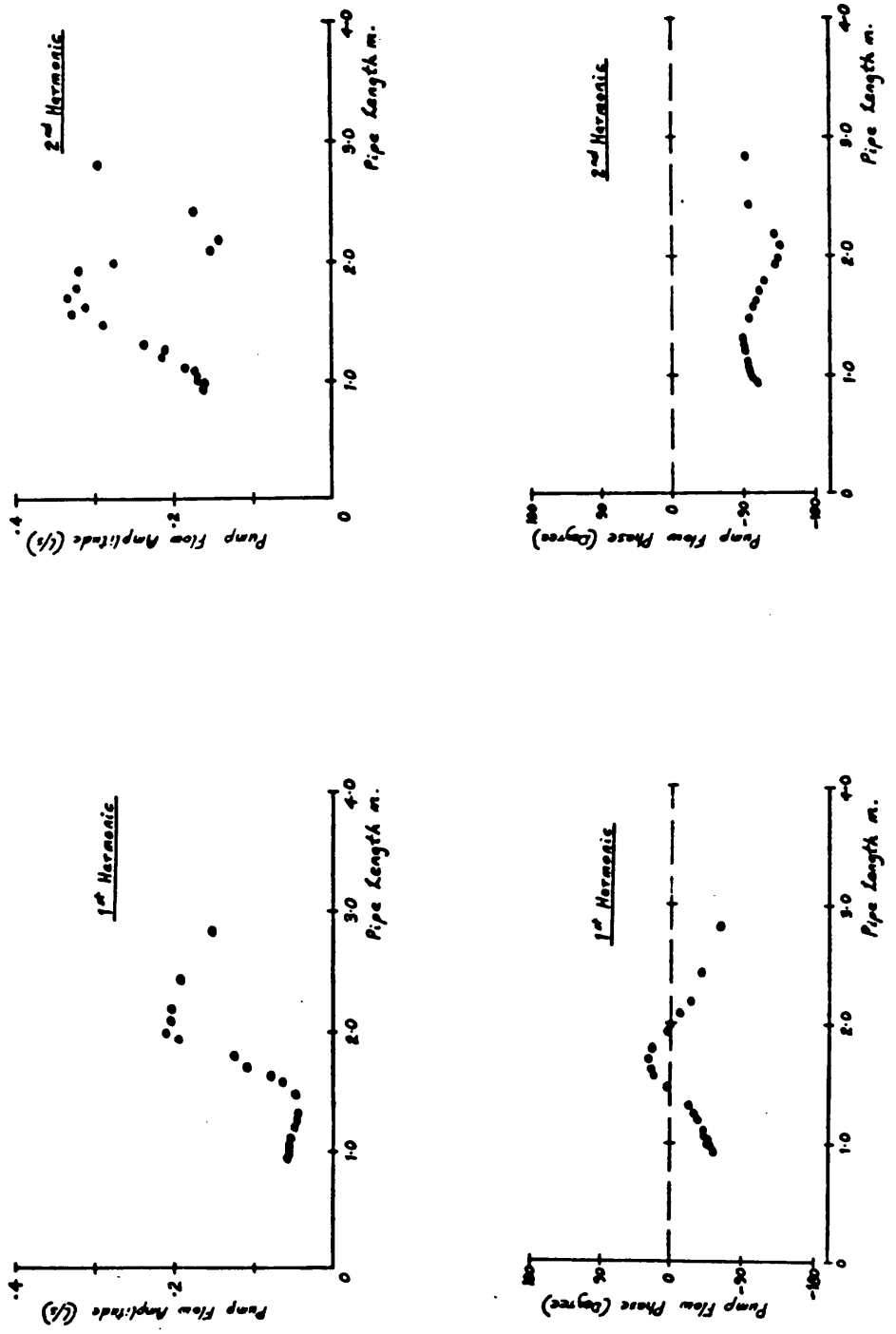

FIG 5·17 Pump Flow Values predicted for each pipeline length.

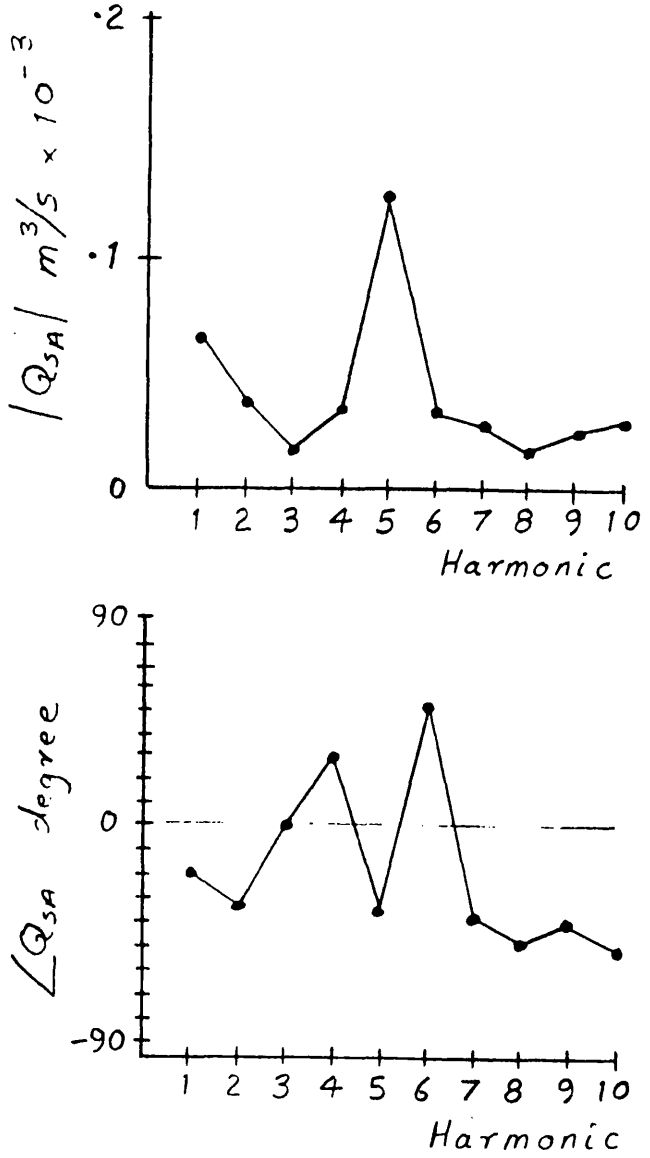

FIG 5·18 Pump flow at the port plate.

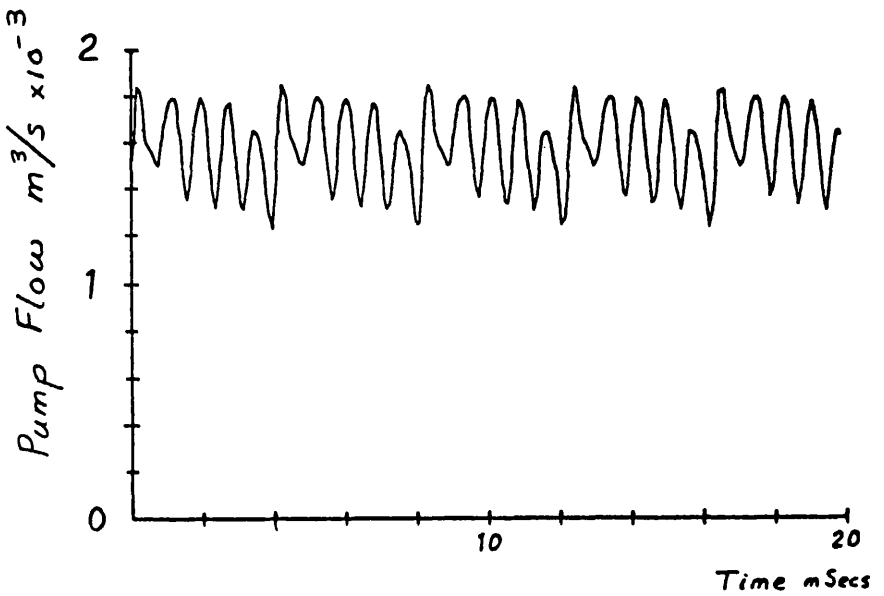

FIG 5·19 Synthesised pump flow at the port plate.

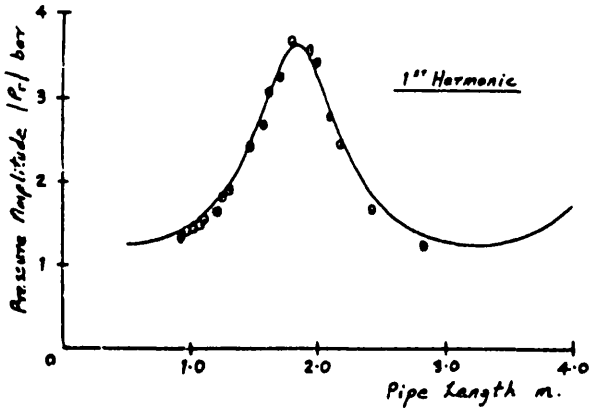

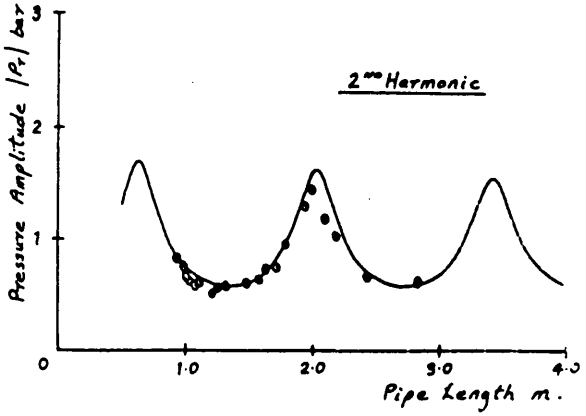

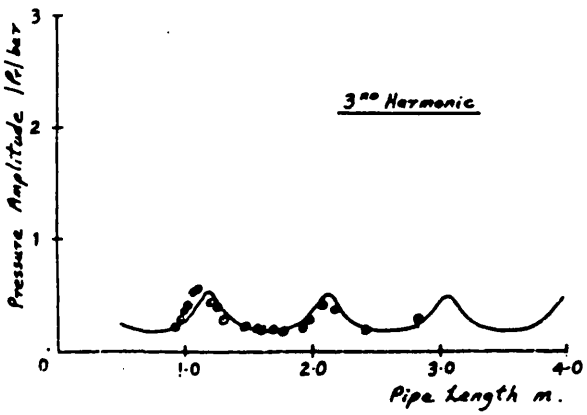

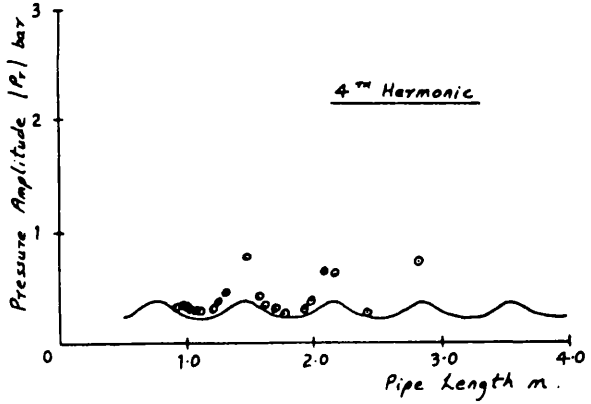

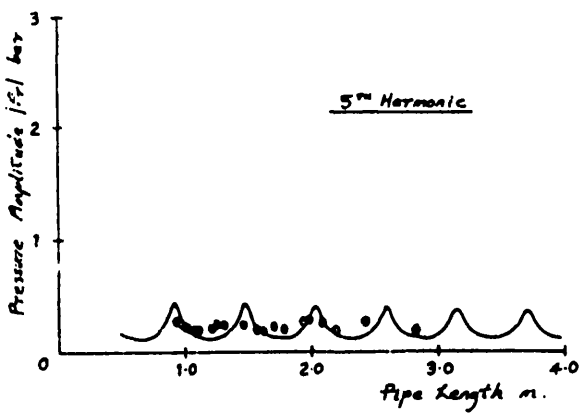

FIG 5·20

Pressure Amplitude at the Valve, $|P_T|$

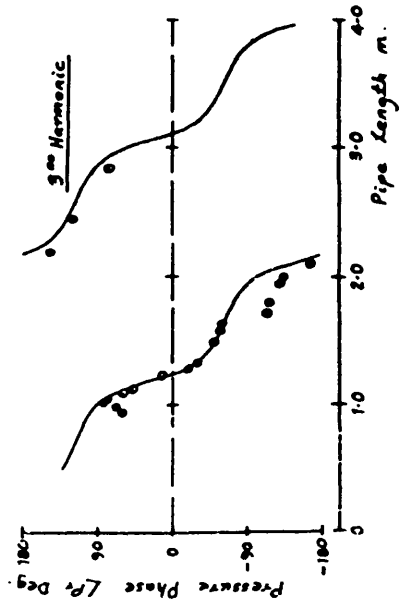

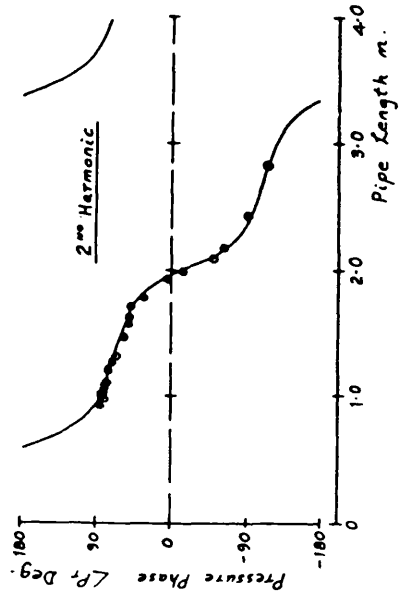

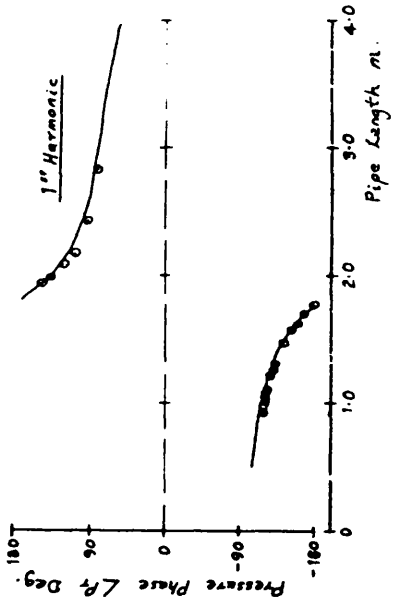

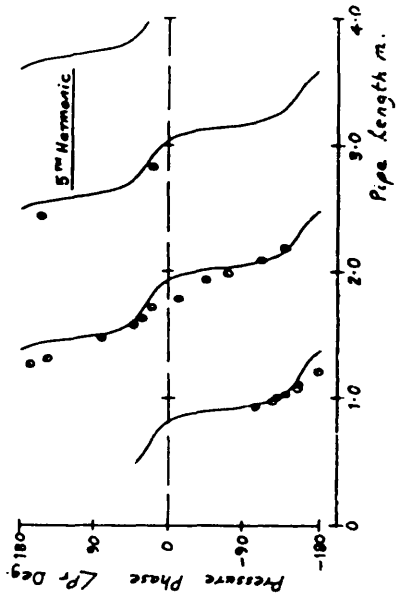

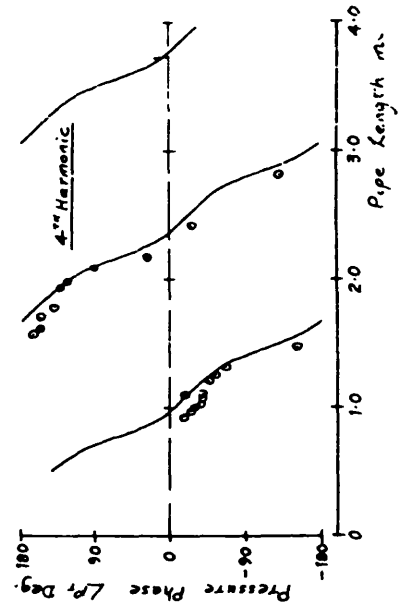

FIG 5·21

Pressure Phase at the Valve, $\angle P_T$

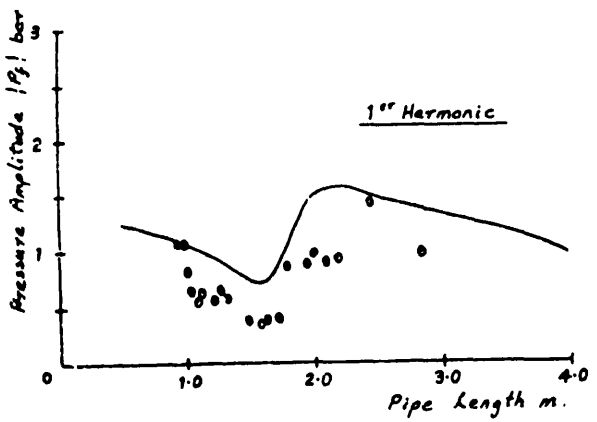

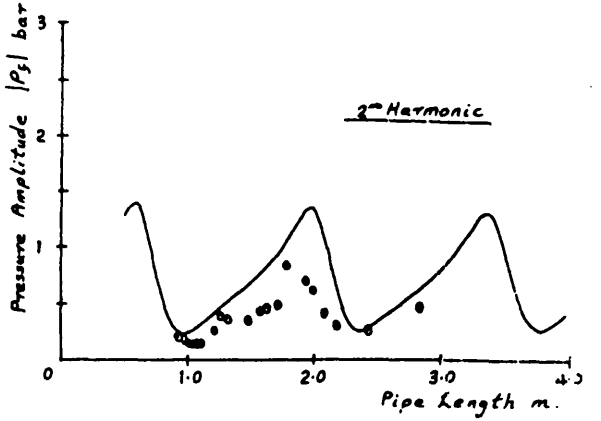

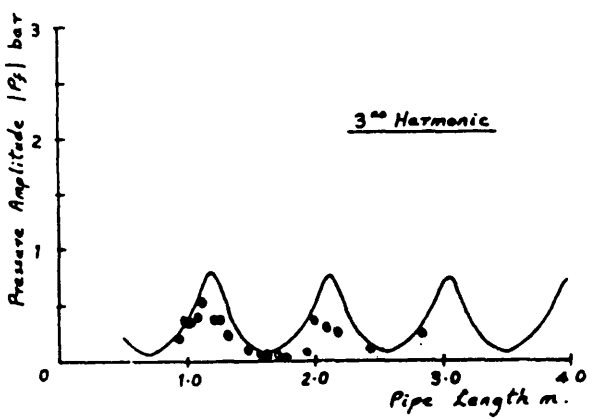

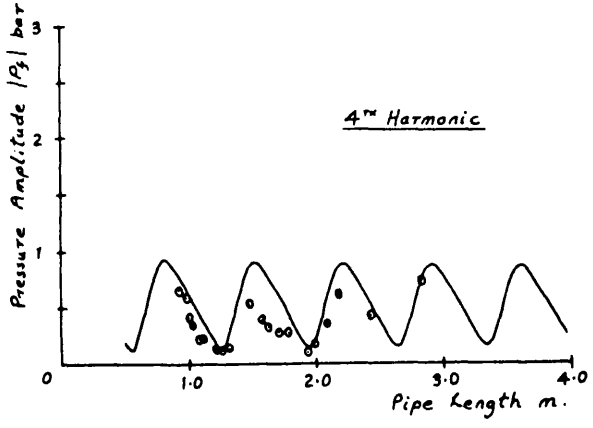

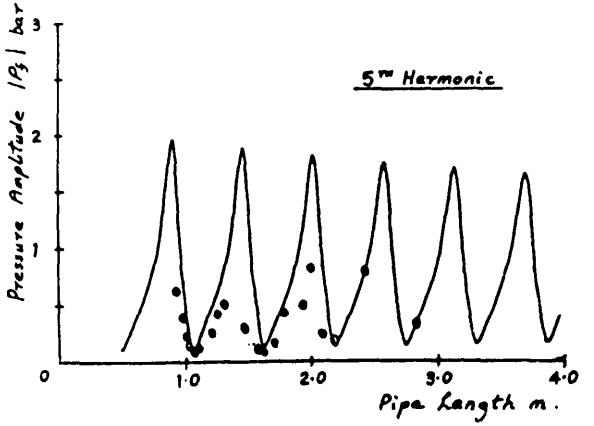

FIG 5·22

Pressure Amplitude at the Flowmeter, $|P_f|$

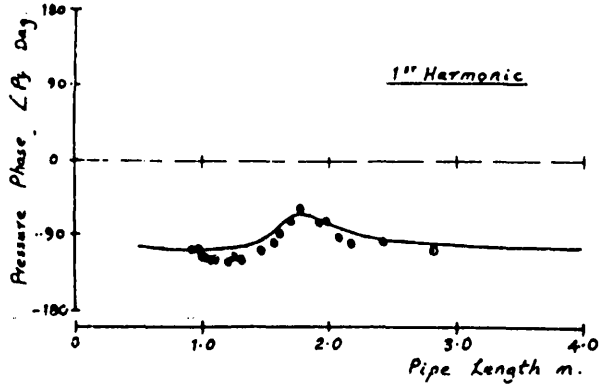

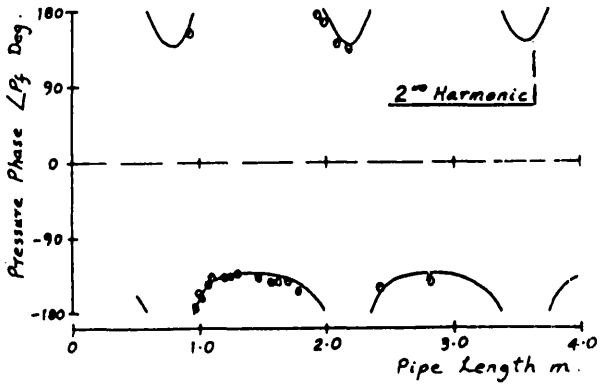

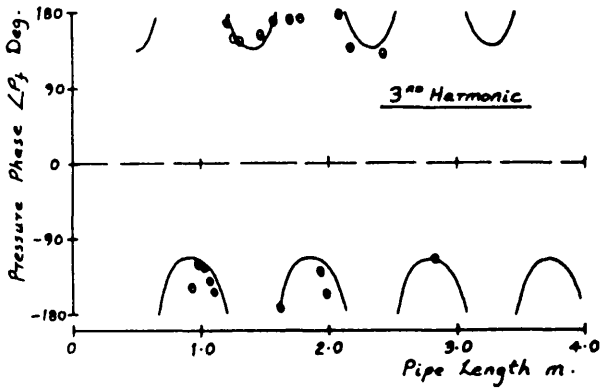

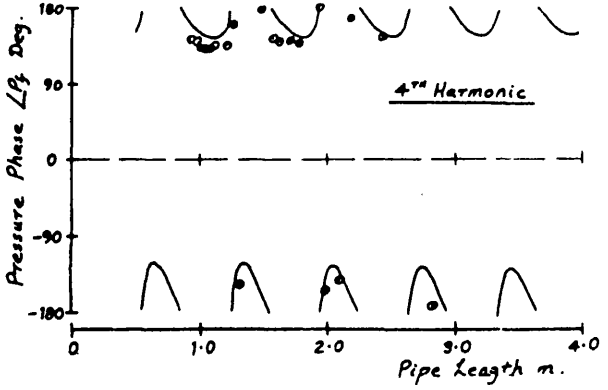

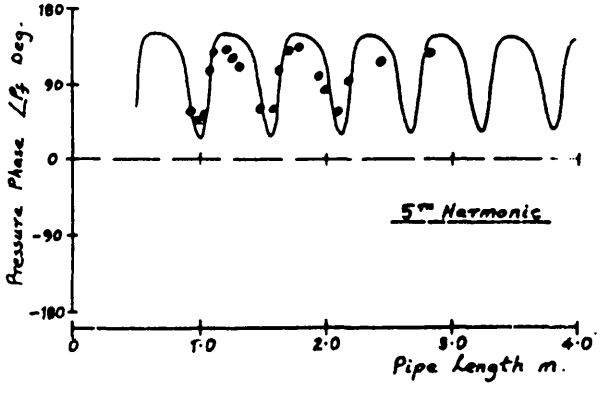

FIG 5·23

Pressure Phase at the Flowmeter, $\angle P_f$

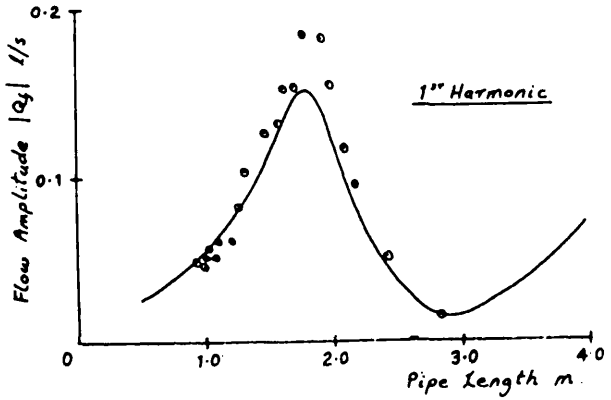

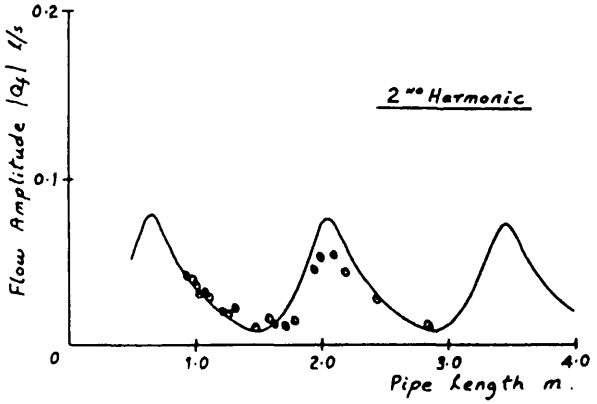

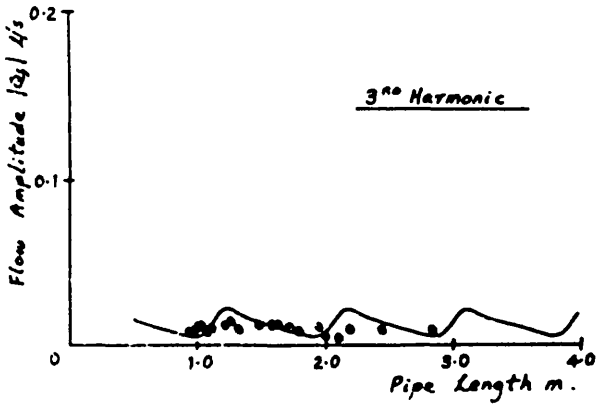

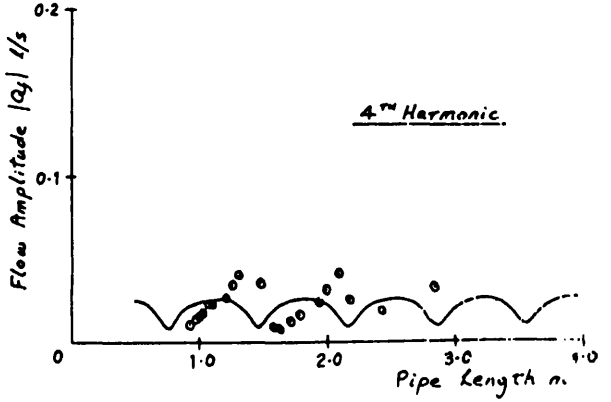

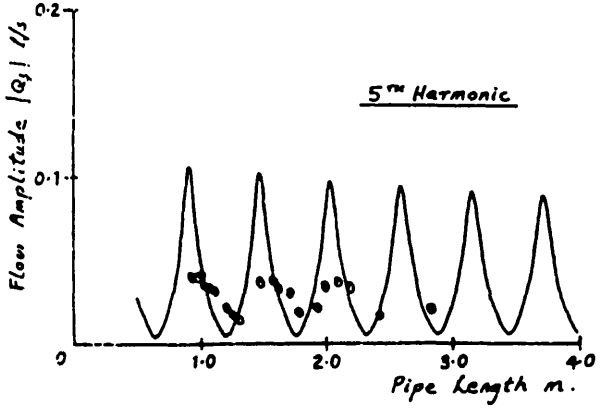

FIG 5·24

Flow Amplitude at the Flowmeter, $|Q_f|$

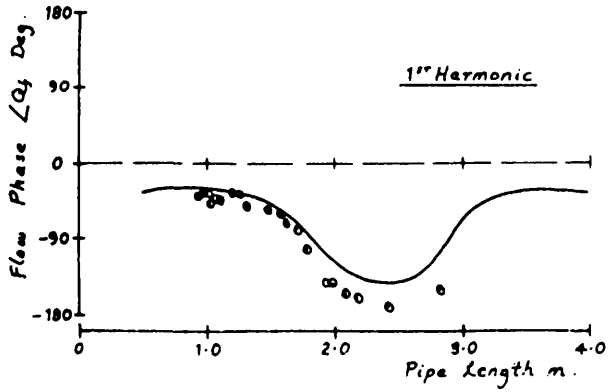

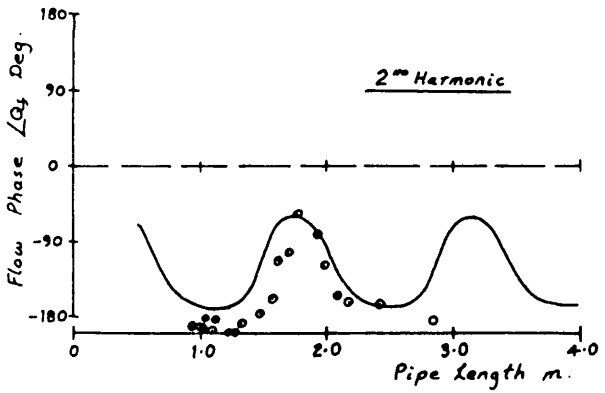

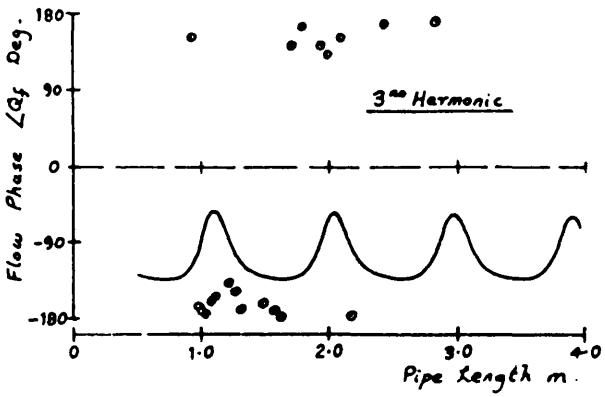

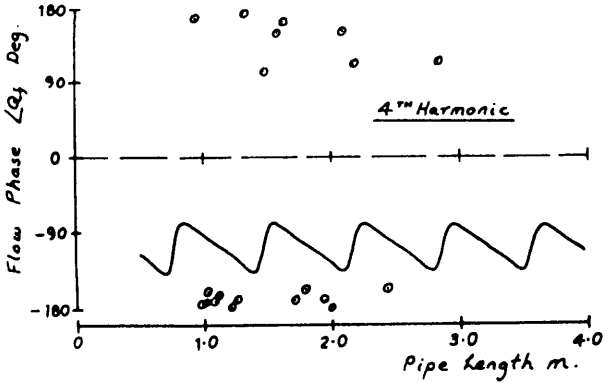

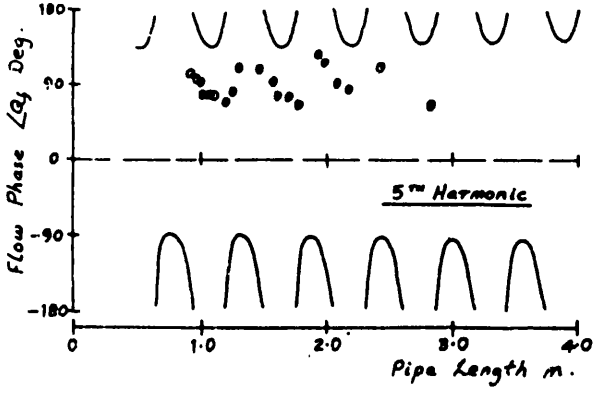

FIG 5·25

Flow Phase at the Flowmeter, $\angle Q_f$

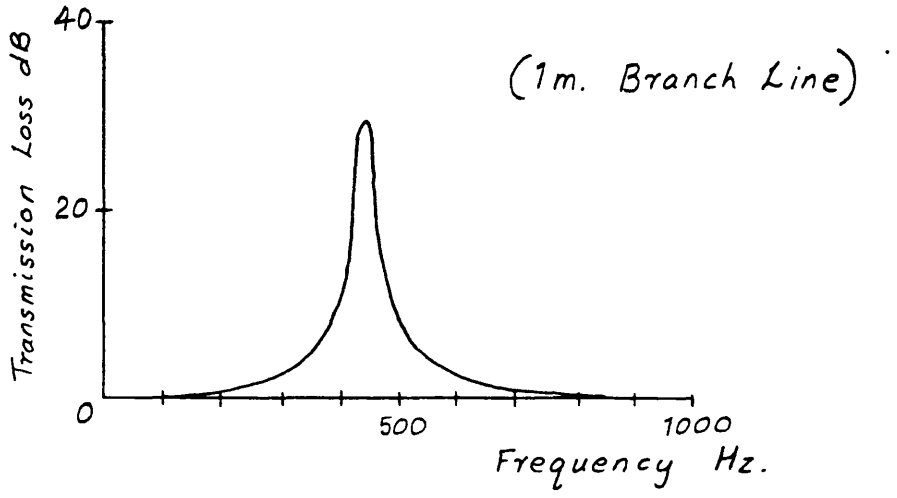

FIG 6·1 Performance Curve for a Closed Ended Branch Line

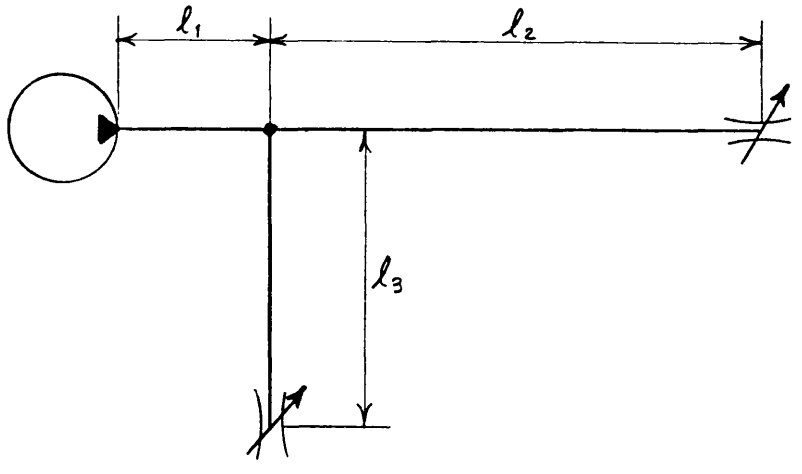

FIG 6·2 A Simple Hydraulic Circuit with a Single Branch Line.

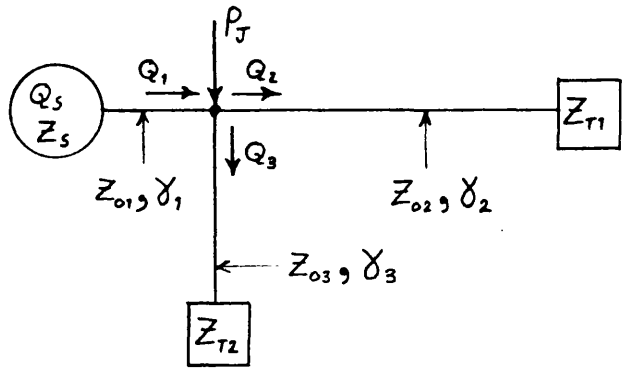

FIG 6·3 Impedance Representation of a Branch Line System.

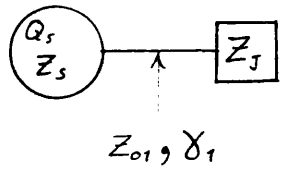

FIG 6·4 Equivalent Circuit Model

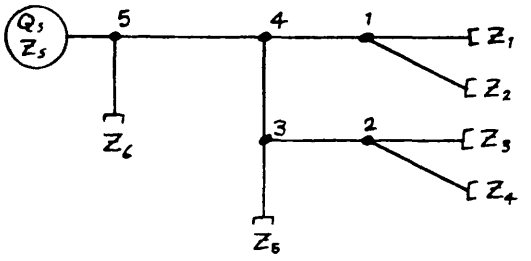

a) Number the Terminations and Junctions

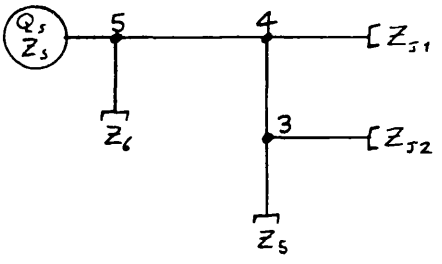

b) Evaluate the Junction Impedance were possible

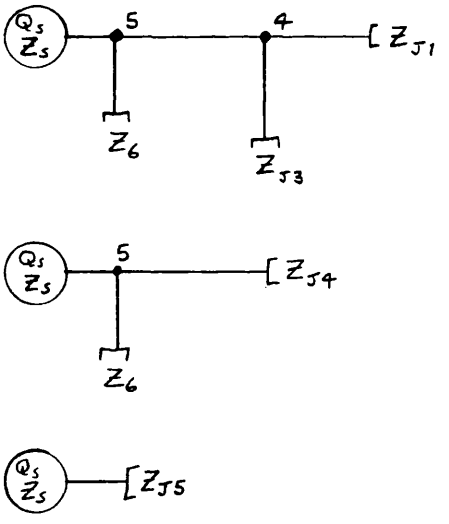

c) Repeat b) until the system has been reduced to a single termination.

d) Determine the pressures in this simple system

e) Reverse the above process. Determine the pressures at each junction.

f) The pressure at any part of the system can now be derived.

FIG 6·5 Step by Step Guide to Modelling Systems with Multiple Branch Lines.

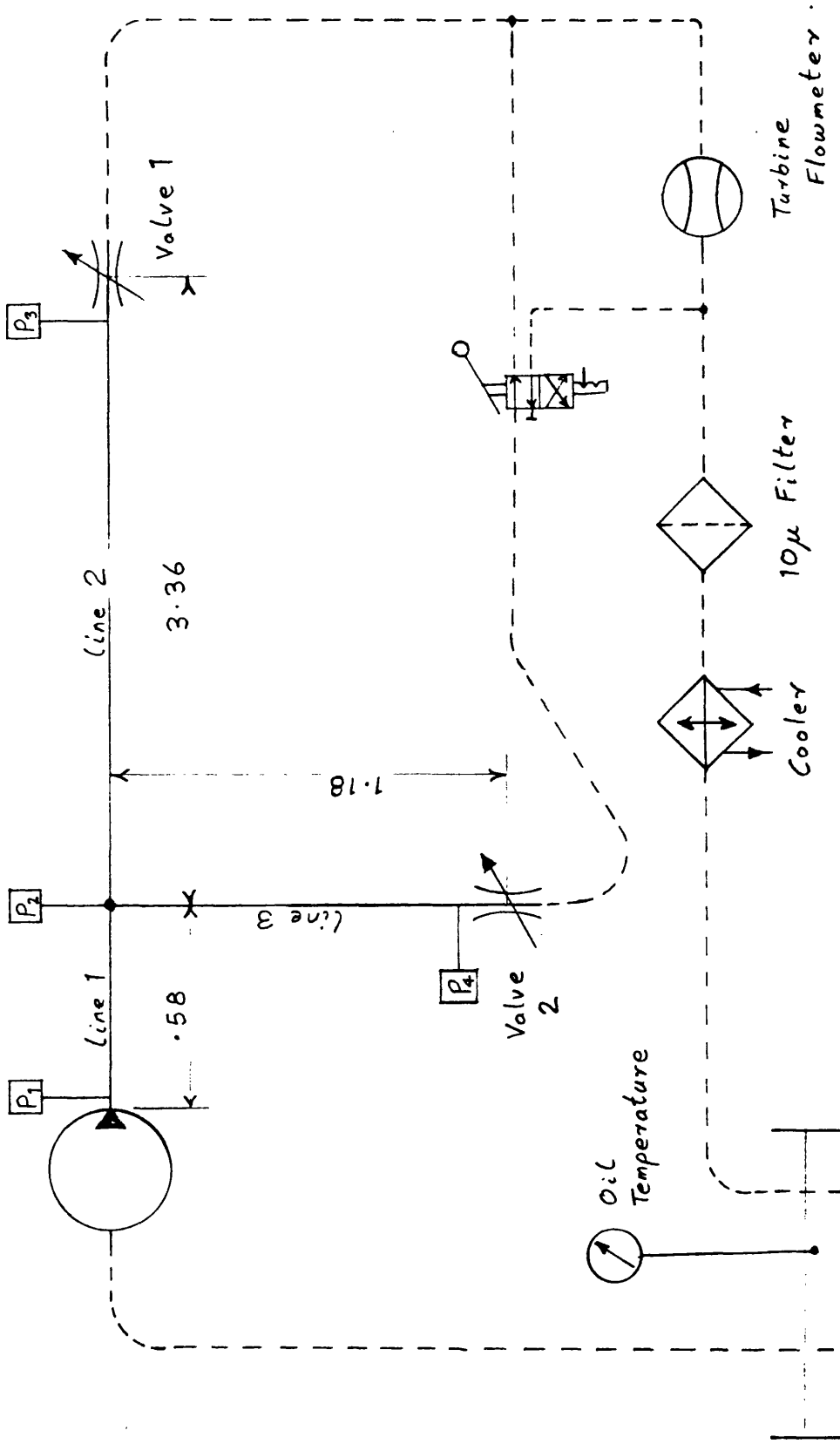

FIG 6·6 Line Diagram of the Branch Circuit Test Rig

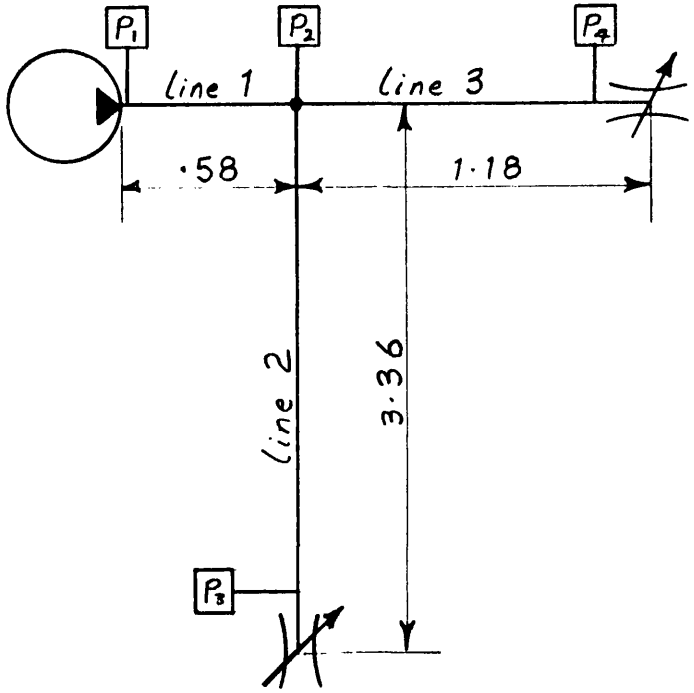

FIG 6·7 Line diagram of the branch circuit with lines 2 and 3 interchanged.

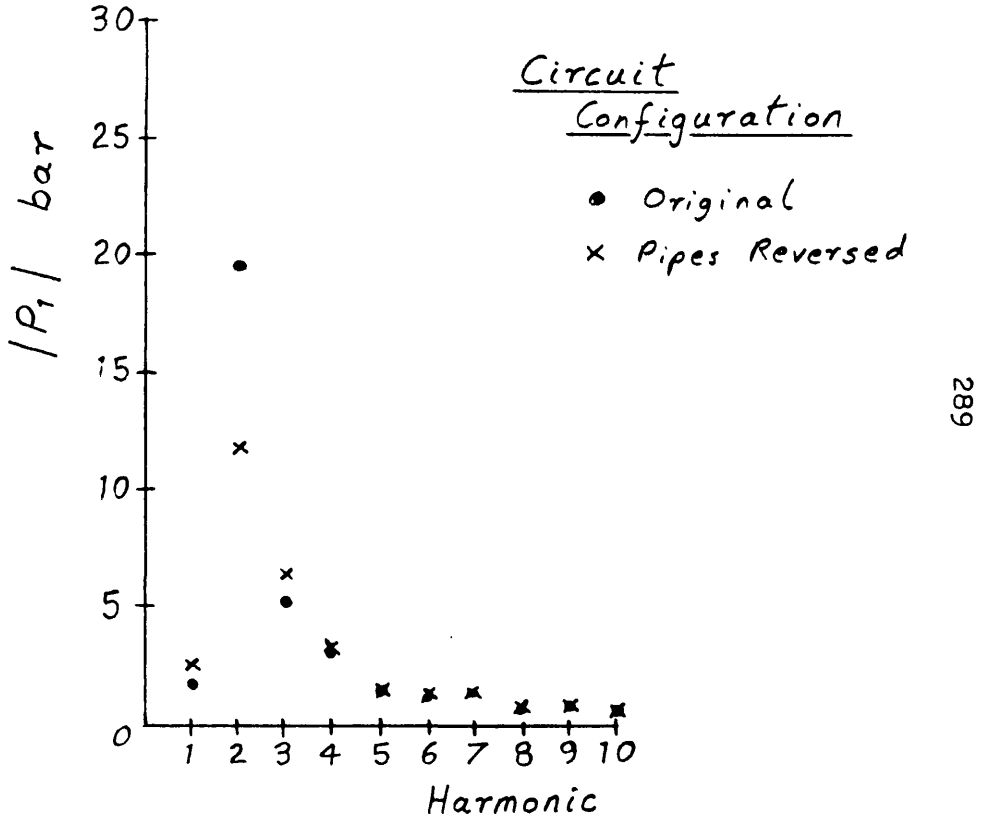

FIG 6·8 Effect of circuit configuration on the pressure levels.

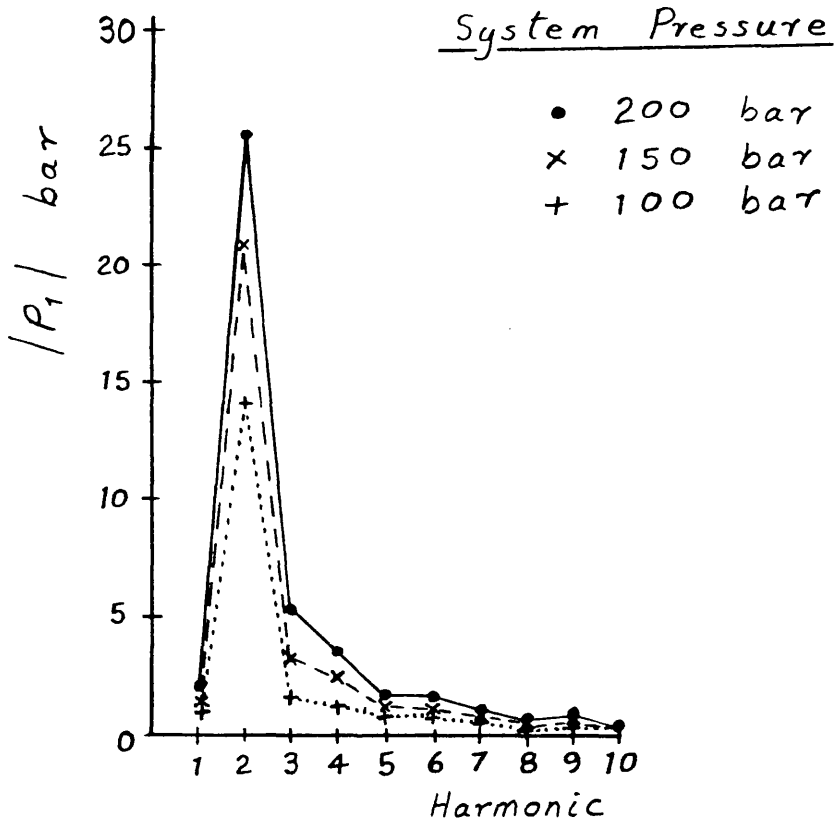

FIG 6·9 Effect of mean system pressure on the pressure levels.

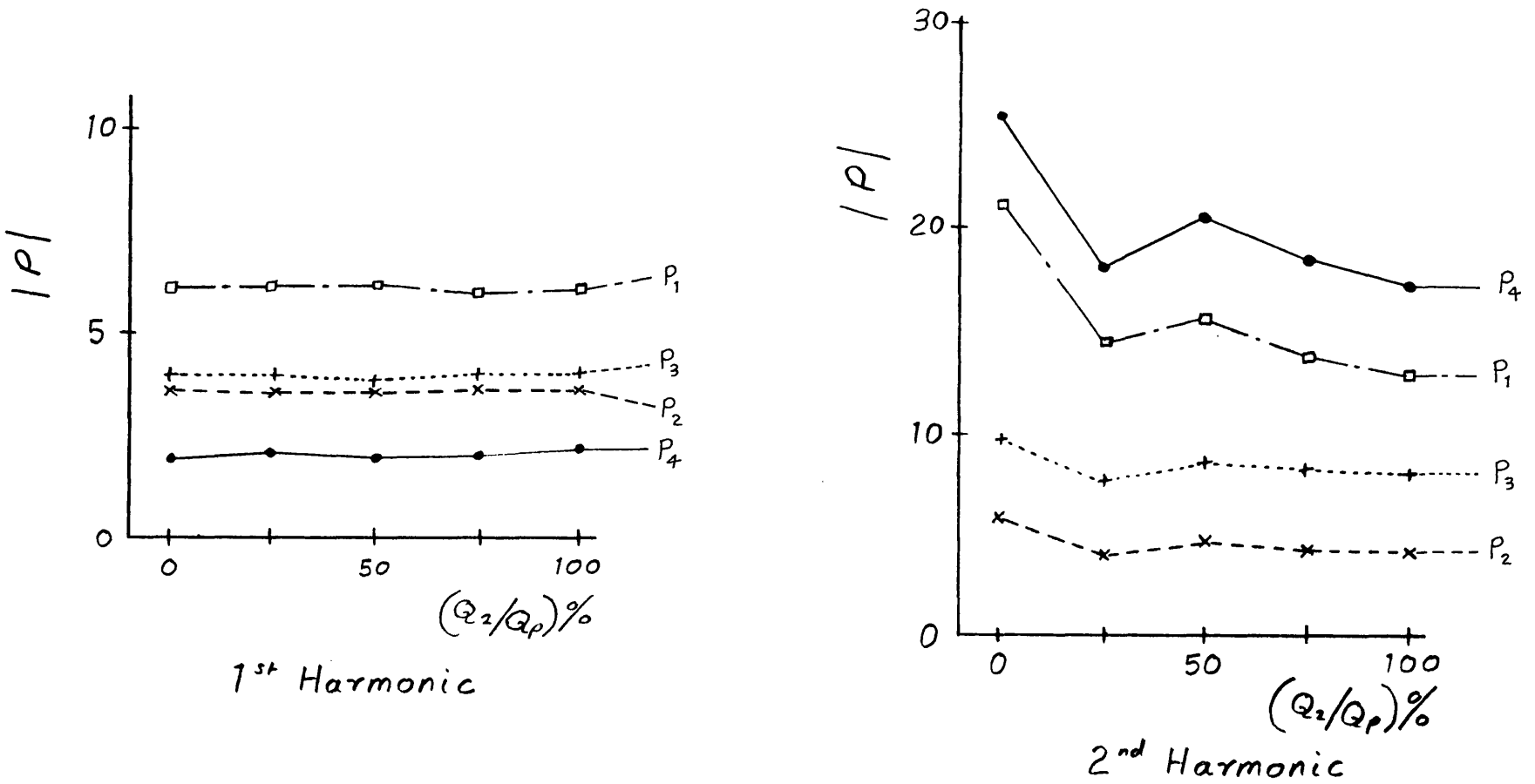

FIG 6·10 Effect of mean flowrate on the pressure levels.

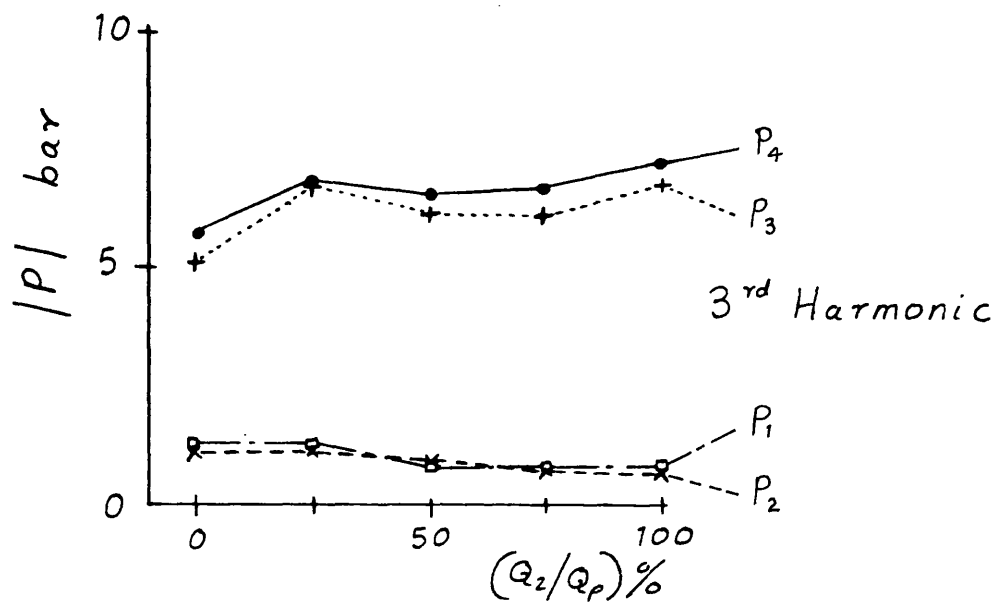

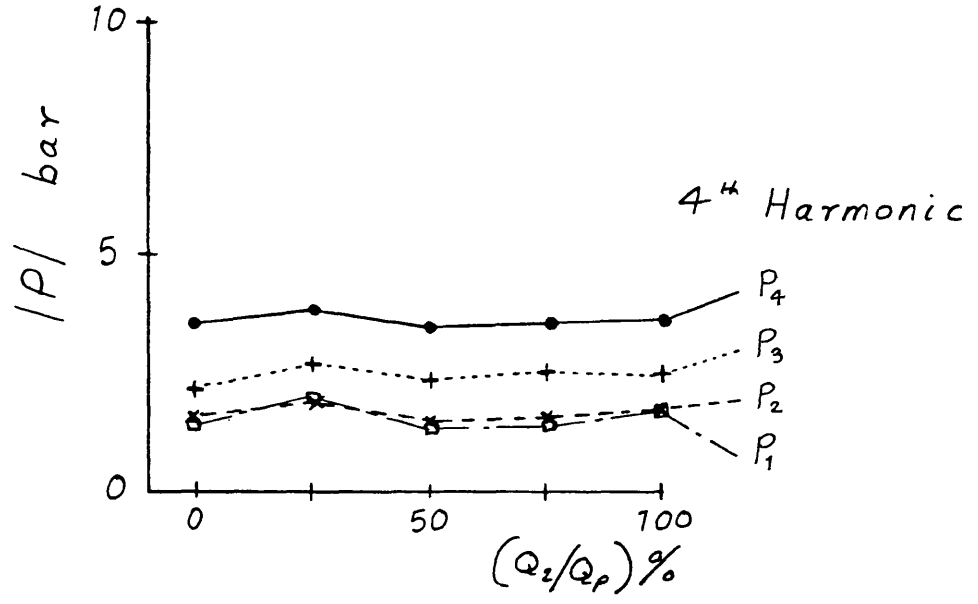

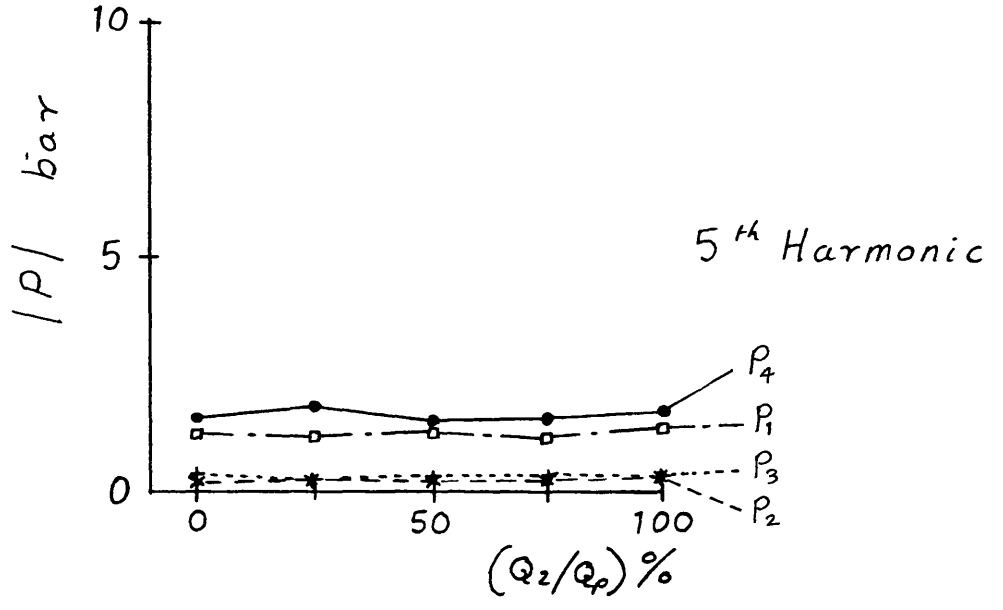

FIG 6·10 Continued.

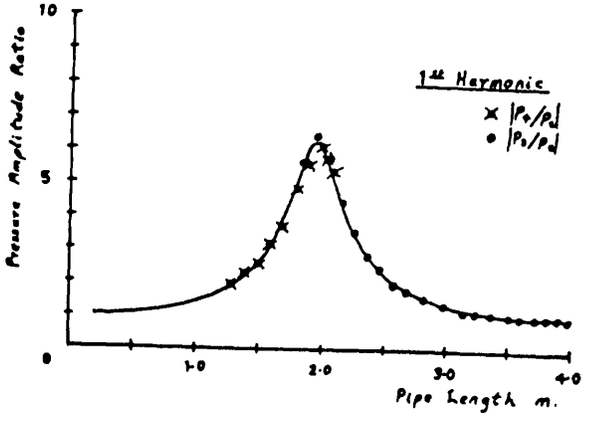

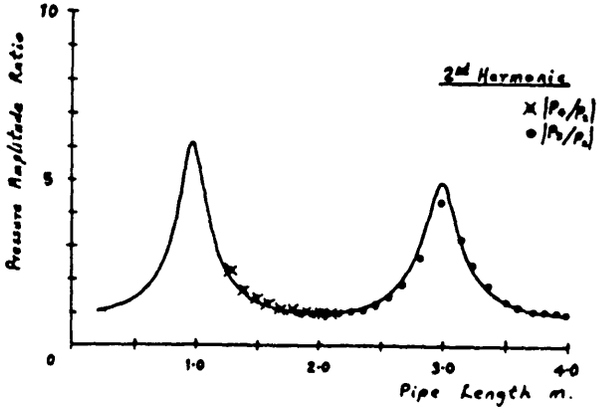

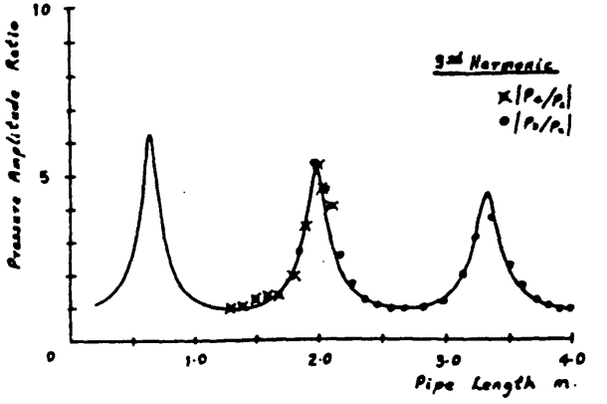

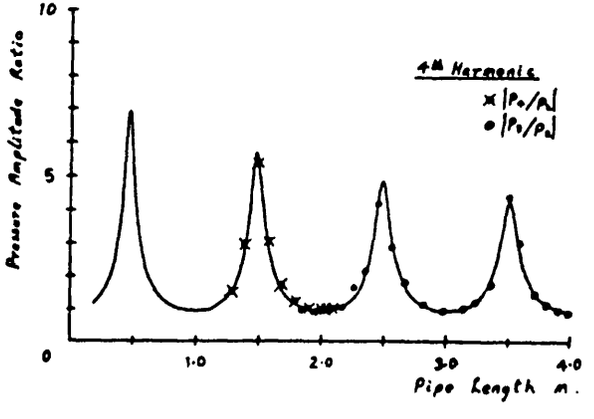

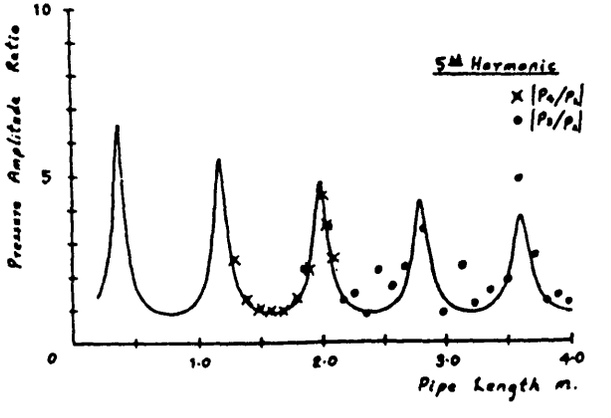

FIG 6·11

Pressure Amplitude Ratios

$|P_3/P_2|$ and $|P_4/P_2|$ (Full Flow)

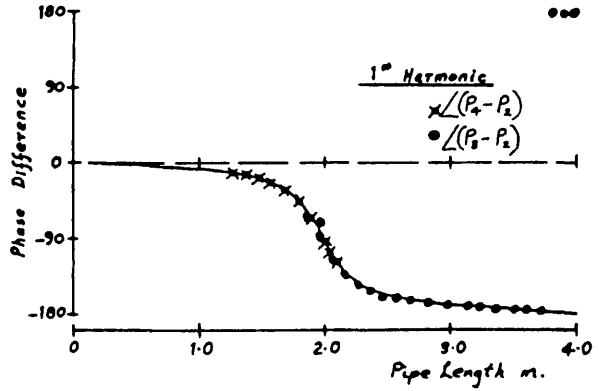

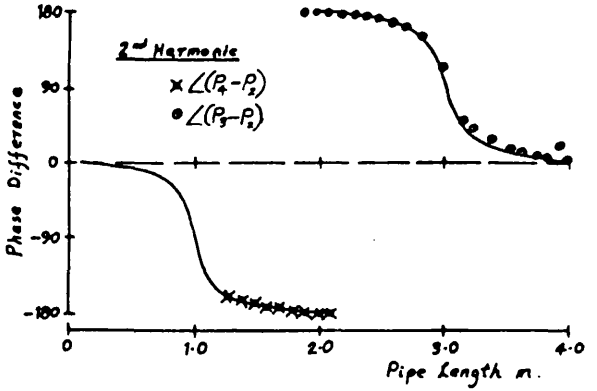

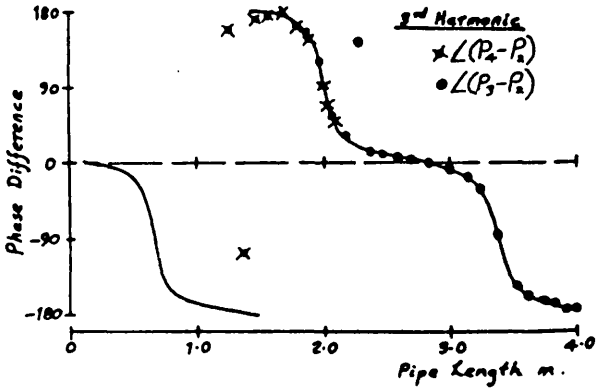

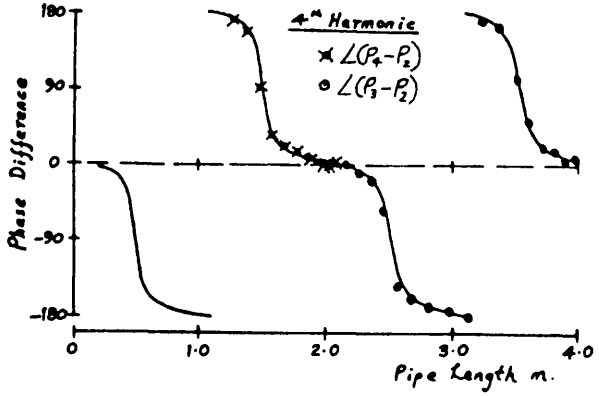

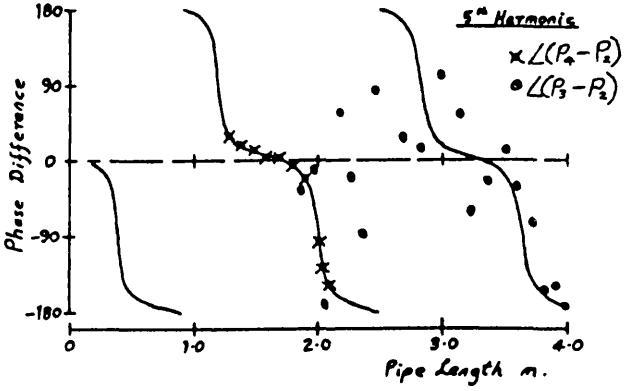

FIG 6·12

Pressure Phase Differences

$\angle(P_3 - P_2)$ and $\angle(P_4 - P_2)$ (Full Flow)

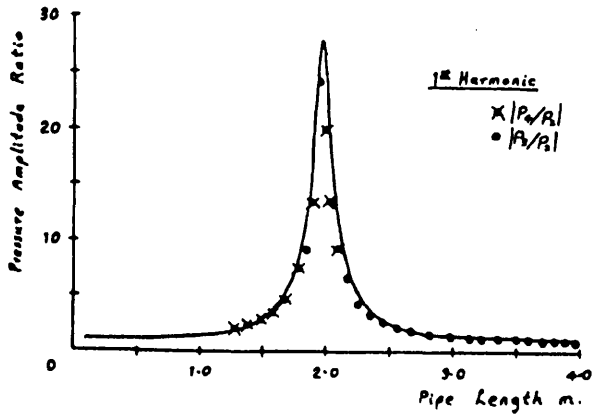

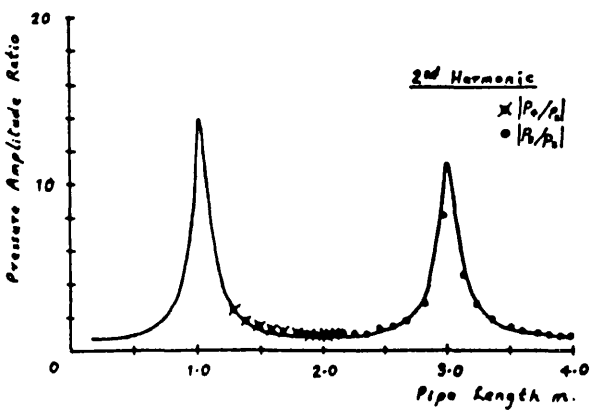

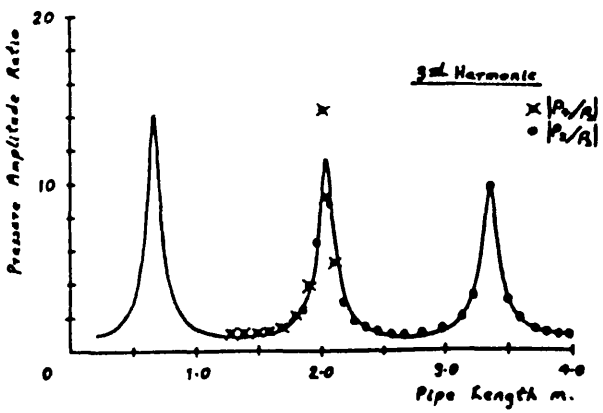

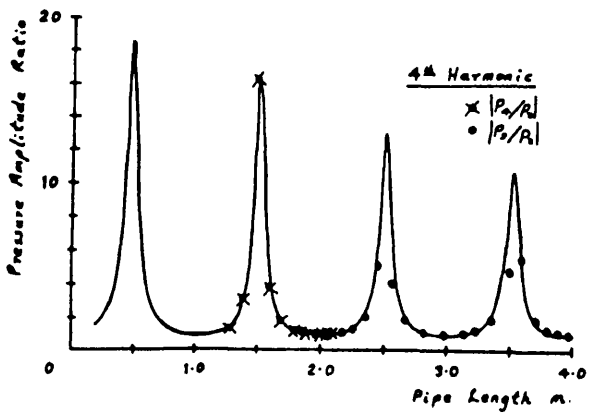

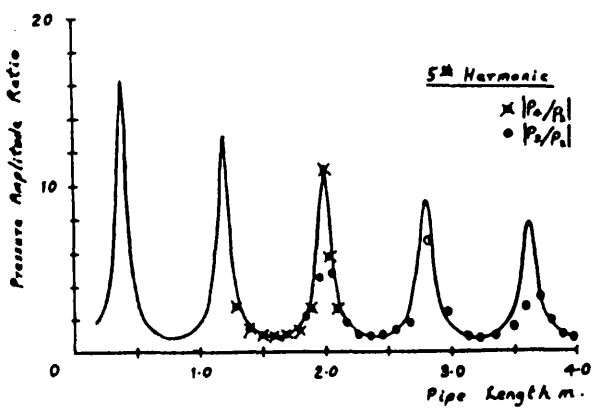

FIG 6·13

Pressure Amplitude Ratios

$|P_3/P_2|$ and $|P_4/P_2|$ (No Flow)

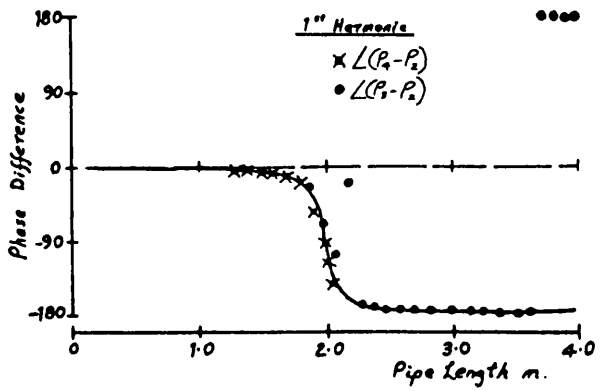

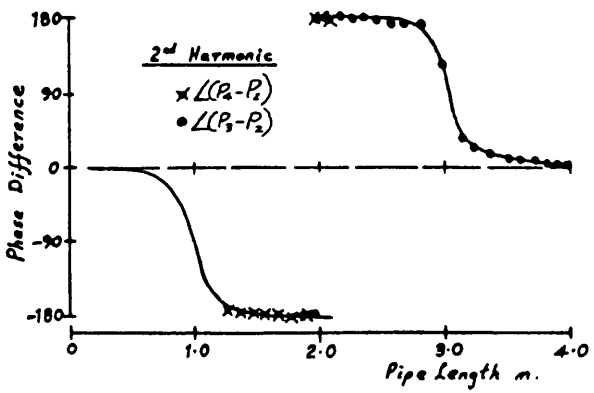

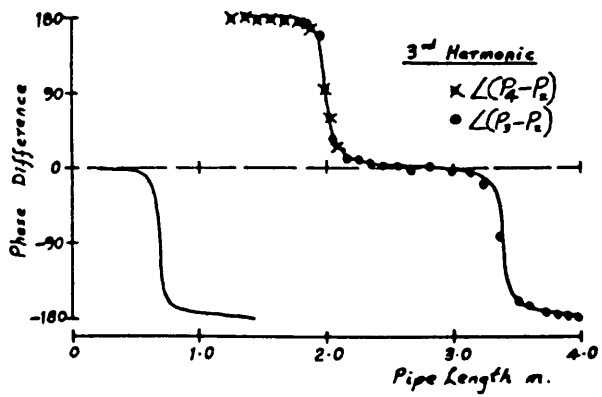

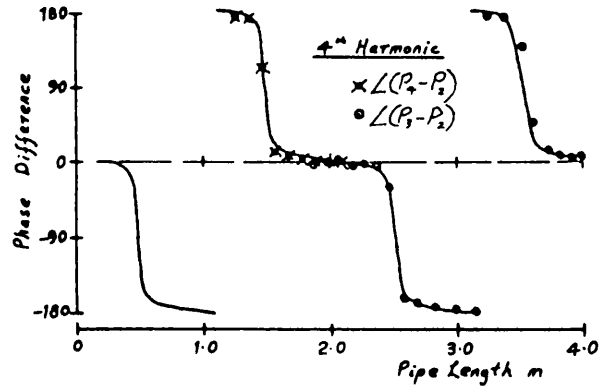

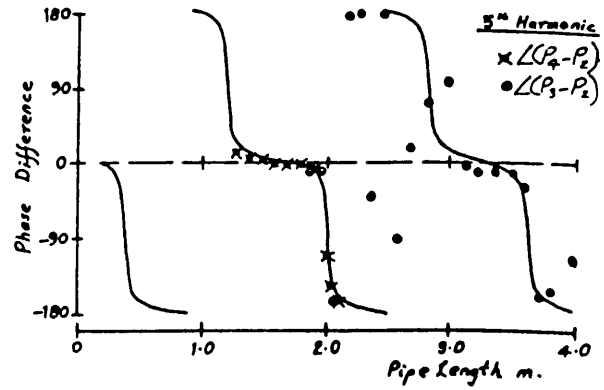

FIG 6·14

Pressure Phase Differences

$\angle(P_3 - P_2)$ and $\angle(P_4 - P_2)$ (No Flow)

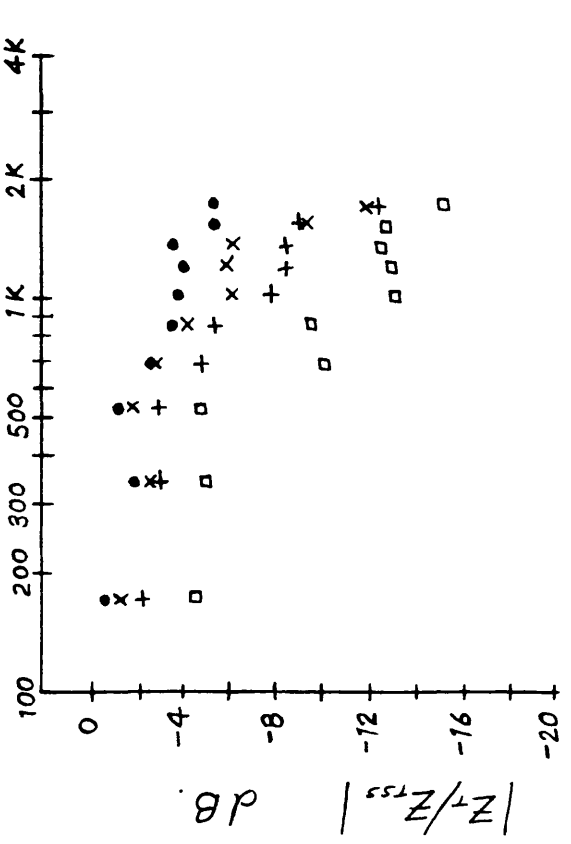

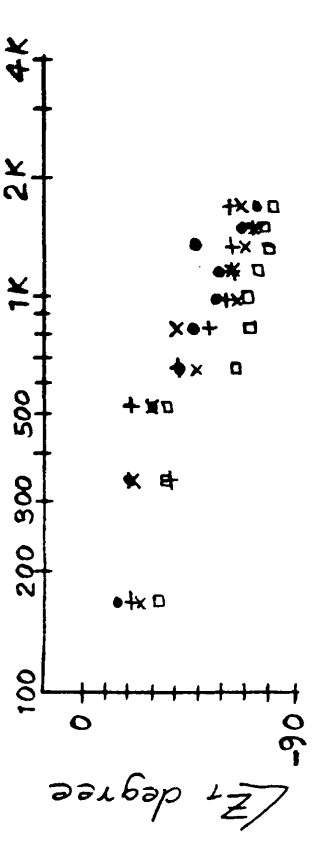

FIG 6·16 Valve impedance, variation with frequency and mean flowrate.

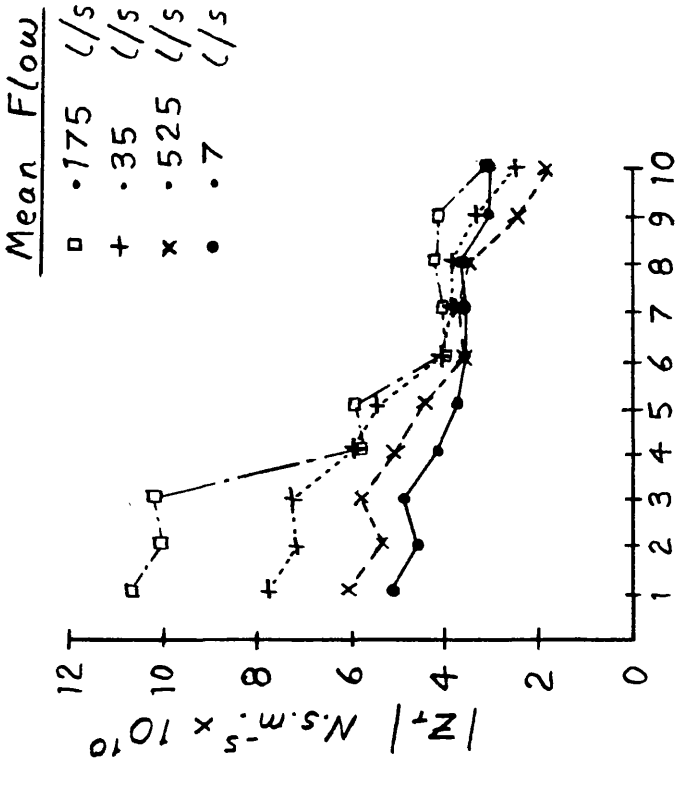

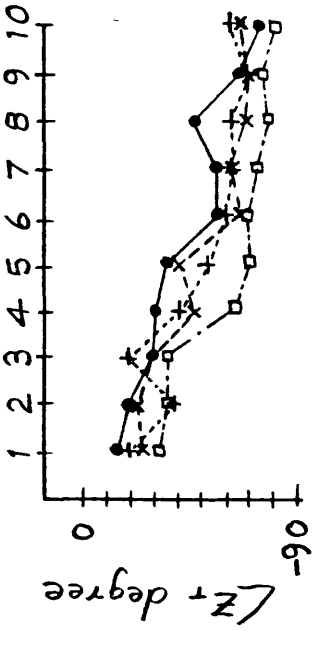

FIG 6·15 Valve impedance spectra

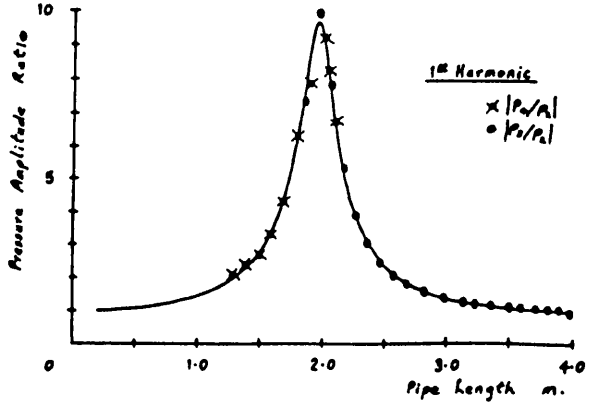

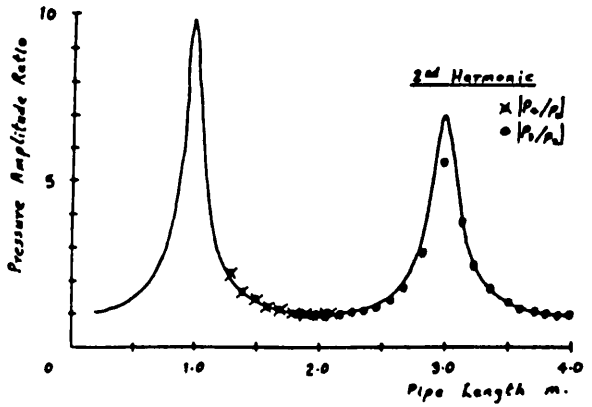

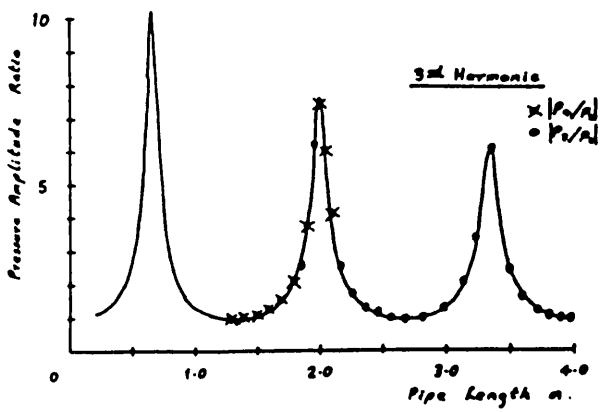

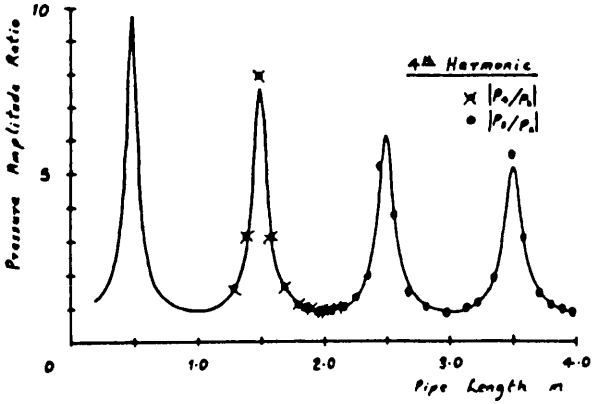

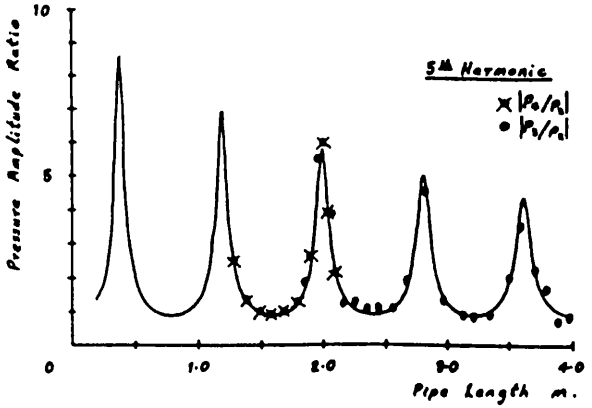

FIG 6·17

Pressure Amplitude Ratios

$|P_3/P_2|$ and $|P_4/P_2|$ (Flow · 5 l/s)

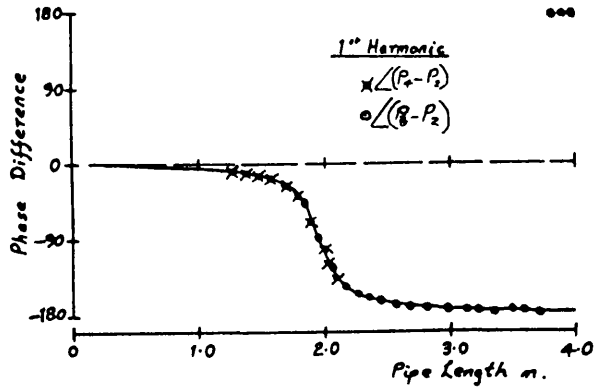

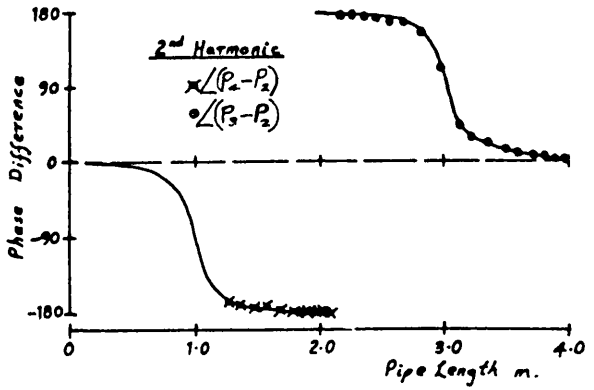

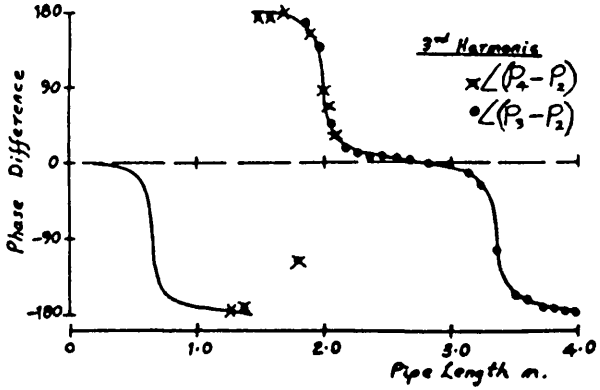

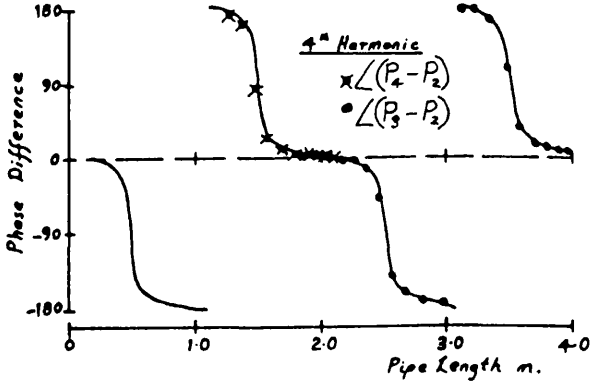

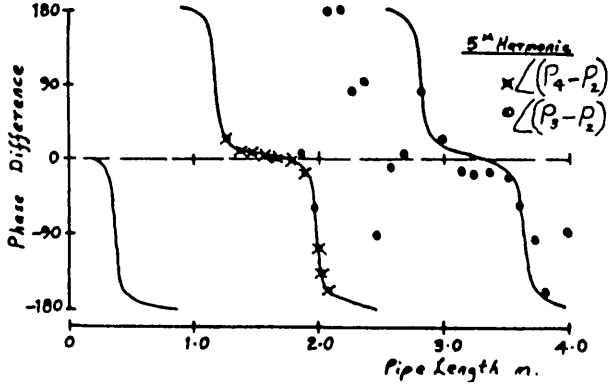

FIG 6·18

Pressure Phase Differences

$\angle(P_3-P_2)$ and $\angle(P_4-P_2)$ (Flow ·5 l/s)

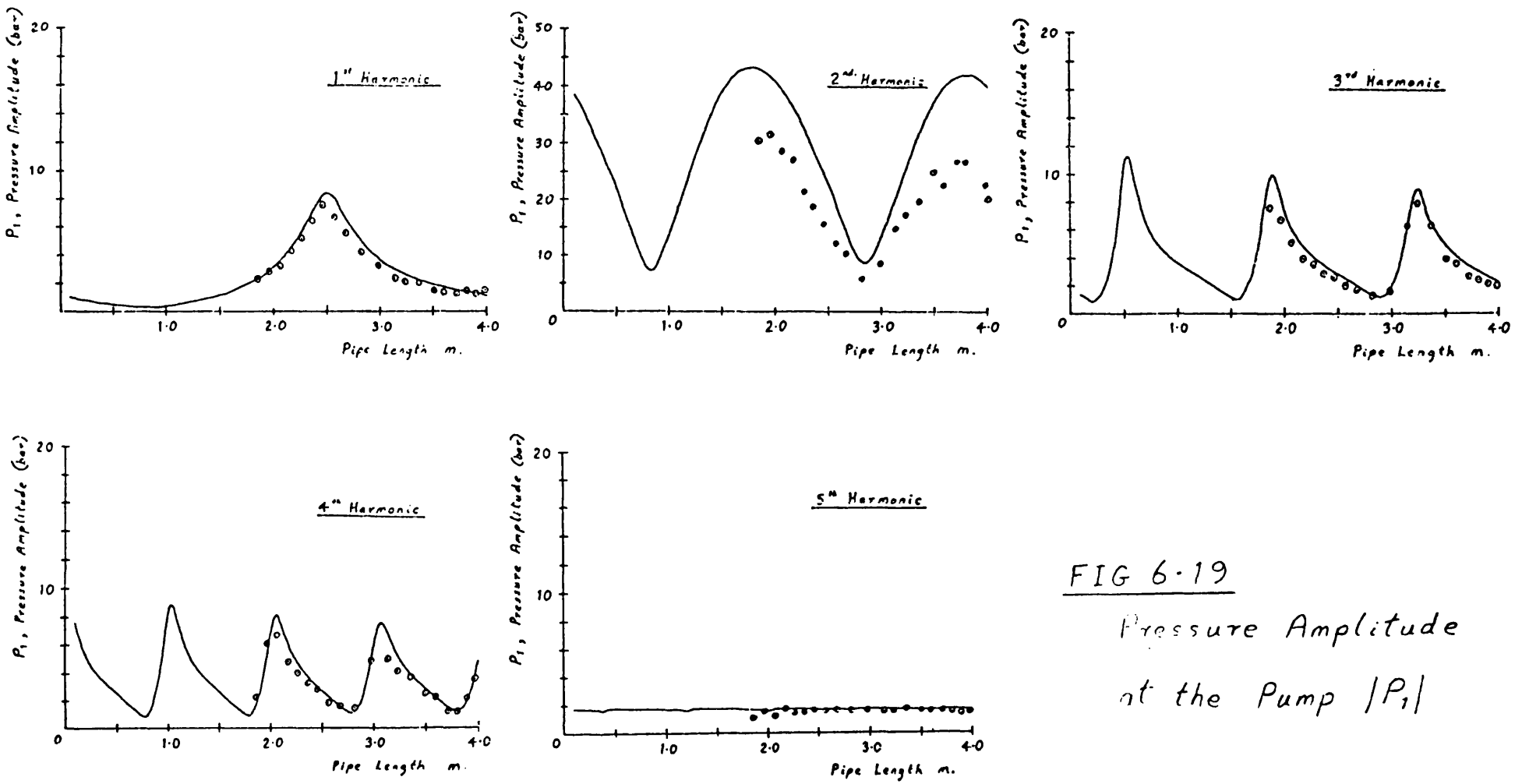

FIG 6·19

Pressure Amplitude at the Pump $|P_1|$

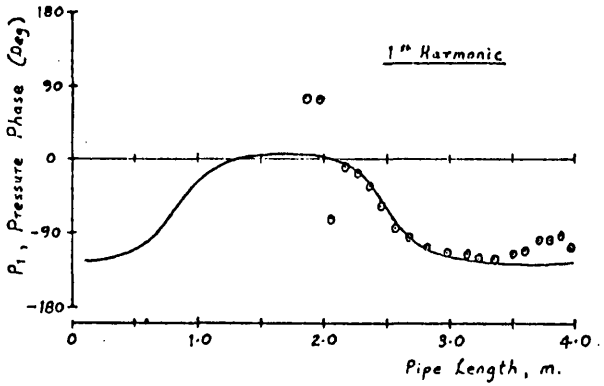

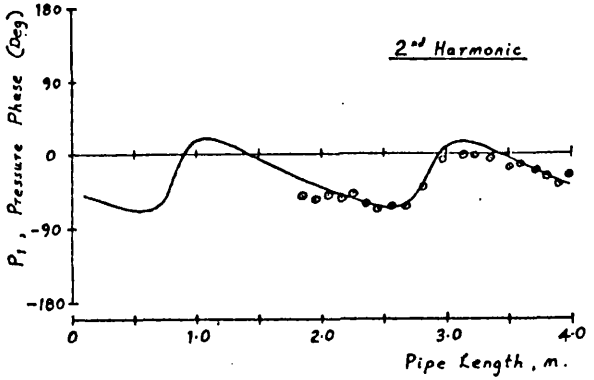

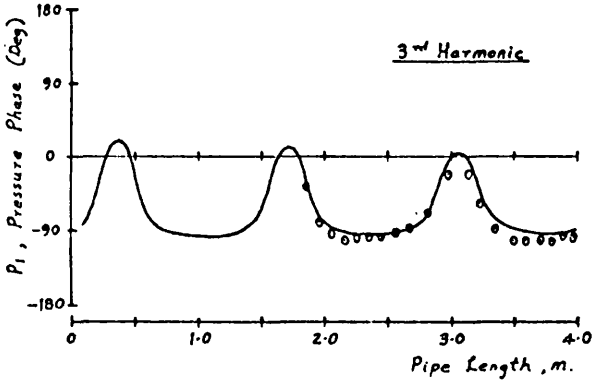

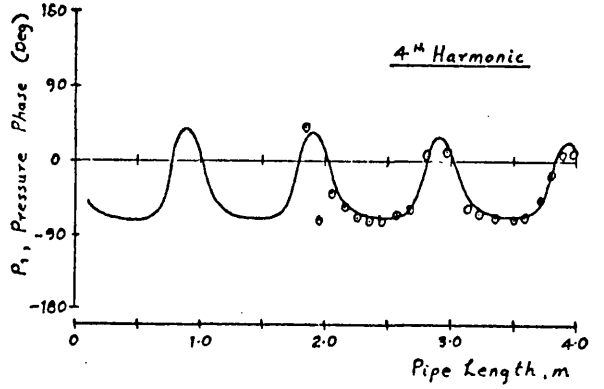

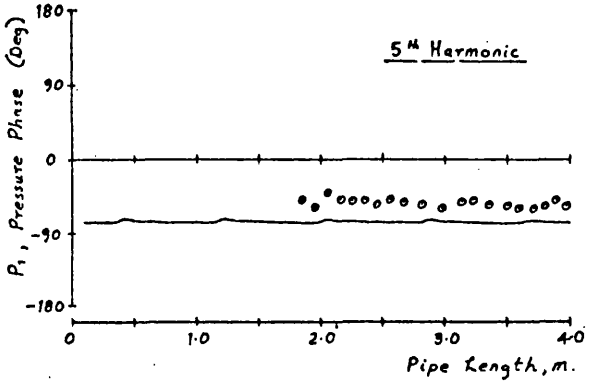

FIG 6·20 Pressure phase at the pump $\angle P_1$

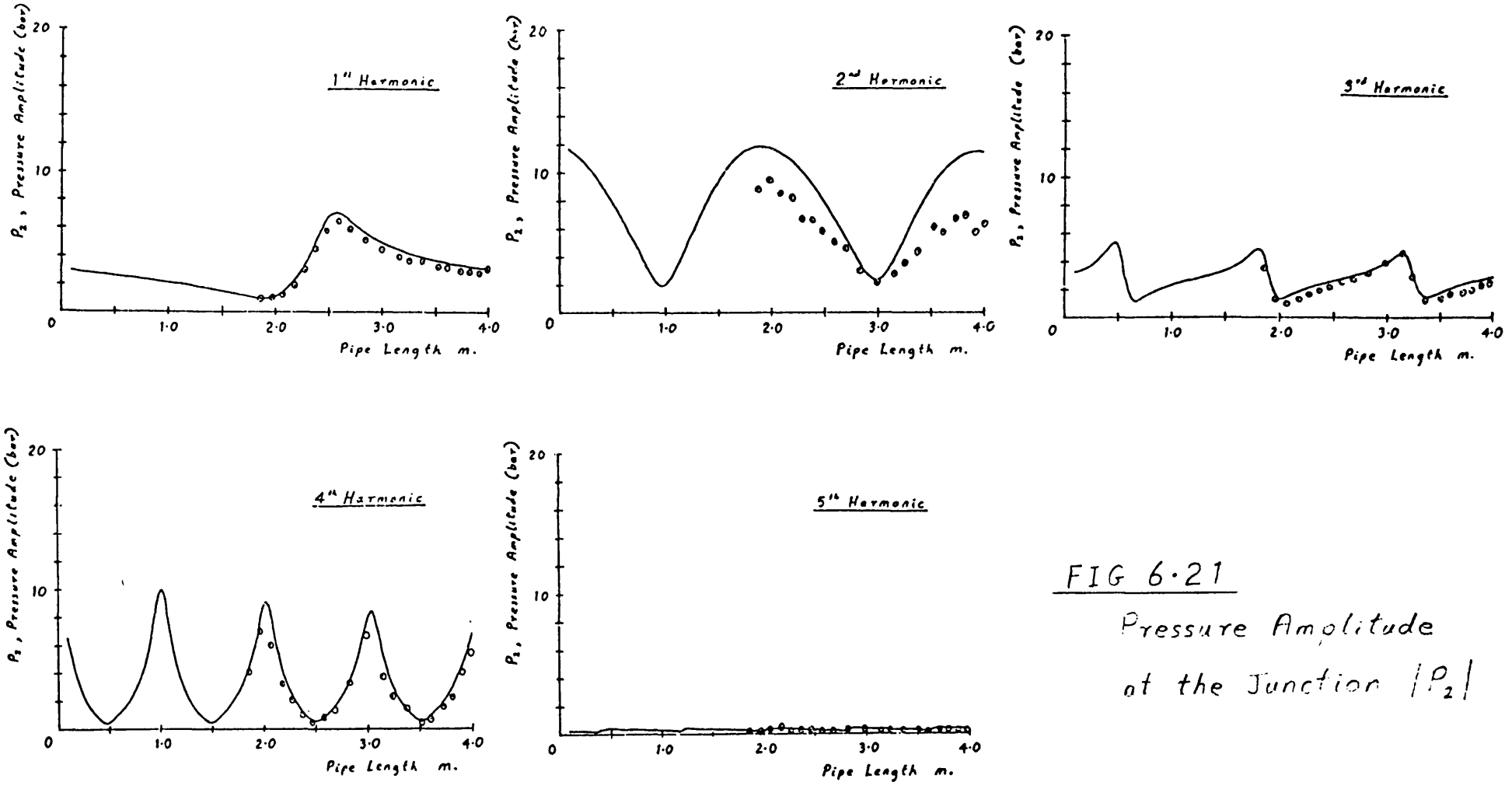

FIG 6·21

Pressure Amplitude at the Junction $|P_2|$

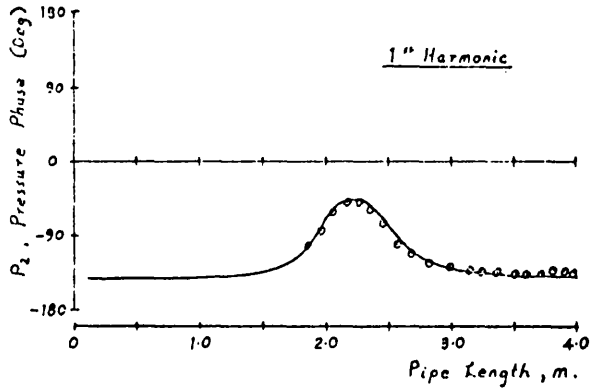

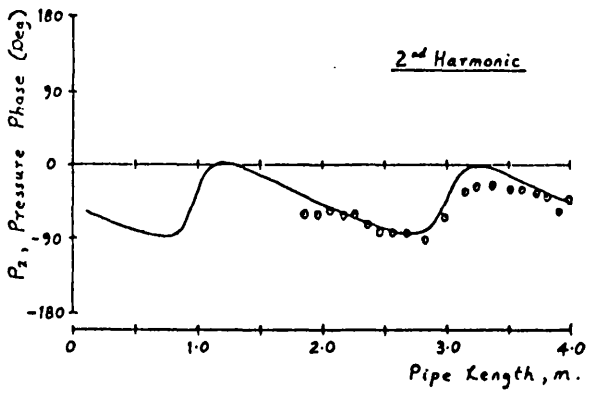

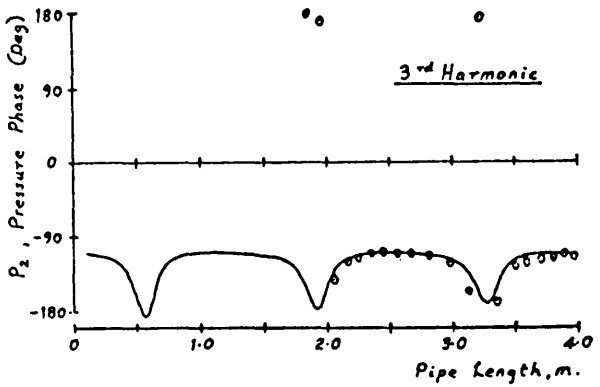

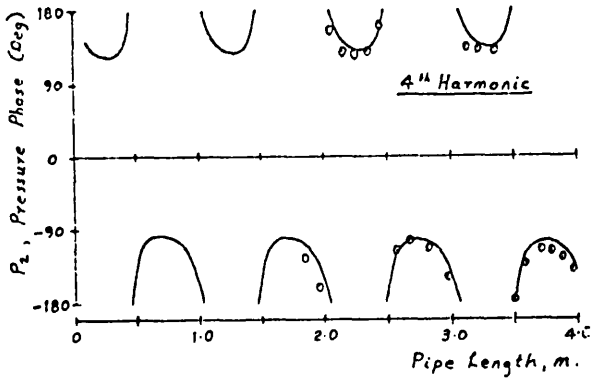

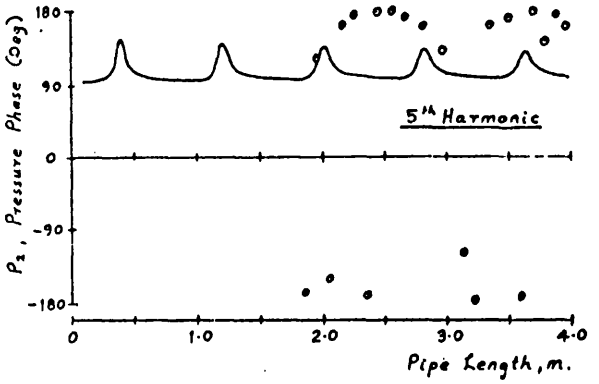

FIG 6·22 Pressure phase at the junction $\angle P_2$

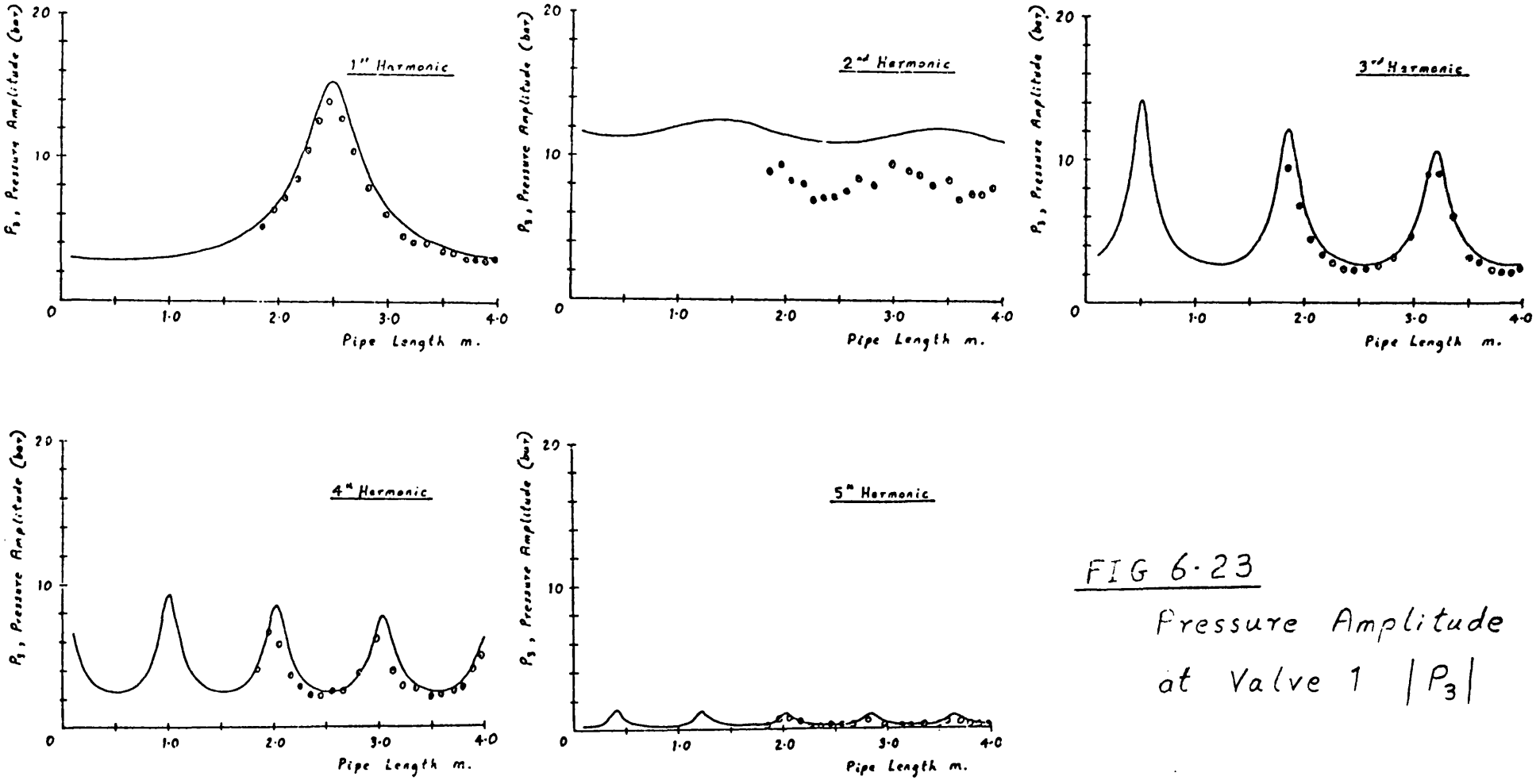

FIG 6·23

Fressure Amplitude at Valve 1 $|P_3|$

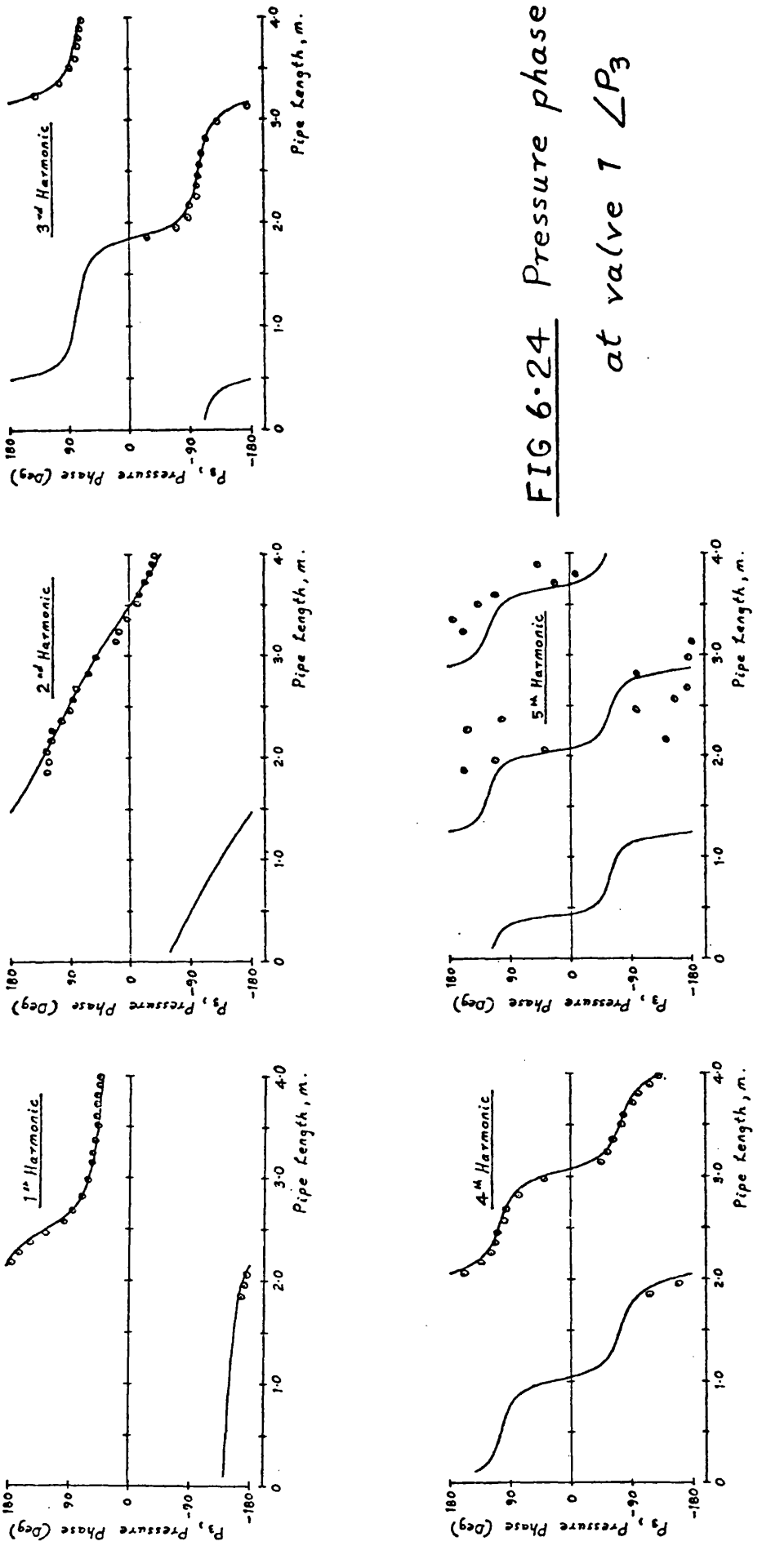

FIG 6.24 Pressure phase at valve 1 $\angle P_3$

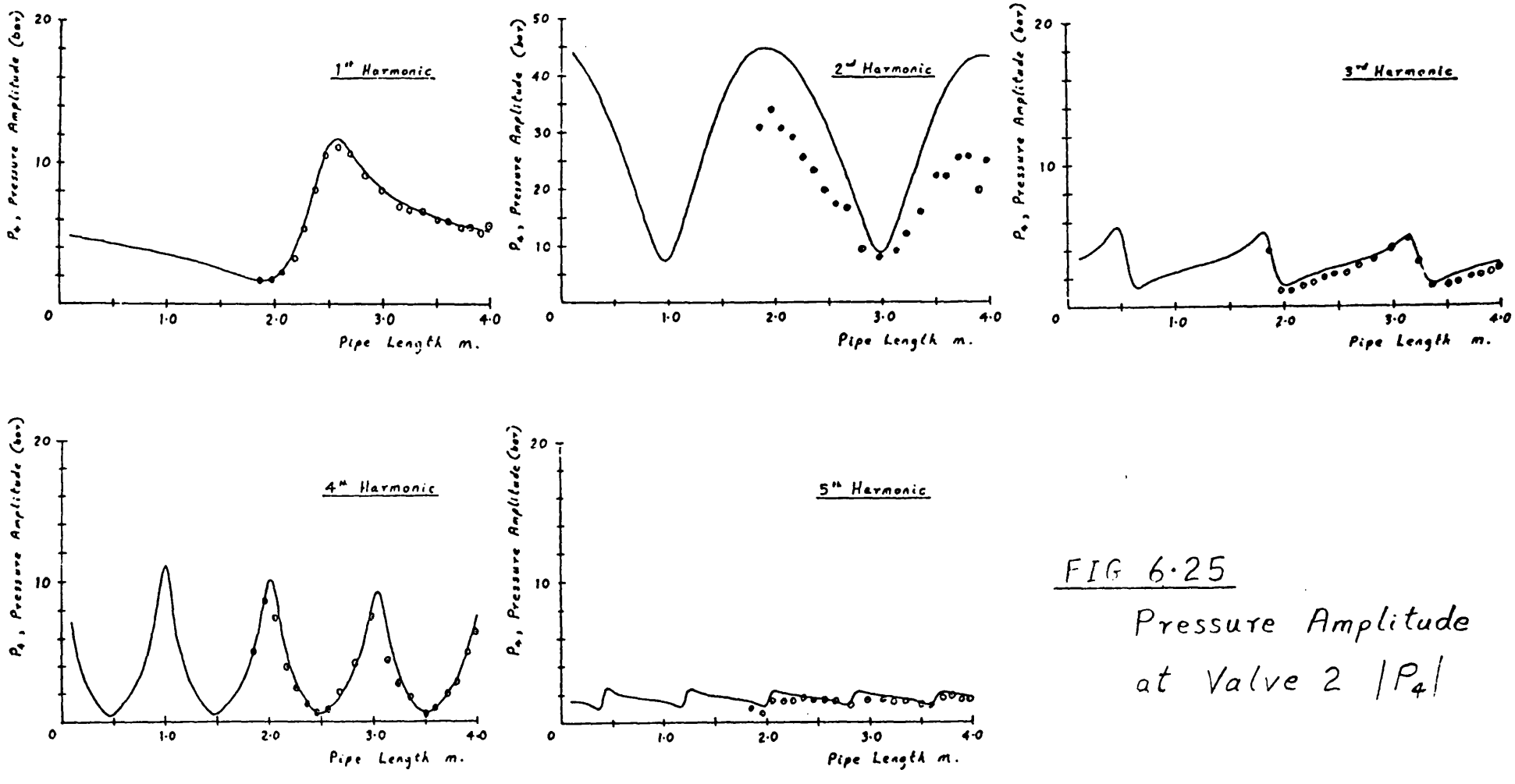

FIG 6·25

Pressure Amplitude at Valve 2 $|P_4|$

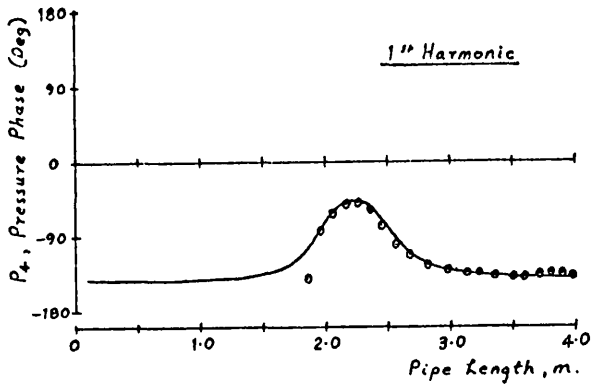

FIG 6·26 Pressure phase at valve 2 $\angle P_4$

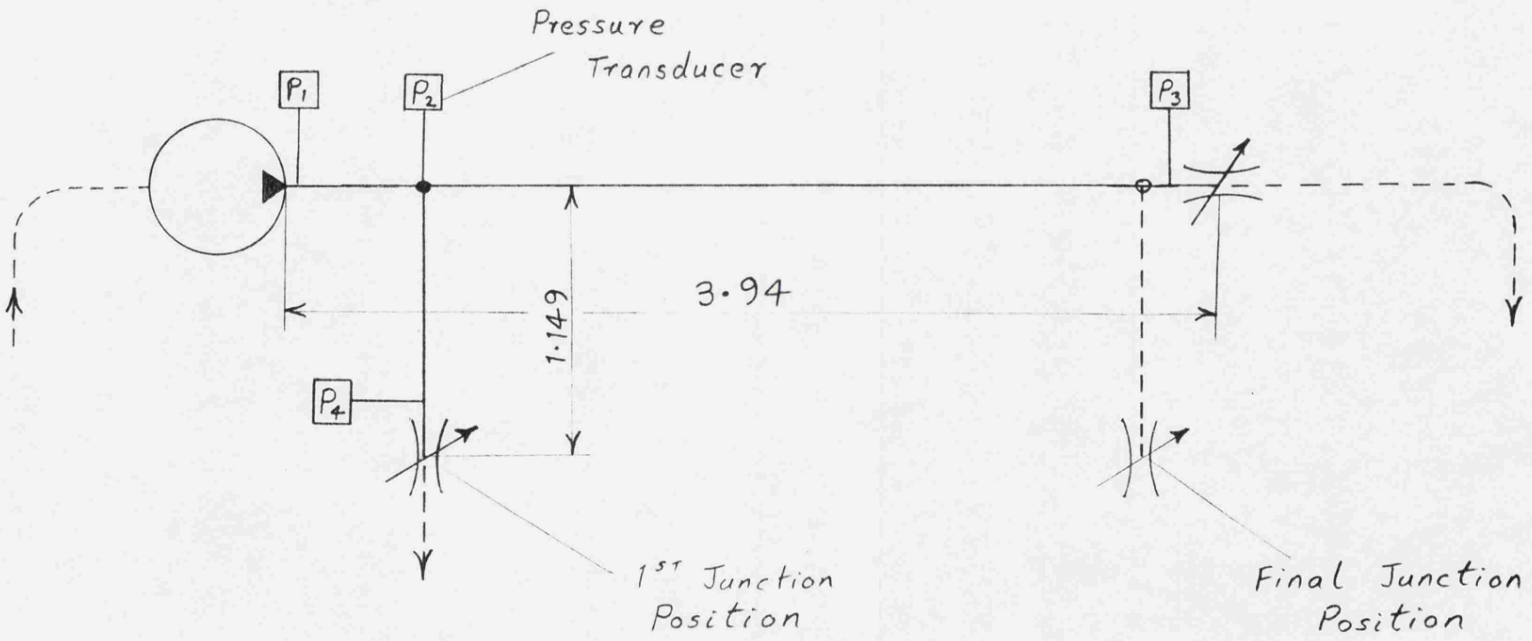

Suction and Return lines
as for the Branch Circuit
Rig, Fig 6·6.

FIG 6·27 Line Diagram of Junction Position Test Rig

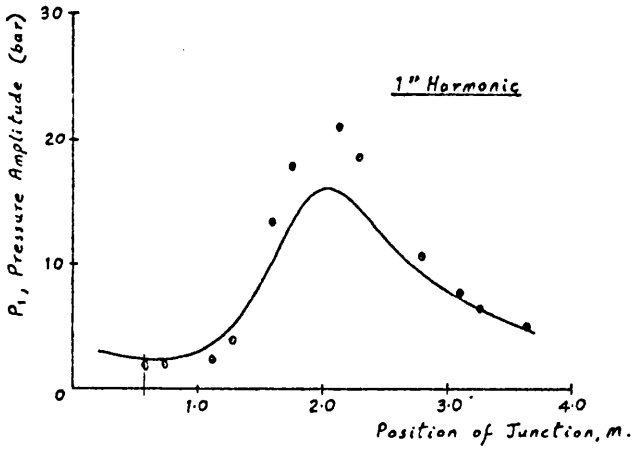

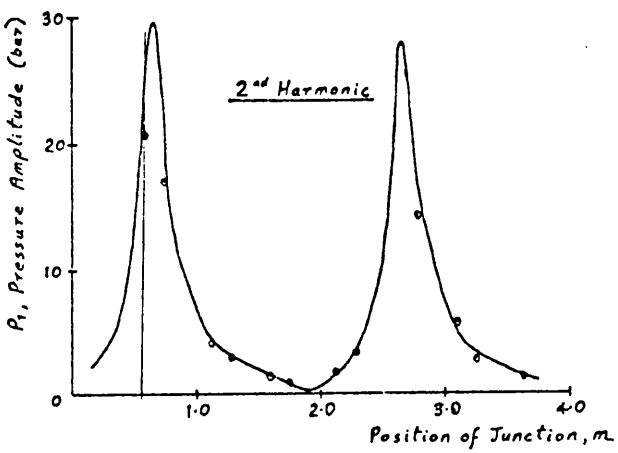

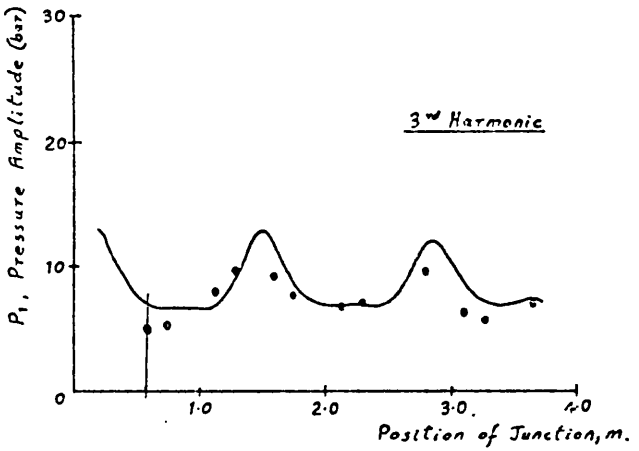

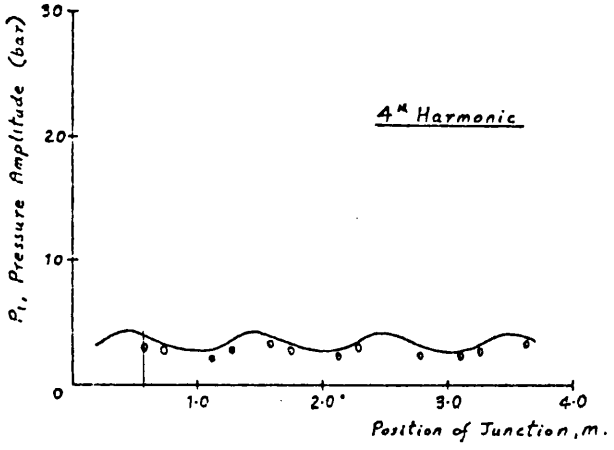

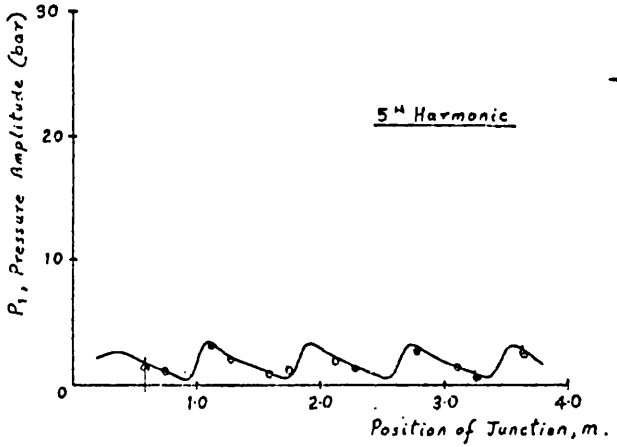

FIG 6·28

Effect of junction position on pressure amplitude $|P_1|$

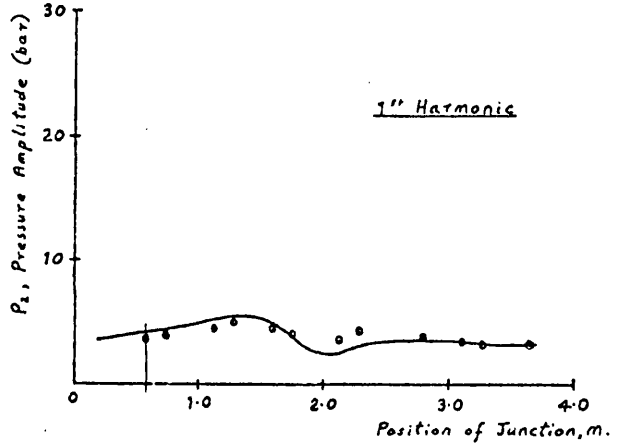

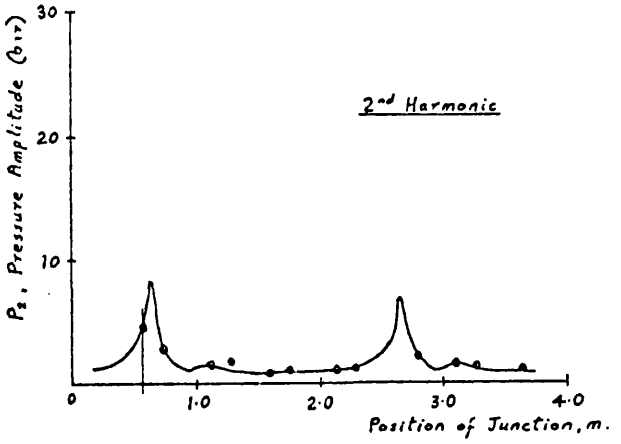

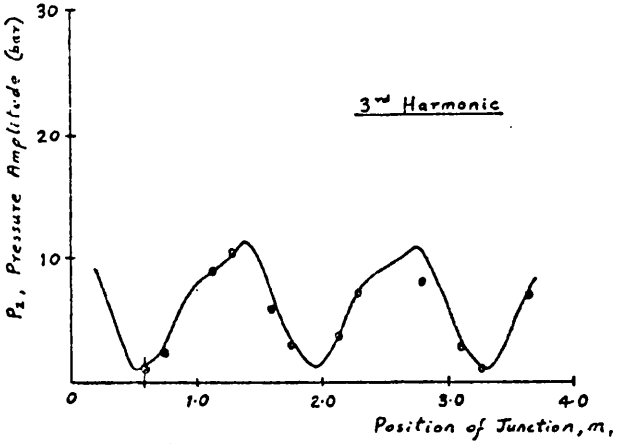

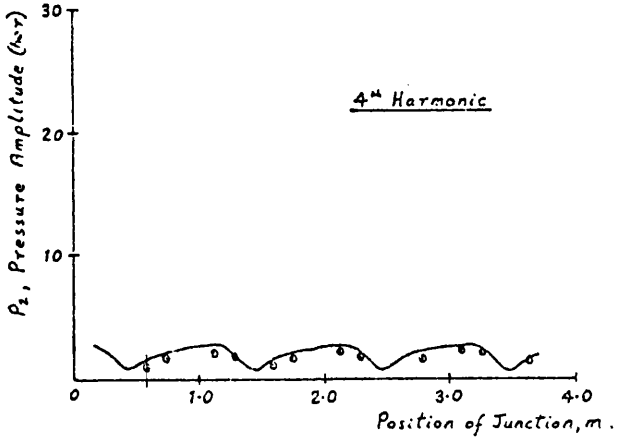

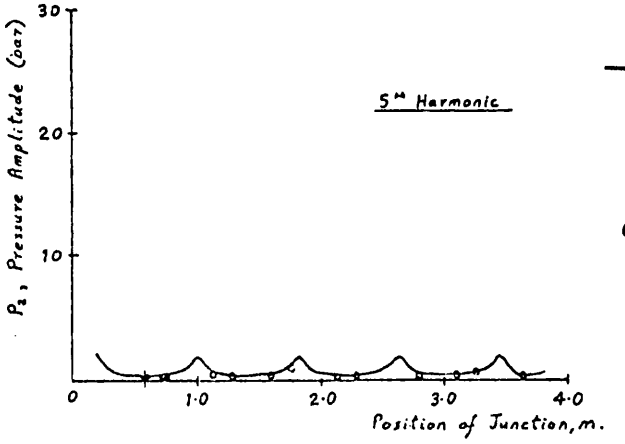

FIG 6·29

Effect of junction position on pressure amplitude $|P_2|$

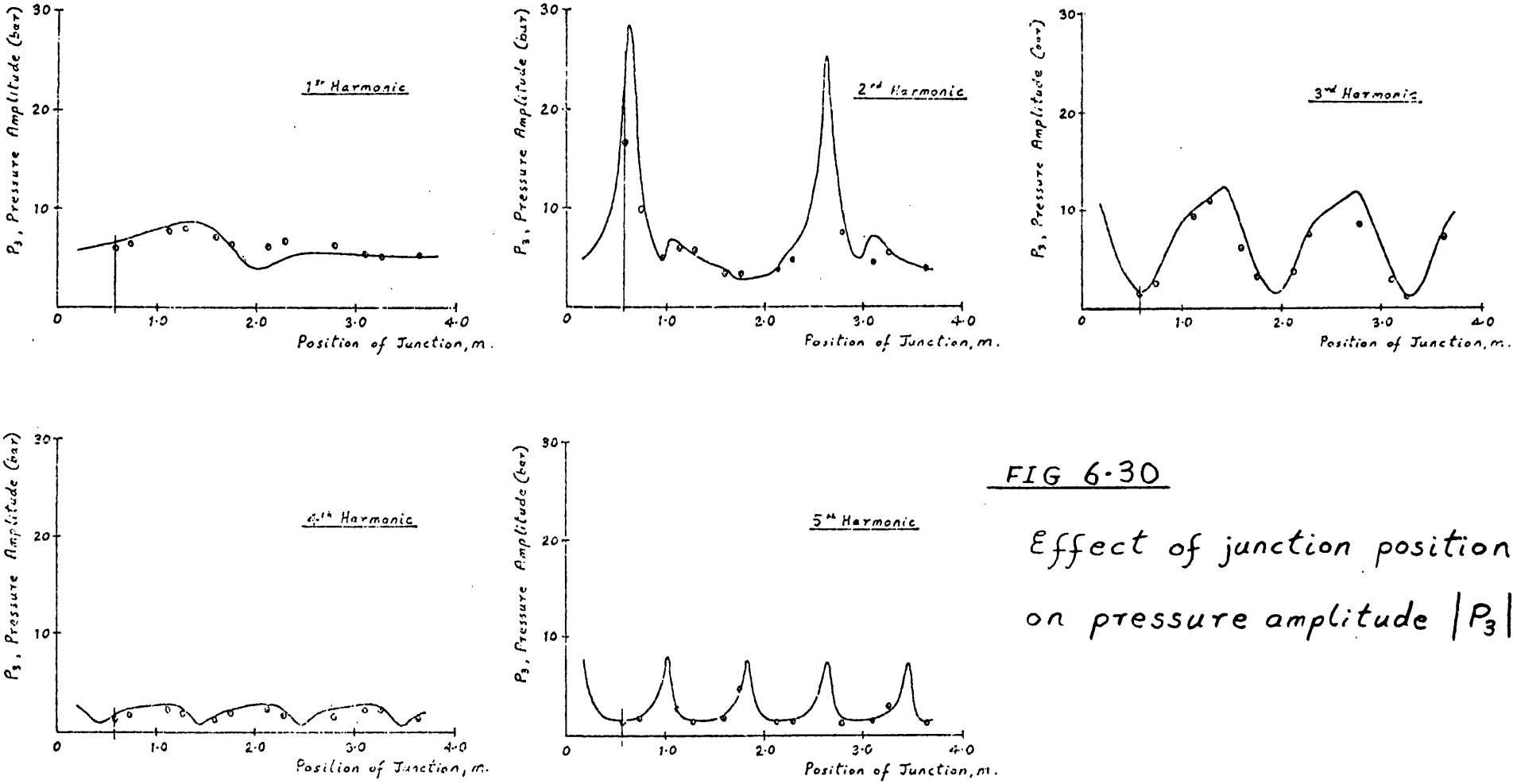

FIG 6·30

Effect of junction position on pressure amplitude $|P_3|$

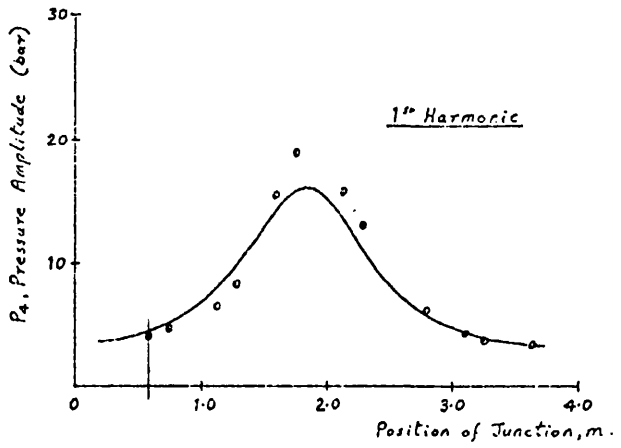

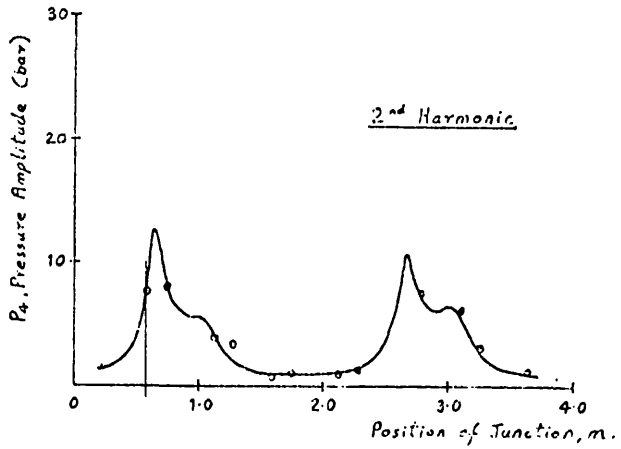

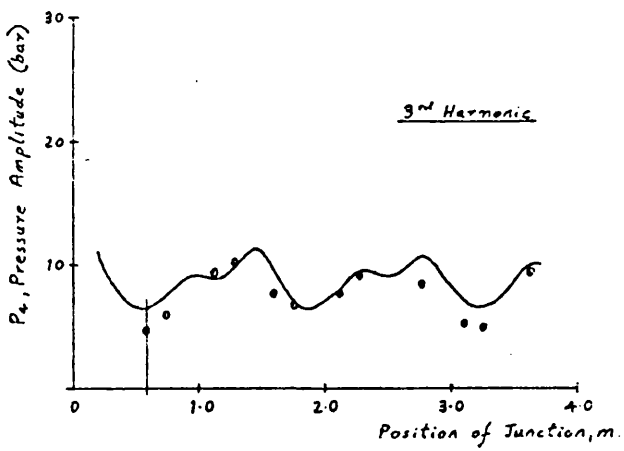

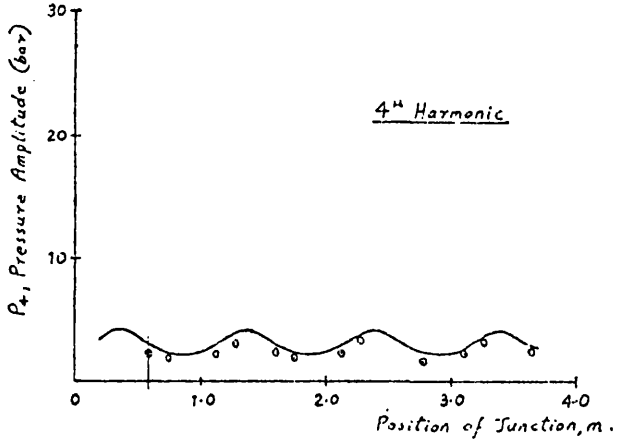

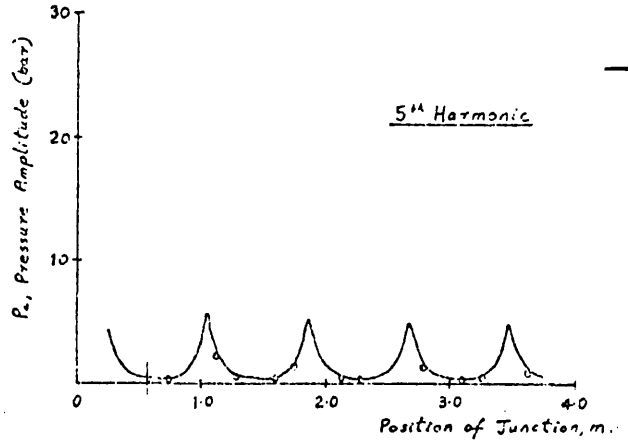

FIG 6·31

Effect of junction position on pressure amplitude $|P_+|_o$

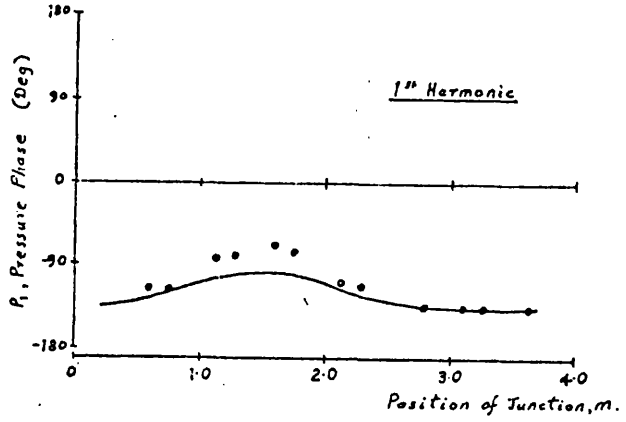

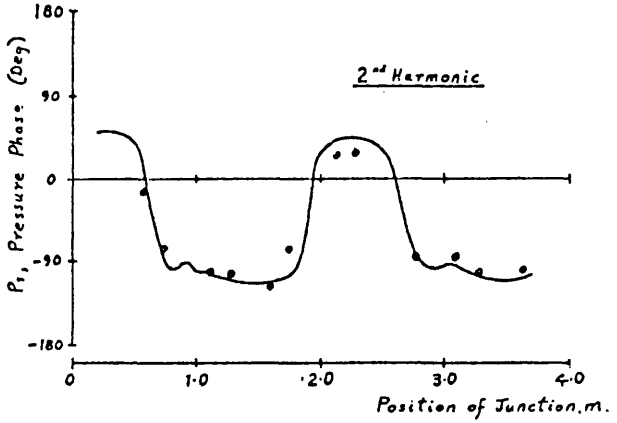

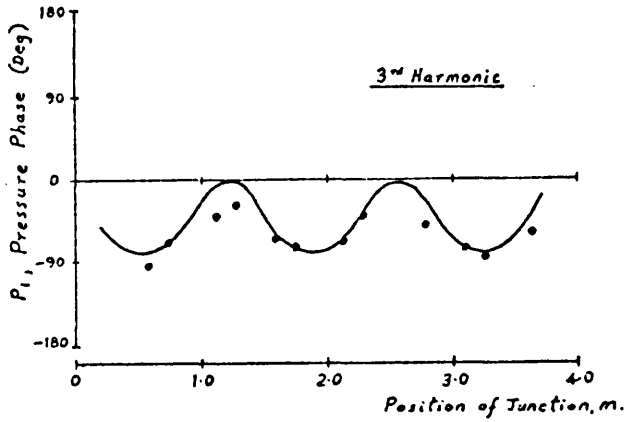

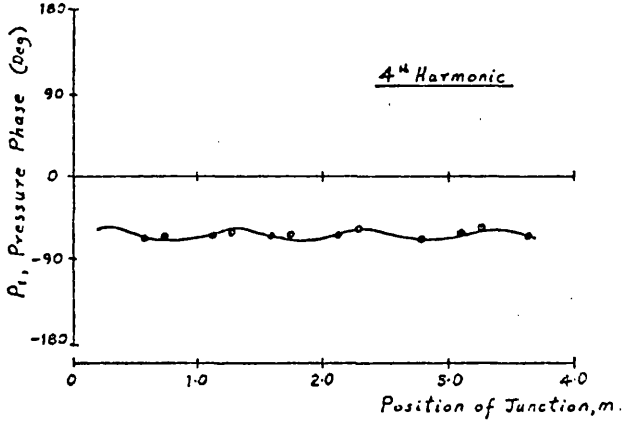

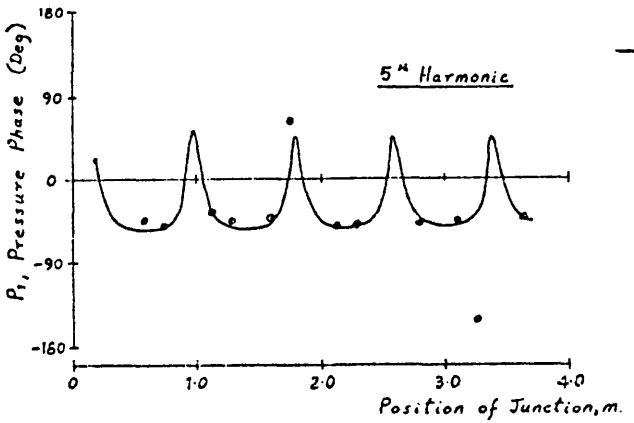

FIG 6·32

Effect of junction position on pressure phase $\angle P_1$

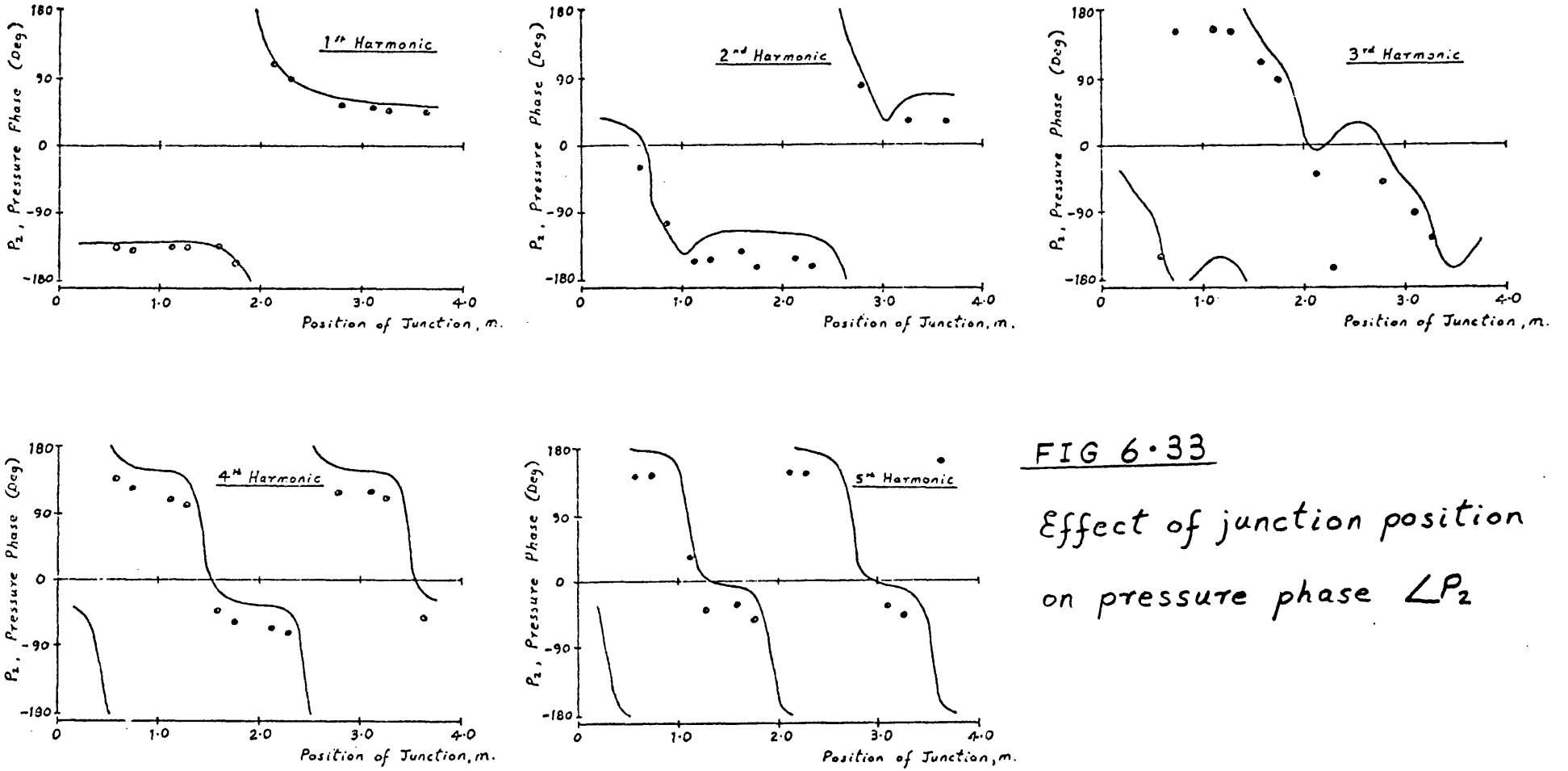

FIG 6·33

Effect of junction position on pressure phase $\angle P_2$

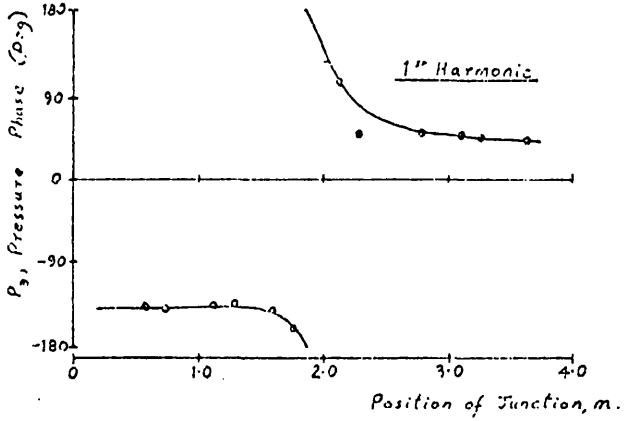

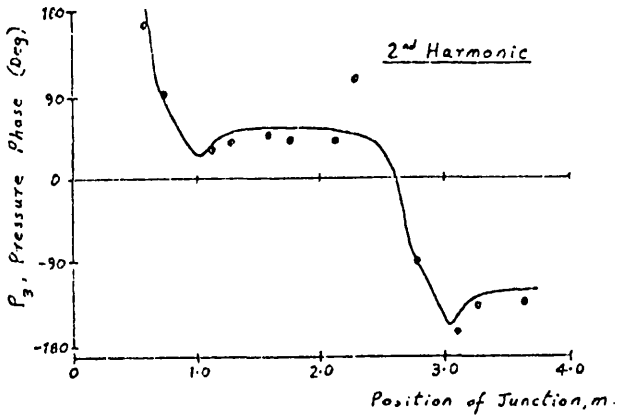

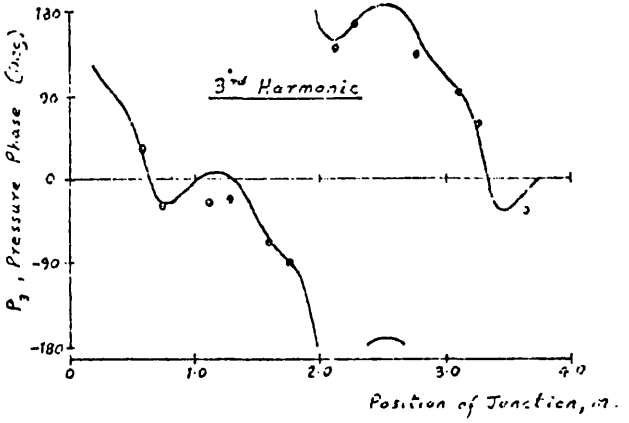

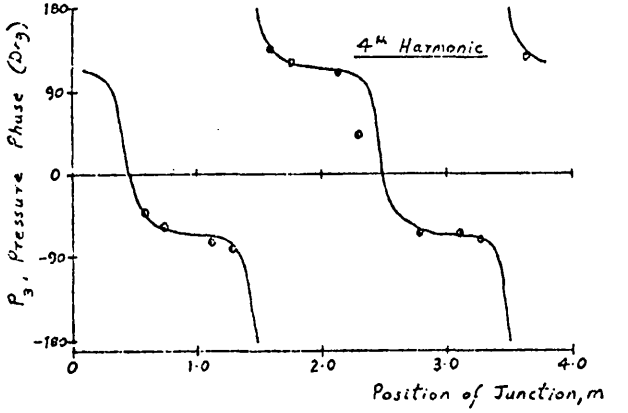

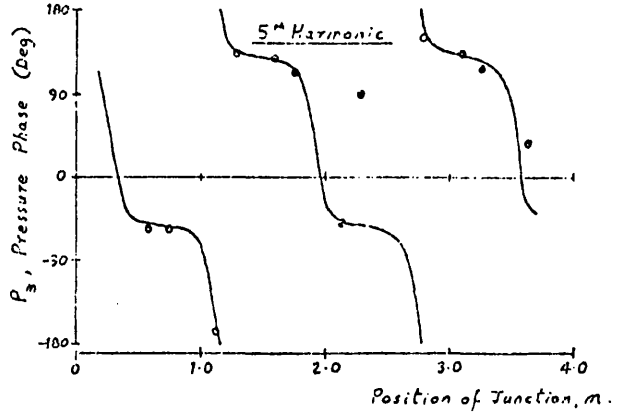

FIG 6·34

Effect of junction position on pressure phase $\angle P_3$

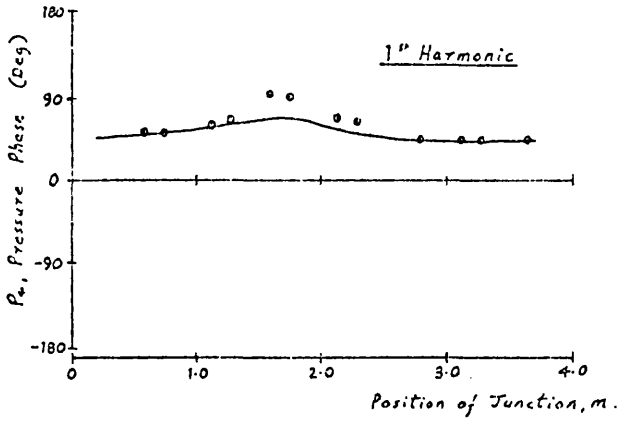

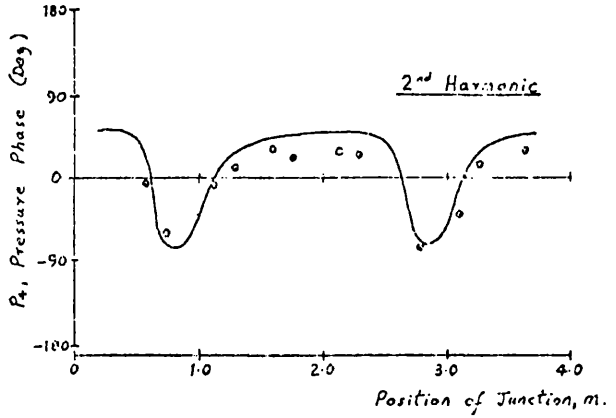

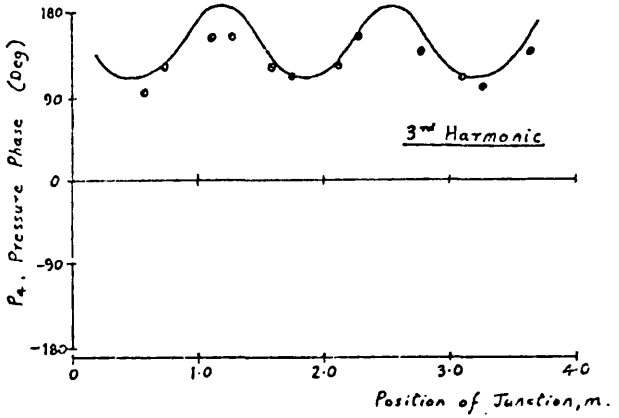

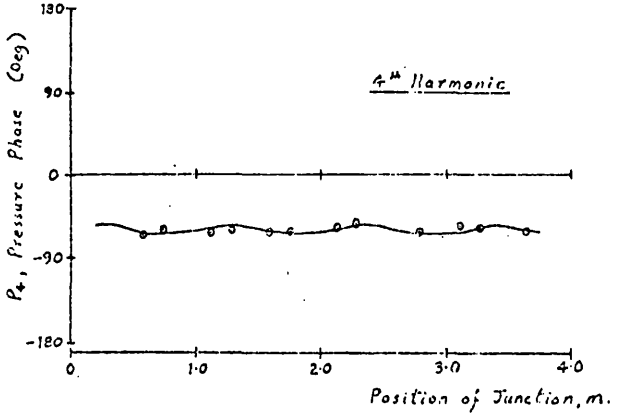

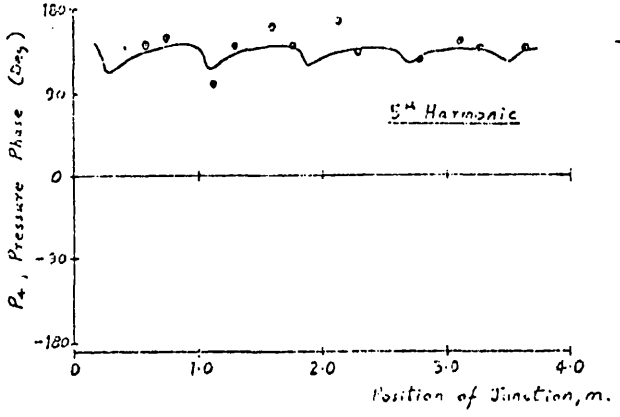

FIG 6·35

Effect of junction position on pressure phase $\angle P_4$

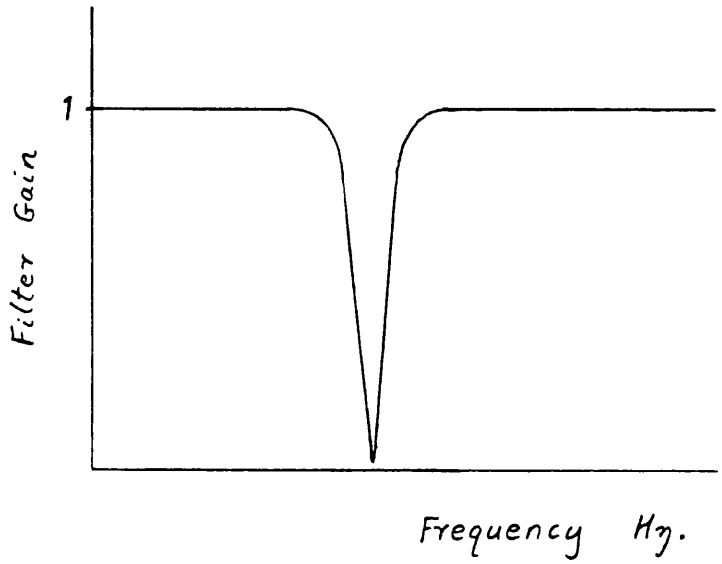

FIG 6·36 Characteristics of a Notch Filter

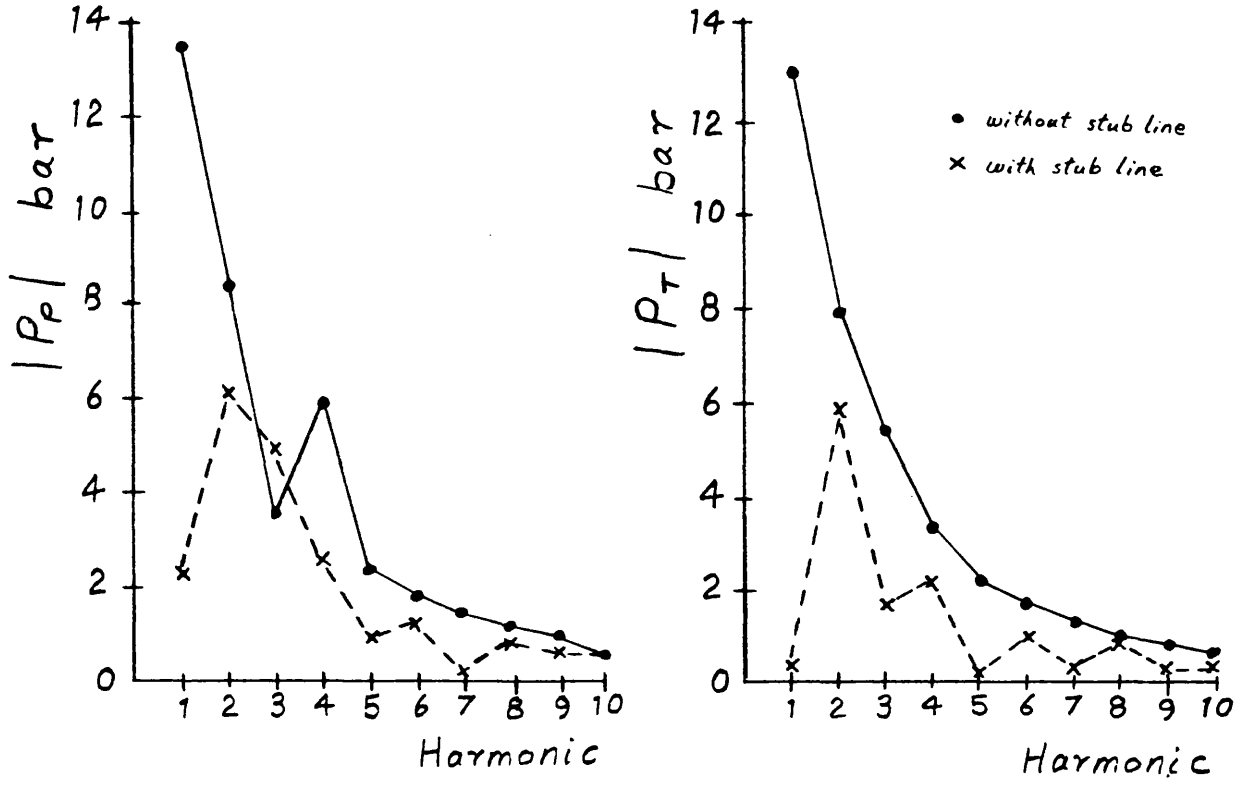

FIG 6·37 Addition of a stub line to a simple system with a pipeline 1·76 m.

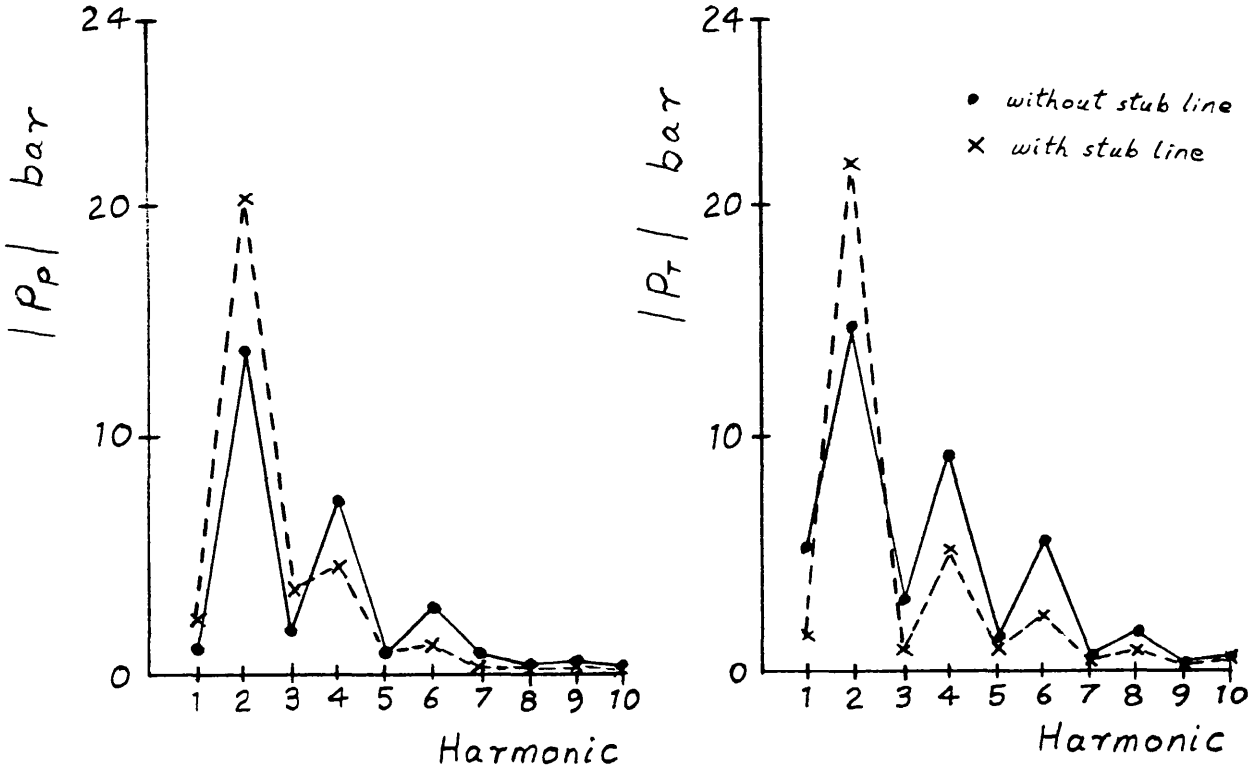

FIG 6·38 Addition of a stubline to a simple system with a pipeline 3·94 m.

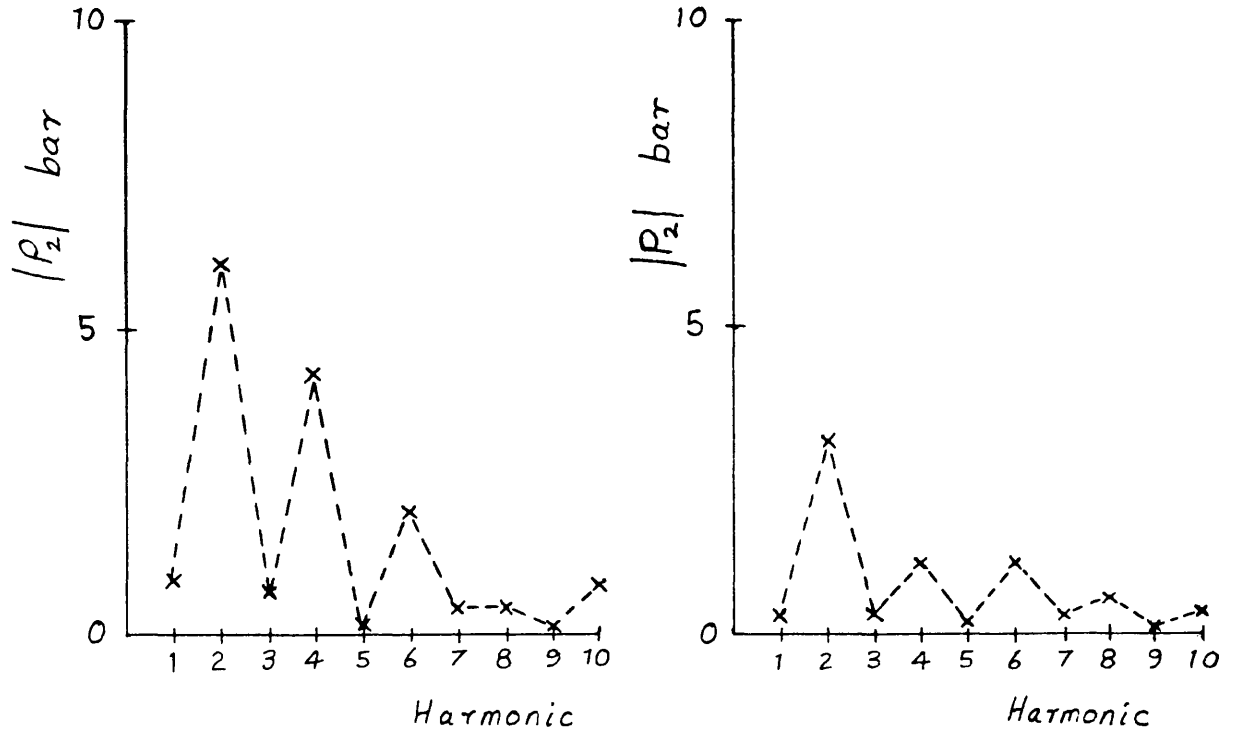

FIG 6·39 Effect of a stub line on the pressures at the junction.

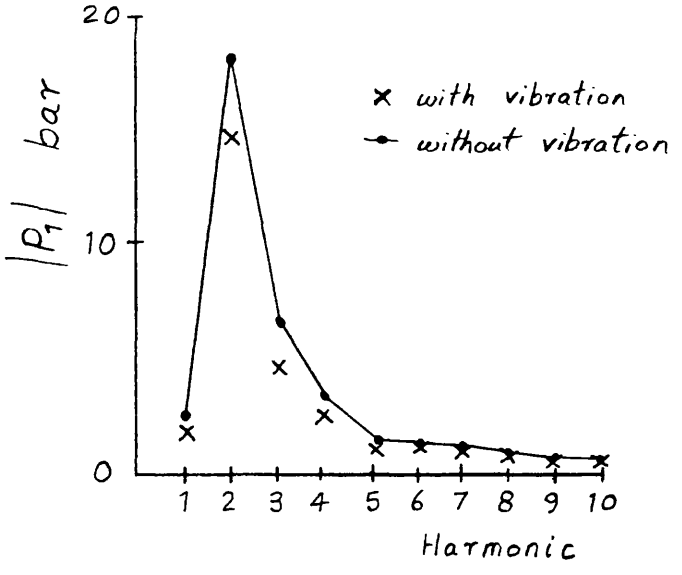

FIG 6·40 Effect of pipe vibration on pressure amplitude, $|P_1|$

× Results obtained with first test circuit FIG 6·6

• Results obtained with second test circuit FIG 6·7

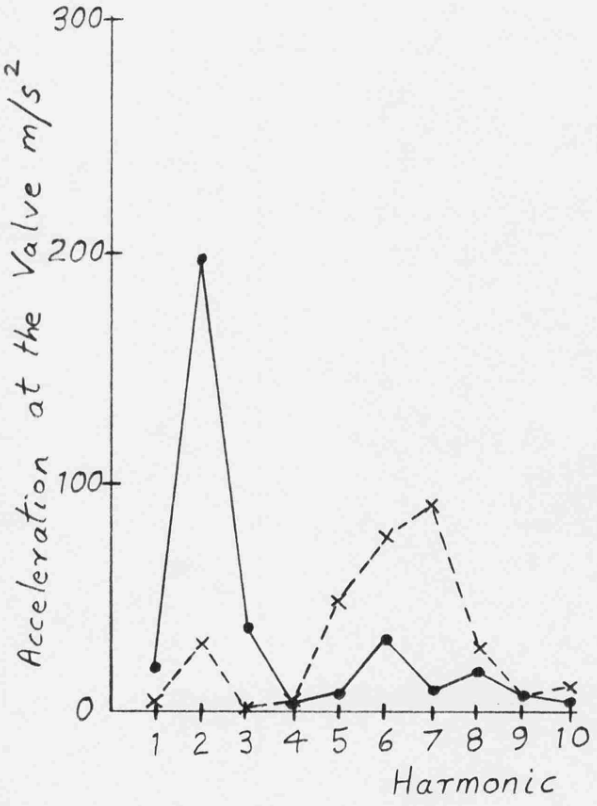

FIG 6·41 Vibration at the valve.

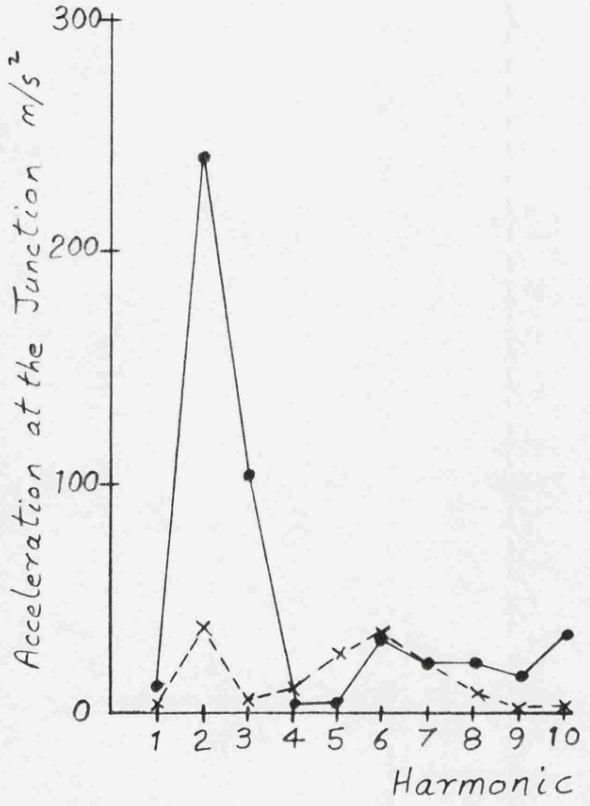

FIG 6·42 Vibration at the junction.

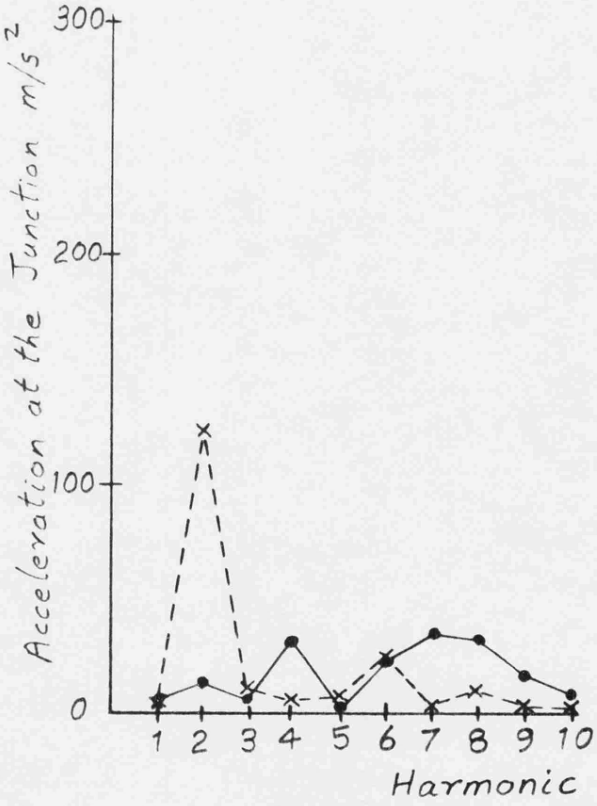

FIG 6·43 Vibration at the junction when clamped to a large mass.

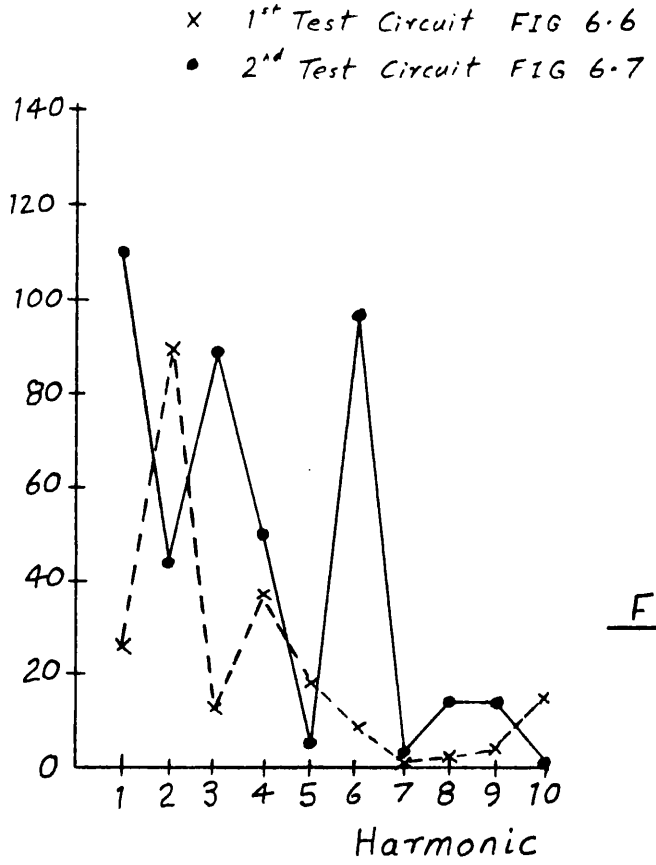

FIG 6·44 Pressure forces generated in the branch line.

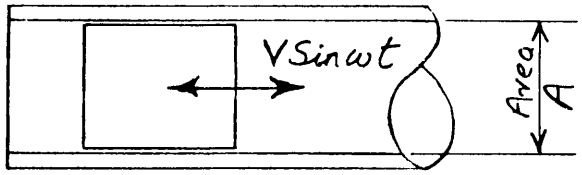

$Q_v = A \cdot V \sin \omega t$

FIG 6·45 Flow generation by the vibration of the valve.

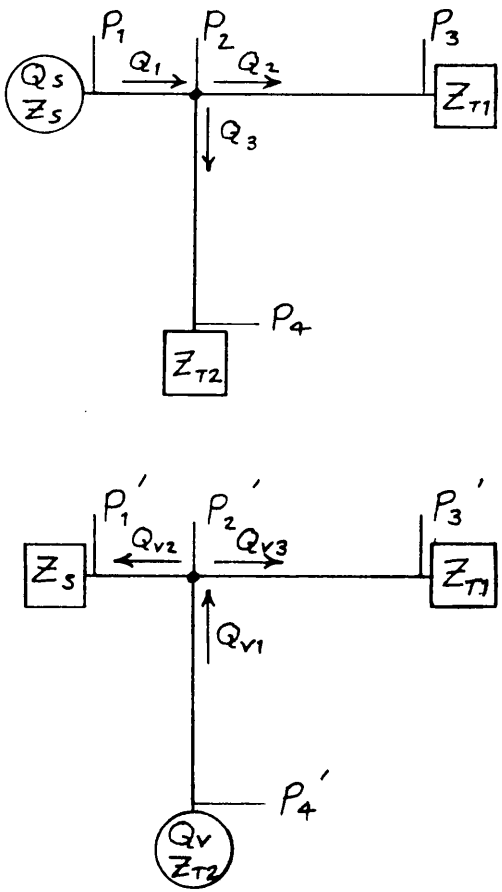

FIG 6·46 Impedance representation of two superimposed flow systems.

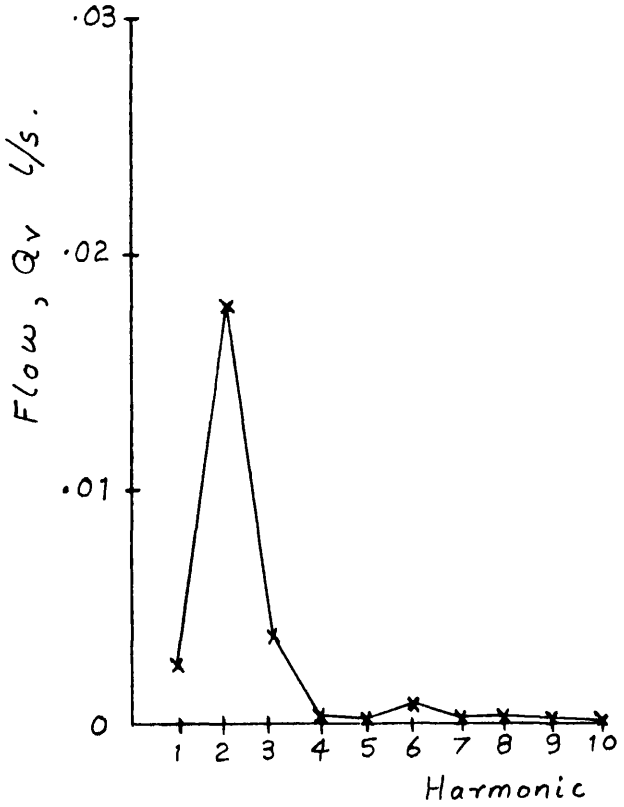

FIG 6·47 Apparent flow generated at the valve

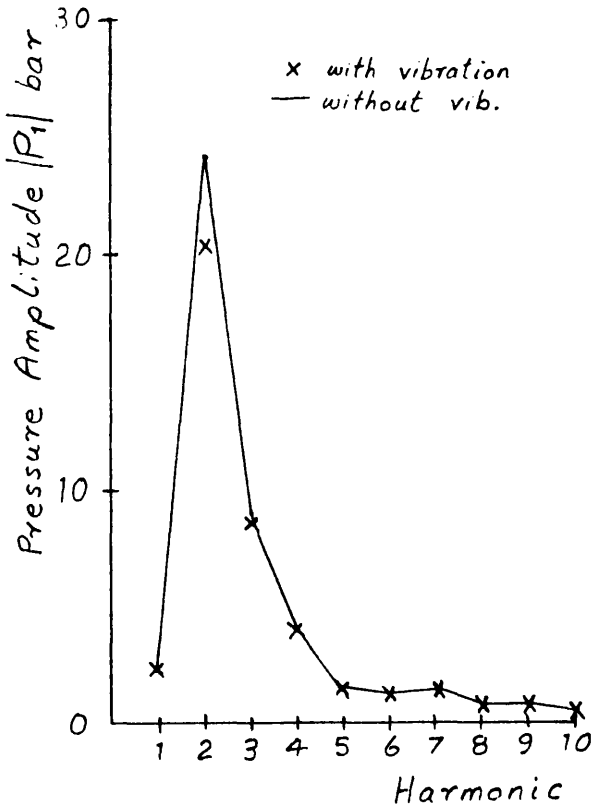

FIG 6·48 Predicted Pressure amplitudes at P_1 including the effects of vibration.

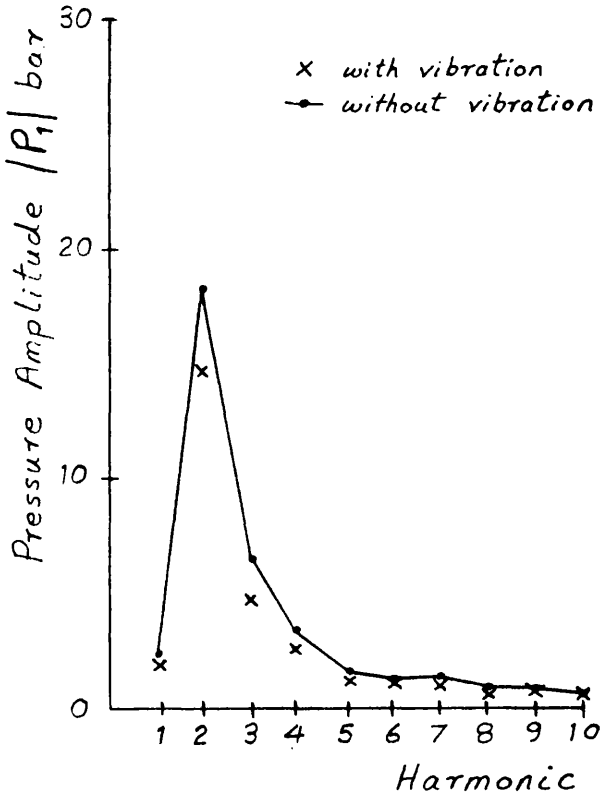

FIG 6·49 Pressure amplitude $|P_1|$ recorded with and without pipe vibration.

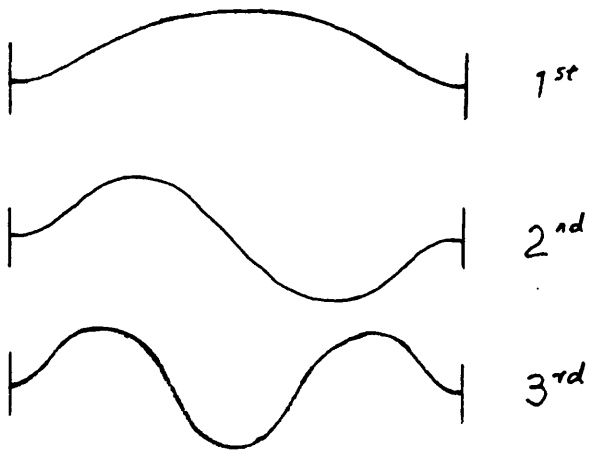

FIG 6·50 Modes of pipe vibration (Clamped Ends)

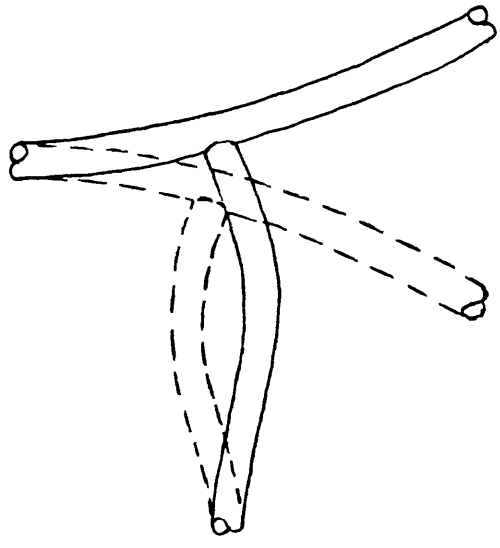

FIG 6·51 Bending modes at the junction.

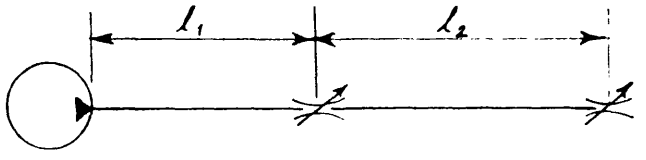

FIG 7·1 A Simple Hydraulic System with Impedances in Series

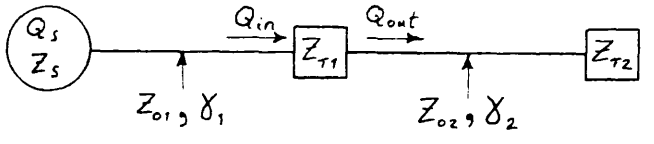

FIG 7·2 Impedance Representation of a Series Impedance System

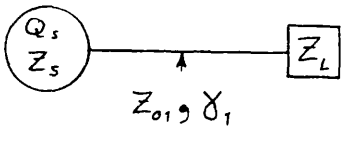

FIG 7·3 Equivalent Circuit Model

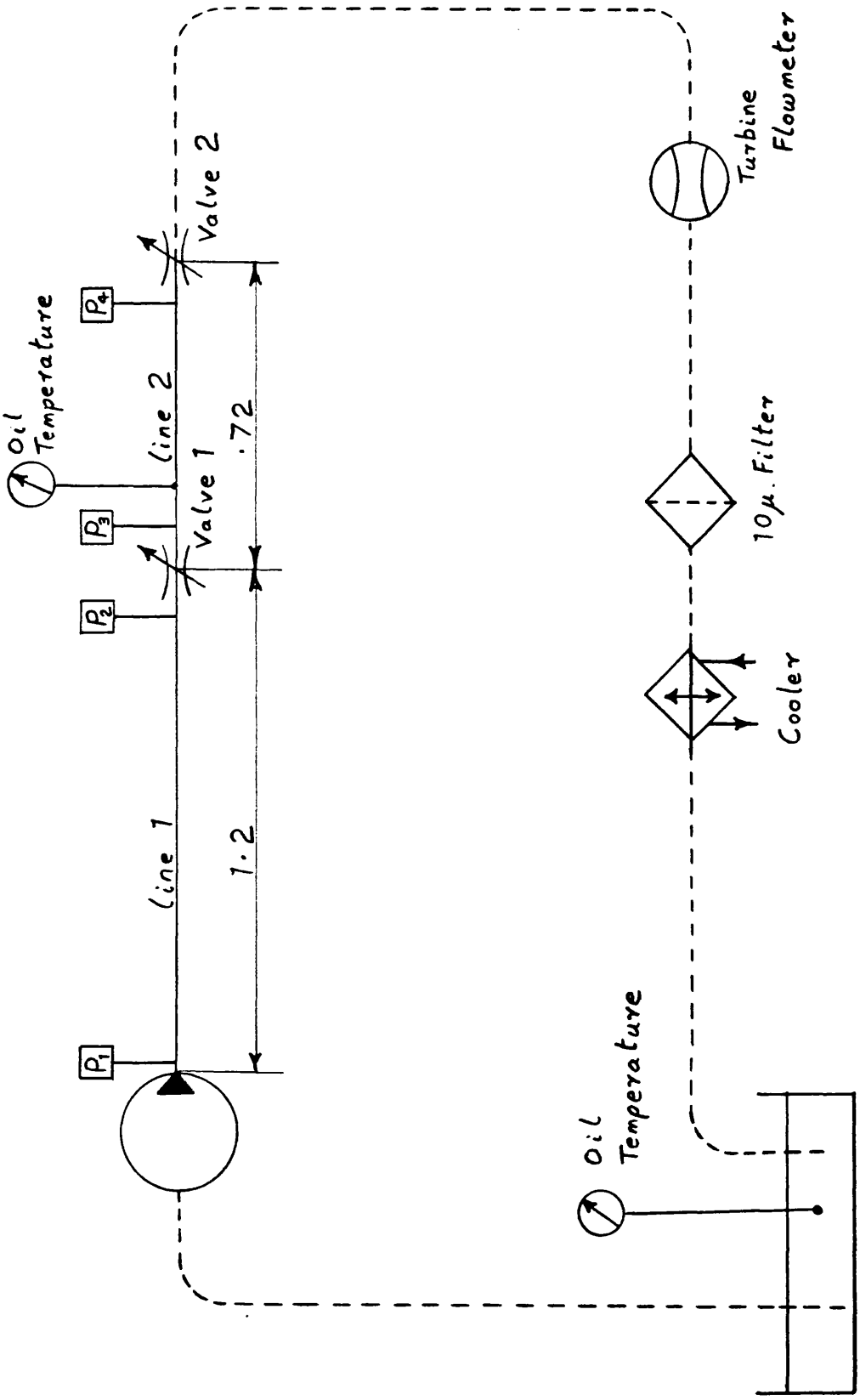

FIG 7.4 Line Diagram of Test Circuit.

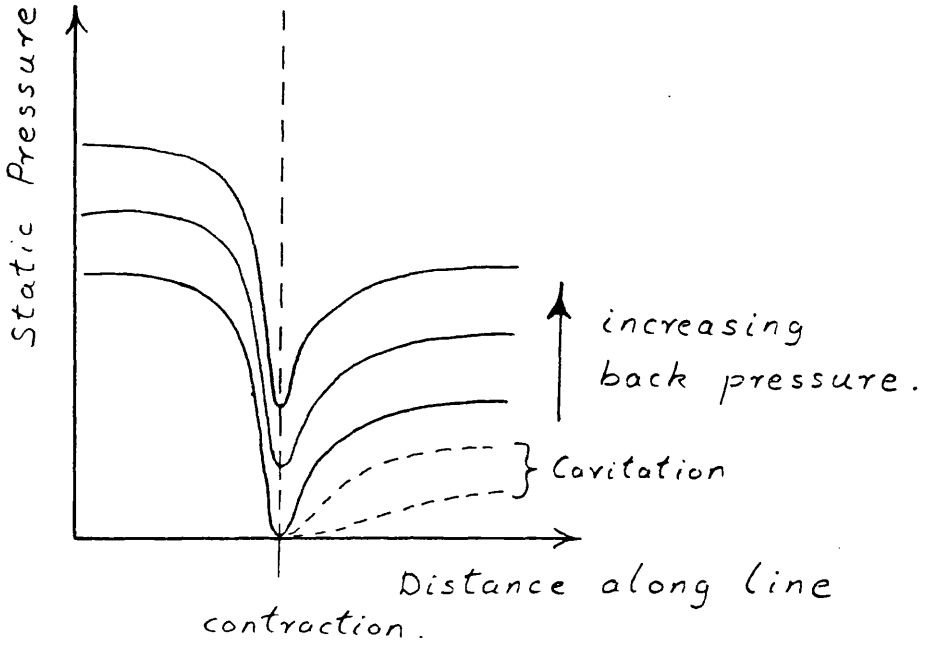

FIG 7·5 Effect of back pressure on cavitation.
(Taken from ref. [24])

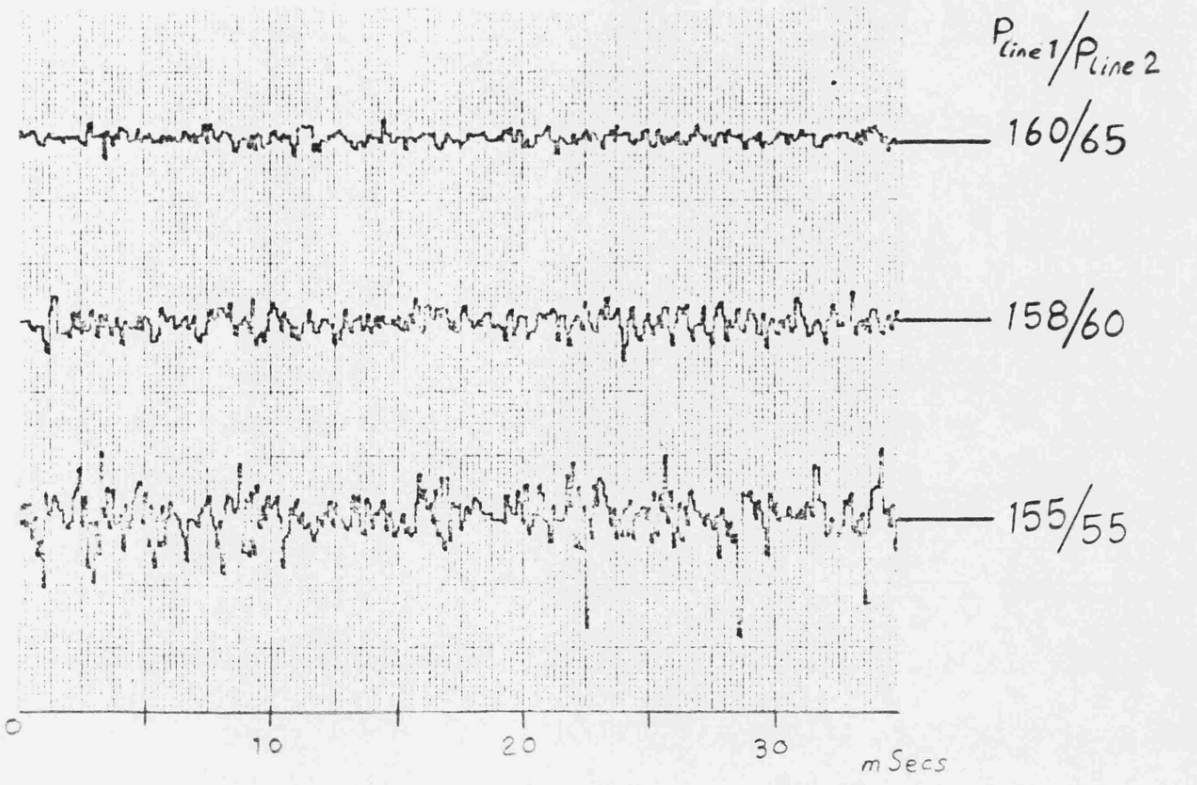

FIG 7·6 Variation in acceleration levels with back pressure

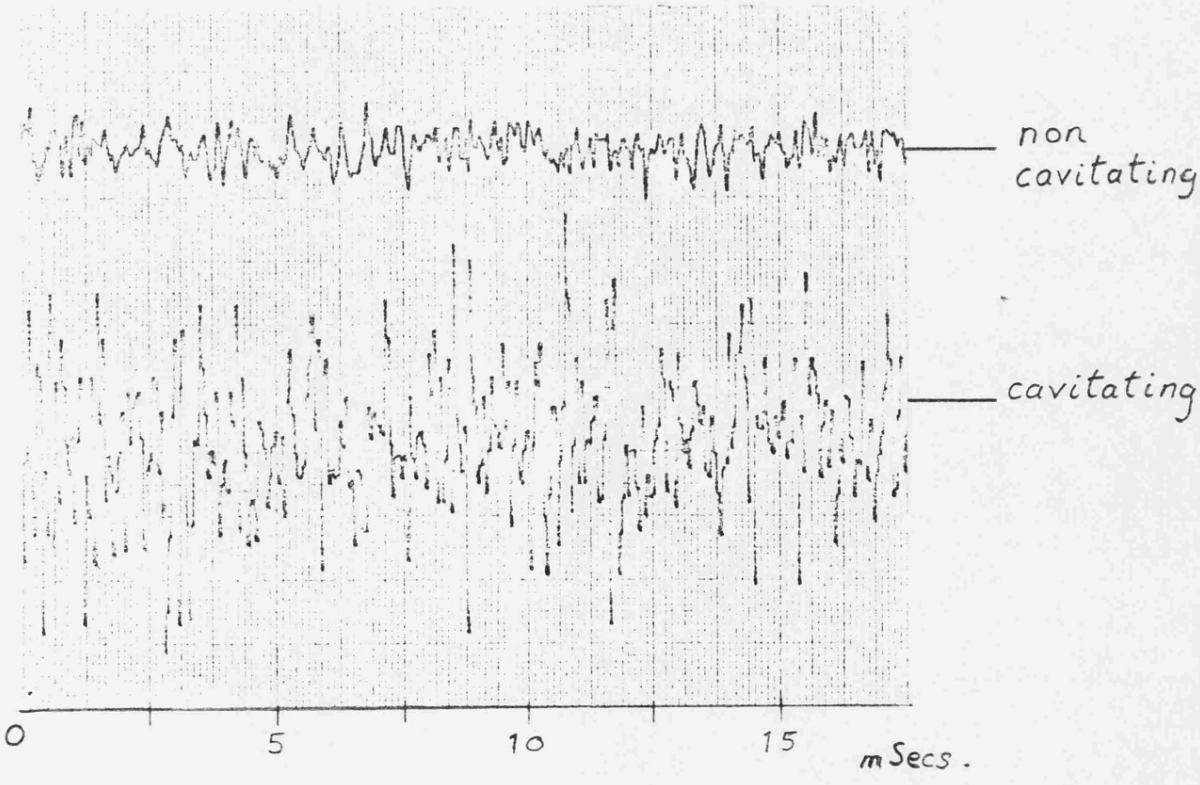

FIG 7·7 Acceleration levels for cavitating and non cavitating conditions.

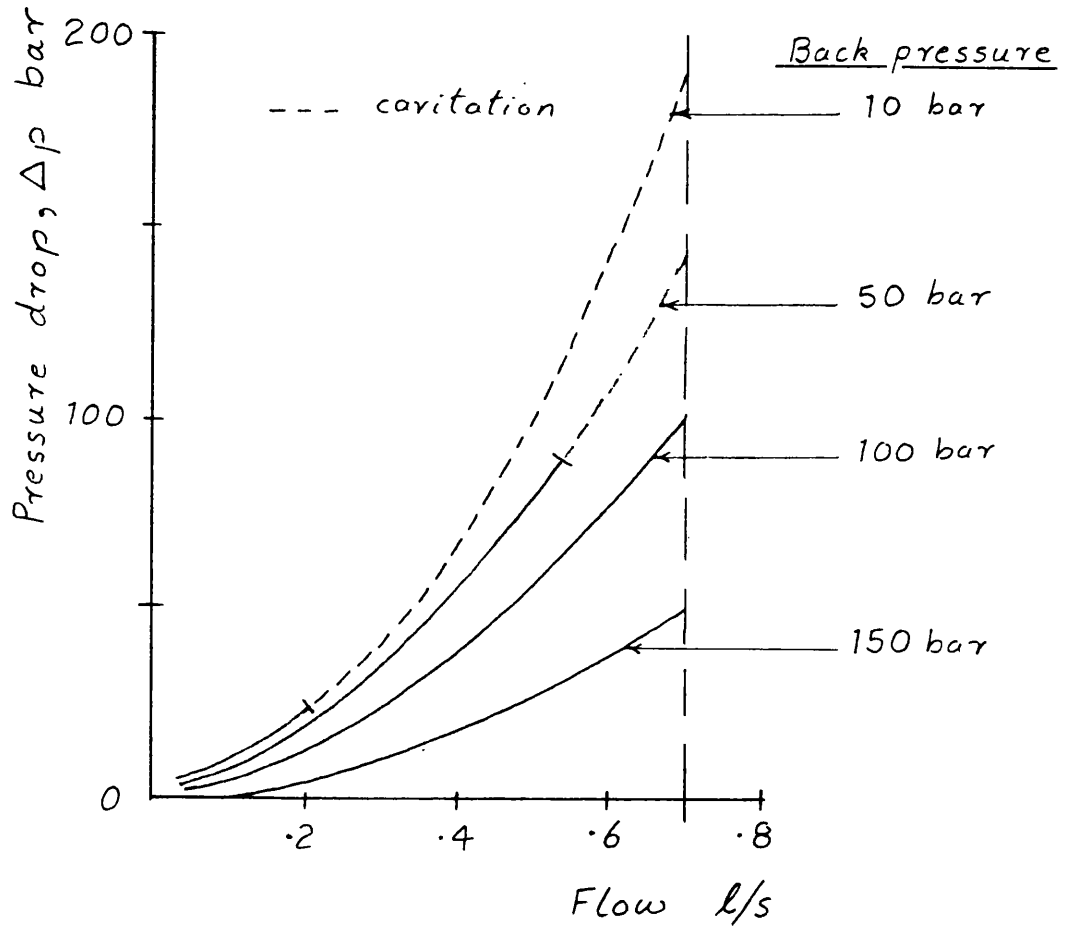

FIG 7·8 Valve pressure - flow characteristics with constont back pressure levels.

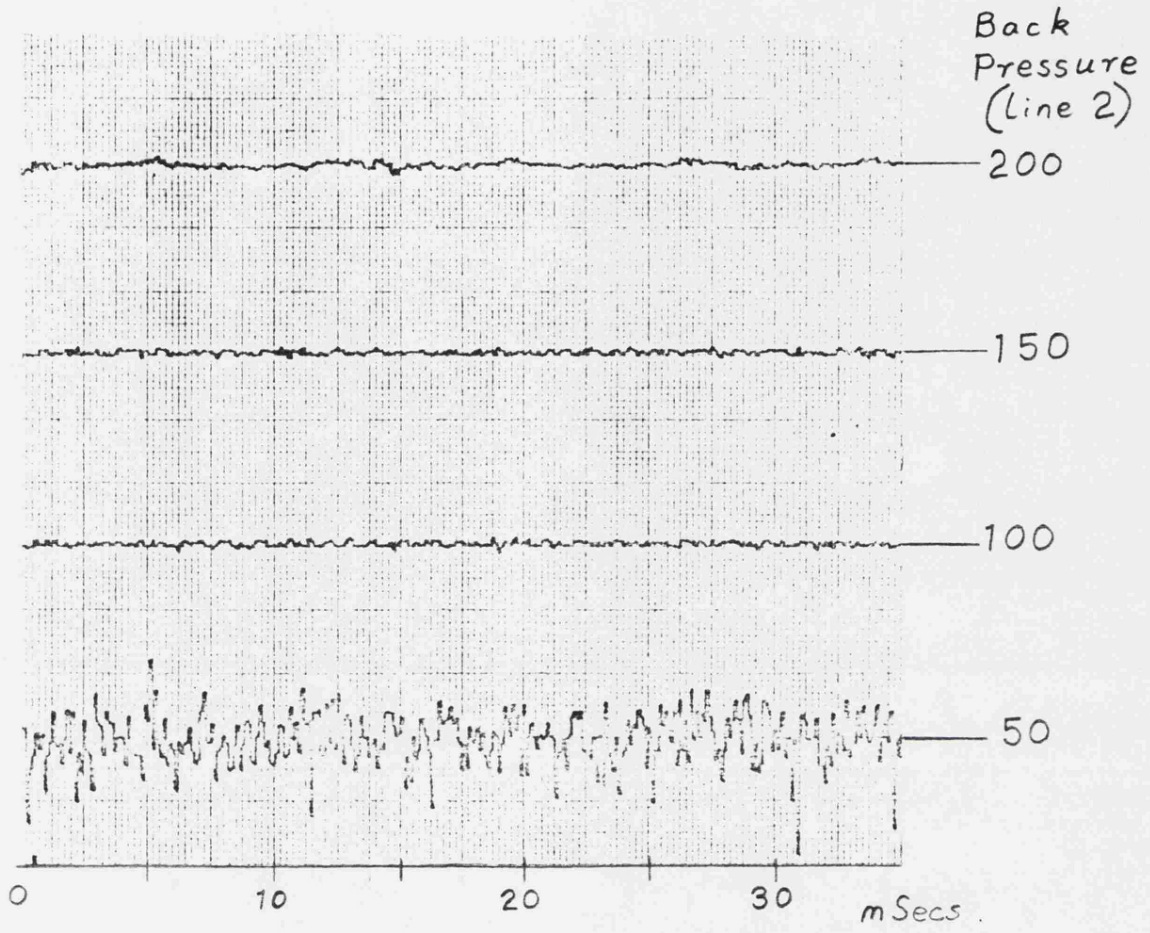

FIG 7·9 Valve acceleration levels at each test condition.

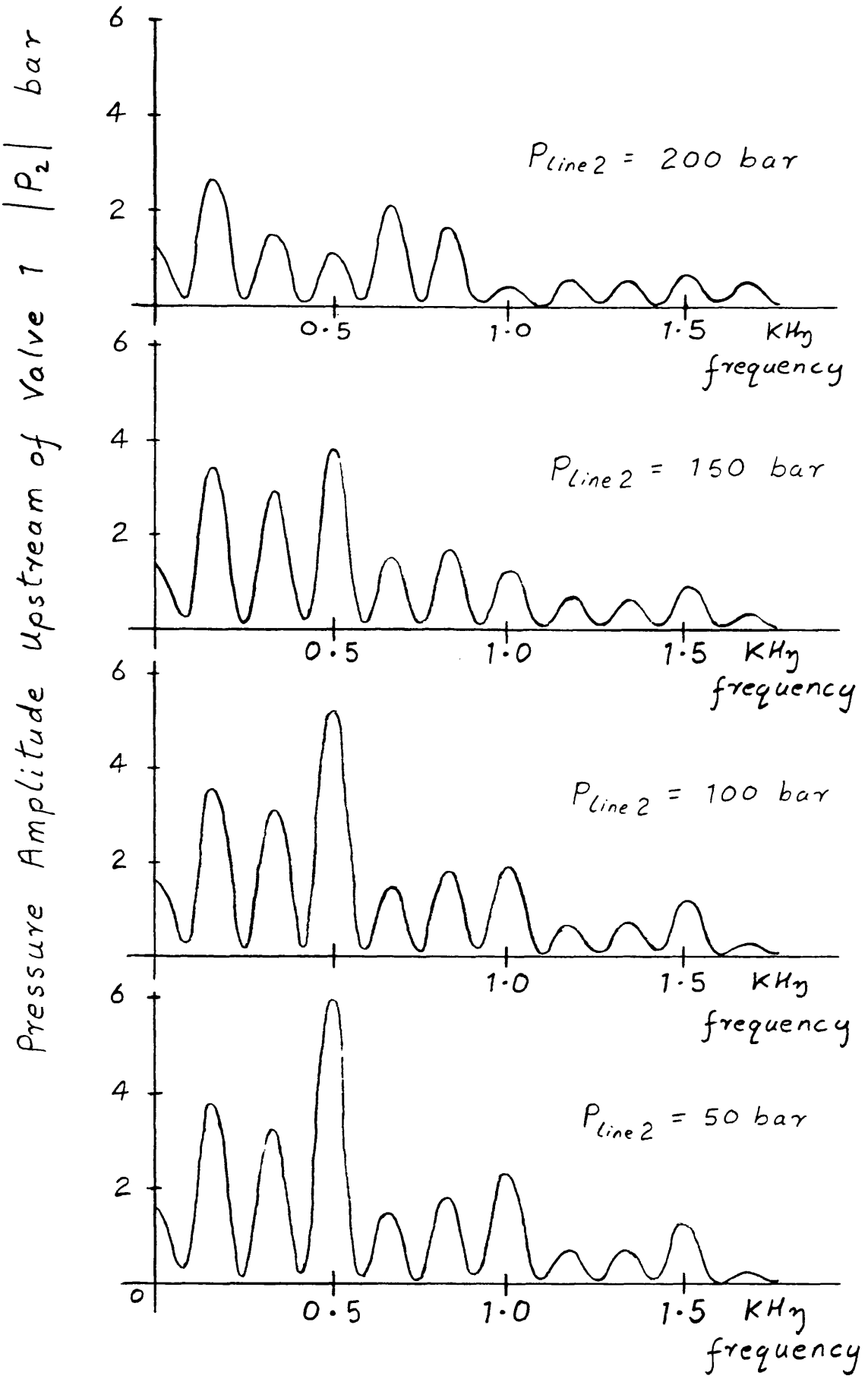

FIG 7·10 Pressure amplitudes upstream $|P_2|$ and downstream $|P_3|$ of valve 1.

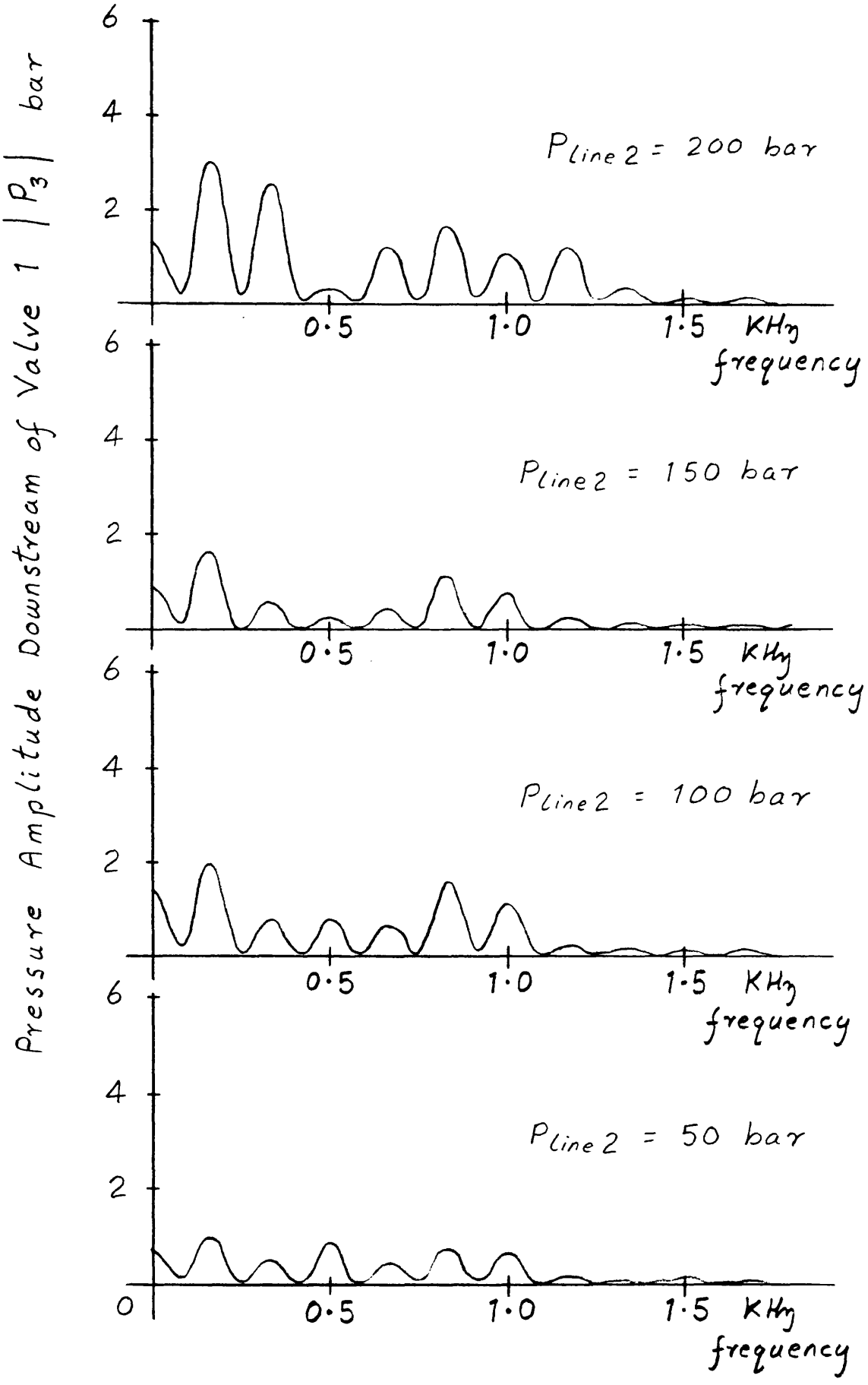

FIG 7·10 Continued.

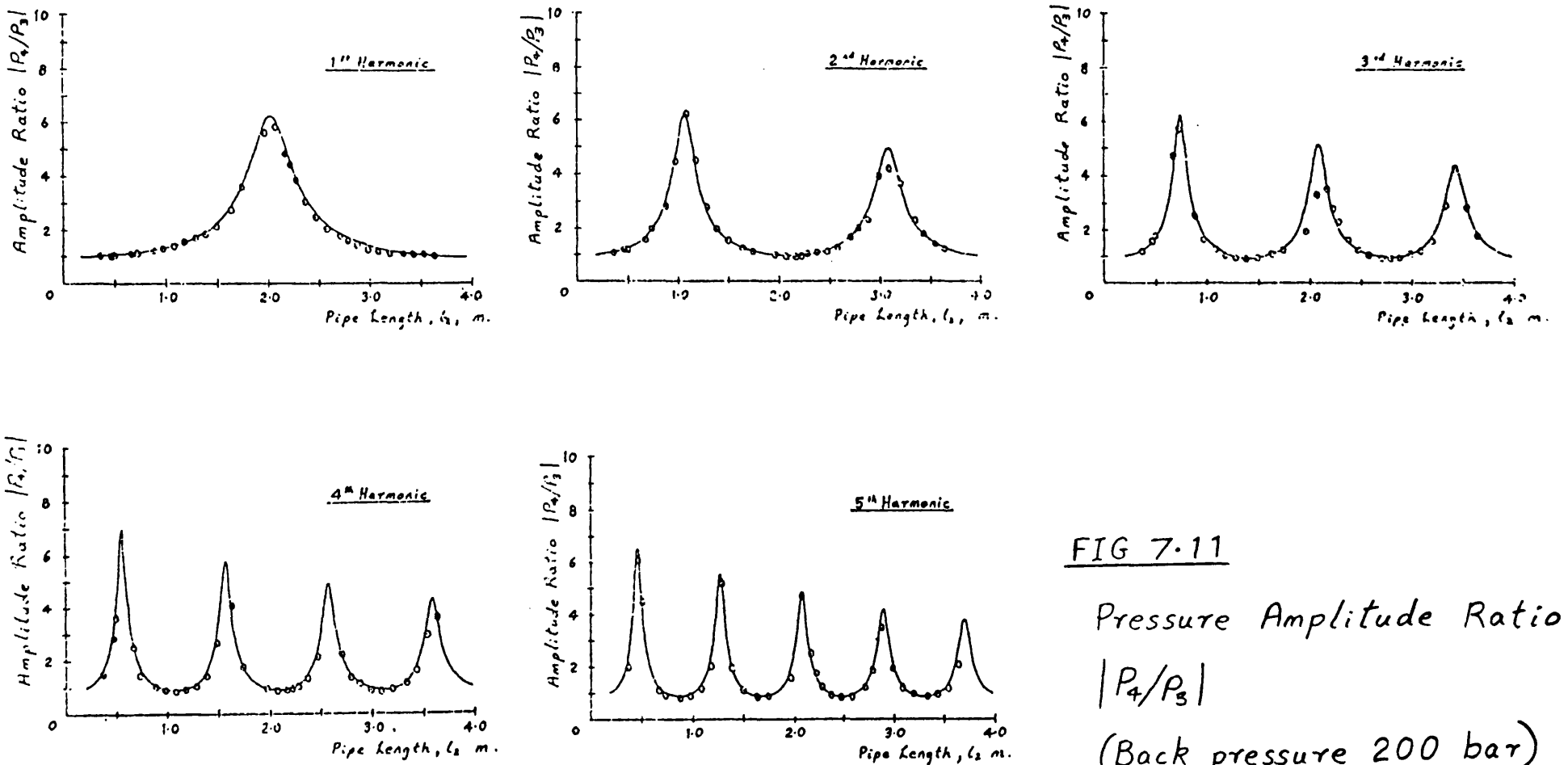

FIG 7·11

Pressure Amplitude Ratio $|P_4/P_3|$

(Back pressure 200 bar)

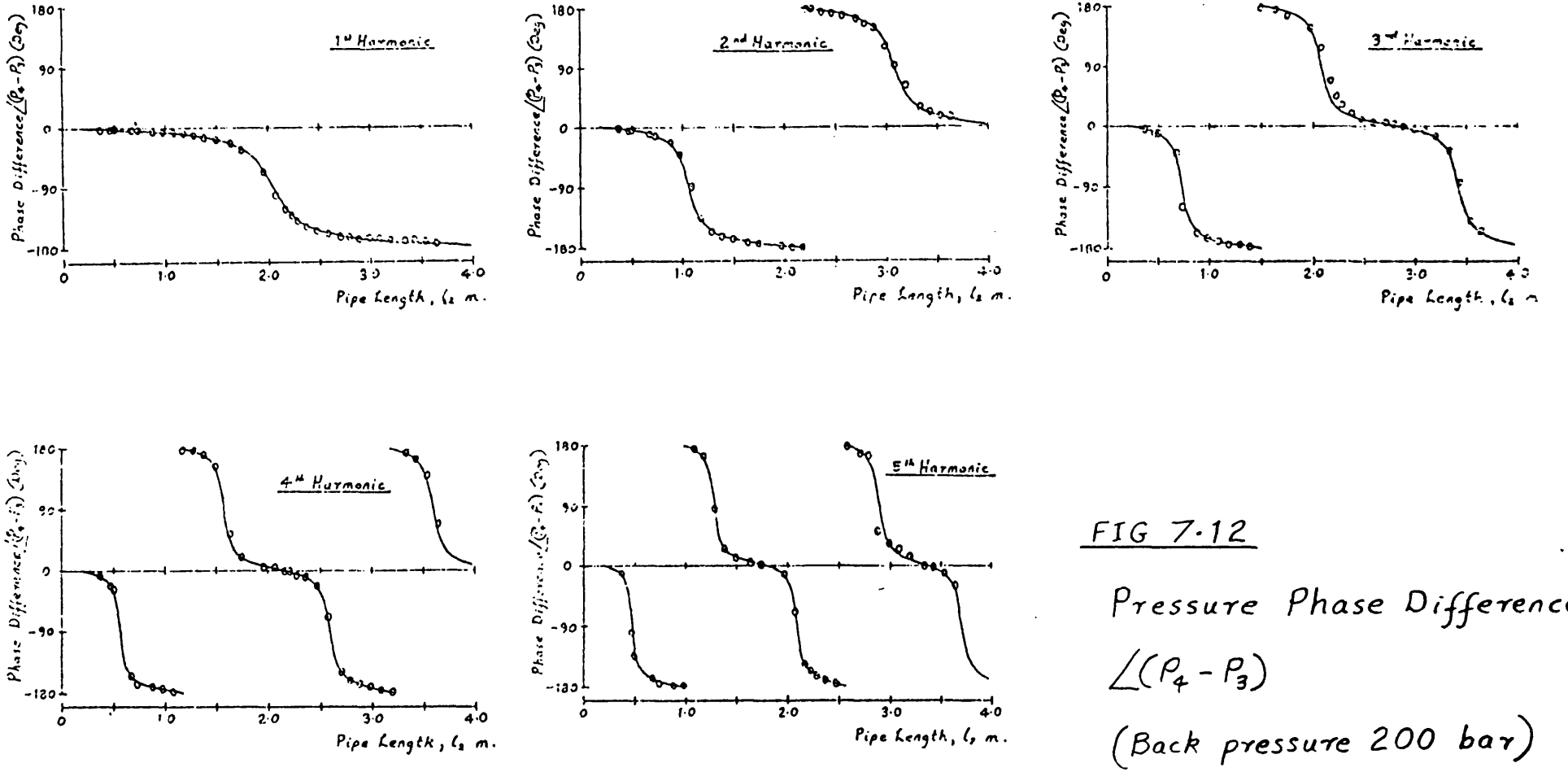

FIG 7·12

Pressure Phase Difference

$\angle(P_4 - P_3)$

(Back pressure 200 bar)

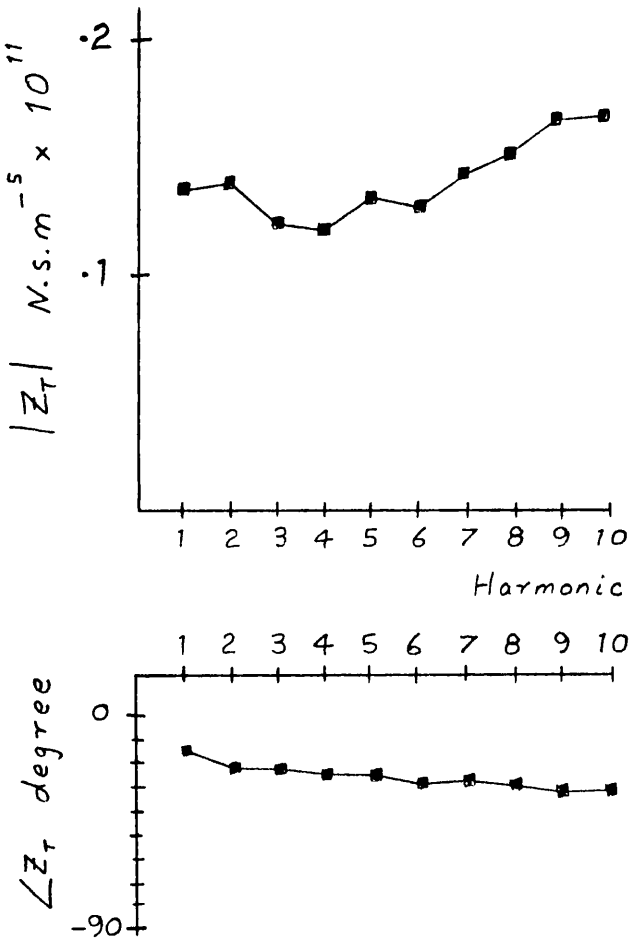

FIG 7·13 Valve impedance spectrum.

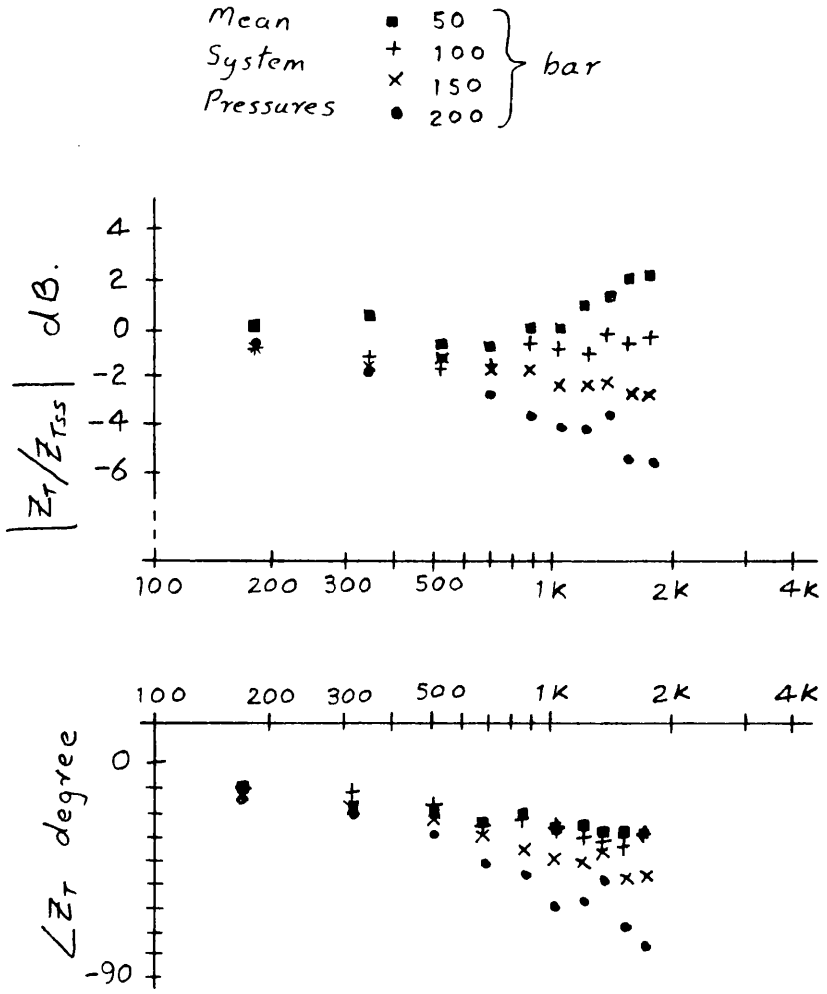

FIG 7·14 Valve impedance variation with frequency and setting.

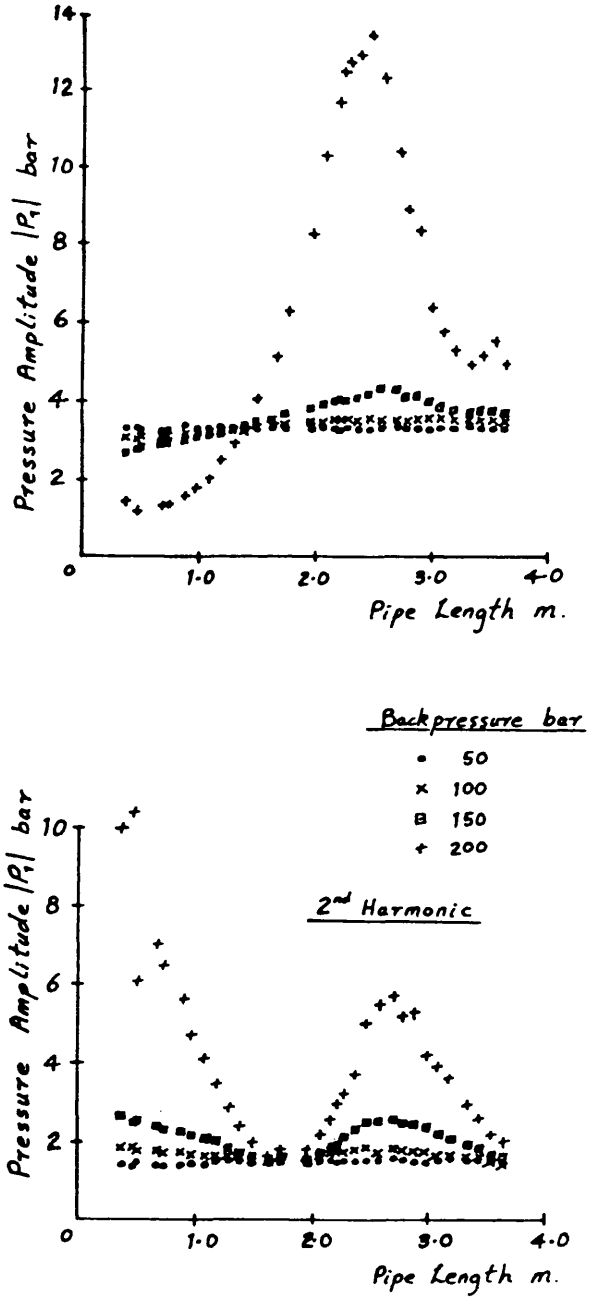

FIG 7·15 Pressure Amplitudes at the Pump $|P_1|$, variation with Back Pressure.

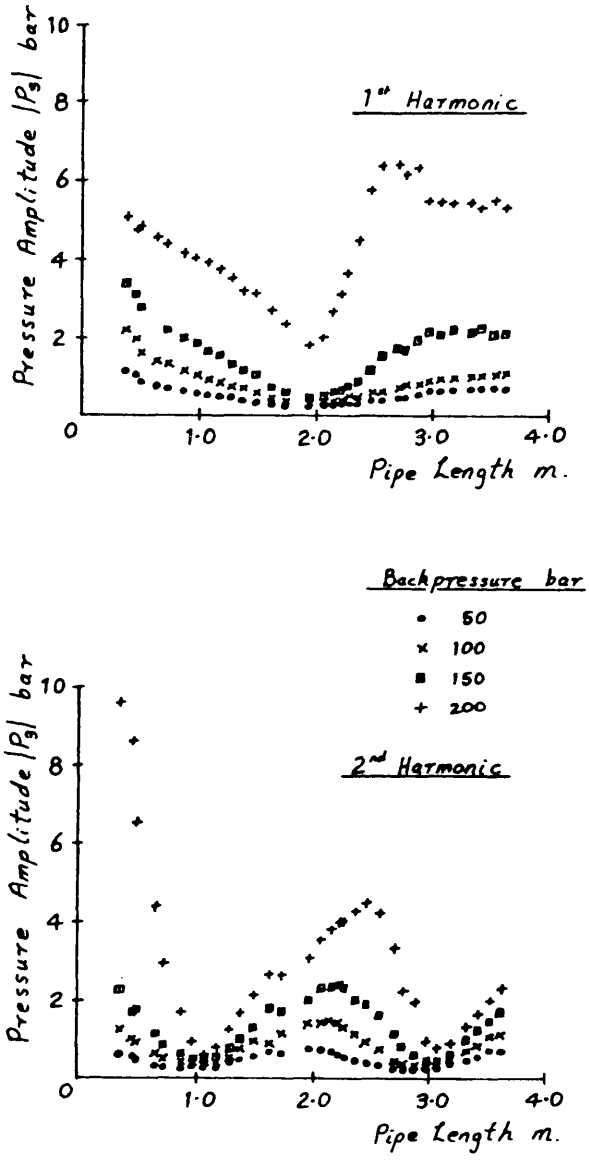

FIG 7·16 Pressure Amplitudes Downstream of Valve 1, $|P_3|$, variation with System Pressure and Line Length, ℓ_2.

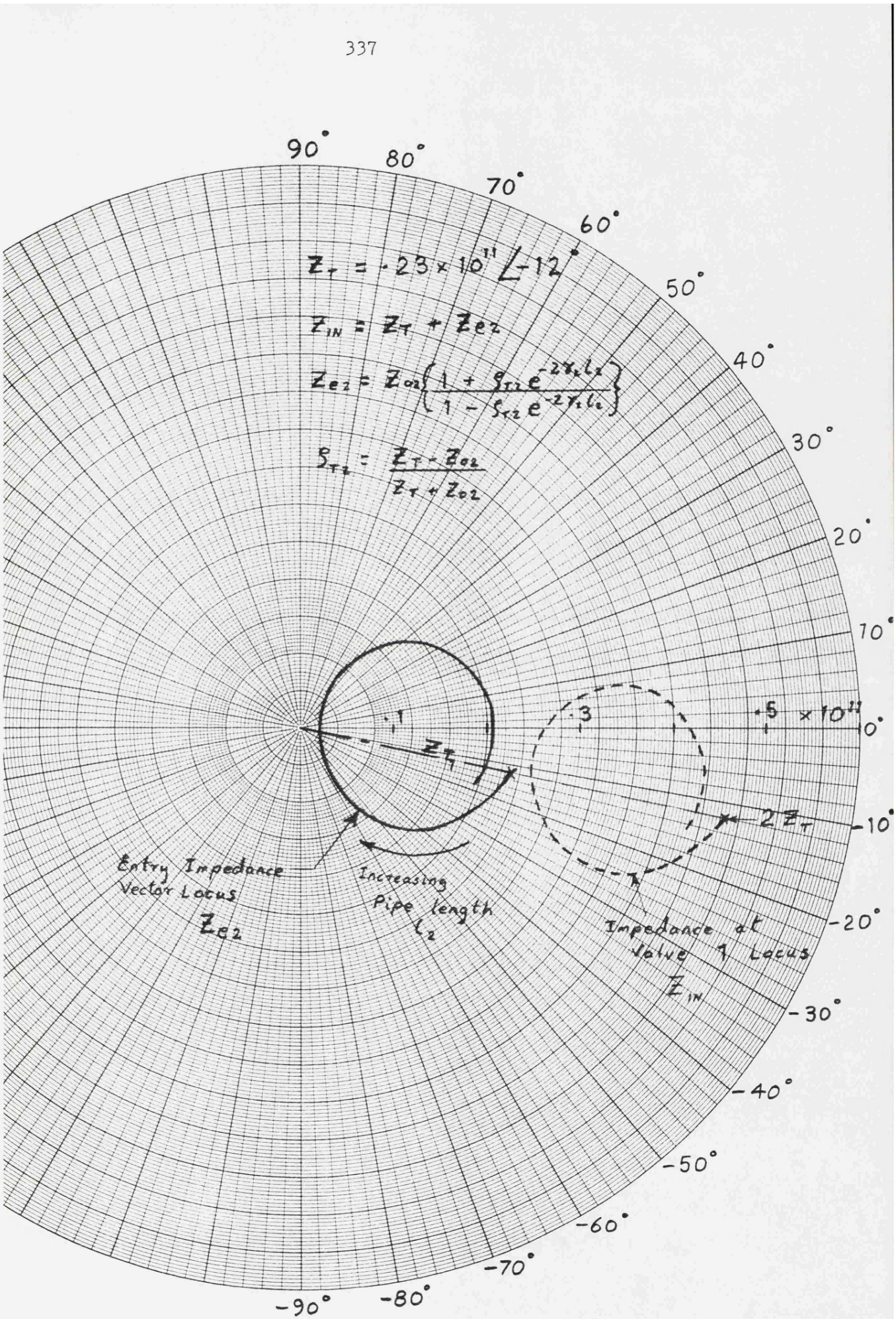

FIG 7·17 Graphical evaluation of the lumped impedance, Z_{IN}.

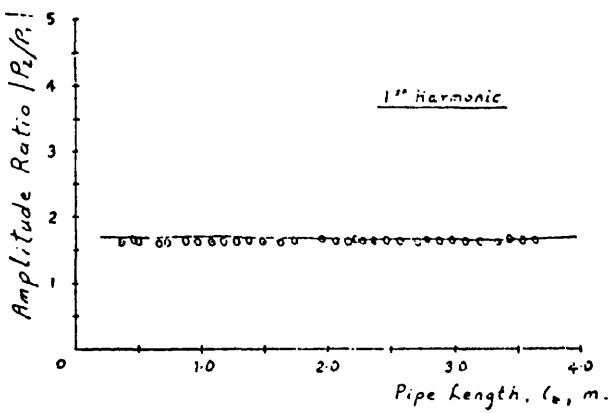

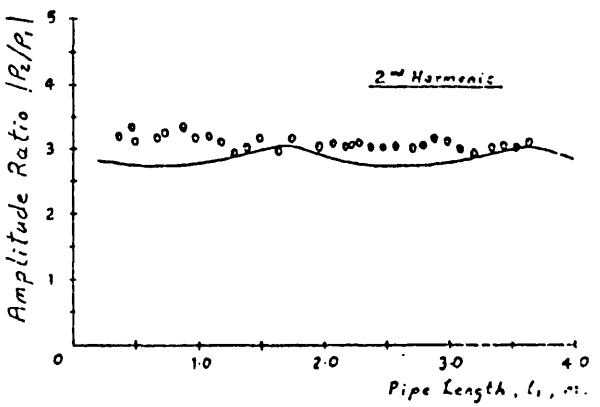

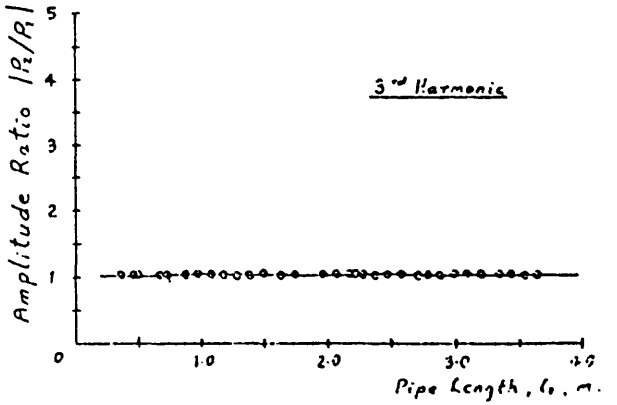

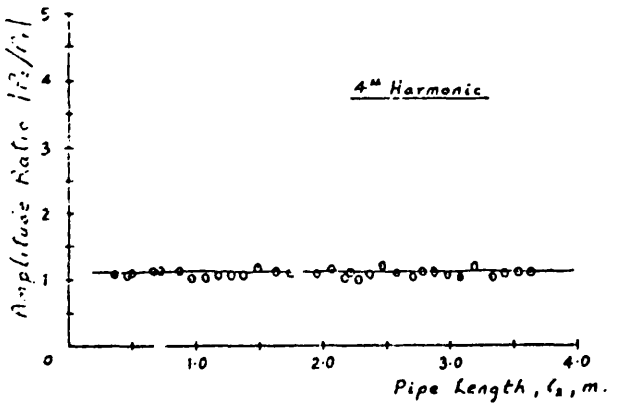

FIG 7·18

Pressure Amplitude Ratio

$|P_2/P_1|$

(Back pressure 50 bar)

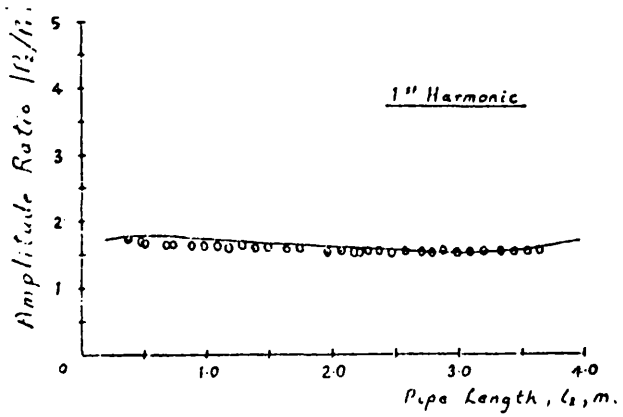

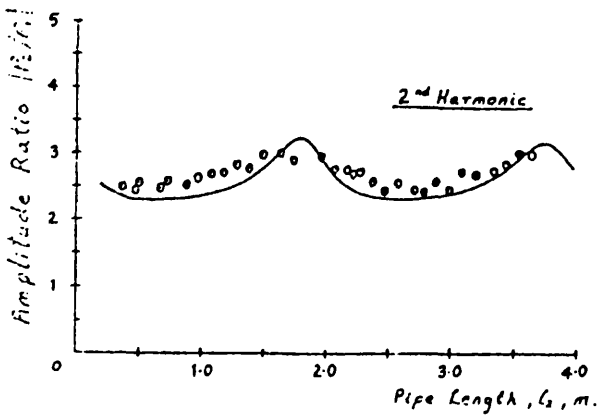

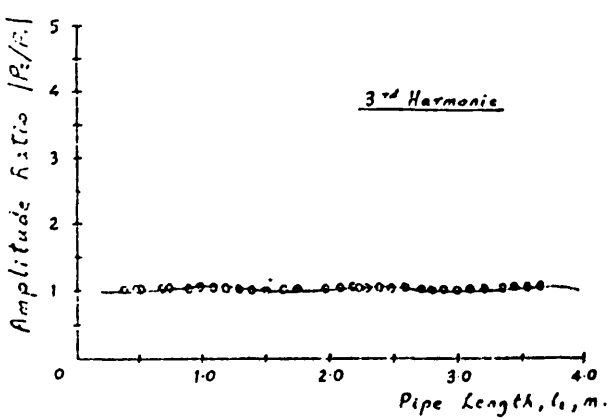

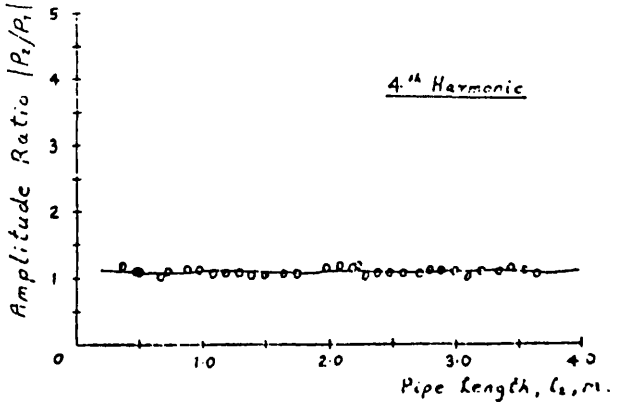

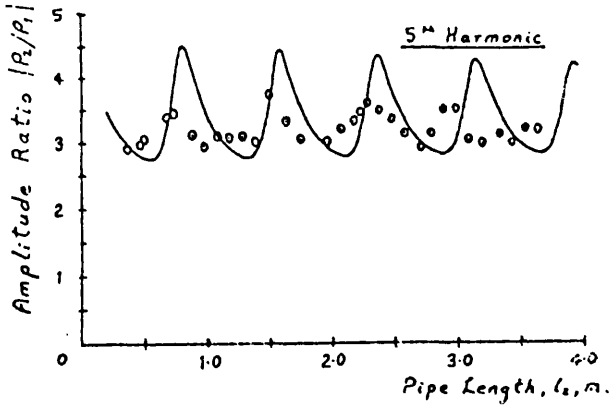

FIG 7·19

Pressure Amplitude Ratio

$|P_2/P_1|$

(Back pressure 100 bar)

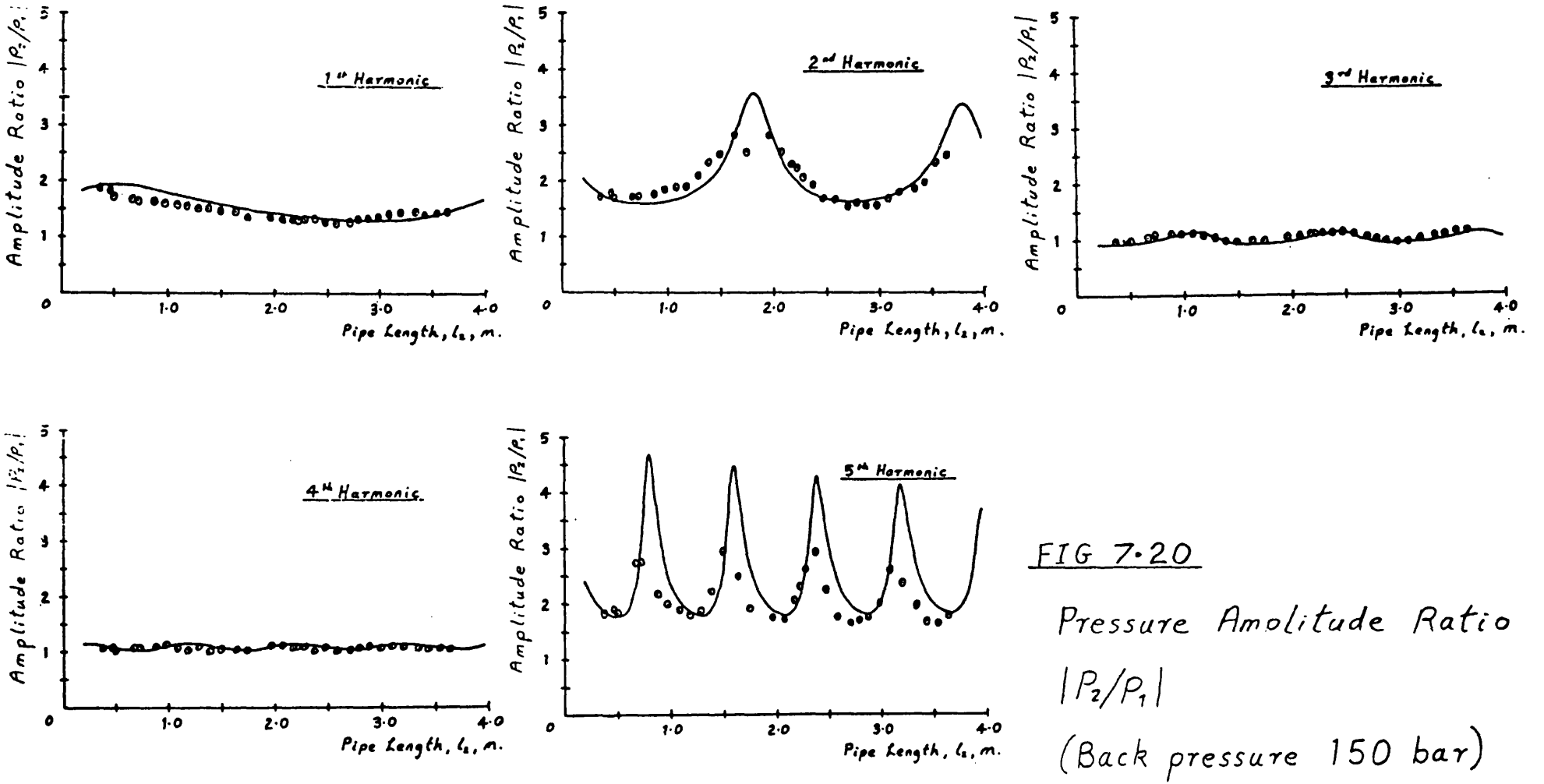

FIG 7·20

Pressure Amolitude Ratio

$|P_2/P_1|$

(Back pressure 150 bar)

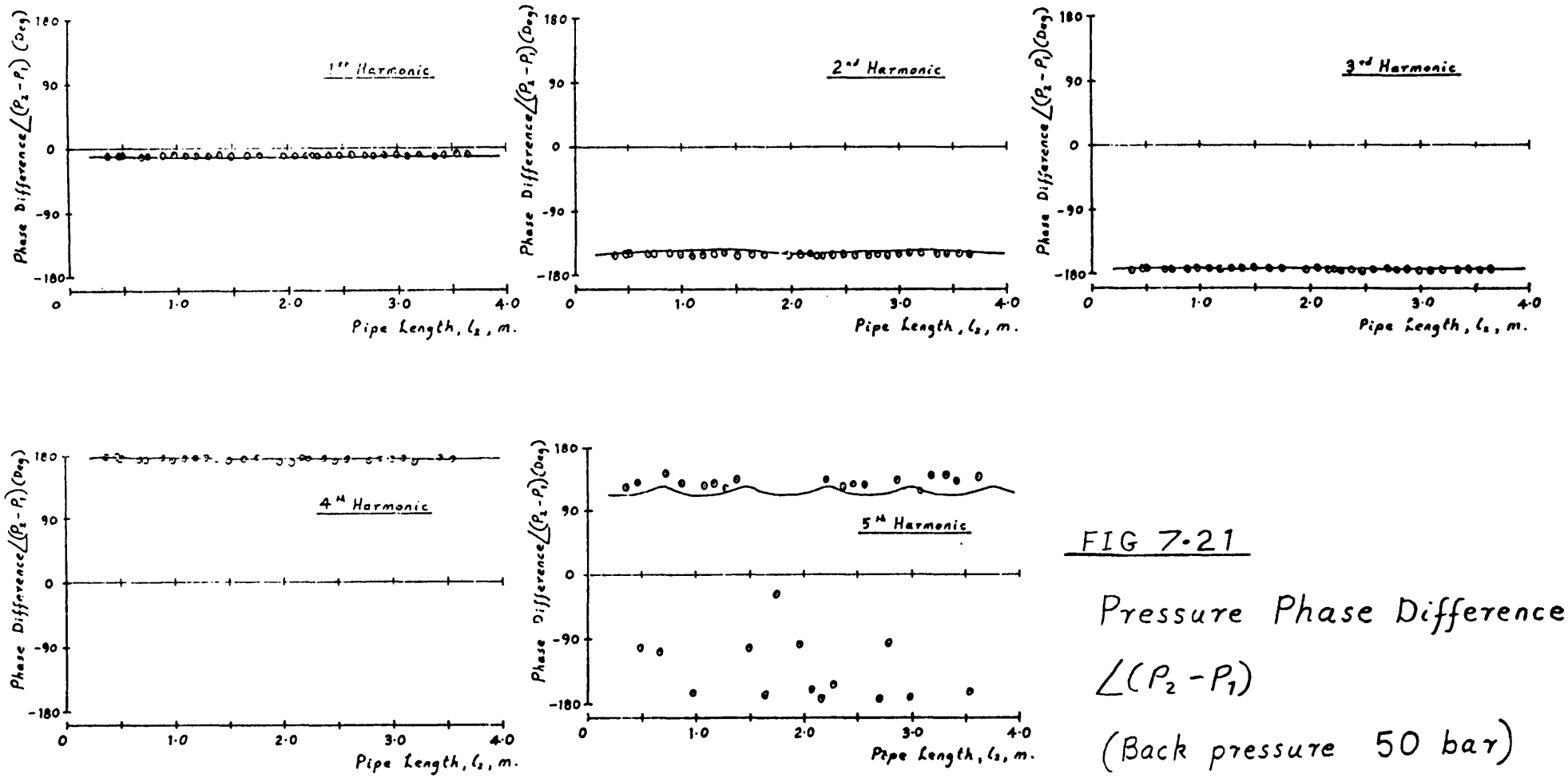

FIG 7·21

Pressure Phase Difference

$\angle(P_2 - P_1)$

(Back pressure 50 bar)

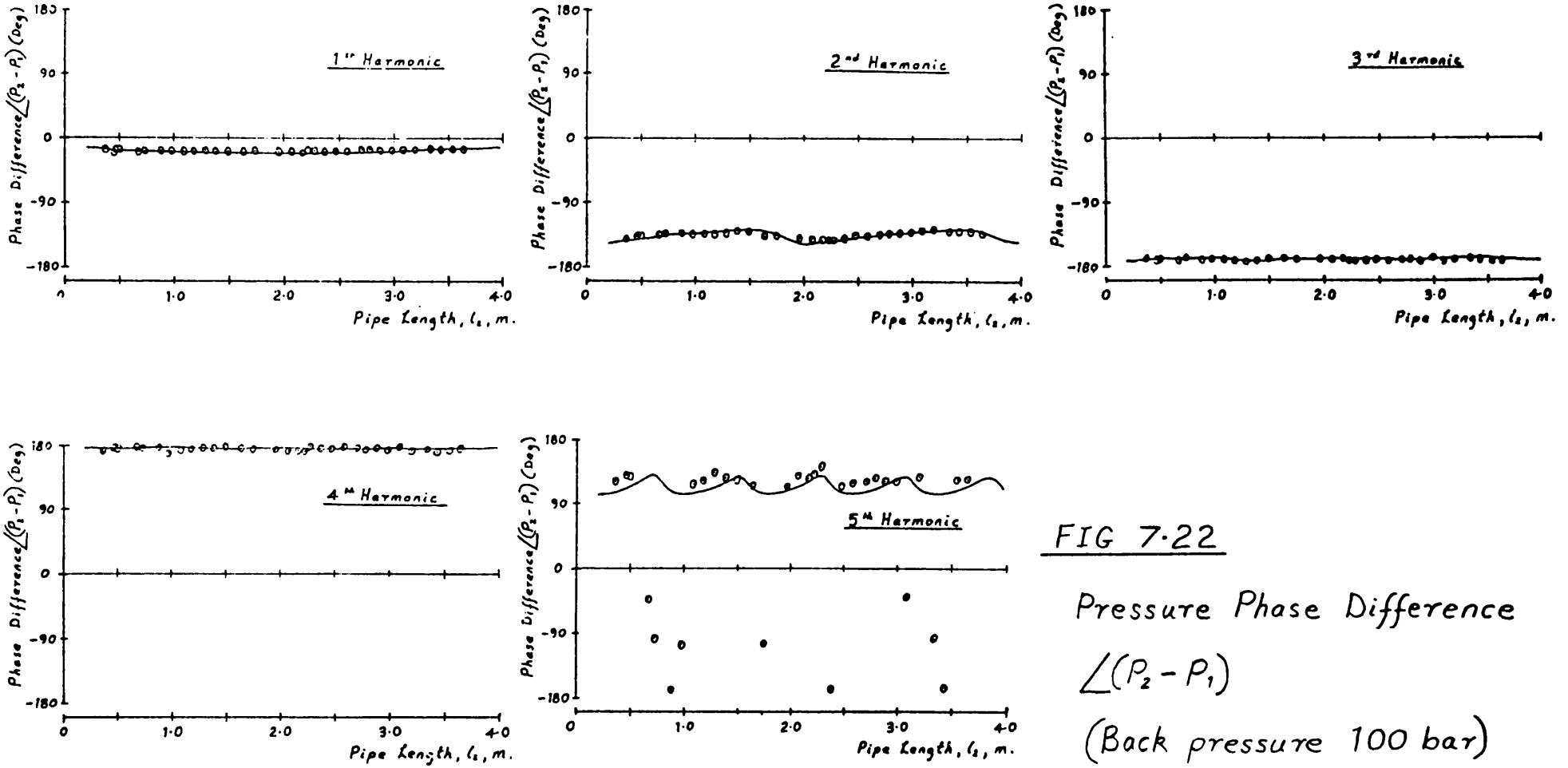

FIG 7·22

Pressure Phase Difference

$\angle(P_2 - P_1)$

(Back pressure 100 bar)

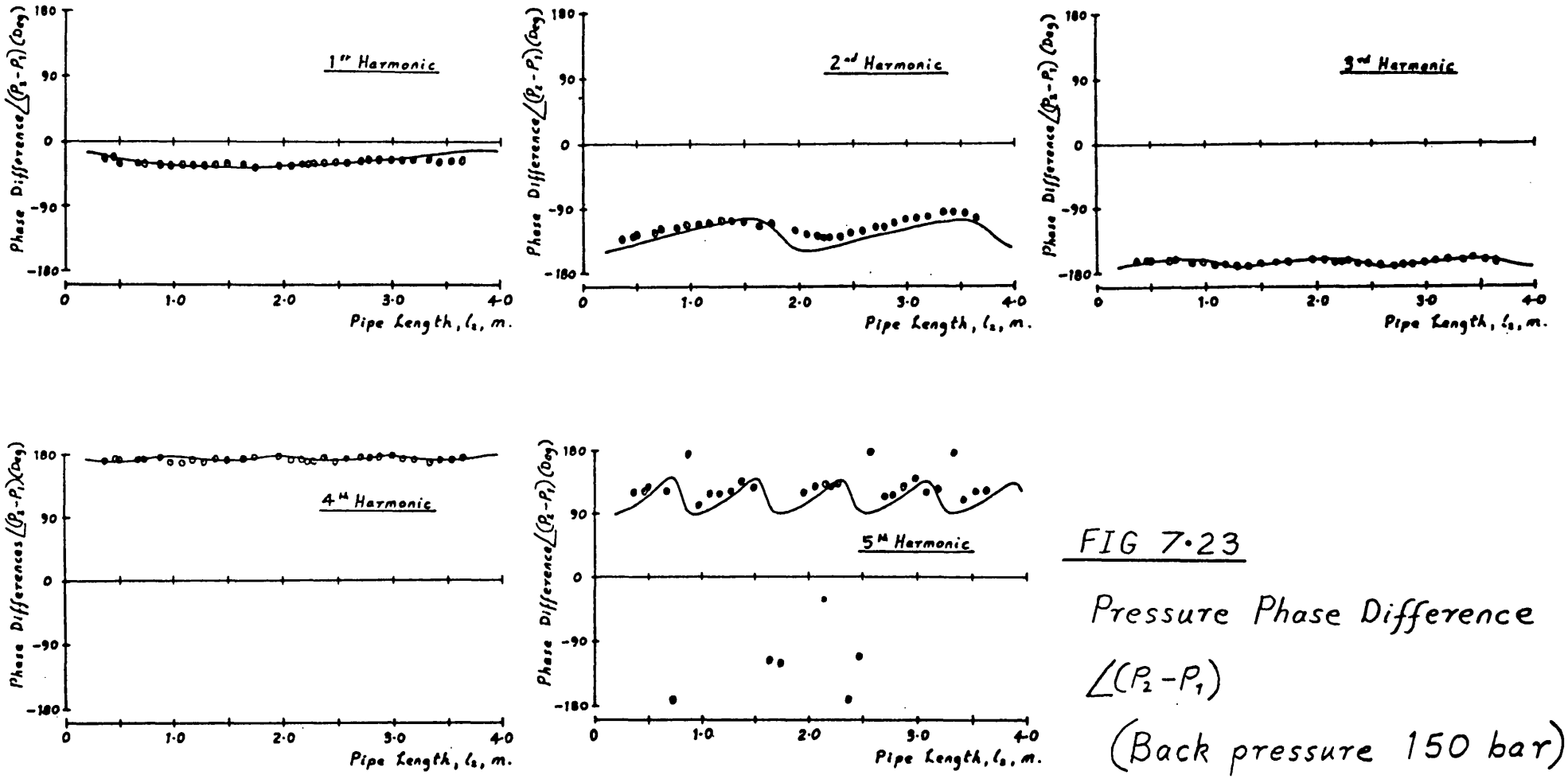

FIG 7·23

Pressure Phase Difference

$\angle(P_2 - P_1)$

(Back pressure 150 bar)

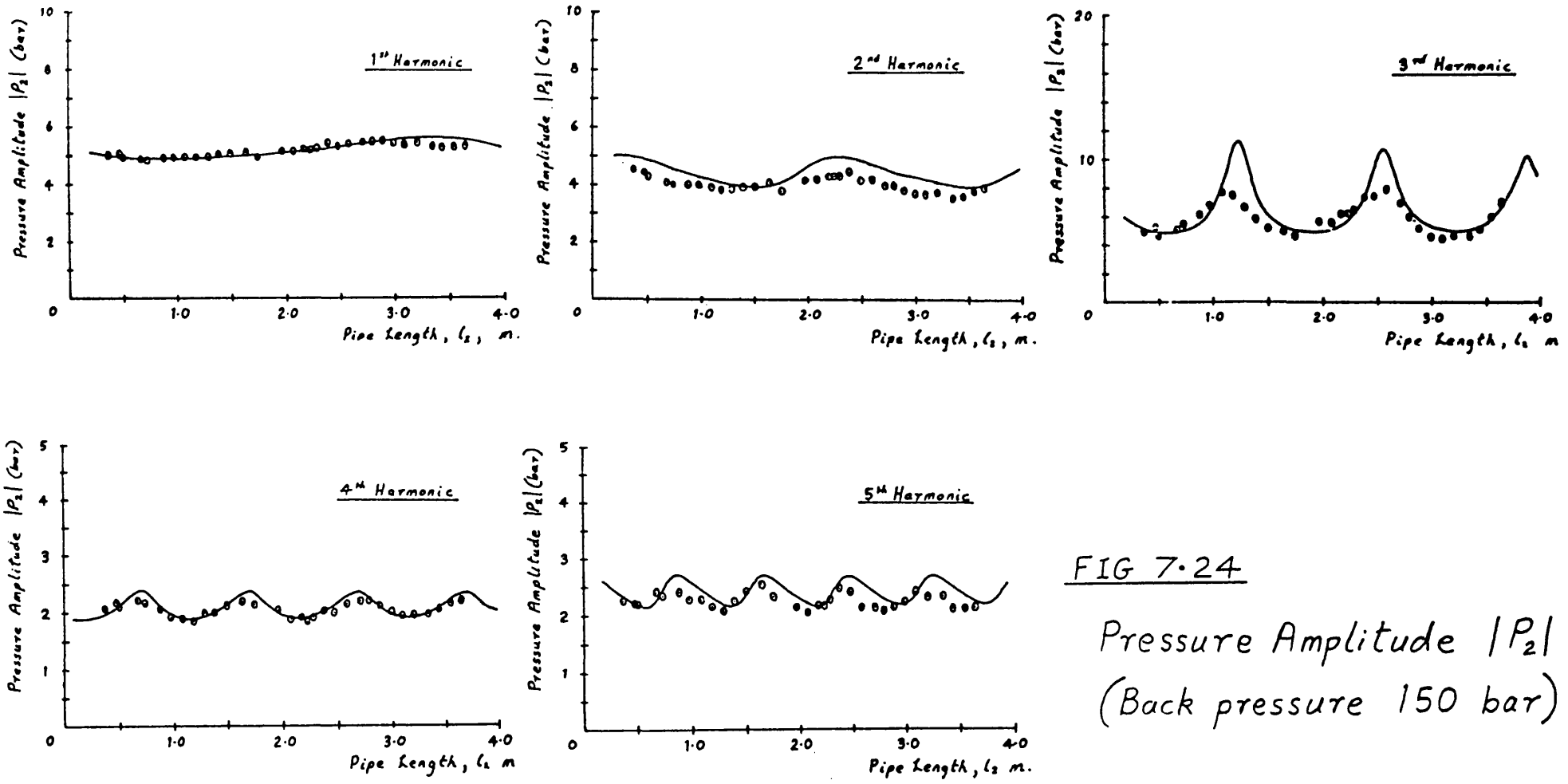

FIG 7·24

Pressure Amplitude $|P_2|$
(Back pressure 150 bar)

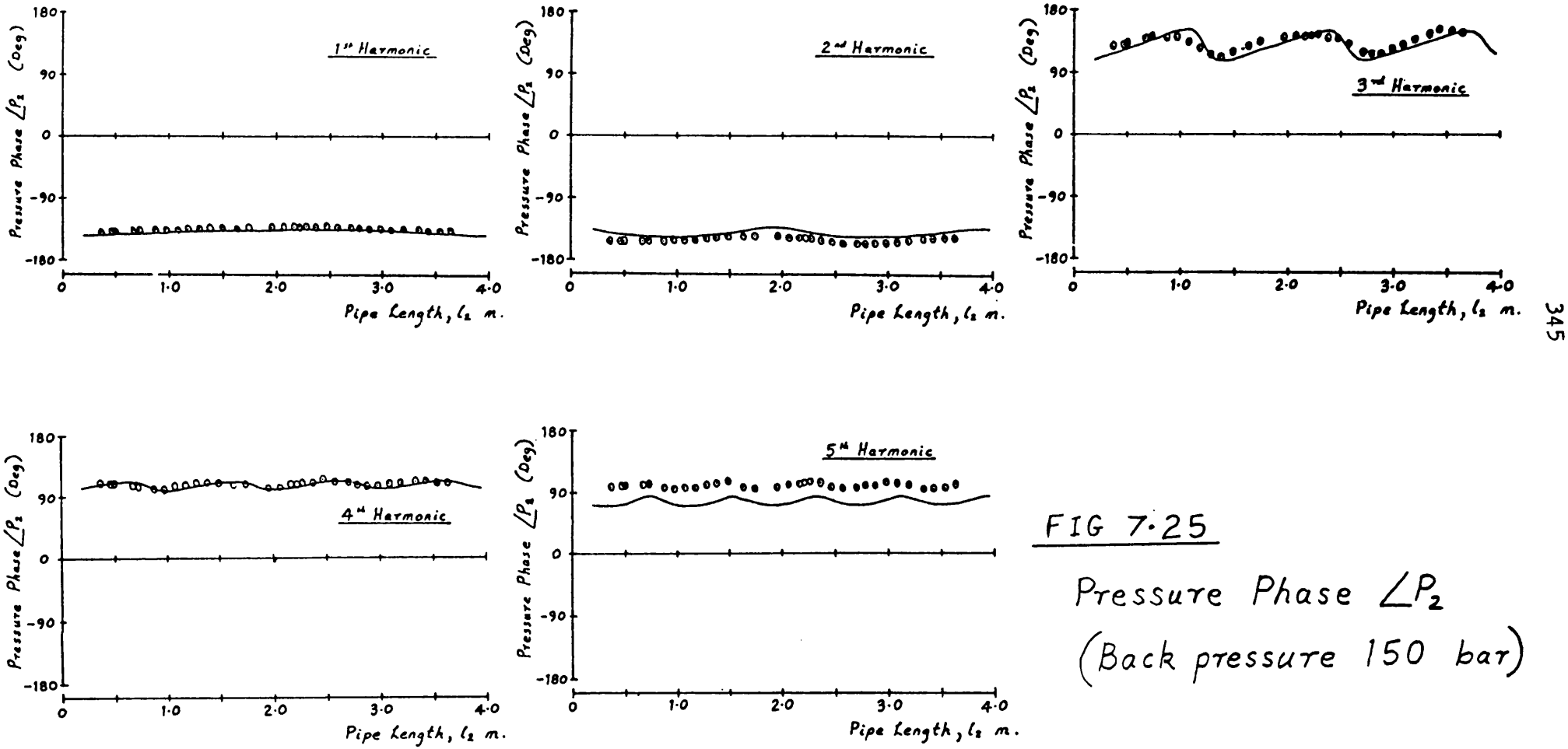

FIG 7·25

Pressure Phase $\angle P_2$

(Back pressure 150 bar)

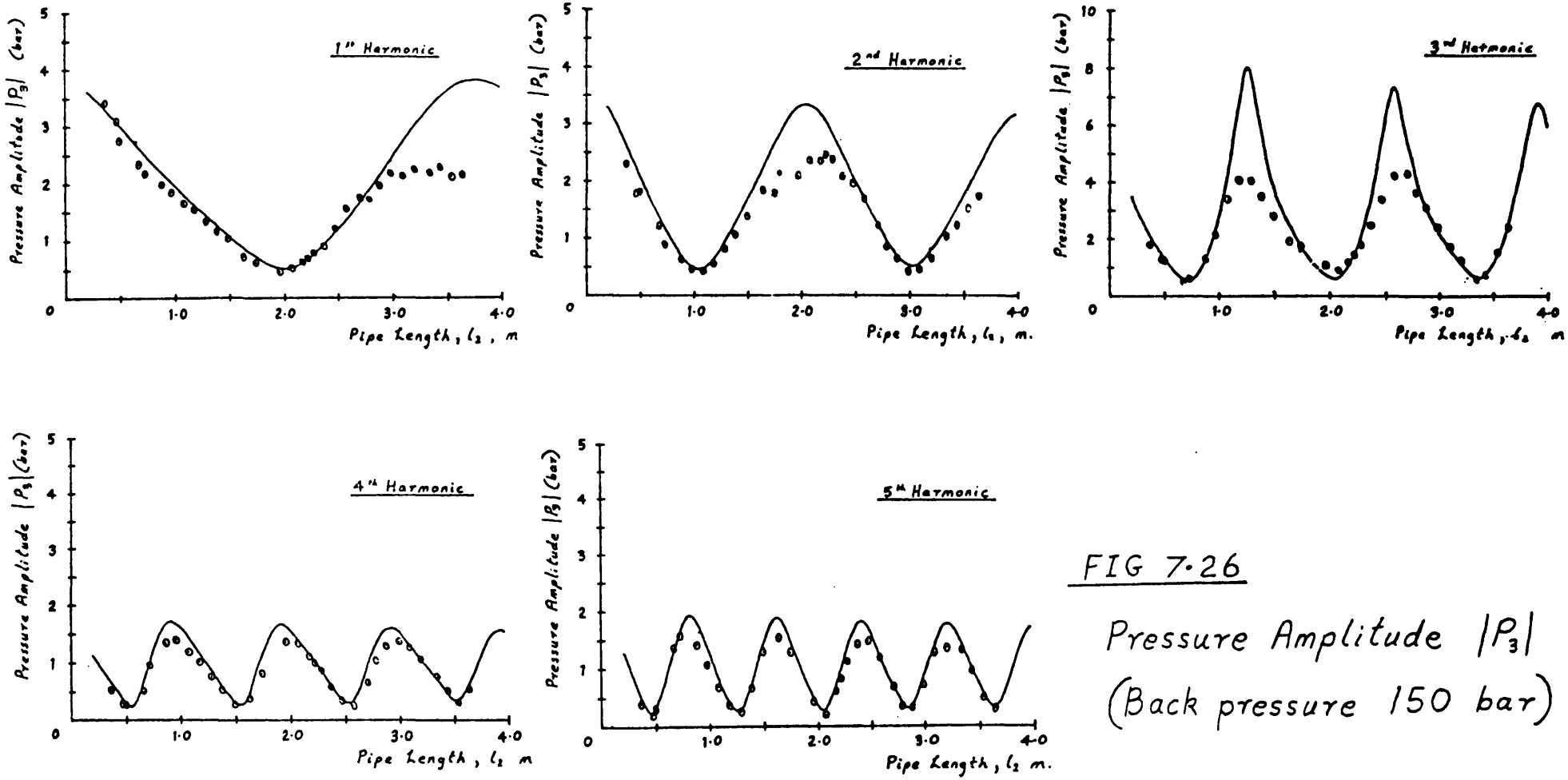

FIG 7·26

Pressure Amplitude $|P_3|$
(Back pressure 150 bar)

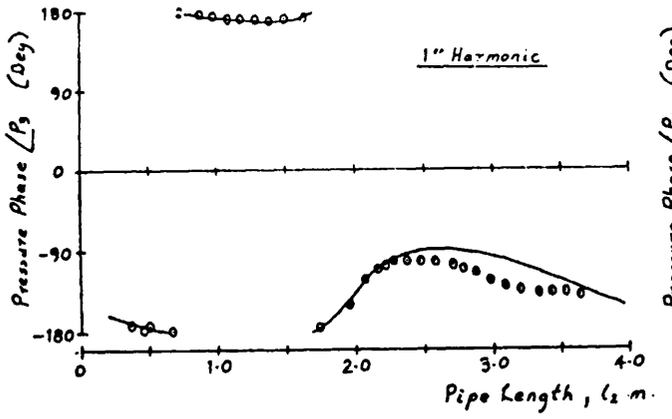

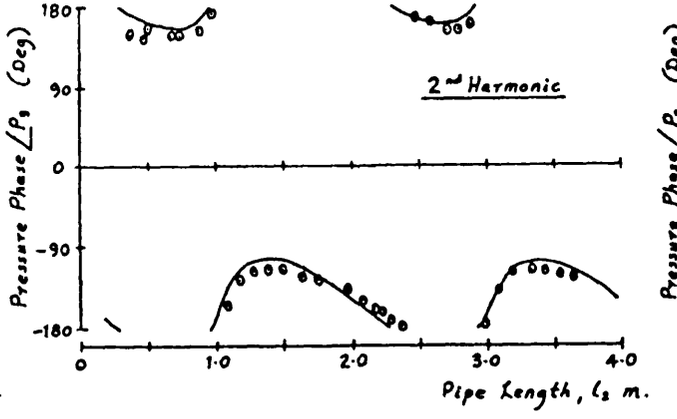

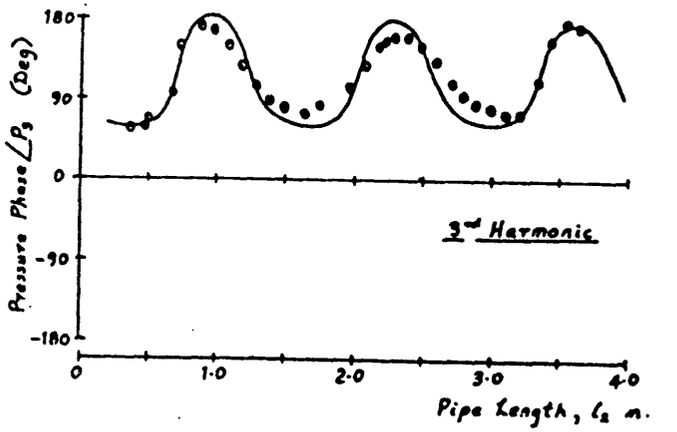

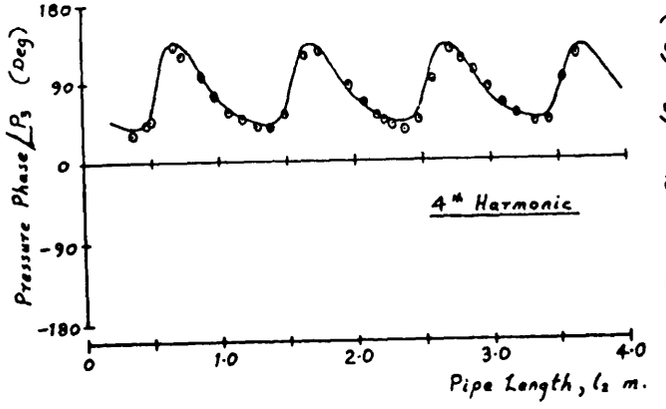

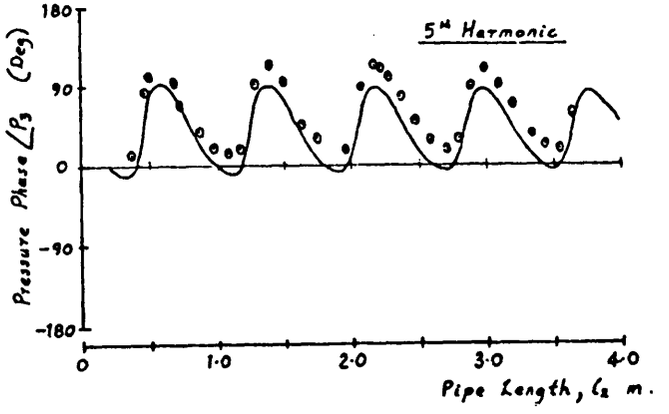

FIG 7·27

Pressure Phase $\angle P_3$

(Back pressure 150 bar)

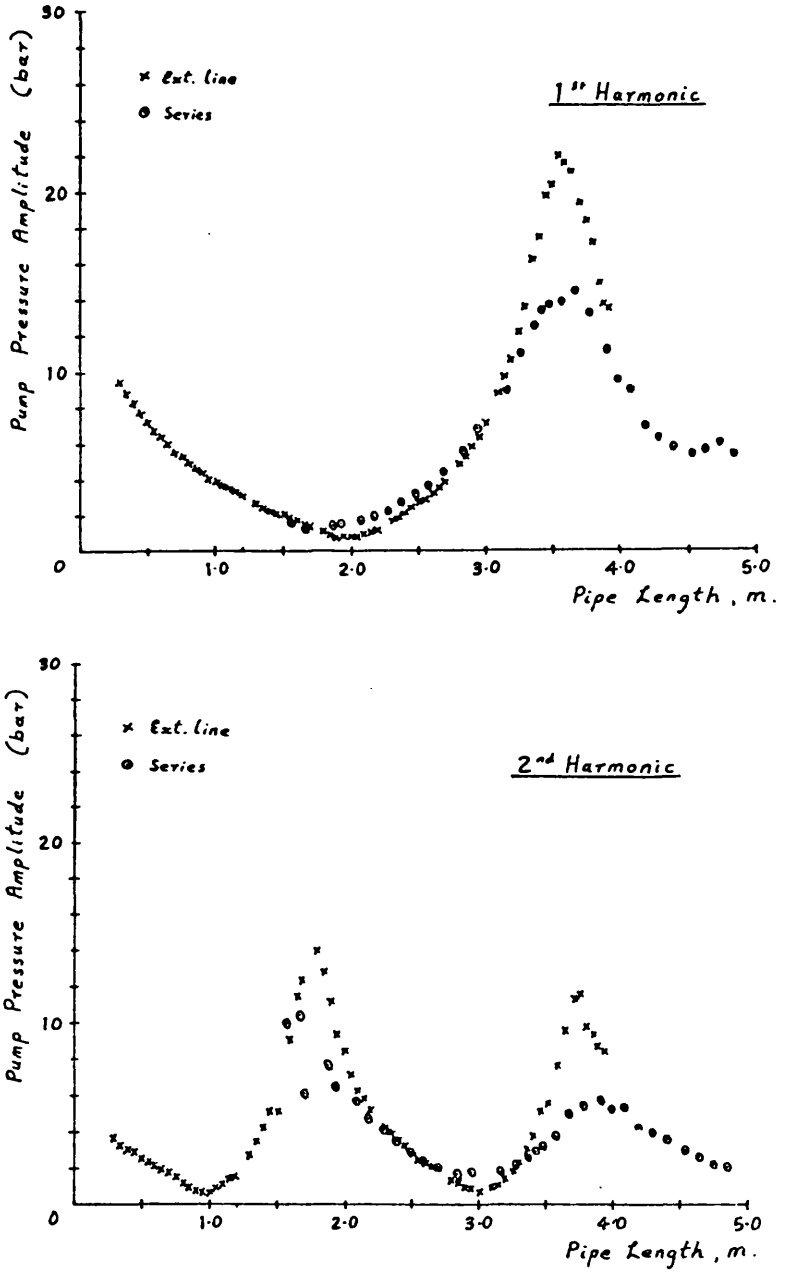

FIG 7·28 Comparing Pressures Recorded at the Pump $|P_1|$ and $|P_p|$

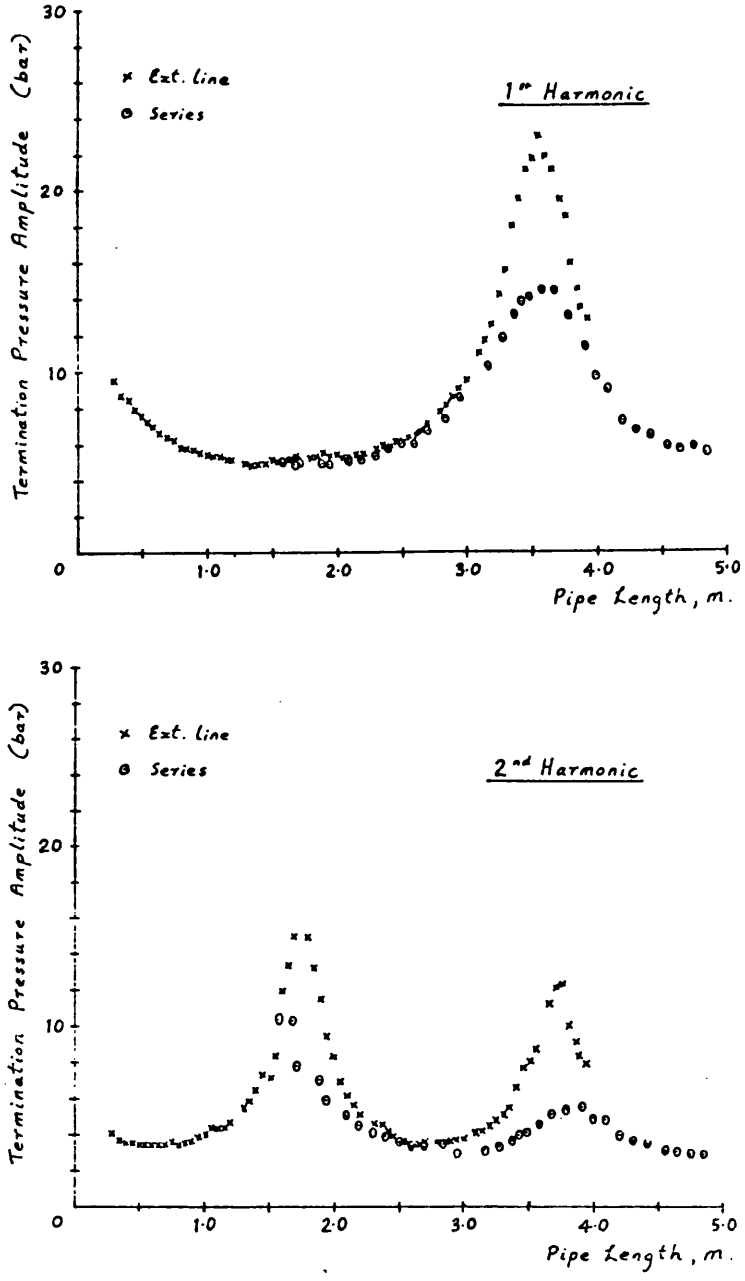

FIG 7·29 Comparing Pressures Recorded at the Termination $|P_4|$ and $|P_T|$

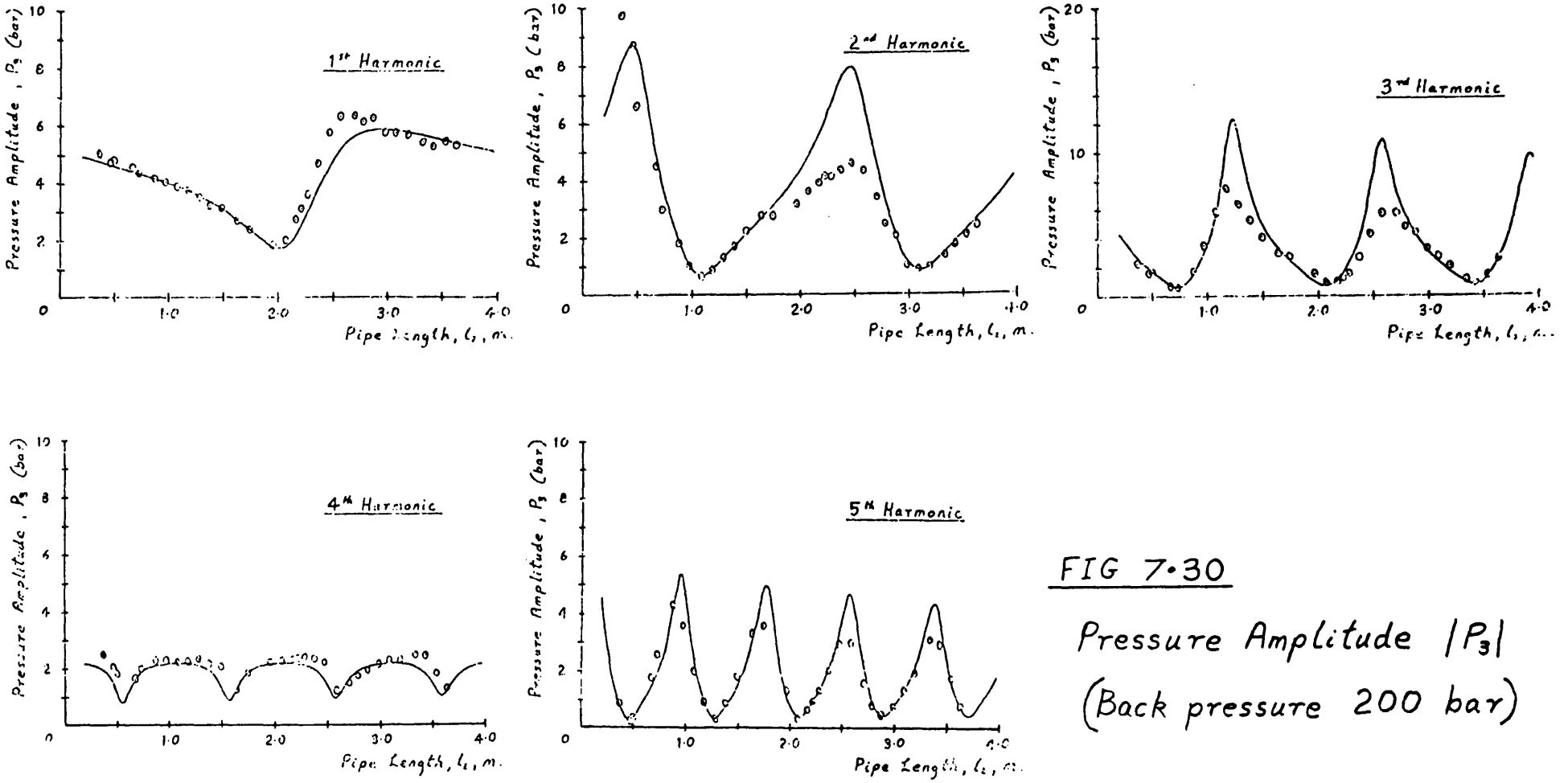

FIG 7·30

Pressure Amplitude $|P_3|$

(Back pressure 200 bar)

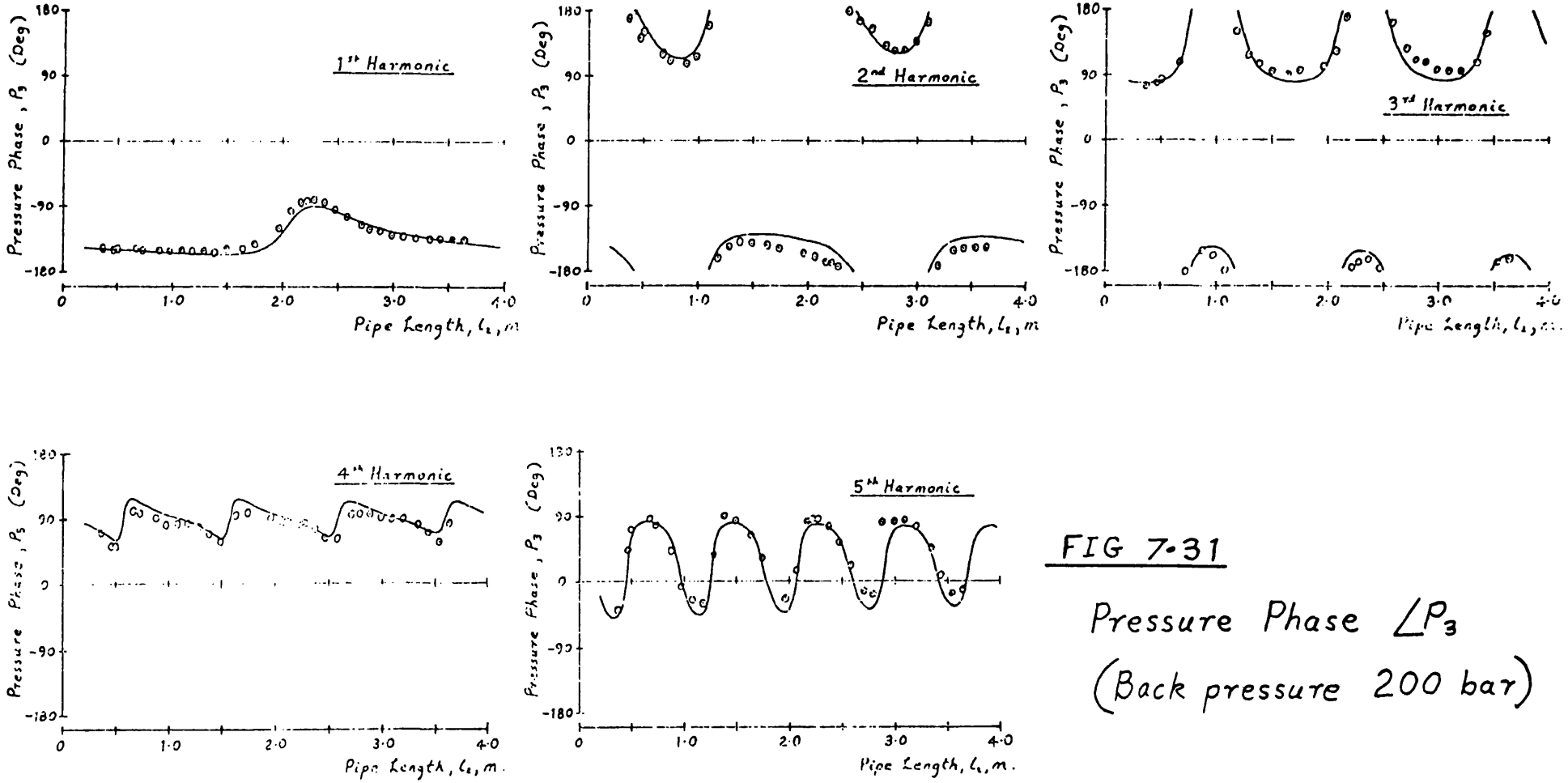

FIG 7·31

Pressure Phase $\angle P_3$

(Back pressure 200 bar)

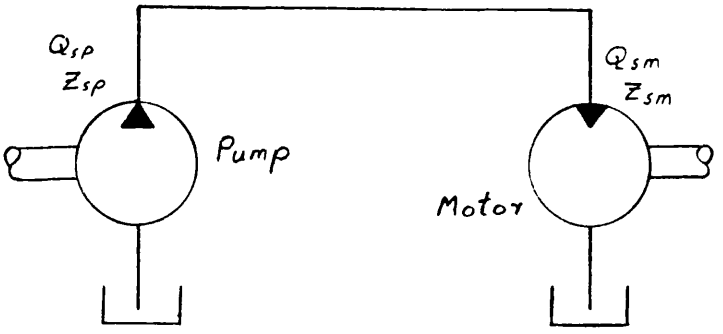

FIG 8·1 Simplified Pump/motor Transmission Circuit

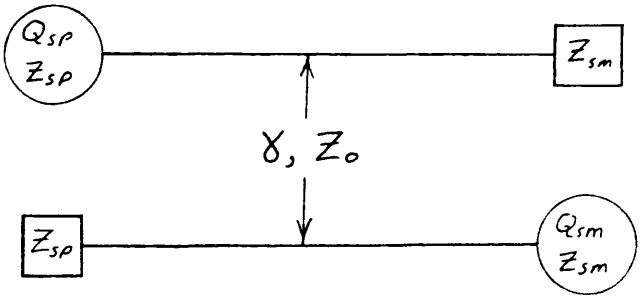

FIG 8·2 Impedance representations of a pump/motor circuit with either unit as the flow ripple source.

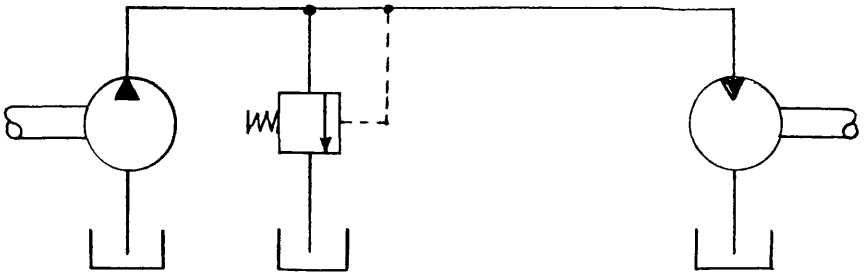

FIG 8·3 A simple practical pump/motor transmisson circuit

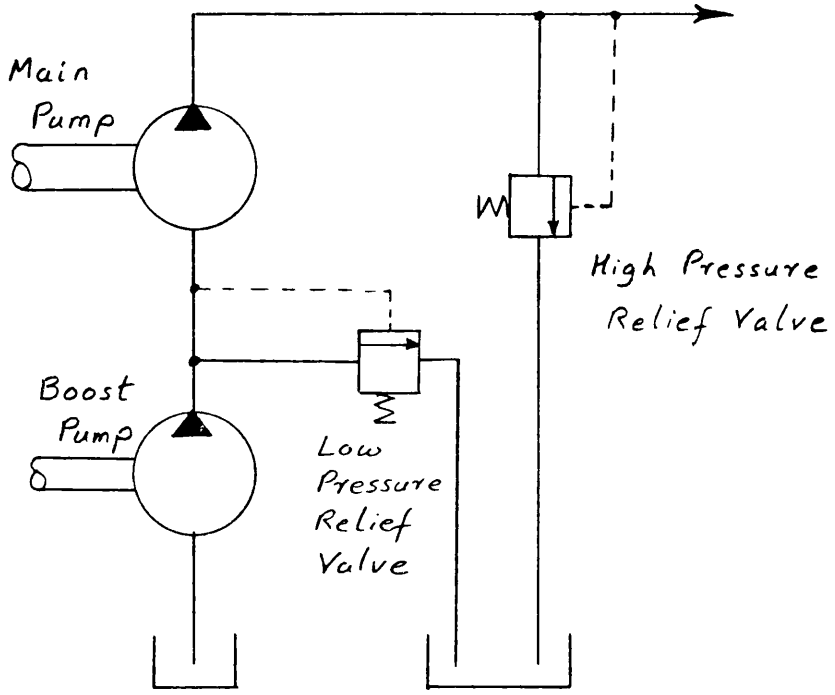

FIG 8·4 A Typical Boost Pump Circuit

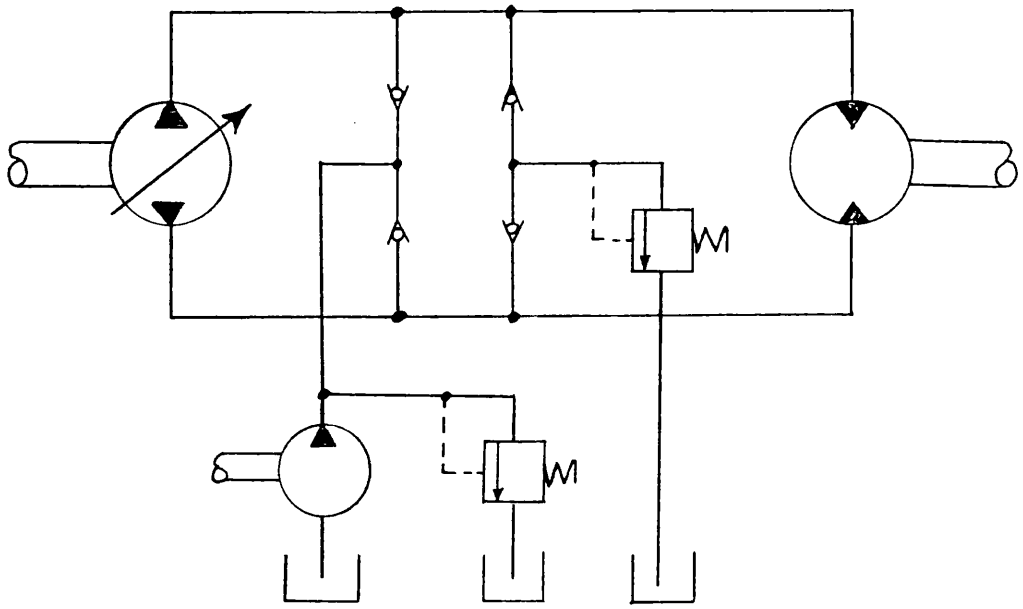

FIG 8·5 A Closed Loop Pump/motor Transmission System with Boost Pump Make Up Flow.

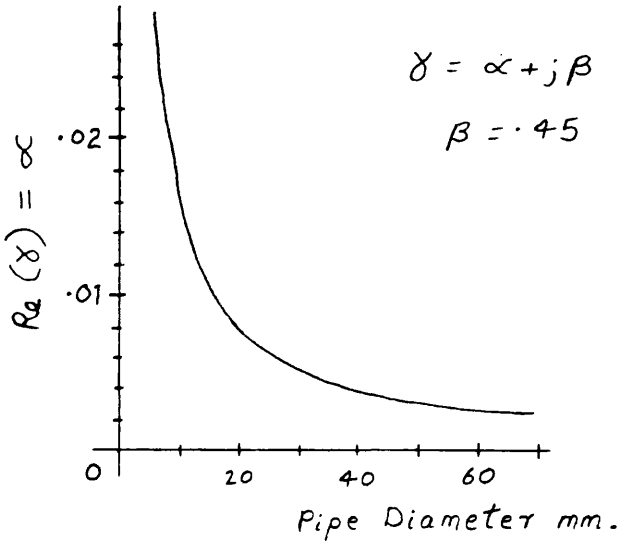

FIG 8·6 Variation in the values for the propagation constant γ with pipe diameter.

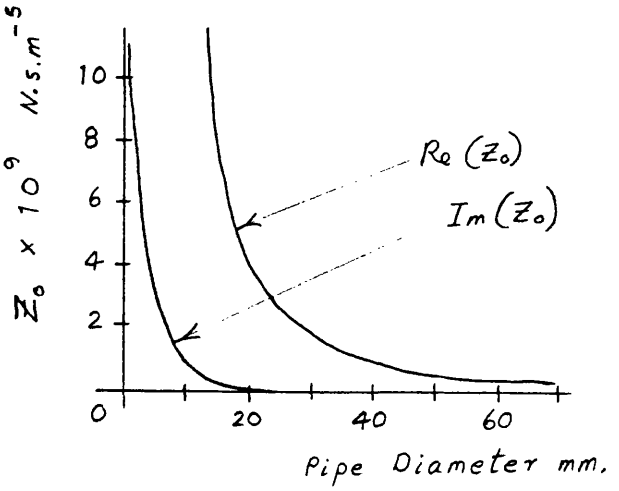

FIG 8·7 Variation in the values for the characteristic impedance Z_o with pipe diameter.

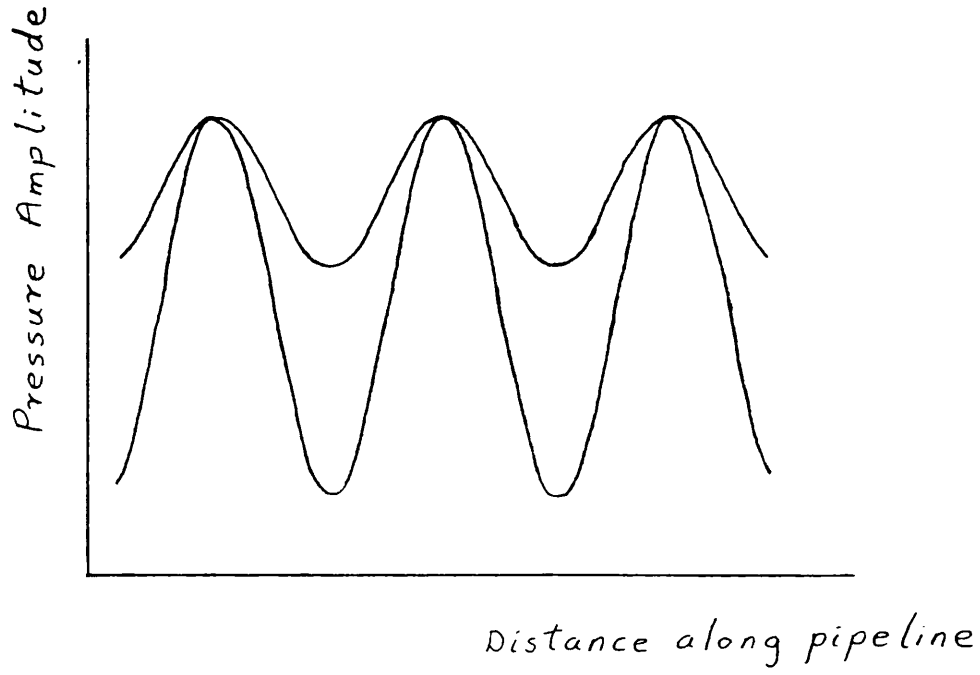

FIG 8·8 Pressure Ripple with Equal Maximum Pressure Levels

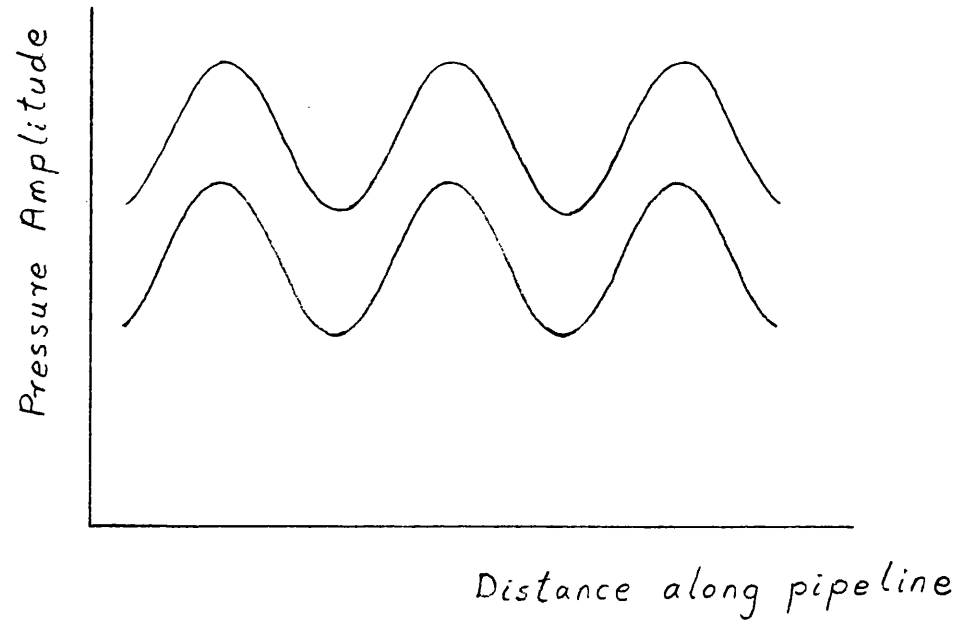

FIG 8·9 Pressure Ripple with Equal PSWR's

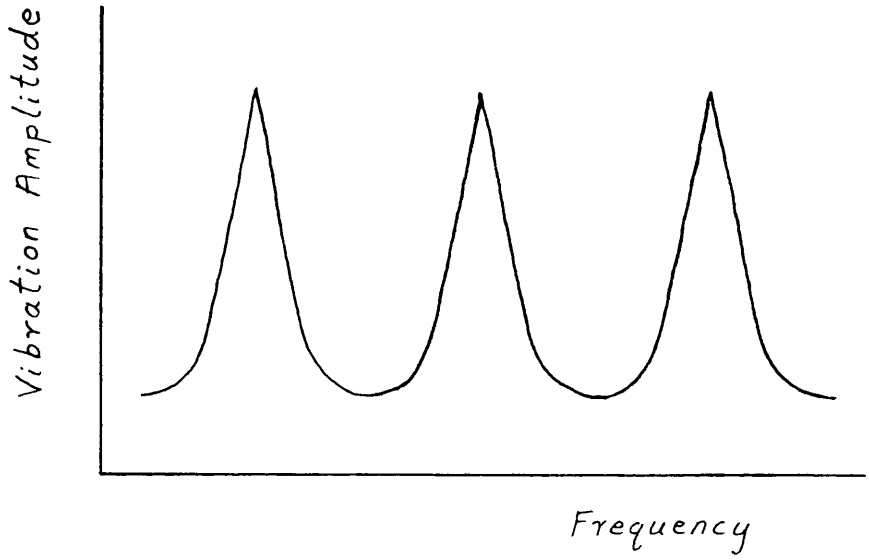

FIG 8·10 Response of a Mechanical System to Excitation

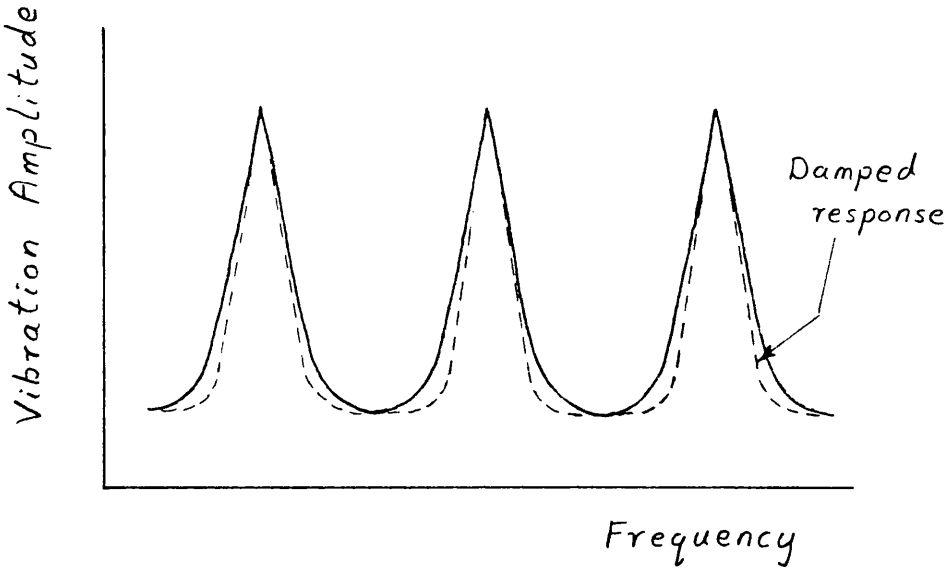

FIG 8·11 Effect of Damping on the System Response

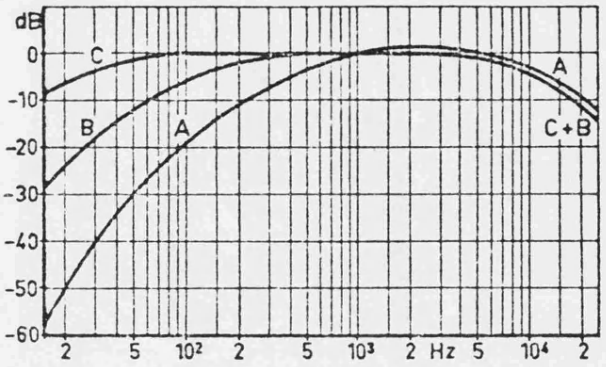

FIG 8·12 Noise measurement filter characteristics

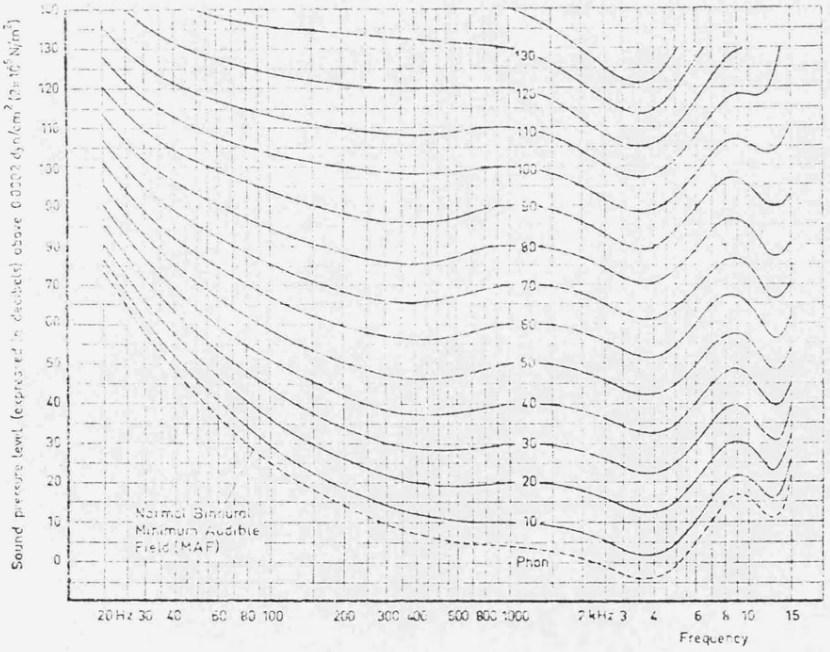

FIG 8·13 Equal loudness contours - Response of a human ear to noise levels